NASA CR-171,838

NASA-CR-171838
19850008985

A Reproduced Copy

OF

NASA CR-171,838

Reproduced for NASA

by the

NASA Scientific and Technical Information Facility

LIBRARY COPY

MAY 14 1985

LANGLEY RESEARCH CENTER
LIBRARY, NASA
HAMPTON, VIRGINIA

NF01599

FFNo 672 Aug 65

CR-171838 c.1

FINAL REPORT

(NASA-CR-171838) DESIGN AND TEST OF A FOUR CHANNEL MOTOR FOR ELECTROMECHANICAL FLIGHT CONTROL ACTUATION Final Report (Sundstrand Energy Systems) 245 p HC A11/MF A01 CSCL 09A G3/33

N85-17294

Unclas 14081

DESIGN AND TEST OF A FOUR CHANNEL MOTOR FOR ELECTROMECHANICAL FLIGHT CONTROL ACTUATION

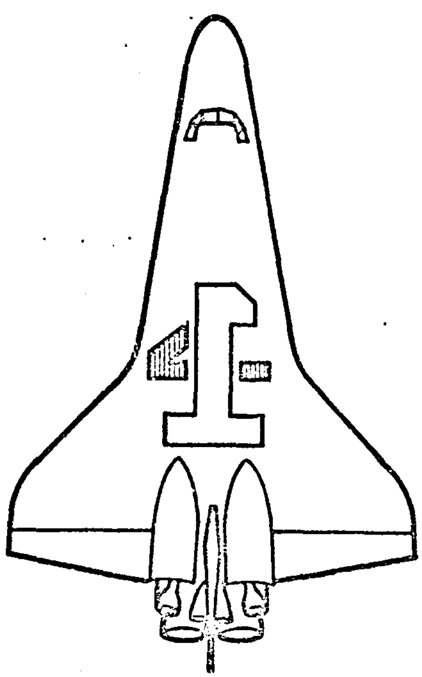

Sundstrand Energy Systems

ROCKFORD, ILLINOIS

unit of Sundstrand Corporation

N85-17294

FINAL REPORT S8308-R1

DESIGN AND TEST OF A FOUR CHANNEL PERMANENT MAGNET BRUSHLESS D.C. MOTOR FOR

ELECTROMECHANICAL FLIGHT CONTROL ACTUATION

FOR

NASA CONTRACT: NAS 9-16535

DATA ITEM: MA-640T

TO

NASA-LYNDON B. JOHNSON SPACE CENTER

HOUSTON, TEXAS 77058

By

SUNDSTRAND ENERGY SYSTEMS

Unit of Sundstrand Corporation
4747 Harrison Avenue, P.O. Box 7002
Rockford, IL 61125

DECEMBER 1984

TABLE OF CONTENTS

1.0 Introduction

2.0 Summary

3.0 Approach

4.0 Motor Design Studies

5.0 Motor Fabrication

6.0 Design Verification Test

7.0 Conclusion

Appendix A Test Data

Appendix B Control Strategy

1.0 INTRODUCTION

1.0 INTRODUCTION

Advances in power electronics and electric motor design have made possible Electromechanical Actuation Systems (EMA), Figure 1-1, with performance and weight characteristics comparable to conventional hydraulic and hydromechanical systems. Present trends in aircraft and spacecraft toward use of electric power for more accessories and services make EMA an attractive candidate for primary flight control actuators.

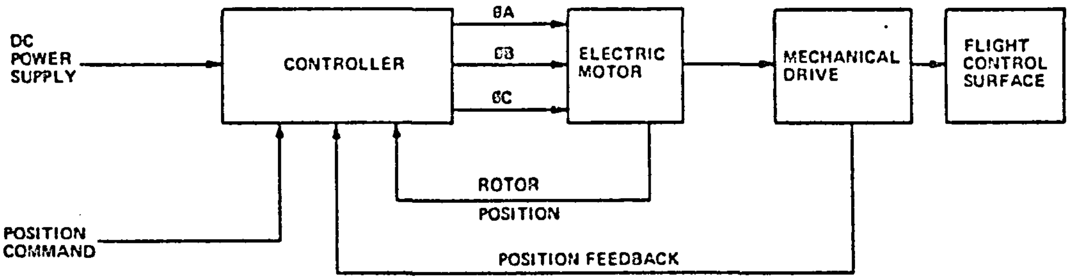

Figure 1-1 Electromechanical Servoactuator System Block Diagram (Simplified)

The reliability requirements for primary flight control actuators, however, dictate a level of redundancy. Conventional approaches have included multi-actuator, Figure 1-2, or multi-motor systems, Figure 1-3.

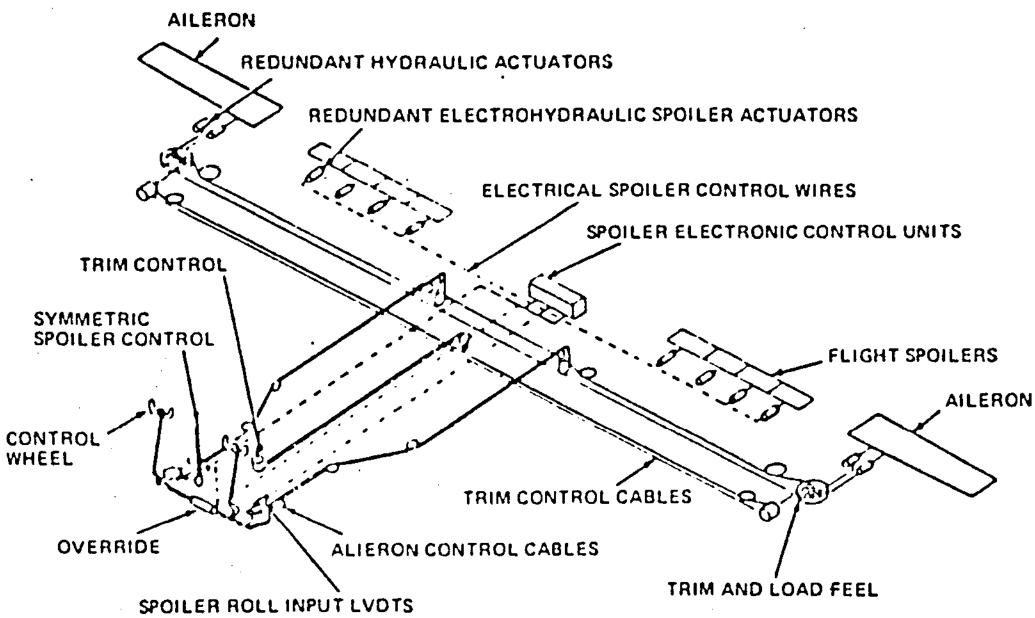

Figure 1-2 Typical Lateral Flight Control System

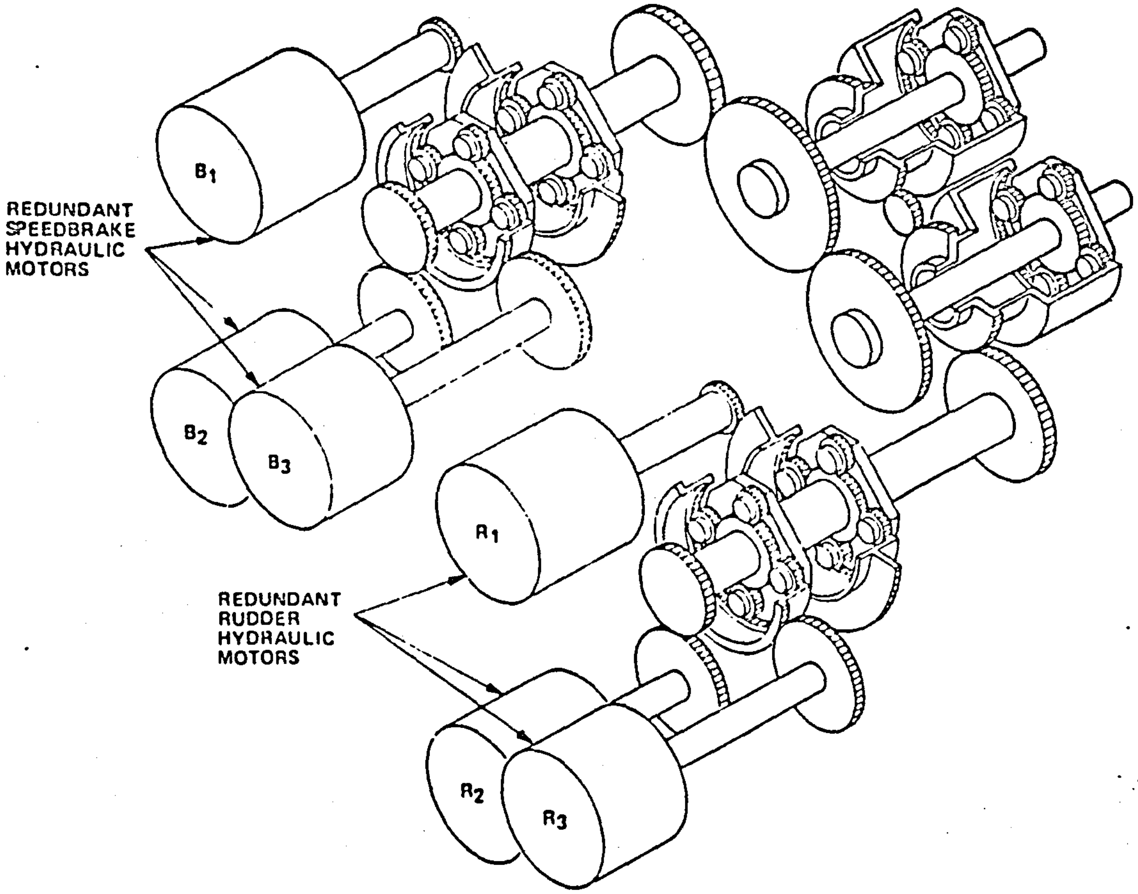

Figure 1-3 Space Shuttle Rudder/Speedbrake Schematic

To achieve the full potential of EMA technology, it is desirable to obtain the required redundancy with a multi-channel motor which could electromagnetically sum the torque of the individual channels on a single rotor, Figure 1-4. Complex mechanical gearing arrangements could then be eliminated.

To reduce this concept to practical application requires knowledge of the failure modes and effects and innovative approaches to control and redundancy management.

As the first step in this effort, NASA-JSC and Sundstrand Advanced Technology Group undertook a joint program to design, develop and test a highly reliable, lightweight, multi-channel motor. This program was conducted under contract NAS-9-16535.

This project concentrated on establishing a suitable electromagnetic torque summing approach to flight control system redundancy. The objective was to design, fabricate, and test a brushless dc motor with four-channel/two fault tolerant redundancy. This motor provided the means for validation of the analytical models and permits future development of a compatible four-channel control technique.

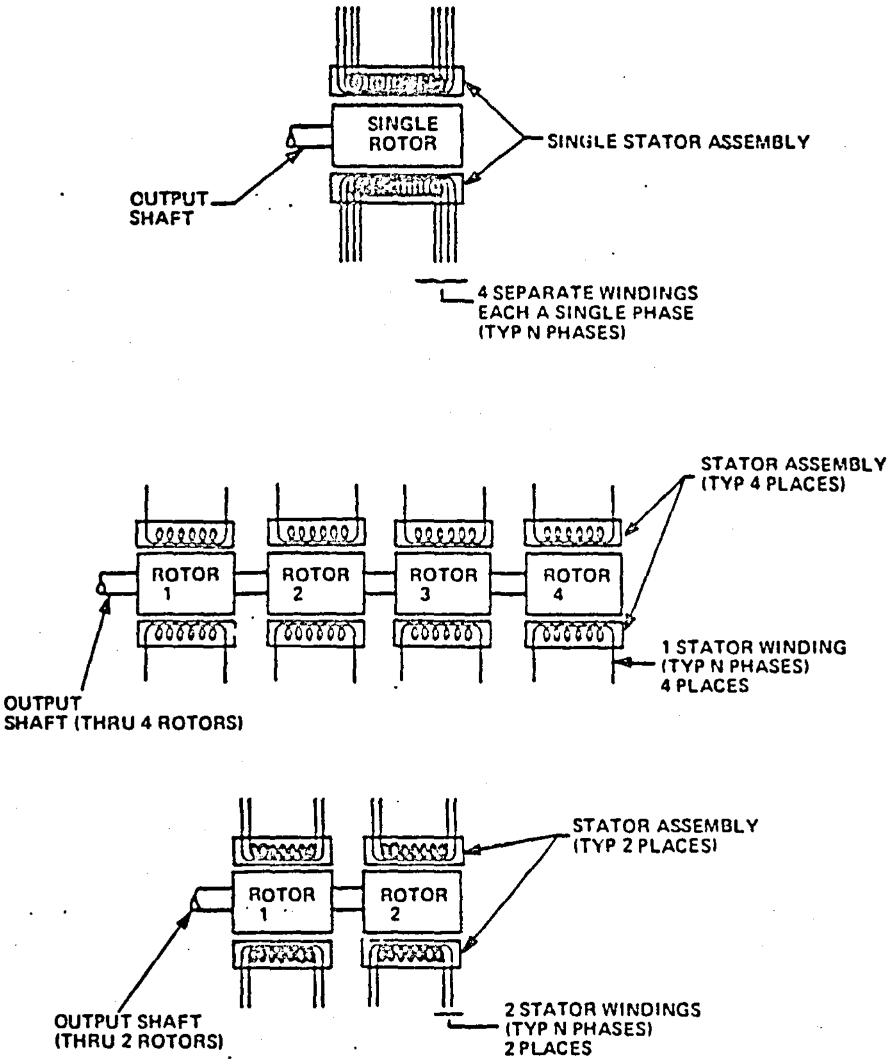

Figure 1-4 Typical Electromagnetic Torque Summing Concepts

Within this context, several specific objectives were defined:

1. Establish a Preferred Motor Concept — With emphasis on failure modes and effects, different mechanical arrangements were evaluated and a preferred concept selected.

2. Minimize Weight of Preferred Concept — The weight of the preferred concept was evaluated with respect to performance, reliability, and efficiency. Electromagnetic design parameters were traded to achieve a suitable balance of these characteristics.

3. Validate Electrical Performance Model — Single-channel tests of the motor characterized its performance and were used to validate the design models.

In achieving these objectives, the intent of this project was to demonstrate the feasibility of electromagnetic torque summing and establish the credibility of weight and performance

predictions. In conjunction with this work, NASA-JSC separately funded the development of finite element electromagnetic performance models. The combination of these analytical techniques, the characterization data obtained from motor tests, and the availability of a four-channel motor provide the foundation for the future development of a compatible control strategy.

2.0 SUMMARY

2.0 SUMMARY

A four-channel motor, capable of sustaining full performance after any two credible failures was successfully designed, fabricated, and tested. Configured as illustrated in Figure 2-1, the design consisted of a single samarium cobalt permanent magnet rotor with four separate three phase windings arrayed in individual stator quadrants around the periphery.

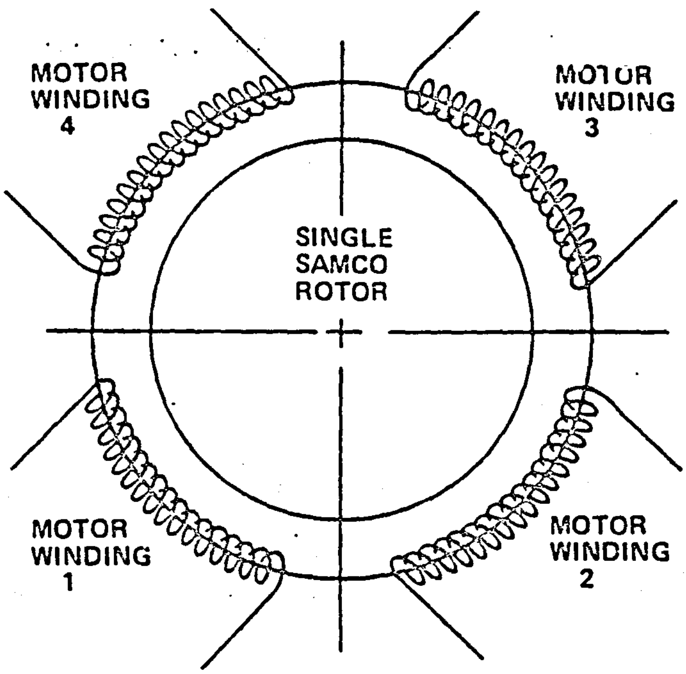

Figure 2-1 Electromagnetic Torque Summing Candidate

Trade studies which culminated in this design established the sensitivities of weight and performance to such parameters as design speed, winding pattern, number of poles, magnet configuration and strength. With this information, individual design details were selected to provide a reasonable balance between weight and performance. The resulting motor, at 33.31 pounds, achieved a project goal, bettering a 34 pound maximum established by comparison to comparable hydraulic systems. With a demonstrated efficiency of 92.9% at a design point of 4333 rpm, 17.2 hp, the motor also achieved the goal of 90% minimum efficiency. The prototype motor is shown in Figure 2-2.

Manufacturing techniques refined in the construction of this unit demonstrated that electromagnetic torque summing is a practical concept. Methods of coil winding and insertion plus rotor fabrication techniques provided a light, compact assembly without exotic and expensive processes.

Equally significant, testing demonstrated excellent electromagnetic separation among the individual channels. Performance was virtually unaffected as channels were added or subtracted from the circuit. Extensive static and dynamic data were developed. Included in the Appendix to this report, these data provide the essential information necessary to design a compatible four-channel controller and ultimately bring an electromechanical flight control system to fruition.

ORIGINAL PAGE
BLACK AND WHITE PHOTOGRAPH

Figure 2-2 Prototype 4 Channel Motor

3.0 APPROACH

3.0 APPROACH

The approach used in this project is summarized as follows:

i) ESTABLISH REQUIREMENTS — Sundstrand and NASA-JSC jointly reviewed the functional requirements of an EMA system, assessed their influence on motor design and selected a working set of design criteria.

ii) ESTABLISH PREFERRED GEOMETRY — A variety of configurations were conceived and compared, establishing a preferred mechanical arrangement.

iii) DEFINE POINT OF DEPARTURE DESIGN — A detailed design of the preferred geometry was executed using historical information to select individual part configurations.

iv) ESTABLISH POINT OF DEPARTURE PERFORMANCE — In-depth analyses were conducted for the preferred geometry to fully define its predicted performance.

v) ITERATE ON POINT OF DEPARTURE — Individual design parameters were varied to develop sensitivity information enabling a refined final design to be established.

vi) FABRICATE FINAL DESIGN — One motor was built. Design changes necessary for manufacturing reasons were factored into the analyses.

vii) TEST FINAL DESIGN MOTOR — Motor and single channel motor/controller tests were conducted to confirm and correct the analytical techniques and provide a data base for controller development by NASA.

viii) NASA-JSC TESTING — The motor was provided to NASA-JSC for planned performance and failure mode evaluation testing.

4.0 MOTOR DESIGN STUDIES

4.0 MOTOR DESIGN STUDIES

The objective of the design studies was to establish a design which offered a reasonable balance of the desired criteria. Trades were conducted to define a preferred geometry which was then optimized. Variables such as magnet material, lamination material, number of poles, rotor construction, design speed and winding pattern were considered.

The method employed entailed establishing the preferred arrangement using reliability criteria. The details of this configuration were then selected, based on prior experience, to establish a point of departure design. This baseline was analyzed in depth to fully characterize its performance and physical properties.

Next, each parameter was varied individually by carrying out complete alternate motor designs, calculating the resulting performance and comparing to the baseline. After all the variables had been evaluated in this manner, a final motor design was performed using the optimum value for each parameter. This version was later fabricated to assess the accuracy of the predictions, to validate the models and to provide a tool for further system development.

A flow diagram of the trade studies is found in Figure 4-1.

4.1 REQUIREMENTS

The design for the motor is based on the Space Shuttle inboard elevon performance requirements, Figure 4-2. The Space Shuttle requirements were chosen because, at the time, interest in an electric Orbiter offered a likely opportunity for a near-term demonstration of this technology.

Fault Tolerance and Torque vs. Speed

The two-fault tolerant requirement dictates that the actuator's motor provide full performance even after two credible failures. A further stipulation for safe operation at reduced performance with any three credible failures was also imposed, in essence dictating a four-channel motor. Quadruple redundancy is compatible with the Shuttle flight control system of four general purpose computers with four reconfigurable data strings.

The resulting actuator, therefore, requires the torque vs. speed characteristics illustrated in Figure 4-3. Note that to provide this full performance with only two healthy motor channels requires that each channel be capable of supplying one-half full actuator output power plus one-half of any losses engendered by the failed channels. Theoretically then a fully healthy motor would be capable of supplying, at least instantaneously, the torque shown in Figure 4-4.

The four channel concept thus carries the potential for overdriving the actuation system and perhaps damaging structure. Control of this situation must be considered in ensuing system definition activities.

Duty Cycle

The duty cycle defined in the contract statement of work is shown in Figure 4-5. Representing original Orbiter design criteria, this cycle comprises approximately 2000 watt-hours.

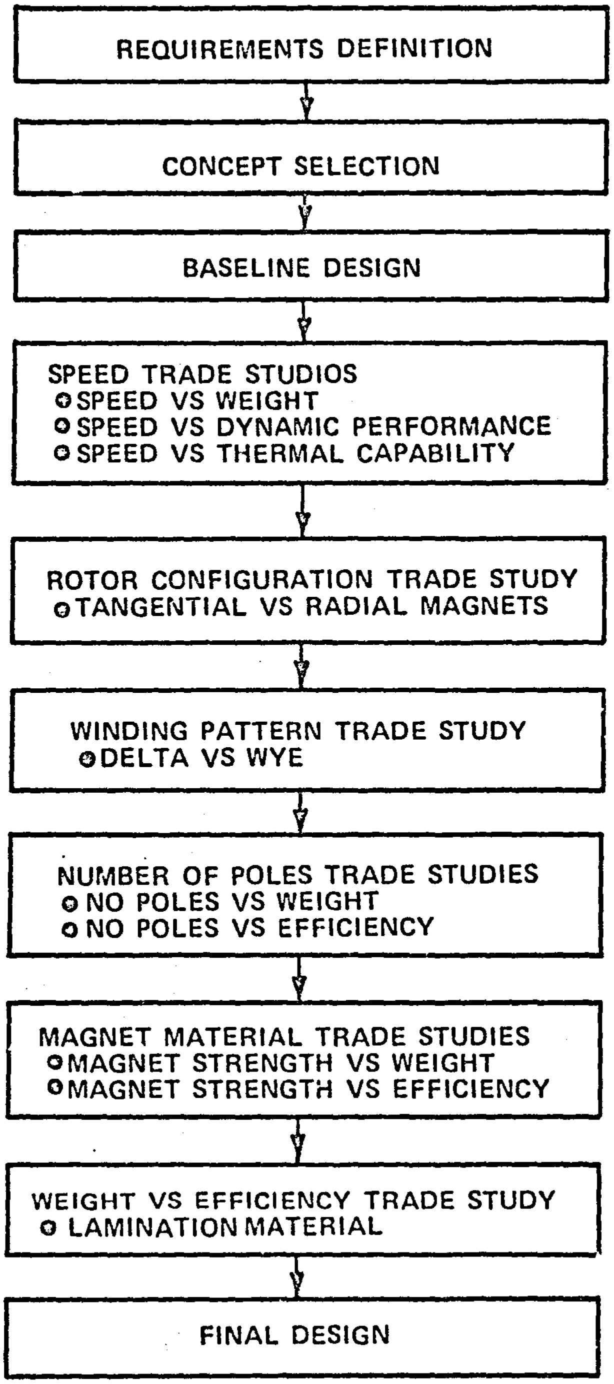

Figure 4-1 Trade Study Flow Diagram

INPUT VOLTAGE	270 VDC
STROKE	± 12.5°
NO LOAD VELOCITY	± 30°/SEC
STALL LOAD	500,000 IN–LB
DYNAMIC PERFORMANCE	–3DB @ 3.3 HZ + 2% COMMAND
RELIABILITY	TWO FAULT TOLERANT

Figure 4-2 Space Shuttle Inboard Glevon Requirements

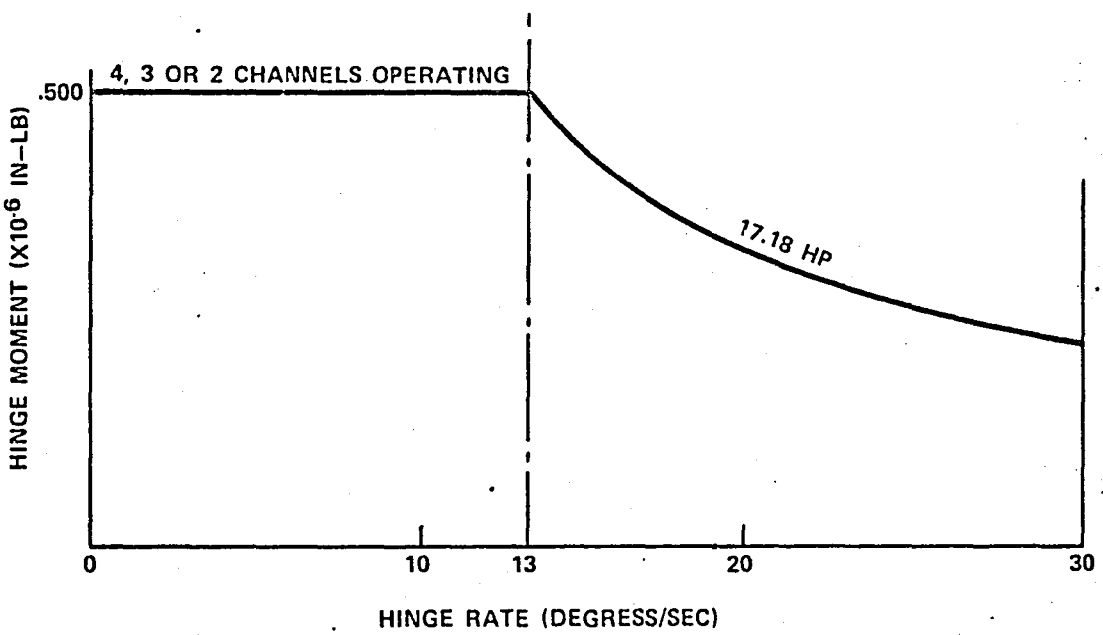

Figure 4-3 Motor Speed-Torque Requirements

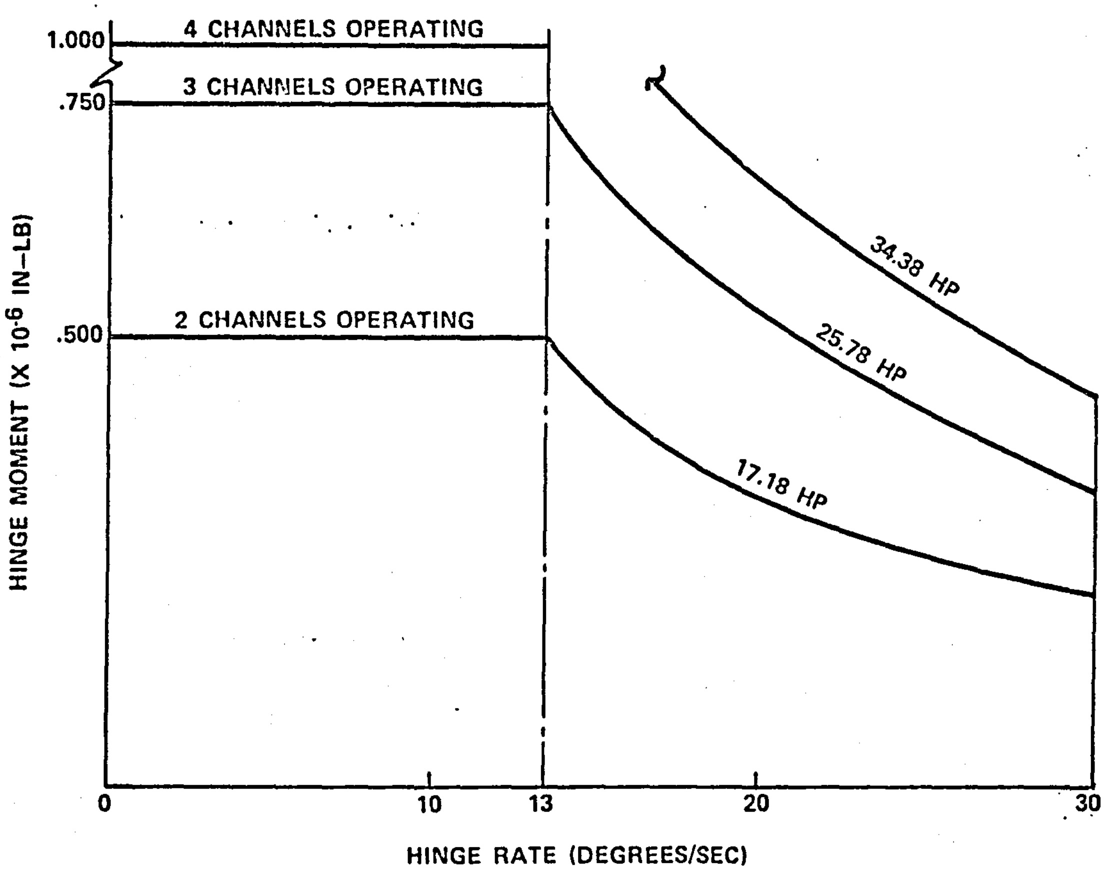

Figure 4-4 Motor Speed-Torque Capabilities

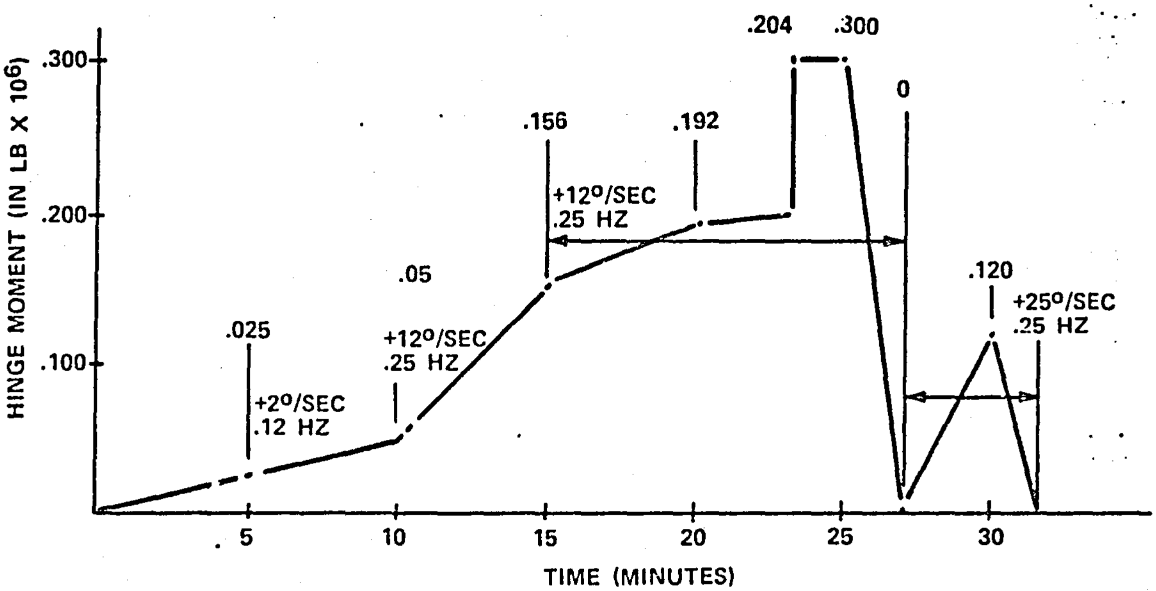

Figure 4-5 Duty Cycle

At the time of this project, data from initial flights were revealing a large degree of conservatism in that value. Sufficient capability was anticipated to require no more than 500 watt-hours.

In order not to penalize this design study by using overly conservative criteria, NASA-JSC and Sundstrand jointly redefined the duty cycle. The resulting cycle, summarized in Table 4-1 on a per channel basis, was predicated on the following:

1. Elevon hinge moment and rate using STS-1 data and three sigma winds.
2. Approximately 500 watt-hours total energy.
3. At least one maximum power point in each flight regime.
4. Output horsepower less than 1.5 horsepower 98% of the time.
5. Nine minutes of surface holding against inertia loads, assumed to be equal to 5% of the maximum load, during the initial phase of de-orbit prior to entering the atmosphere.

Table 4-1 Derived Single Channel Duty Cycle

Cycle Number	Duration, Minutes	Motor Power, Horsepower	Surface Rate, Degrees/Sec.	Motor Speed*, RPM	Remarks
1	9	Holding	0	0	Holding 12,500 in-lb/GR**
2	17.5	0.3	5	1666	
3	0.5	2.3	5	1666	
4	7.5	0.3	13	4333	
5	0.5	10.0	13	4333	Max. Hinge Moment
6	3.5	0.3	20	6666	
7	0.5	10.0	20	6666	
8	1.5	0.3	30	10,000	
9	0.5	10.0	30	10,000	Max. Surface Rate

* Based on 10,000 RPM Motor
** Gear Ratio (GR) = 2,000:1 for 10,000 RPM Motor

4.2 EVALUATION CRITERIA

A principal emphasis of this project was to ascertain the realistic weight savings which could be anticipated with electromechanical technology. For that reason, all design options were compared primarily on the basis of their effect on motor weight.

However, from an overall vehicle perspective, the lightest actuator may not yield the lightest system. If a heavy battery was the power source, for example, the motor would be only a small percentage of system weight. It would thus be advantageous to emphasize efficiency in the motor design to lower battery weight. For this reason, motor efficiency was the second criteria used for evaluating design options.

The theme which pervaded the trades then was to strive for the lightest design which would satisfy a minimum efficiency. Having selected candidates on this basis, a final evaluation of weight vs. efficiency was made to ascertain if efficiency gains would warrant some weight growth. The project goal was to produce a motor no heavier than 34 pounds with a 90% minimum efficiency at the design operating point.

4.3 CONTROL CONSIDERATIONS

Although the primary emphasis of this project was development of a four channel motor, the interrelationship of the motor and its controller required that some control method be assumed. The following paragraphs describe the control strategy that was envisioned. Note that these assumptions relate to providing compact and efficient control of the actuation functions and do not address redundancy management. How faults are detected and controlled is the subject of futuer NASA-JSC activity.

Figure 4-6 is a block diagram of the actuation system. The controller converts the 270 volts dc to three-phase power suitable for driving the motor. It consists of an inverter and associated control electronics that process the commanded position, the rotor position, and the actuator position information to suitably switch the inverter.

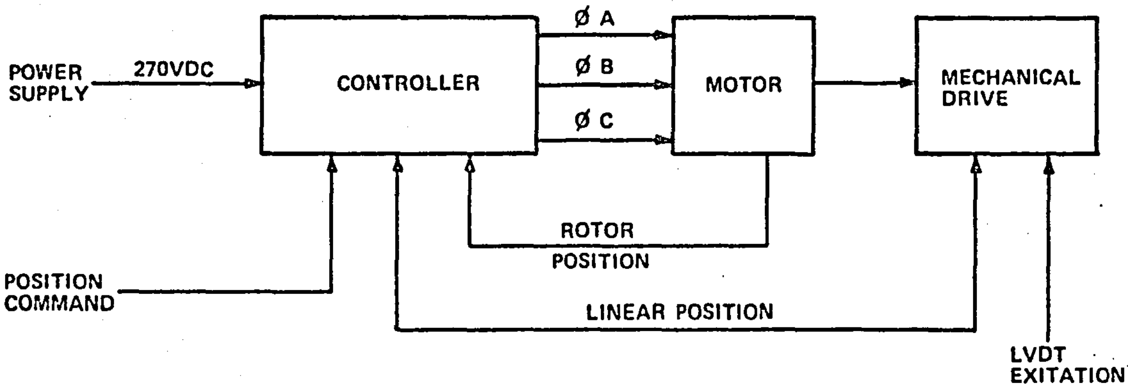

Figure 4-6 Actuation System Block Diagram (Single Channel)

A voltage source, six-step inverter was selected because it is smaller and lighter than a current source inverter and is more suitable for pulse width modulation (PWM) control.

As shown in Figure 4-3, the motor must produce constant horsepower from the maximum speed down to 43% of the maximum speed. This can be accomplished by holding the commutation angle constant. However, the motor power factor and current will vary as the speed varies.

To minimize controller current, it is desirable to have the same motor current at the extreme speeds. This can be achieved by designing the motor such as to have a leading power factor at the maximum speed and a lagging power factor of the same magnitude at the lowest speed. The power factor depends on the ratio of the speeds, the higher the speed range, the lower the power factor. At the intermediate speeds, the power factor is always greater than the value at the extreme speeds as is the motor current. The motor design was based on this concept and optimized for operation at the extreme speeds.

For output powers less that full output power at speeds down to 43% of the maximum speed, reducing the commutation angle will reduce the output power since the output power is proportional to the sine of the commutation angle. Below 43% of the maximum speed, the output power can be controlled by simultaneously varying the commutation angle and the input voltage. PWM is used to control the input voltage.

More detail on the assumed control scheme is found in Appendix B.

4.4 DESIGN PROCEDURE

Two Sundstrand developed computer programs were used to design the brushless dc motor options and calculate performance.

The first program calculates the motor flux densities, back EMF, winding resistance, winding inductance, and other basic motor parameters from the motor dimensions, number of turns, wire size, permanent magnet characteristics, etc.

The second program calculates the motor losses, torque, power factor, efficiency, current and the transistor currents. The inverter and motor are represented by an electrical network model and the motor performance is calculated by solving the network nonlinear differential equations.

4.5 SELECTION OF THE PREFERRED GEOMETRY

A variety of mechanical arrangements can be envisioned to provide a motor with four channel capability. For the purpose of this study, the six configurations shown in Figures 4-7 through 4-12 were selected as representative of the most likely approaches.

Single rotor concepts (Figure 4-7) are generally lighter and do not suffer from critical speed problems. Multirotor designs (Figure 4-8) offer better fault isolation and greater torque to inertia ratio but have more parts plus critical speed limitations. The concept in Figure 4-9 represents a combination of the single and multirotor approaches.

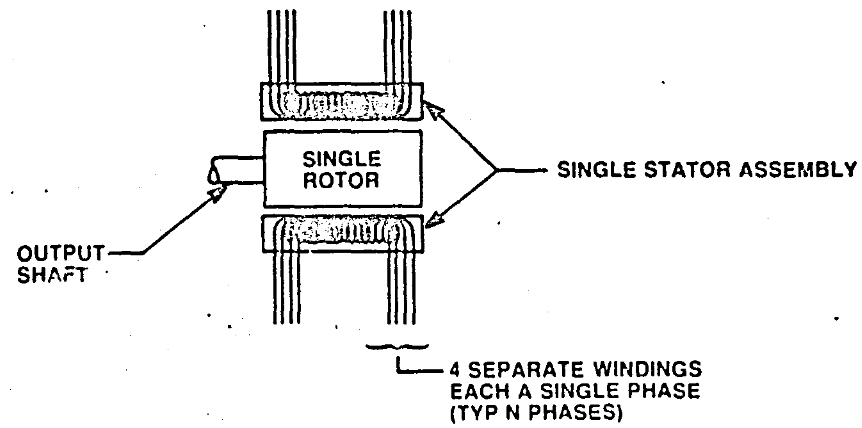

Figure 4-7 Four Channel Concept A

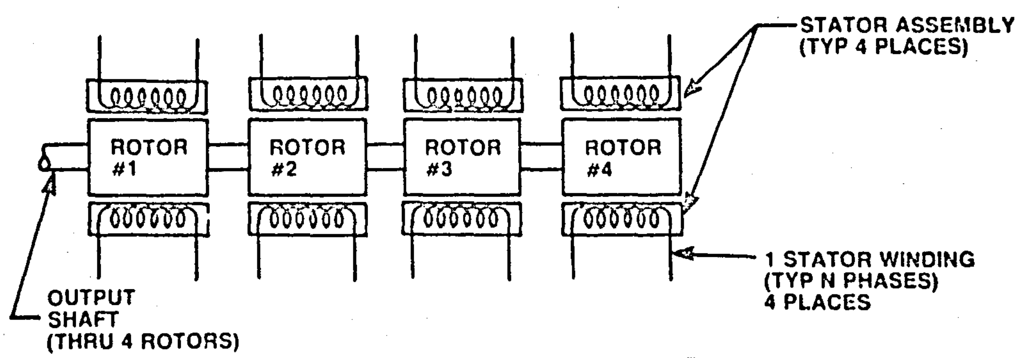

Figure 4-8 Four Channel Concept B

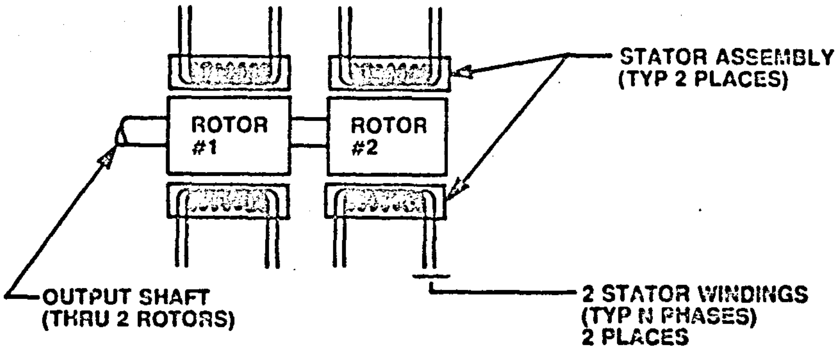

Figure 4-9 Four Channel Concept C

Multishaft approaches, shown in Figures 4-10 through 4-12, have the drawback of needing clutch mechanisms, but afford more straightforward methods of redundancy management.

In choosing among these options, mechanical and reliability criteria were applied. Mechanical considerations included qualitative assessment of complexity, volume, weight, and performance capability. Reliability considerations addressed the ability to provide two fault tolerant performance. This included an evaluation of the ability of each configuration to isolate faults and prevent subsequent propagation to secondary failures. The nature of likely failure modes and their implications to overall system architecture were also considered.

The above considerations indicated the single rotor configuration, Figure 4-7, offered the best design solution. As a further refinement, several stator options for this configuration were conceived. These included intertwining the windings of the individual channels, completely separating them, or partially overlapping them. The four quadrant geometry shown in Figure 4-13 was selected as offering the best isolation without affecting performance. Thus, the preferred concept is a single rotor geometry with a four quadrant stator.

As noted, dual fault tolerance requires two healthy channels to carry half the output load plus half any losses accruing to faults. Having selected a preferred geometry, it was then necessary to assess the probable failure modes, estimate the resulting additional losses, and thus establish the sizing criteria for the individual channels.

Mechanical failure modes are straightforwardly controlled with multipe rotating surfaces, dual retaining devices, generous structural margins of safety, etc. All probable modes entail very small additional losses.

Electrical failures can be generally grouped as open circuits or short circuits. As the scope of this project was directed to permanent magnet brushless dc motors, the presence of permanent magnets enables the motor to also perform as a generator. This fact causes short circuit failures, which present fault current paths, to produce considerable retarding torque. Compensating for two faults of this nature could result in an excessively large motor.

In evaluating this scenario, any failure or failure combination with a probability of 10^{-9}/flight or greater was deemed credible and, therefore, a design consideration. Any failure modes with smaller probabilities were judged noncredible.

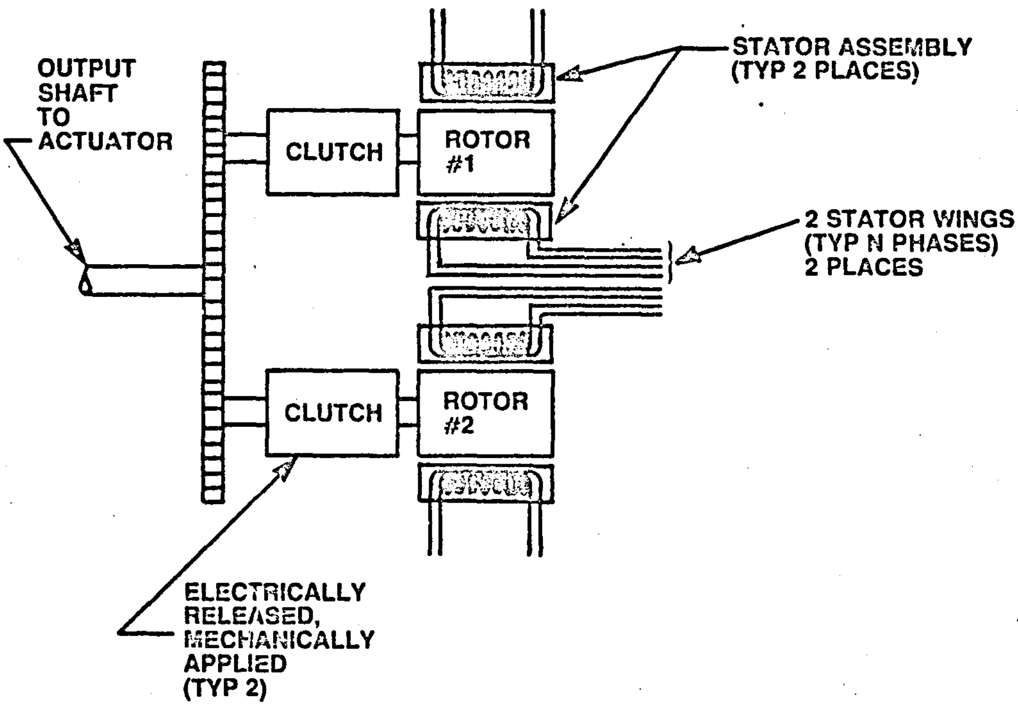

Figure 4-10 Four Channel Concept D

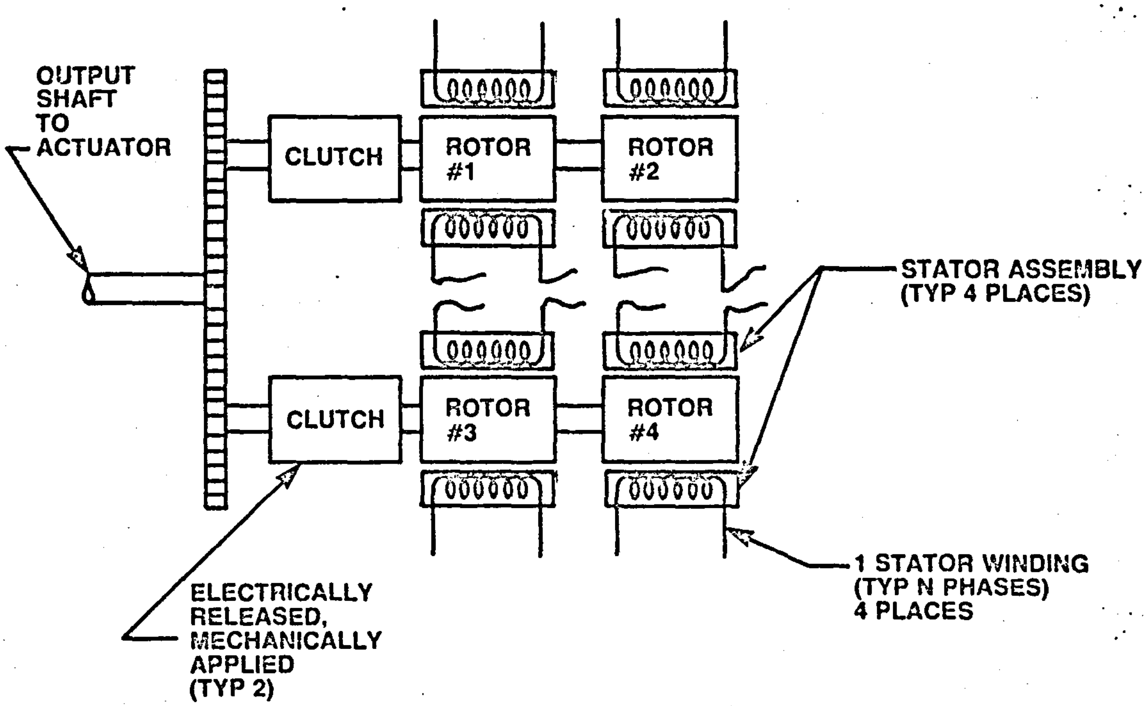

Figure 4-11 Four Channel Concept E

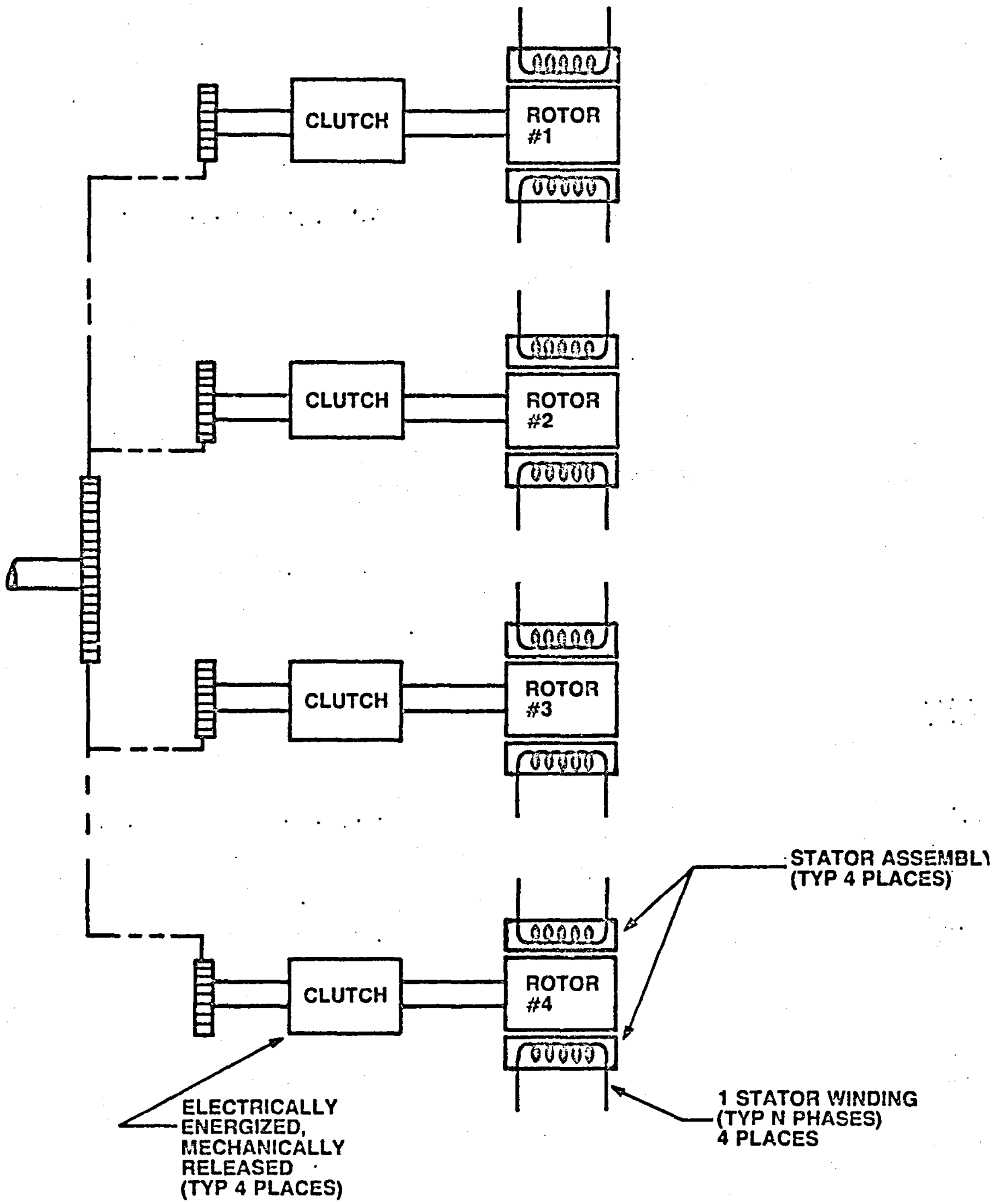

Figure 4-12 Four Channel Concept F

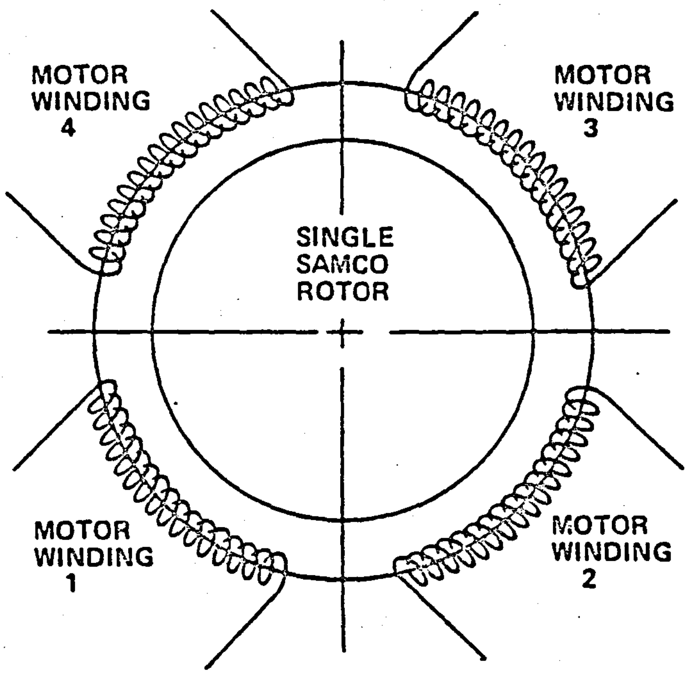

Figure 4-13 Selected Four Channel Geometry

Using MIL-HDBK-217D data plus historical information from similar Sundstrand products, a combination of one short circuit and one open circuit failure per flight was judged credible, but two short circuits were not. Allocating losses in fault down modes, therefore, sized the individual channels at approximately 10 hp apiece to insure 17.18 hp was always delivered.

4.6 POINT OF DEPARTURE DESIGN CONCEPT

As noted, the design concept selected was a single stator-single rotor design with the 4 stator windings wound in quadrants around the stator. Evaluation of different winding schemes showed that isolation of the 4 windings could be achieved with a consequent pole, full-pitch winding if the number of stator slots is an integral multiple of the number of poles times the number of phases. The total number of poles is 4 times the number of poles per quadrant. Therefore, the possibilities for the motor design are 8, 16, 24, etc. poles. Previous brushless dc motor design experience led to choosing 16 poles for the baseline motor. The minimum number of stator slots is 48 which was selected for the baseline motor. A wye connected winding was selected for the design. The winding design is shown in Figure 4-14.

Hiperco 50 was selected for the stator laminations because the high magnetic saturation results in minimum weight. The stator iron areas were sized to obtain flux densities of 130,000 and 140,000 lines/in^2 for the stator core and stator teeth, respectively.

The rotor configuration is shown in Figure 4-15. Samarium-cobalt with an energy product of 21 x 10^6 gauss-oersteds was chosen for the permanent magnets. The rotor design is based on tangentially oriented permanent magnets as shown.

The stator slot area was sized for a winding current density of 8,000 amperes/in^2.

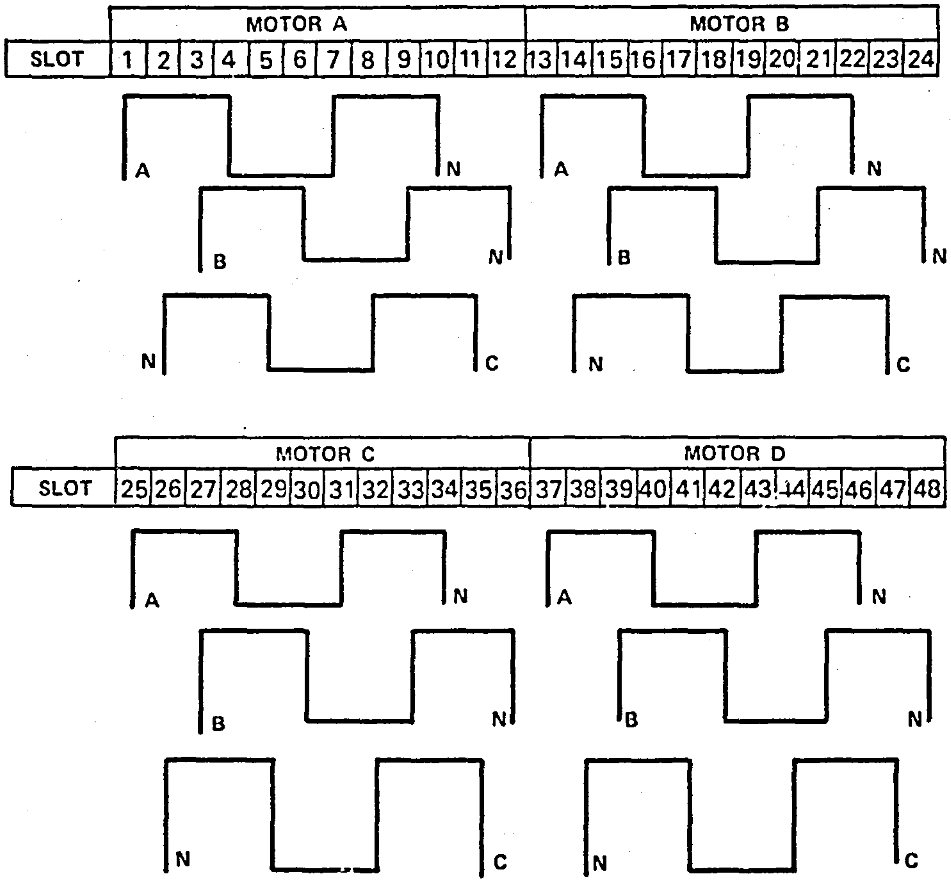

Figure 4-14 Quad Motor Winding Insertion - Connection Diagram

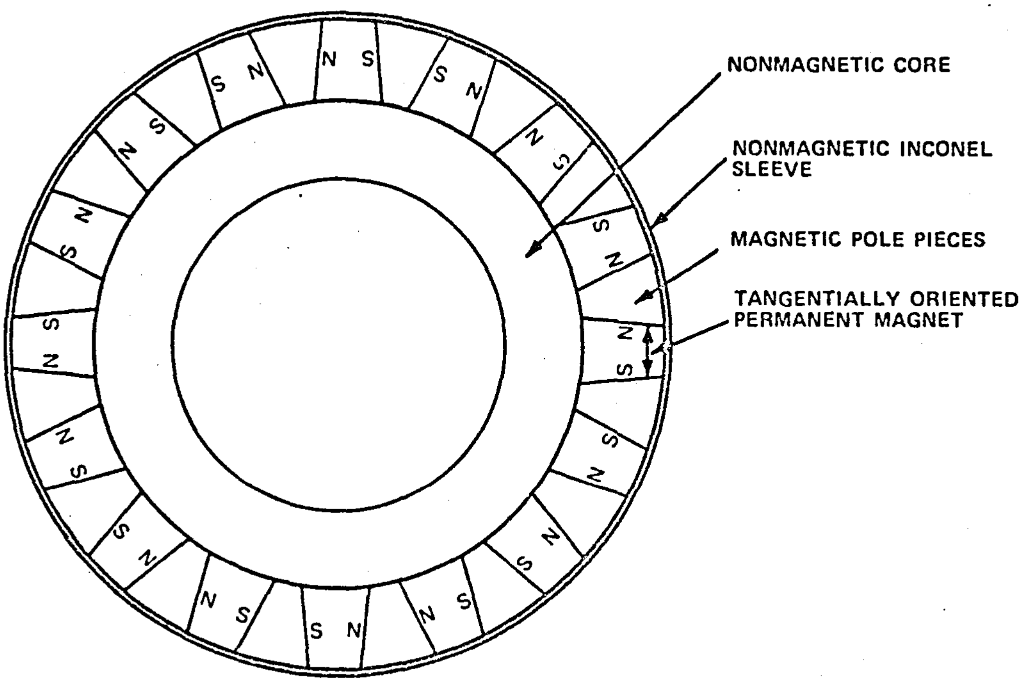

Figure 4-15 Baseline Motor Rotor Configuration

For the motor performance calculations, the stator copper was assumed to be at a temperature of 150°C and the rotor magnets at 160°C.

The calculated motor performance at the duty cycle load points is shown in Table 4-2. The total electromagnetic weight is 15.3 pounds, 10.2 pounds for the stator, and 5.1 pounds for the rotor.

Table 4-2 Baseline Motor Performance (Per Channel)

Load Point	Speed, RPM	Output, HP	Period, Minutes	Motor Losses, Watts	Inverter Duty Cycle, Per Unit	Inverter Commutation Angle, Degrees	Inverter PWM Frequency, Hertz	Inve. Input Current, DC Amps	Motor Phase Current, RMS Amps	Power Factor, Per Unit	Efficiency, Percent
1	0	0	9	15							0
2	1666	0.3	17.5	106	0.3	9.3	5330	3.8	4.1	0.22	64.1
3	1666	2.3	0.5	237	0.3	36.0	5330	10.2	21.6	0.45	88.6
4	4333	0.3	7.5	357	0.65	10.0	6930	5.2	6.7	0.33	46.3
5	4333	10.0	0.5	574	1.0	36.0	—	33.1	28.1	0.77	92.8
6	6666	0.3	3.5	627	1.0	3.9	—	5.9	6.4	0.35	26.5
7	6666	10.0	0.5	771	1.0	38.5	—	33.9	23.2	0.95	90.6
8	10000	0.3	1.5	1158	1.0	6.5	—	7.9	16.5	0.22	16.2
9	10000	10.0	0.5	1270	1.0	41.5	—	35.7	25.7	0.91	85.4

4.7 THERMAL ANALYSIS

A thermal analysis of the baseline motor design was performed for the duty cycle shown in Table 4-1. Two motors were assumed to be operating in a 200°F ambient and all of the dissipated energy was considered to be absorbed by the iron and copper.

The results of the thermal analysis are shown in Table 4-3. The maximum safe operating temperatures are 200°C for the magnets and 250°C for the stator copper. Since both the copper and the magnet temperatures exceeded these limits at the end of the fourth cycle, the thermal analysis was not carried any further.

Table 4-3 Baseline Motor Thermal Analysis

Load Point	Duration, Minutes	Maximum Temperature, °C — Copper Initial	Copper Final	Magnet Initial	Magnet Final
1	9.0	93.3	100.2	93.3	96.1
2	17.5	100.2	173.8	96.1	154.2
3	0.5	173.8	179.5	154.2	155.8
4	7.5	179.5	262.3	155.8	218.9

The thermal analysis assumed that all of the losses were absorbed by the motor mass. In reality, there will be heat transfer due to convection, conducction, and radiation. Also, the duty cycle needs validation. Since the primary objective of this study was to demonstrate a concept,

NASA-JSC and Sundstrand decided that thermal capability would not be a design criterion. The objective would be to design the lightest motor satisfying the performance requirements and to then define its thermal capability.

4.8 MOTOR SPEED TRADE STUDY

The speed trade study was performed for speeds of 6,000, 10,000, and 15,000 rpm. Six thousand and 15,000 rpm motors were designed and compared to the baseline 10,000 rpm motor. The 6,000 and 15,000 rpm motors were based on the same design constraints that were used for the baseline motor.

The motor performance at the rated load is shown in Tables 4-4 and 4-5 for the 6,000 and 15,000 rpm designs, respectively. Table 4-6 is a tabulation of the motor characteristics for all three motors.

The system inertia at the motor shaft for the three speeds was calculated and compared to the motor inertia to determine the influence on the dynamic response. The actuation system is shown in Figure 4-16. A ballscrew was chosen over a geared rotary actuator because it is more efficient and results in more efficient packaging for a flight control surface. The following assumptions were made for the analysis:

1. Actuator stroke: ±1.85 in.
2. Efficiencies
   a. Ballscrew: 92%
   b. Thrust bearing: 97%
   c. Gear: 99%
   d. Gearbox: 99% (98% for 15,000 rpm motor)

The motor and system inertias are tabulated in Table 4-7. Since the system inertia is small compared to the motor inertia, it can be neglected in a dynamic analysis.

The frequency response requirement for a command with an amplitude of ±2% of full stroke is shown in Figure 4-17. The system model that was used for the analysis is shown in Figure 4-18. The dynamic response for the three speeds is shown in Figure 4-19. The 6,000 and 10,000 rpm motors meet the frequency response requirements with a slower motor having the better frequency response. However, the system is a second order system and as such has a 40 db/decade fall-off whereas the specified response has a 20 db/decade fall-off. If the corner frequency were changed from 1.5 to 3 Hertz and the fall-off from 20 to 40 db/decade as shown in Figure 4-19, the 15,000 rpm motor would meet this requirement.

The trade study shows that the 15,000 rpm motor is the smallest and lightest. Being the smallest means it would have the highest temperature rise. The 6,000 rpm motor has the best frequency response and, since it is the heaviest, would have the lowest temperature rise. The 10,000 rpm motor was selected as the best compromise between size, thermal capability, and frequency response.

Table 4-4 6,000 RPM Motor Performance (Per Channel)

Load Point	Speed, RPM	Output, HP	Period, Minutes	Motor Losses, Watts	Inverter Duty Cycle, Per Unit	Inverter Commutation Angle, Degrees	Inverter PWM Frequency, Hertz	Inverter Input Current, DC Amps	Motor Phase Current, RMS Amps	Power Factor, Per Unit	Efficiency, Porcent
1	0	0	9	15							0
2	1000	0.3	17.5	91	0.33	8.0	3200	3.7	6.3	0.23	71.8
3	1000	2.3	0.5	240	0.33	34.0	3200	11.2	20.3	0.52	89.9
4	2600	0.3	7.5	278	0.69	8.0	4160	4.64	4.95	0.33	47.4
5	2600	10.0	0.5	578	1.0	35.3	—	33.3	27.8	0.77	92.9
6	4000	0.3	3.5	482	1.0	3.4	—	5.3	6.1	0.30	31.6
7	4000	10.0	0.5	676	1.0	38.0	—	33.4	22.8	0.95	91.7
8	6000	0.3	1.5	906	1.0	5.6	—	7.0	16.6	0.18	20.1
9	6000	10.0	0.5	1051	1.0	40.0	—	34.9	25.4	0.90	87.6

Table 4-5 15,000 RPM Motor Performance (Per Channel)

Load Point	Speed, RPM	Output, HP	Period, Minutes	Motor Losses, Watts	Inverter Duty Cycle, Per Unit	Inverter Commutation Angle, Degrees	Inverter PWM Frequency, Hertz	Inverter Input Current, DC Amps	Motor Phase Current, RMS Amps	Power Factor, Per Unit	Efficiency, Percent
1	0	0	9	15							0
2	2500	0.3	17.5	94	0.3	9.4	8000	3.87	4.5	0.34	70.4
3	2500	2.3	0.5	165	0.3	31.8	8000	9.8	17.8	0.51	91.2
4	6500	0.3	7.5	359	0.65	8.9	10400	4.7	6.7	0.26	33.0
5	6500	10.0	0.5	557	1.0	34.5	—	33.6	28.7	0.76	93.2
6	10,000	0.3	3.5	657	1.0	3.75	—	5.9	6.6	0.35	24.3
7	10,000	10.0	0.5	774	1.0	36.1	—	33.7	23.0	0.95	90.6
8	15,000	0.3	1.5	1234	1.0	6.5	—	8.22	17.4	0.22	16.5
9	15,000	10.0	0.5	1333	1.0	39.0	—	37.0	26.7	0.90	85.3

Table 4-6 Motor Speed Trade Study Summary

	6000 RPM Motor	10,000 RPM Motor	15,000 RPM Motor
Overall Diameter, Inches	5.83	5.42	5.26
Overall Length, Inches	5.08	4.44	4.21
Electromagnetic Weight, Pounds	23.3	15.3	13.4
Inductance, Microhenries	1176	694	441
Maximum Phase Current, RMS Amperes	27.8	28.1	28.7
Energy Loss Over Duty Cycle, Watt-Hours	135.5	167.1	167.3

Table 4-7 Actuation System Parameters

Motor Speed, RPM	Gearbox Ratio	Overall Ratio	Motor Inertia, Lb. In. Sec.^{2}	System Inertia at Motor, Lb. In. Sec.^{2}	Percentage of Motor Inertia
6,000	2.11:1	1200:1	4×10^{-2}	7.5×10^{-4}	1.9
10,000	3.52:1	2000:1	2.31×10^{-2}	2.6×10^{-4}	1.1
15,000	5.28:1	3000:1	2.01×10^{-2}	3.41×10^{-4}	1.7

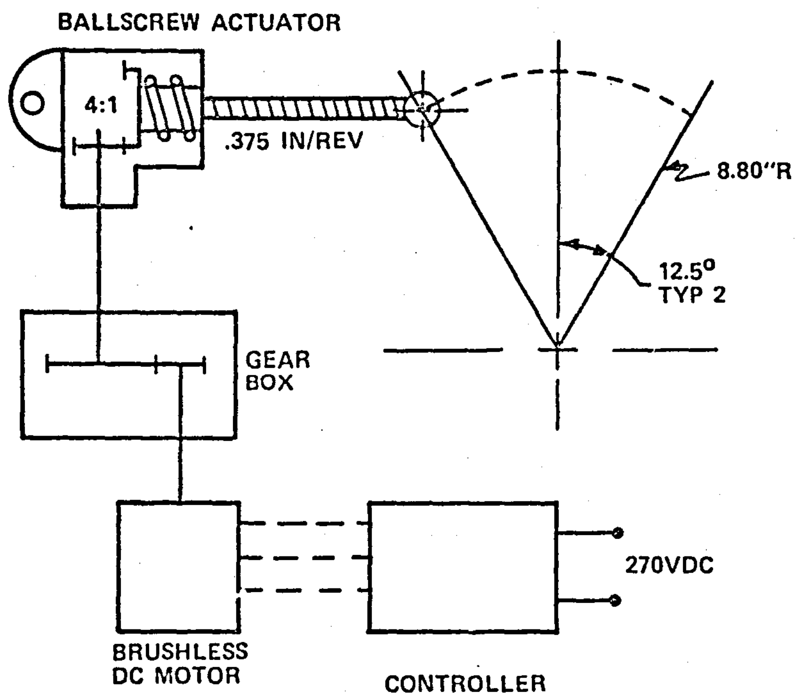

Figure 4-16 System Schematic

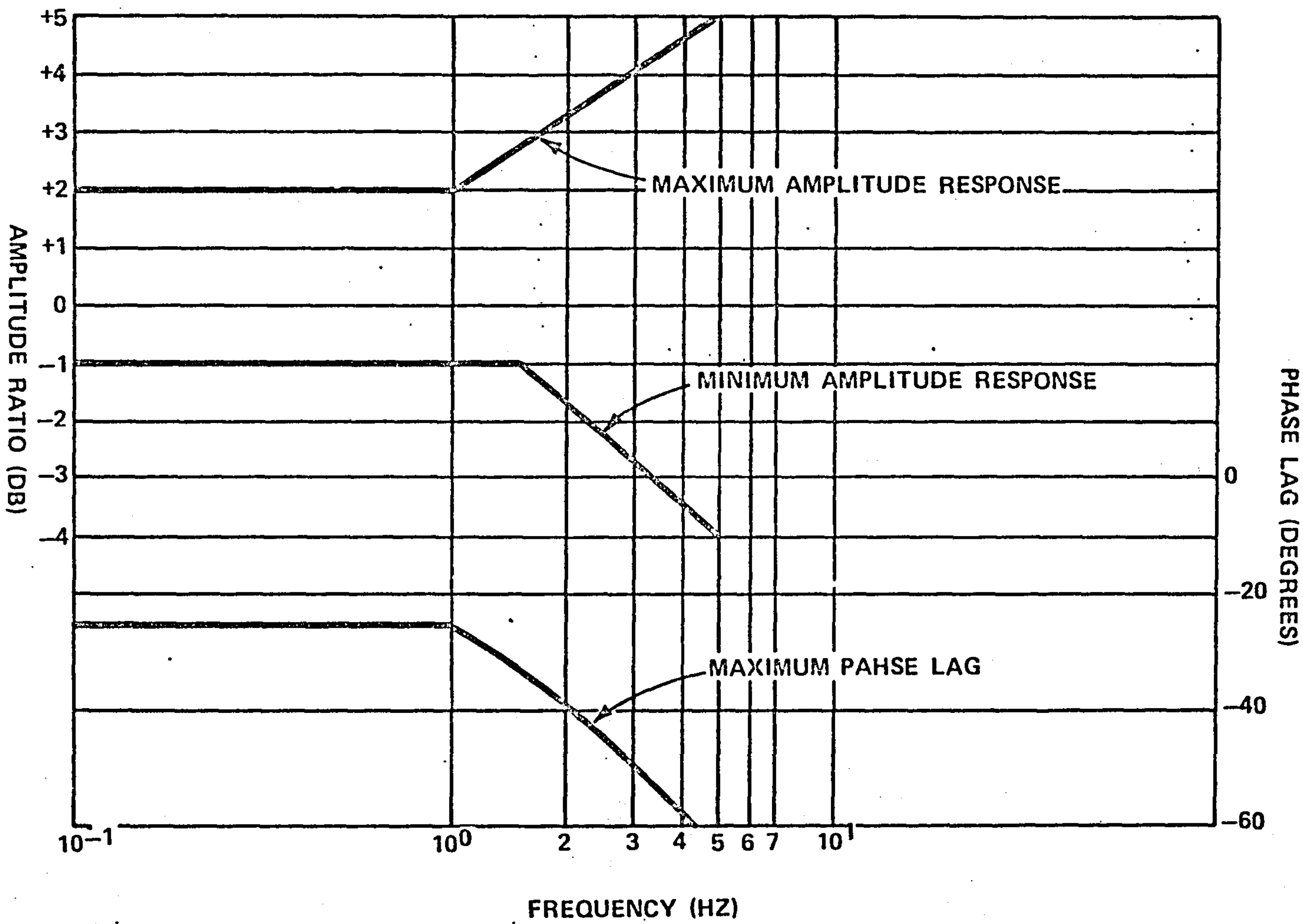

Figure 4-17 Frequency Response Requirements

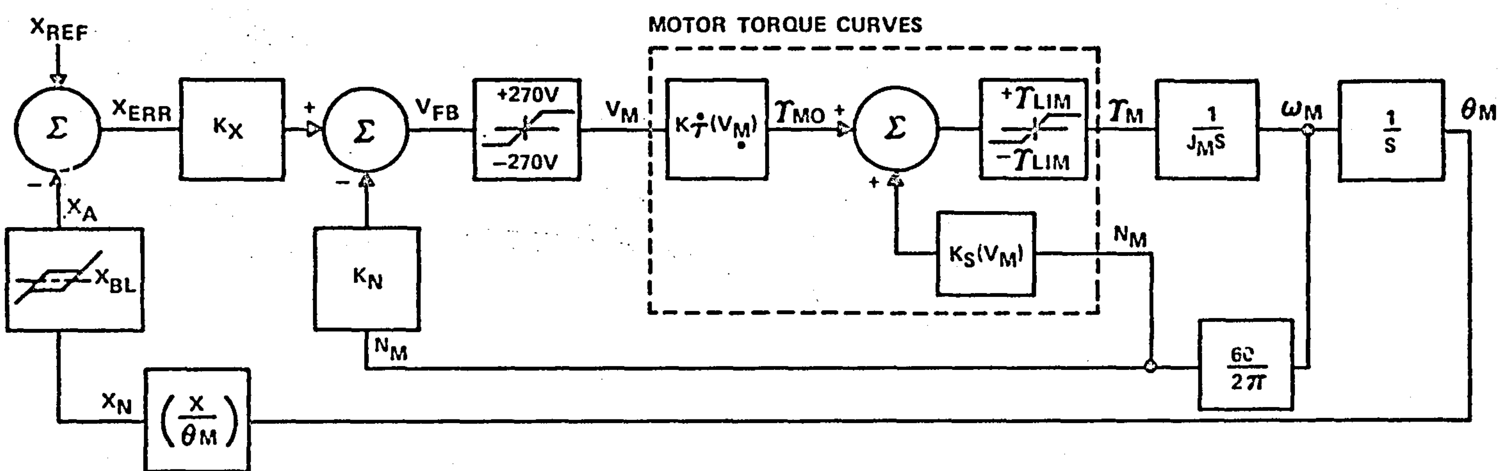

K_X = POSITION FEEDBACK GAIN
K_N = VELOCITY FEEDBACK GAIN
X_{BL} = BACKLASH REFLECTED TO BALL SCREW
τ_{LIM} = ACTUATOR TORQUE LIMIT REFLECTED TO MOTOR

$K_S(V_M) = \dfrac{\Delta \tau_M}{\Delta N_M}$ FOR GIVEN V_M
J_M = MOMENT OF INERTIA OF ROTOR AND GEARS REFLECTED TO MOTOR
$K_\tau(V_M) = \tau_M(N_M{=}0)$ FOR GIVEN V_M
$\left(\dfrac{X}{\theta_M}\right)$ = ACTUATOR RADIUS/OVERALL GEAR RATIO

Figure 4-18 Model for Dynamic Analysis

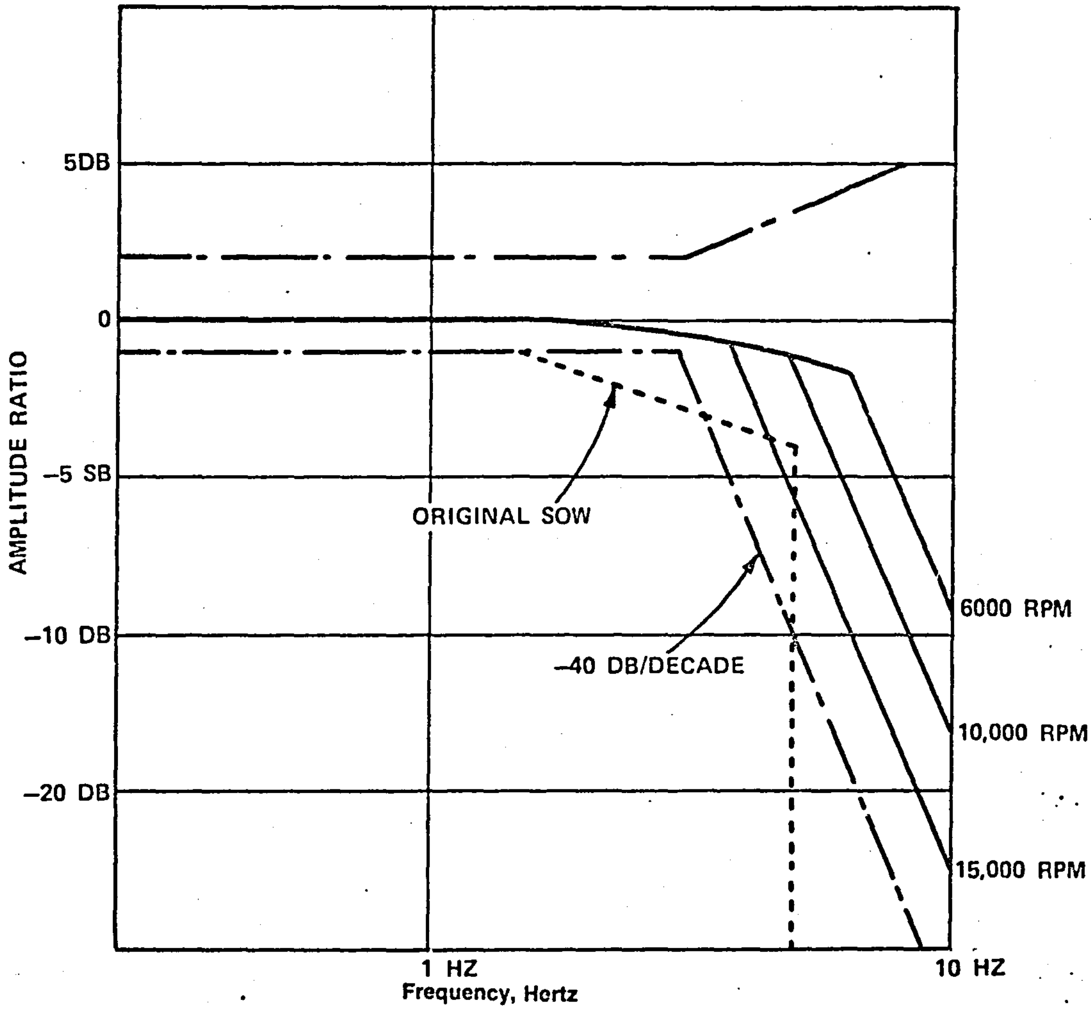

Figure 4-19 Frequency Response

4.9 ROTOR CONFIGURATION TRADE STUDY

The baseline motor design had a rotor with tangentially oriented permanent magnets as shown in Figure 4-15. This design was compared to one employing a rotor with radially oriented permanents as shown in Figure 4-20. This alternate version was executed using the same design constraints that were employed for the baseline motor design. The stator iron densities were kept at the same values and the same wire size was used so as to achieve the same current density. The permanent magnet material (21 x 10^6 gauss-oersteds energy product) was the same as was used for the baseline motor design.

The comparative performance of the two designs is shown in Table 4-8.

Since the tangential design is smaller, lighter, and more efficient, it was chosen over the radial design.

Table 4-8 Radial vs. Tangential Performance

	Radial Design	Tangential Design
Motor Speed, RPM	10,000	10,000
Output HP (Per Channel)	10	10
Efficiency, %	83.9	85.4
Overall Diameter, Inches	5.70	5.42
Overall Length, Inches	6.70	4.44
Electromagnetic Weight, Pounds	20.8	15.3

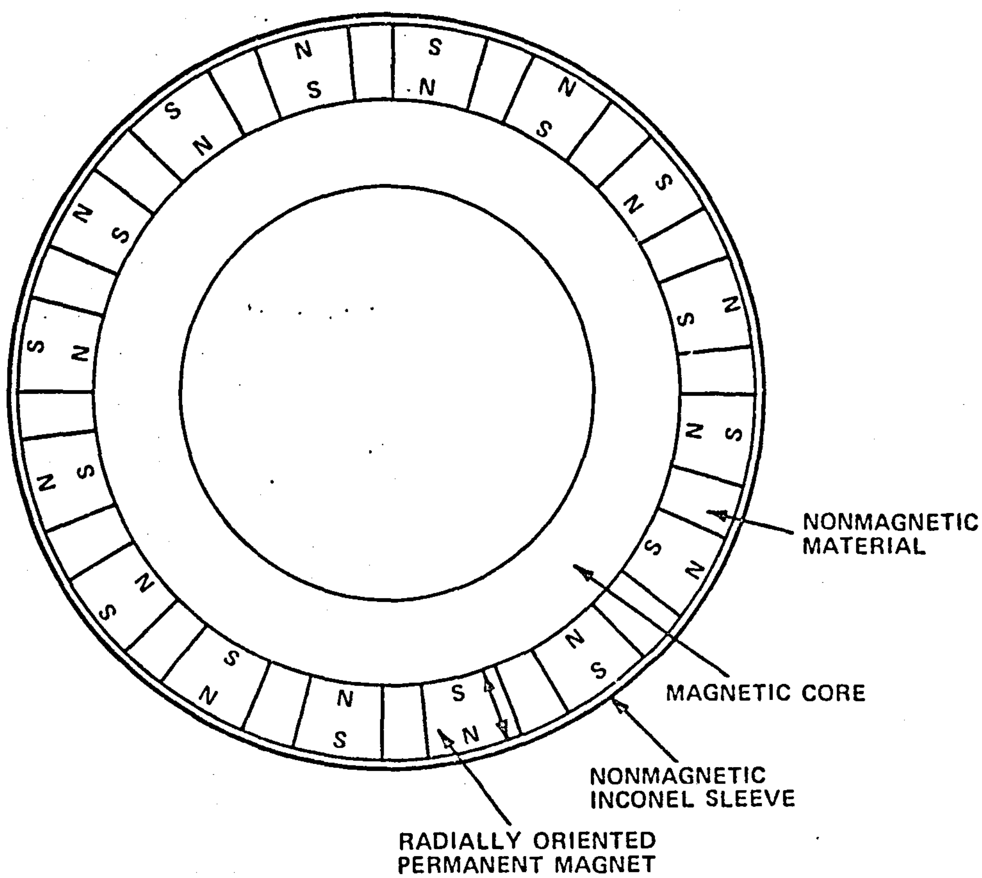

Figure 4-20 Rotor Design With Radially Oriented Permanent Magnets

4.10 WYE VS. DELTA WINDING TRADE STUDY

A motor with a delta connected winding was designed using the same design constraints and assumptions that were used for the baseline motor design.

The motor performance and electromagnetic weights for the two windings are compared in Table 4-9. The motor performance at the duty cycle load points for the delta winding is tabulated in Table 4-10.

Table 4-9 Wyo vs. Dclta Winding

	Wye Winding	Delta Winding
Motor Speed, RPM	10,000	10,000
Output HP	10	10
Efficiency, %	85.4	85.0
Energy Loss During Duty Cycle, Watt-Hours	167.1	175.4
Electromagnetic Weight, Pounds	15.3	15.6

Table 4-10 Pcrformancc of 10,000 RPM Delta Wcund Motor (Per Channcl)

Load Point	Speed, RPM	Output, HP	Period, Minutes	Motor Losses, Watts	Inverter Duty Cycle, Per Unit	Inverter Commutation Angle, Degrees	Inverter PWM Frequency, Hertz	Inverter Input Current, DC Amps	Motor Phase Current, RMS Amps	Power Factor, Per Unit	Efficiency, Percent
1	0		9	15							0
2	1666	0.3	17.5	113	0.3	6.5	5330	7.8	4.3	0.3	53.6
3	1666	2.3	0.5	223	0.3	3.6	5330	10.9	12.0	0.51	89.7
4	4333	0.3	7.5	385	0.65	12.9	6930	5.9	7.54	0.17	34.4
5	4333	10.0	0.5	582	1.0	30.5	—	33.4	16.5	0.76	92.8
6	6666	0.3	3.5	648	1.0	3.9	—	6.0	3.8	0.36	28.2
7	6666	10.0	0.5	802	1.0	37.1	—	34.1	14.1	0.90	89.9
8	10,000	0.3	1.5	1201	1.0	6.5	—	8.1	10.1	0.21	16.1
9	10,000	10.0	0.5	1306	1.0	39.5	—	35.9	15.1	0.90	85.0

Size and weight of the two motors are almost identical with the delta winding motor being slightly heavier and larger.

For the delta winding, there are circulating currents for the 3rd harmonic and multiples of the 3rd harmonic. The wye winding doesn't have these circulating currents which add to the copper losses without producing torque.

With the delta winding, if one of the phases opens, the motor will continue to operate and provide approximately two-thirds torque. With the wye winding, an open circuit will result in the motor single-phasing with greatly reduced output. In either case, however, if a failure occurs the input power will most likely be disconnected.

In the event of a short circuit fault in one of the windings, it is hard to say which winding pattern would have the greatest effect on the controller. Further study would be required to answer this question.

The wye winding was selected as the optimum winding because it is smaller, more efficient, and winding faults are more readily detectable.

4.11 NUMBER OF POLES TRADE STUDY

The total number of poles is four times the number of poles for each motor winding or quadrant and since each winding must have an even number of poles, the possibilities are 8, 16, 24, etc. poles. Eight, sixteen, and twenty-four poles were chosen for the trade study.

The baseline motor design is sixteen poles. Eight and twenty-four pole motor designs were completed for comparison to the baseline motor design. The same design criteria and assumptions were used for all the motor designs. Current density and the stator flux densities were maintained at the same levels. The number of stator slots was kept at one per pole per phase.

The motor performance at 4,333 and 10,000 rpm is shown in Table 4-11 along with the weights.

Table 4-11 Motor Performance vs. Number of Poles

	8 Pole Motor	16 Pole Motor	24 Pole Motor
Efficiency at 10 HP and 4333 RPM	93.6	92.8	91.5
Efficiency at 10 HP and 10,000 RPM	90.0	85.4	82.0
Total Electromagnetic Weight, Pounds	22.2	15.3	18.0

The 16-pole motor is the lightest. It is 7 pounds lighter than the 8-pole motor and 2.8 pounds lighter than the 24-pole motor. The 8-pole motor is the most efficient.

Since the 16-pole motor was the smallest and the lightest, it was selected as the best choice because it also had good efficiency.

4.12 PERMANENT MAGNET MATERIAL TRADE STUDY

Samarium-cobalt permanent magnets are available with energy products up to 30 x 10^6 gauss-oersteds. The desirable characteristics for the permanent magnet material are: high energy product, high coercive force, capable of 200°C operation, good temperature stability, ability to withstand physical shock, and availability. Since these requirements are best met by samarium-cobalt permanent magnets, other materials were not considered.

Table 4-12 lists the characteristics for samarium-cobalt premanent magnets with energy products ranging from 21 to 30 x 10^6 gauss-oersteds. The 21 and 24 x 10^6 gauss-oresteds permanent magnets have straight line demagnetization curves as illustrated in Figure 4-21. The 26 and 30 x 10^6 gauss-oersteds materials do not have straight line demagnetization curves and can demagnetize due to armature reaction depending on the operating point.

Table 4-12 Samarium-Cobalt Permanent Magnet Characteristics

Energy Product, Gauss-Oersteds	21 x 10^6	24 x 10^6	26 x 10^6	30 x 10^6
Density, Pounds/In.^{3}	0.295	0.295	0.295	0.295
Br, Residual Flux Density, Gauss	9300	9500	9500	11,200
Coercive Force, Oersteds	8860	9200	10,000	6300
Reversible Temperature Coefficient, %/°C	0.04	0.04	0.05	0.05
Relative Cost	1.0	1.5	2.0	—
Maximum Useable Temperature, °C	220	220	200	150

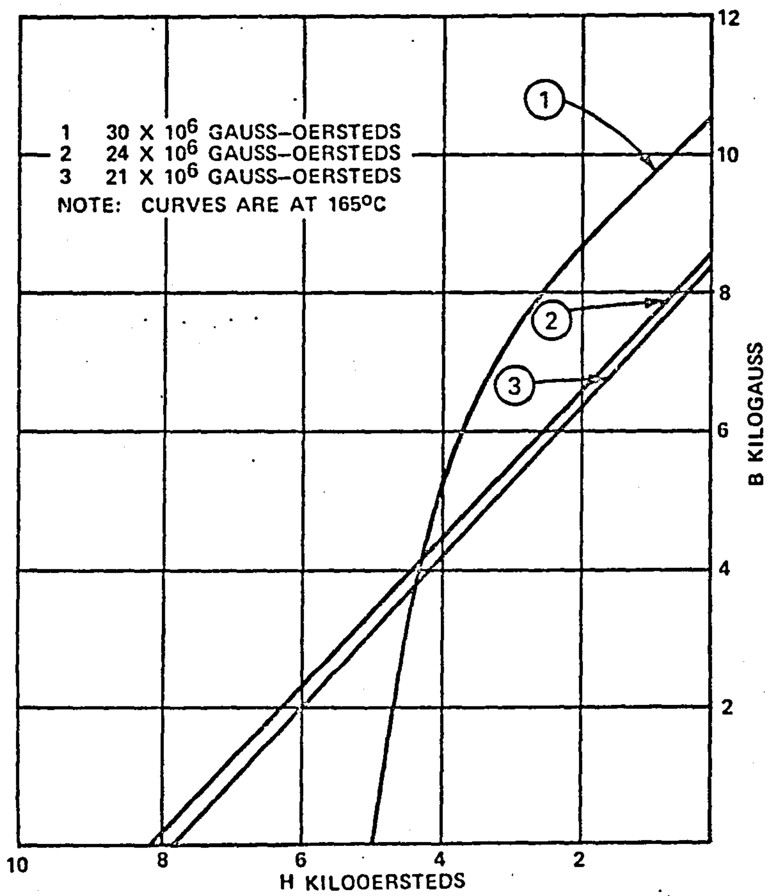

Figure 4-21 Samarium-Cobalt Demagnetization Curves

Because of the straight line demagnetization curve, operating temperature range, and availability, the 21 and 24 x 10^6 gauss-oresteds materials were chosen to be evaluated for the trade study.

The baseline motor design has 21 x 10^6 gauss-oresteds permanent magnets. A motor using 24 x 10^6 gauss-oresteds permanent magnets was designed using the same design criteria and assumptions. The 24 x 10^6 gauss-oresteds motor performance at the duty cycle load points is shown in Table 4-13. Table 4-14 compares the motor performance for two magnet materials. The 24 x 10^6 gauss-oresteds permanent magnet material was chosen for the final motor design because it results in a motor that is 0.8 pounds lighter and reduces the energy consumption over the duty cycle by 15.7 watt-hours.

Table 4-13 Motor Performance 24 x 10^6 Gauss-Oersteds Permanent Magnets (Per Channel)

					Inverter						
Load Point	Speed, RPM	Output, HP	Period, Minutes	Motor Losses, Watts	Duty Cycle, Per Unit	Commutation Angle, Degrees	PWM Frequency, Hertz	Inverter Input Current, DC Amps	Motor Phase Current, RMS Amps	Power Factor, Per Unit	Efficiency, Percent
1	0	0	9	15							0
2	1666	0.3	17.5	99	0.3	9.7	5330	3.9	4.3	0.36	69.7
3	1666	2.3	0.5	191	0.3	33.0	5330	11.3	18.0	0.51	89.9
4	4333	0.3	7.5	324	0.65	9.2	6930	4.7	6.4	0.27	40.3
5	4333	10.0	0.5	546	1.0	35.9	—	32.9	27.9	0.76	93.2
6	6666	0.3	3.5	559	1.0	3.7	—	5.6	6.2	0.33	28.7
7	6666	10.0	0.5	704	1.0	38.0	—	33.5	22.9	0.95	91.9
8	10,000	0.3	1.5	1027	1.0	5.9	—	7.4	16.5	0.20	17.9
9	10,000	10.0	0.5	1139	1.0	40.8	—	35.3	25.4	0.91	86.8

Table 4-14 Permanent Magnet Trade Study Performance Summary

Permanent Magnet Energy Product, Gauss-Oersteds	21 x 10^6	24 x 10^6
Motor Speed, RPM	10,000	10,000
Output Horsepower Per Channel	10	10
Efficiency, %	85.4	86.8
Energy Loss During Duty Cycle, Watt-Hours	167.1	151.4
Overall Diameter, Inches	5.42	5.335
Overall Length, Inches	4.4	4.555
Electromagnetic Weight, Pounds	15.3	14.5

4.13 MOTOR EFFICIENCY VS. WEIGHT

As a final evaluation, the effect of motor weight on efficiency was examined. This was essentially a comparison of the merits of alternate stator lamination materials.

Three materials were considered for the stator laminations:

1. Hiperco 50
2. Magnesil
3. Metallic glass

Typical mechanical and magnetic properties for these materials are tabulated in Table 4-15.

Table 4-15 Properties of Lamination Materials

Material	Thermal Conductivity, cal/cm³/sec/°C	Electrical Resistivity, ohm-cm.	Saturation Induction, Gausses	Core Loss at 400 Hertz, watts/pound	Tensile Strength, PSI	Density, pounds/in.³	Modules of Elasticity, PSI
Hiperco 50	0.131	45.7×10^{-6}	24,000	7.5	43,300	0.296	34.7×10^{6}
Metallic Glass		130×10^{-6}	17,500	3.1	250,000	0.27	
Magnesil	0.043		20,000	3.5	51,900	0.276	16.3×10^{6}

Hiperco 50 is an iron-cobalt-vanadium alloy with 20% higher magnetic saturation than silicon-iron alloys. It is expensive and difficult to work, but the demand for minimum weight systems has resulted in its use for stators and rotors of high energy density machines.

Magnesil is a silicon-iron alloy designed for applications of 400 Hertz or higher. It is available in thicknesses of 0.005 and 0.007 inches. It has good permeability in all directions of the rolling plane and is designed for laminations with random flux direction. It has a thin, uniform inorganic coating that provides a high degree of electrical insulation and the ability to withstand stress-relief annealing temperatures.

Metallic glass is produced by very rapid quenching in which a molten metal alloy is rapidly cooled through temperatures at which crystallization usually occurs. The result is an alloy that is very hard but very soft magnetically, It has a high resistivity which results in a low eddy current loss. Because of its hardness, it is extremely difficult to punch. Thickness is 0.001 to 0.0025 inches and width is up to 4 inches. Greater widths are expected to be available in the future.

Metallic glass was discarded because of fabrication difficulties and lack of availability in the desired width. Since Hiperco 50 results in the lightest weight design, the baseline motor design used Hiperco 50. Hiperco 50 and Magnesil were compared by carrying out a motor design with Magnesil stator laminations. The same design criteria and assumptions were used as for the Hiperco 50 motor except that permanent magnets with an energy product of 24×10^6 gauss-oersteds were used. Therefore, the Magnesil motor design was compared to the Hiperco 50 motor design with 24×10^6 gauss-oersteds magnets. The electromagnetic weights and efficiencies at 4,333 and 10,000 rpm are compared for the two designs in Table 4-16.

Although Magnesil results in a more efficient motor due to the decreased core loss, the Hiperco 50 motor was selected because it is 5.7 pounds lighter.

Table 4-16 Stator Lamination Trade Study Results

	Hiperco 50 Stator Laminations	Magnesil Stator Laminations
Efficiency at 10 HP and 4333 RPM	93.2	94.1
Efficiency at 10 HP and 10,000 RPM	86.8	90.6
Stator Electromagnetic Weight, Pounds	10.0	14.3
Rotor Electromagnetic Weight, Pounds	4.5	5 9
Total Electromagnetic Weight, Pounds	14.5	20.2

4.14 FINAL MOTOR DESIGN CONCEPT

The trade study resulted in the following motor design configuration:

1. 10,000 rpm speed
2. 16 poles
3. Rotor with tangentially oriented permanent magnets
4. Wye connected winding
5. 24 x 10^6 gauss-oresteds permanent magnets
6. Hiperco 50 stator laminations

However, it was decided to reduce the flux density in the stator iron to allow for the increase in flux density due to armature reaction. The motor was redesigned to reduce the flux density to 127,000 lines/in^2 from 140,000 lines/in^2 in the teeth and 130,000 lines/in^2 in the core.

The performance at the duty cycle load points is shown in Table 4-17. The dimensions and weights are shown in Table 4-18. Performance is essentially the same as the higher flux density motor except for a 1.7 pound weight increase.

The final step in the motor design was to select the electrical insulation materials. The insulating materials in the motor are:

1. Magnet wire insulation
2. Phase and ground insulation
3. Varnish

In all cases, the goal was to use materials with as high a temperature rating as possible.

Table 4-17 Final Motor Design Performance (Per Channel)

Load Point	Speed, RPM	Output, HP	Period, Minutes	Motor Losses, Watts	Inverter: Duty Cycle, Per Unit	Inverter: Commutation Angle, Degrees	Inverter: PWM Frequency, Hertz	Inverter Input Current, DC Amps	Motor Phase Current, RMS Amps	Power Factor, Per Unit	Efficiency Percent
1	0	0	9	15							0
2	1666	0.3	17.5	100	0.3	9.7	5330	3.9	4.3	0.36	69.4
3	1666	2.3	0.5	204	0.3	33.5	5330	10.0	18.4	0.51	89.5
4	4333	0.3	7.5	328	0.65	9.3	6930	4.7	6.6	0.27	40.2
5	4333	10.0	0.5	567	1.0	35.7	—	33.0	27.9	0.77	92.9
6	6666	0.3	3.5	565	1.0	3.7	—	5.6	6.3	0.33	28.3
7	6666	10.0	0.5	723	1.0	37.9	—	33.6	23.0	0.95	91.2
8	10,000	0.3	1.5	1042	1.0	6.0	—	7.4	16.6	0.20	17.6
9	10,000	10.0	0.5	1163	1.0	40.6	—	35.3	25.5	0.90	86.5

Table 4-18 Dimensions and Weights — Final Motor Design

Overall Diameter, Inches	5.025
Overall Length, Inches	5.58
Stator Electromagnetic Weight, Pounds	11.2
Rotor Electromagetic Weight, Pounds	5.0
Total Electromagnetic Weight, Pounds	16.2

Magnet wire with polyimide insulation was chosen because it yields 10,000 hours life at 260°C and it is used almost exclusively at Sundstrand for motors and generators.

A nomex-kapton laminate was chosen for the slot insulators and kapton for the phase insulation. Both materials are Class H as is the magnet wire insulation and are compatible with the varnish.

A polyimide varnish was chosen to impregnate the stator based on material compatibility and manufacturing experience at Sundstrand.

5.0 MOTOR FABRICATION

5.0 MOTOR FABRICATION

With the final concept established as described in Section 4.0, a detailed design was executed. A cross section is shown in Figure 5-1. Modifications that were made as the result of manufacturing or testing information are described in this section.

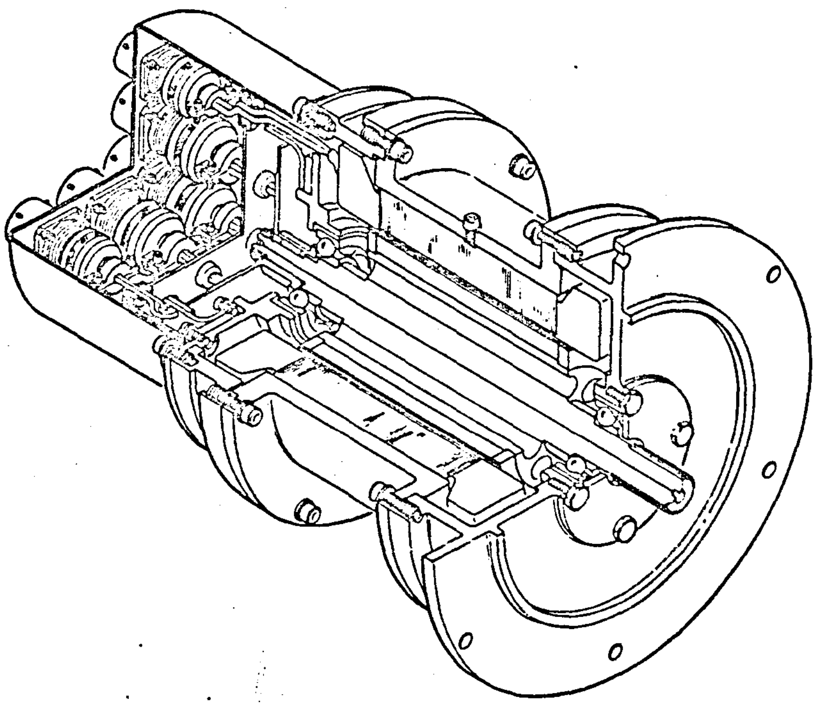

Figure 5-1 Four Channel Motor

5.1 STATOR INSEPARABLE ASSEMBLY (EP 2758-94)

A consequent-pole winding pattern was chosen to provide total winding isolation between adjacent channels, Figure 5-2. Implementation of this scheme caused modifications to the initial motor housing design and slot cell insulation system as described below.

LAP WINDING

CONSEQUENT POLE

• ARROW SHOWS REQUIRED PATH OF ADJACENT COIL

Figure 5-2 Winding Patterns

The initial design approach was to supply a stator core that could be wound, impregnated, and inserted into a one-piece housing. This technique results in a lighter housing than one which utilizes end bells, Figure 5-3.

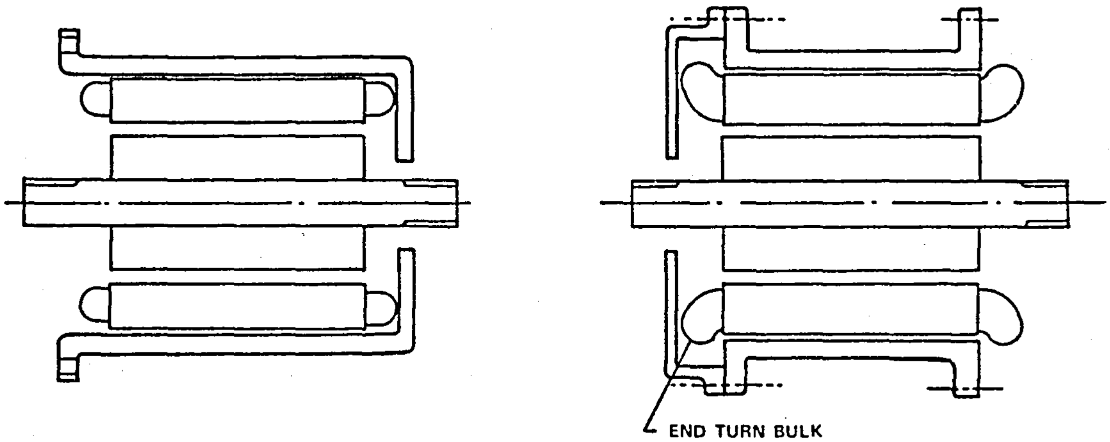

Figure 5-3 Housing Configurations

Several factors, however, prevented implementation of this approach when using the consequent-pole winding. A feature of this pattern is that beginning and ending coil sides do not share slots with adjacent windings. This yields bulky end turn extensions. These extensions must be long enough to allow all coils located within a span to be inserted into their respective slots and enter their return path slots in the outside of the span. In addition, room must be provided for nesting of cross-over coils from adjacent spans.

This end turn bulk is discernible in Figure 5-4. The consequent pole end turn bulk places 50% more copper area in the phase cross-over point than would be found in a lap style winding. As a result of this bulk, the windings flair out over the stator core O.D. Though the bulk can be minimized by adjusting coil lengths, it can't be eliminated.

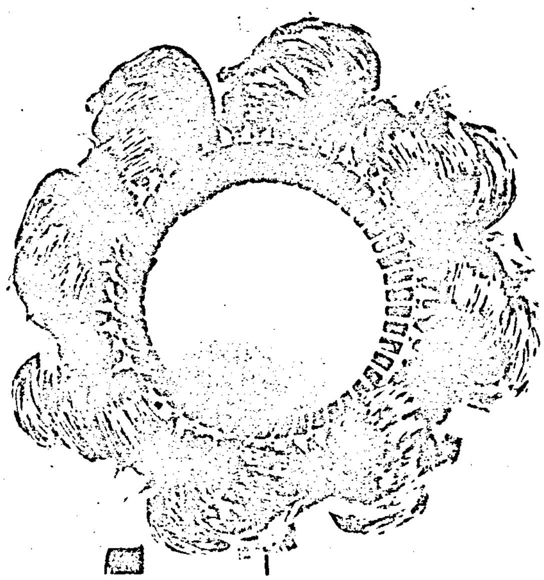

ORIGINAL PAGE
BLACK AND WHITE PHOTOGRAPH

Figure 5-4 End Turn Bulk

ORIGINAL PAGE
BLACK AND WHITE PHOTOGRAPH

Attempts were made to form the coils by hand as they were inserted into the slots. This provided clearance for the inner coils allowing them to be more easily inserted. However, the pressure produced by this technique created cracks in the slot insulation. Some cracks propagated towards the nomex stator end lamination. This can be seen in Figure 5-5.

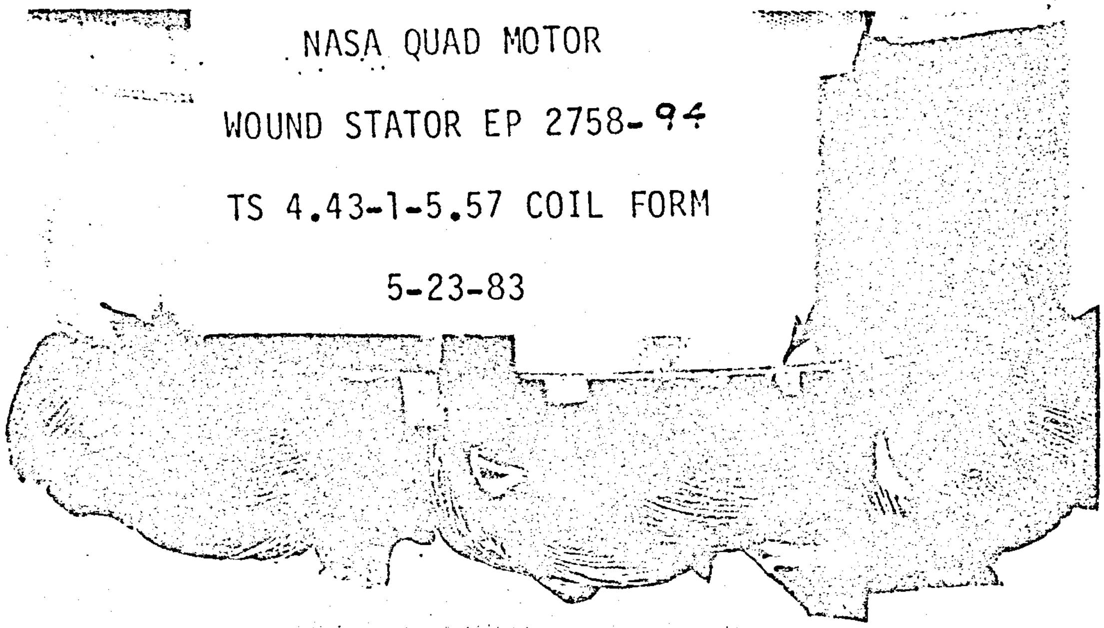

Figure 5-5 Slot Insulation Cracks

An additional result of this coil forming and insertion process was the distortion of the stator core slots. As coils were inserted, stator teeth would deflect, closing down adjacent vacant slots. This made insertion of subsequent coils increasingly difficult.

After reviewing these problems, steps were taken to eliminate their cause or minimize their effect. First, the housing was redesigned to allow the stator core to be wound and impregnated while installed in the housing. This constraint eliminated stator distortion during coil insertion thus allowing the stator slots to maintain their punched dimensions.

Redesign of the housing also entailed implementing an end bell configuration, allowing ample room for the end turns. This minimized the need to hand form the coils during insertion. In turn, minimum pressure was then transmitted to the bottom of the slot insulation.

In conjunction with this, the single layer slot insulation was replaced with two layers of thinner nomex-kapton sandwich. Though the resultant thickness was the same, a greater anti-tear quality was obtained.

Wire gauge was also reduced by paralleling two smaller wires of an area equivalent to the original design. This change facilitated winding insertion without damage to the wire insulation.

The new housing design resulted in a 3.9 pound increase in unit weight over the original design.

Views of the final stator inseparable assembly and its housing are shown in Figures 5-6 and 5-7.

BLACK AND WHITE PHOTOGRAPH

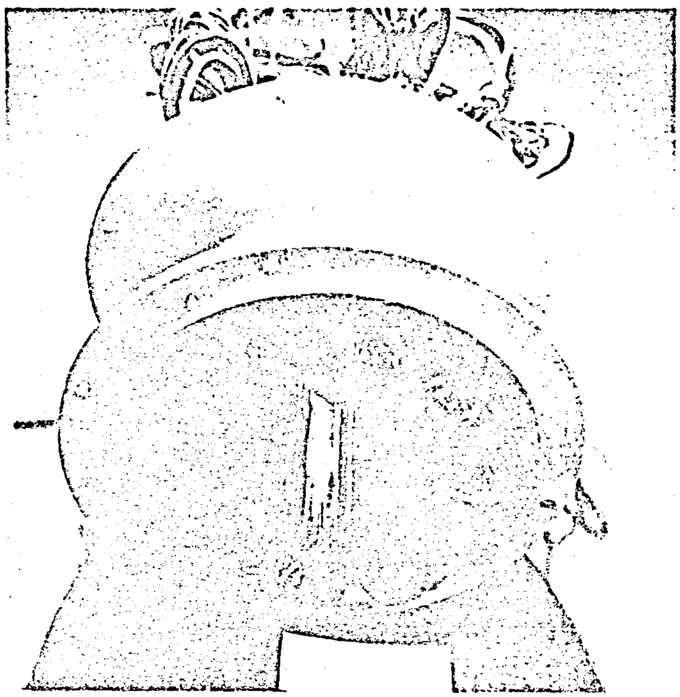

Figure 5-6 Stator/Housing Assy.

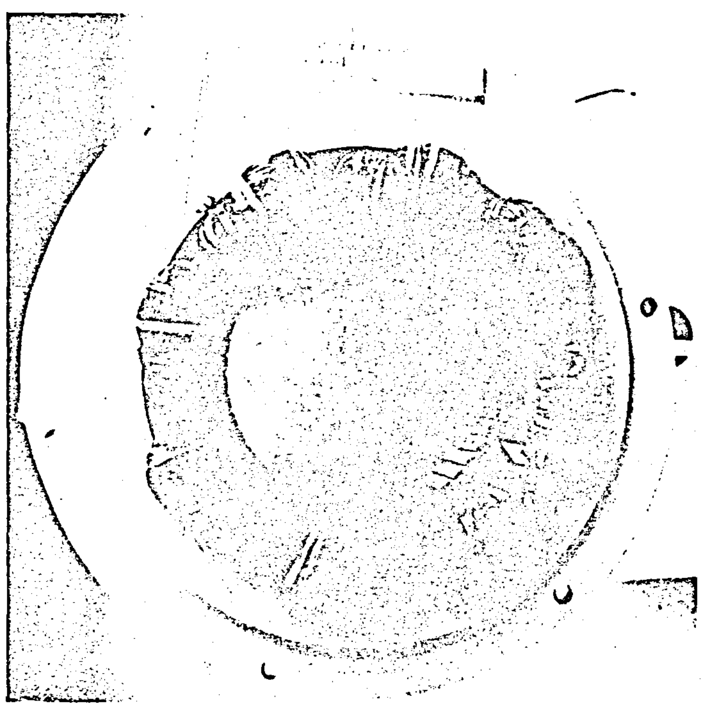

Figure 5-7 Stator/Housing Assy.

5.2 ROTOR BALANCE ASSEMBLY (EP 2758-210)

In the original design approach, a rotor construction containing tangential magnets and utilizing soft iron magnetic pole pieces, electron beam welded to a non-magnetic inner hub, was envisioned. Poles and magnets were contained by a non-magnetic sleeve shrunk over the outer rotor diameter, Figure 5-8.

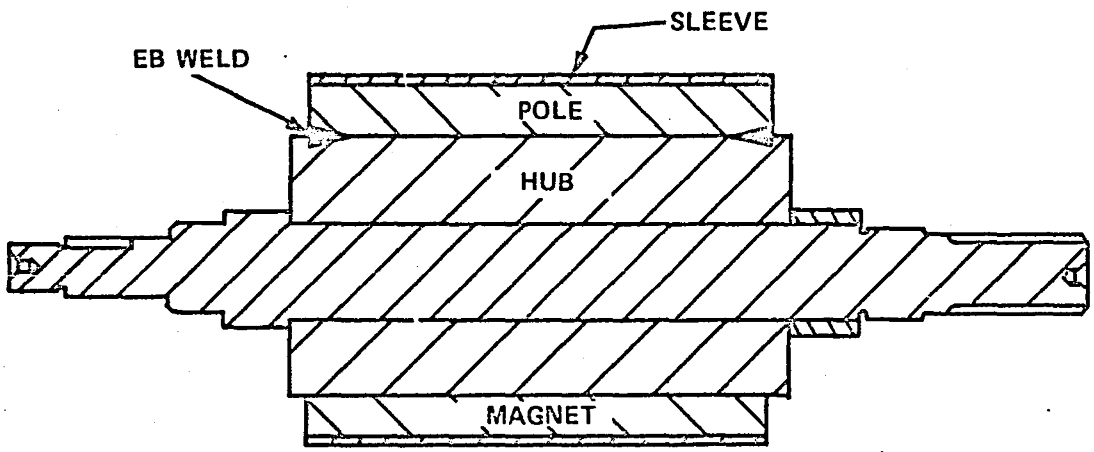

Figure 5-8 Original Rotor Construction

This core construction was patterned after similar Sundstrand products. Subsequent stress analysis, however, revealed that the necessary depth of weld penetration exceeded acceptable manufacturing limits. Not only was this depth difficult to reliably obtain, but it also resulted in an exceeding thick weld zone at the point of entry, Figure 5-9. Material in the weld zone constituted a metallurgical mixing of the magnetic and non-magnetic parent materials, yielding unacceptable mechanical and electromagnetic properties when present in such thickness.

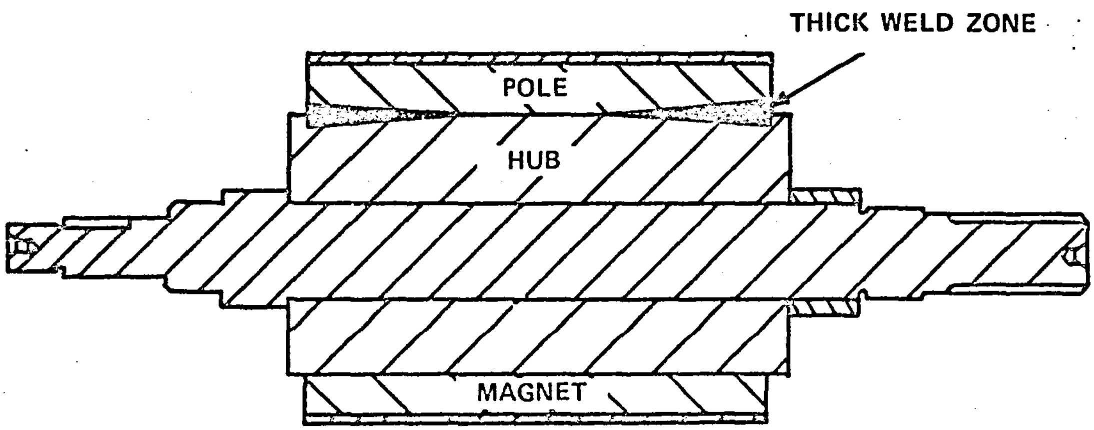

Figure 5-9 Required Weld Penetration

To circumvent this problem, the design was altered to individual core segments stacked together, Figure 5-10. Each segment is composed of an inner non-magnetic core over which an electromagnetic ring is shrunk. The joint between the two pieces is welded axially, forming a completed core segment. These core segments are illustrated in Figure 5-11.

ORIGINAL PAGE
BLACK AND WHITE PHOTOGRAPH

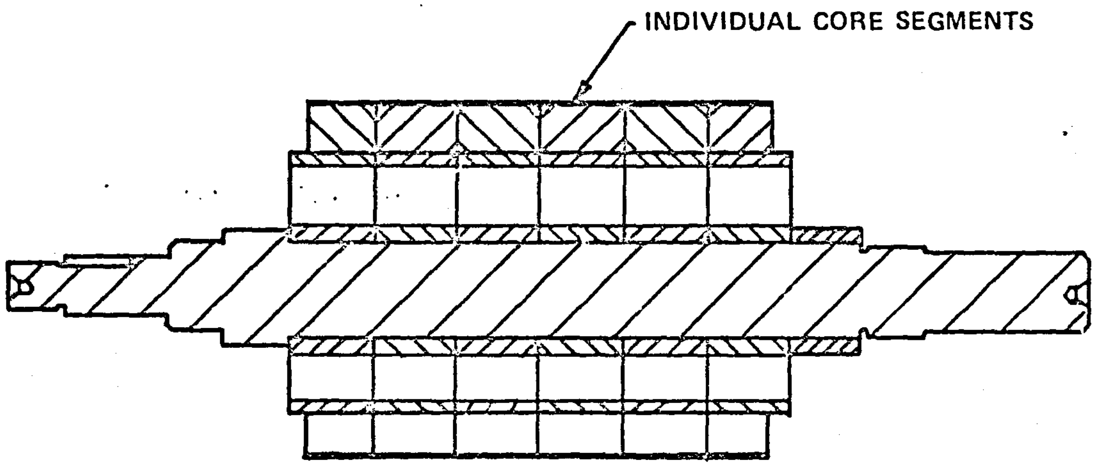

Figure 5-10 Stacked Rotor Construction

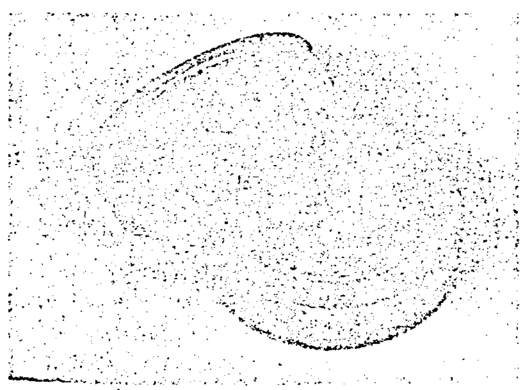

1) EP2758-212-1 SLEEVE

Region on outside of weld bead made of electromagnetic steel

2) EP2758-212-2 CORE

Region on inside of weld bead made of non-magnetic steel.

Figure 5-11 Rotor Element Construction

Each segment is machined so that its faces are flat, removing weld bulges, and exposing a minimum thickness weld zone. In this manner, the weld zone thickness is held to an acceptable value, which in turn facilitates ultrasonic inspection of the weld.

At the point of assembly, weight reduction holes are drilled in the inner core non-magnetic material of each segment. The segments are then stacked and inserted on a shaft to form the rotor core and shaft inseparable assembly. Magnet slots are then machined at predetermined locations. This assembly can be seen in Figure 5-12.

Selection of the non-magnetic material for the inner core was critical in yielding an acceptable weld joint. Weld samples utilizing 347 stainless steel inner cores were determined to contain cold cracks. These resulted from a combination of residual weld stress and a lack of weld ductility. The weld zone was martensitic, Rc 35.

ORIGINAL PAGE
BLACK AND WHITE PHOTOGRAPH

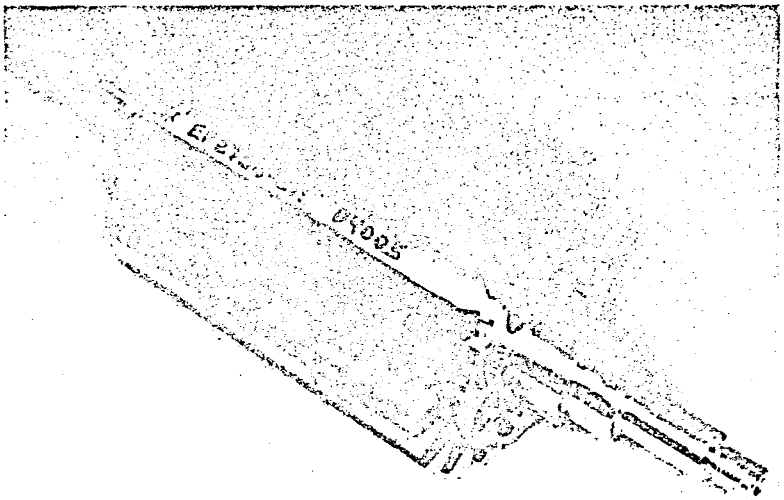

Figure 5-12 Rotor Core Construction

To eliminate cracking problems, the inner core material was changed to Inconel 625, creating an austenite weld zone. Residual stresses were reduced by preheating the core segments and reducing the welding speed.

As noted, the original method envisioned for magnet retention was to utilize a non-magnetic (inconel) sleeve shrunk on the rotor O.D. Concurrent Sundstrand projects, however, were indicating that improved efficiencies could be obtained if a carbon fiber wrap of the same thickness was substituted. The improvement was generally attributed to the elimination of losses associated with eddy currents in the sleeve.

However, to use an equivalent thickness of carbon fiber required that some of the centrifugal forces imparted by the magnets be borne by the pole piece weld and not the fiber wrap. This was achieved by using wedged shaped magnets and dove-tailed slots, Figures 5-12 and 5-13.

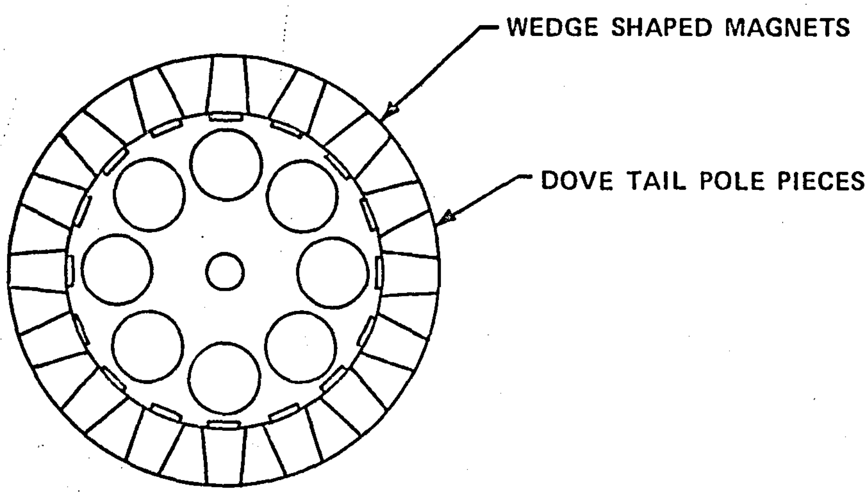

Figure 5-13 Magnet Retention Configuration

ORIGINAL PAGE
BLACK AND WHITE PHOTOGRAPH

As this scheme fully transfers the centrifugal loads to the pole piece welds, it is possible to essentially eliminate the wrapping altogether. Only a thin cosmetic layer needs to be retained to minimize windage losses. However, for this project, it was elected to maintain a wrap thickness equal to that of the originally designed inconel sleeve, providing a secondary retention feature in the event of weld failure.

Two trial rotors of this technique were manufactured. The wrap on these first two pieces, however, did not adhere totally to the rotor pole and magnet surfaces. In addition, the outer epoxy layer used to seal the strand ends was thin, exposing carbon fibers.

Though the wrap exhibited these discontinuities, it was securely bonded to itself. One rotor was tested at speeds up to 10,000 rpm with no failure or change in outer surface appearance.

The second rotor was stripped and rewrapped. Figure 5-14 shows the rotor prior to stripping. The silver colored area on the right side of the rotor is a resin lean region of the fiber system.

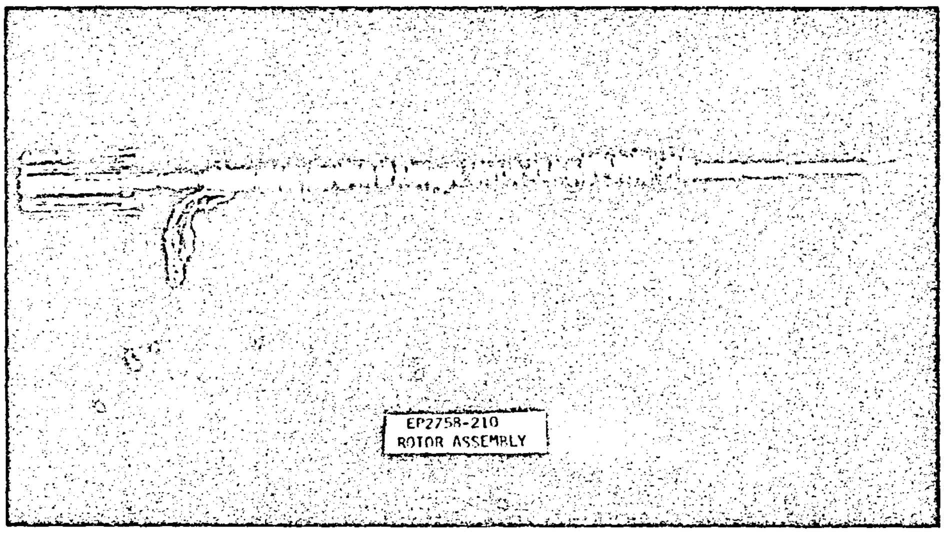

Figure 5-14 Carbon Wrap Distress

After stripping, the rotor was degreased and bead blasted to roughen the O.D. surface. This rougher surface allowed the epoxy to better adhere to the rotor pole and magnet surfaces. The rotor was rewrapped and cured.

Figures 5-15 and 5-16 are views showing a properly wrapped rotor. This rotor was used in the motor assembly tested for this report.

5.3 POSITION SENSOR VANE (EP 2758-41)

The rotor position sensing network was designed to contain 12 hall effect sensors, 1 per motor phase, and 8 sensor vanes, 1 per pole pair. The rotating vanes pass through all 12 sensors which are located on a single plate, Figure 5-17. The vanes are adjustable for either 180° or 120° conduction control schemes. This approach is similar to a Sundstrand design successfully tested for a U.S. Air Force remotely piloted vehicle.

ORIGINAL PAGE
BLACK AND WHITE PHOTOGRAPH

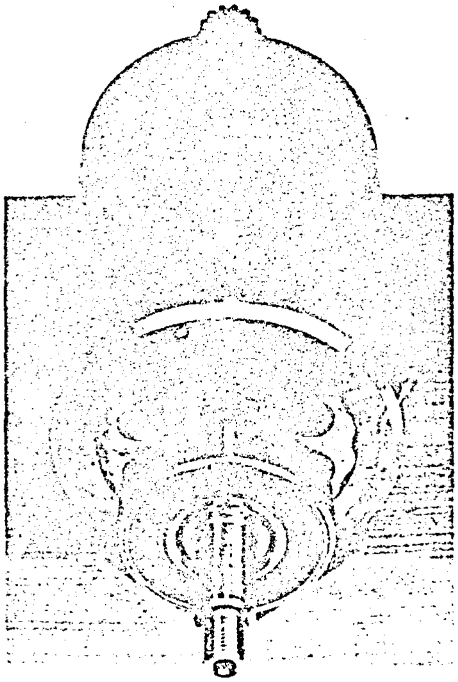

Figure 5-15 Rotor Assy.

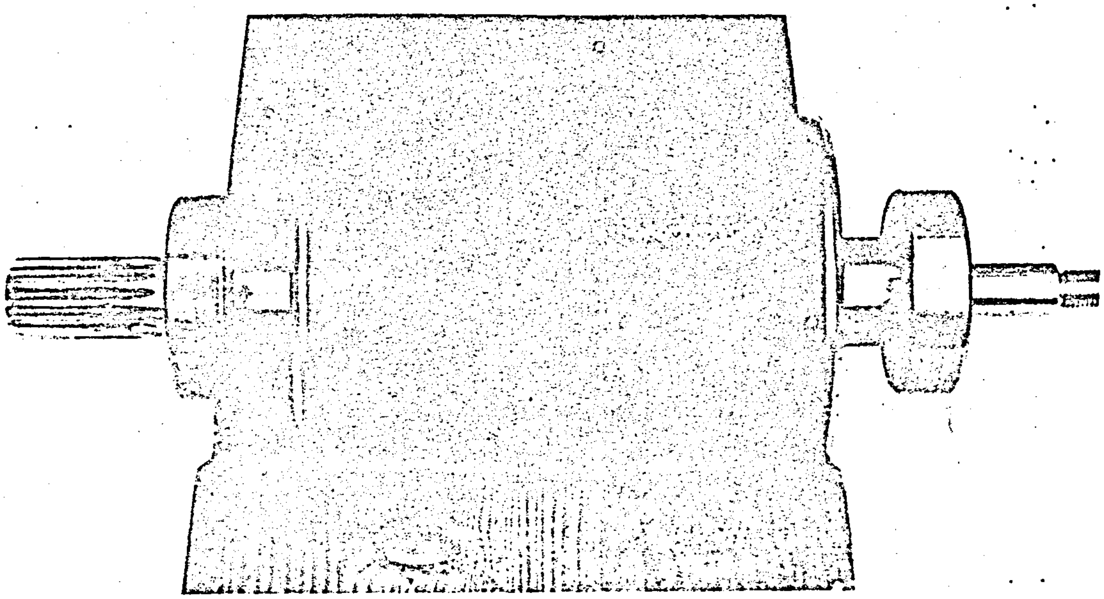

Figure 5-16 Rotor Assy.

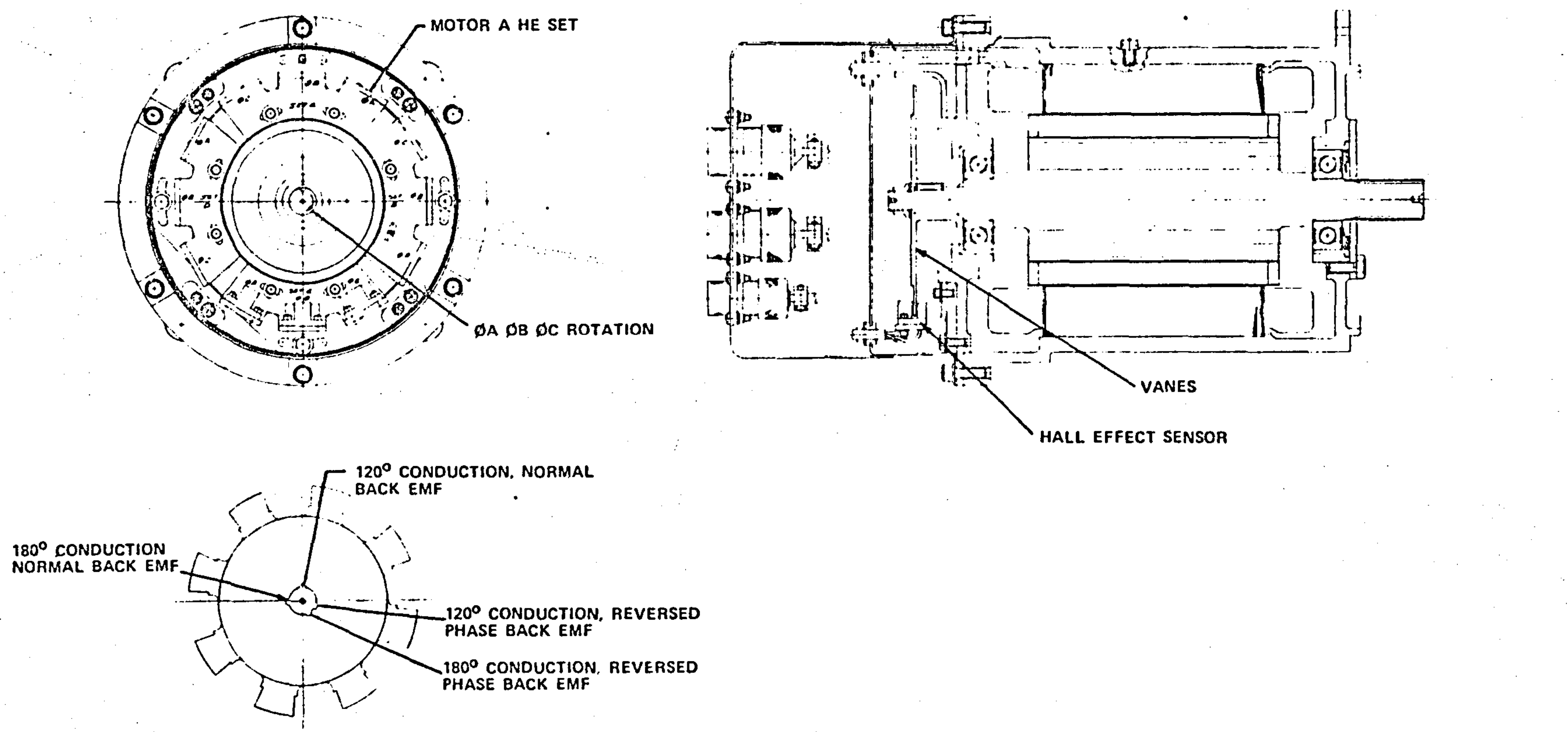

Figure 5-17 Rotor Position Sensing Configuration

In testing, however, the motor exhibited an audible tone at intervals of approximately 900 rpm. Review of the rotor position sensing geometry determined that four vanes would simultaneously pass a sensor every 15 degrees of revolution, creating a 24/rev. excitation of the vane assembly. Multiples of this value were found to correspond to the resonant frequencies of the vane teeth as well as the vane hub.

The immediate solution was to bond a damping material to the central vane hub. The material used was a ployvinylchloride (PVC) filled energy absorbing solid. This configuration was tested to over 10,000 rpm with no bonding failure.

6.0 DESIGN VERIFICATION TEST

6.0 DESIGN VERIFICATION TEST

Extensive tests were conducted on the motor, as a component, to adequately characterize its electromagnetic properties. These tests comprised both a static series where dc voltages were applied and a dynamic series where the motor, performing as a generator, was driven by an external prime mover.

In addition, limited single channel demonstration runs were made using a modified controller from another project. As development of a four channel controller was the objective of subsequent NASA activity, no suitable controller existed at the time of this project to conduct multichannel controller/motor tests.

6.1 TEST PROCEDURE

The test procedure used to determine the performance of the motor is found in Appendix A. Seven test series were conducted:

1) Winding Resistance
2) Winding Inductance
3) Dielectric Strength
4) Permanent Magnet Generator (PMG) Speed vs. Voltage Output
5) Permanent Magnet Generator (PMG) Loading
6) Static Torque vs. Rotor Position
7) Static Torque Summing

6.2 DATA SUMMARY

Complete test data are found in Appendix A. A brief summary of the results follows.

Motor Inductance

The predicted and measured phase inductance values are shown in Table 6-1. The difference is attributed to the consequent pole winding, and the end turn bulk resulting from it.

Table 6-1 Measured Inductance Valves

Test Number	Rotor Number	Predicted Inductance	Average Test Inductance
1	3	352.6 uh	447.4 uh
2	2	352.6 uh	450 uh
3	2	352.6 uh	448.3 uh

PMG Speed vs. Voltage Output

Test data matches predictions within 3% over the range of operating speeds.

PMG Loading

Data show that there is channel independency within the range of loading and speeds tested, Table 6-2.

Table 6-2 Measured Output Voltage — Loaded PMG Operation

	P.M.G. Voltage Output		Motors B, C & D Unloaded
Speed	Predicted	Test	Motor A Loaded
1666	38	37	Unloaded Quadrant Motors
	38	37-31.4	Loaded Quad @ 0 to 15.4 amperes
4333	98	96-107	Unloaded Quadrant Motors
	98	96-56	Loaded Quad @ 0 to 27.3 amperes
10,000	225	222	Unloaded Quadrant Motors
	225	218-157	Loaded Quad @ 0 to 23.3 amperes

Static Torque vs. Rotor Position

The predicted torque output of 12.6 in-lb compares to the average measured torque output of 13.14 in-lb within 4.1%.

Static Torque Summing

The current-torque curves show a linear relationship for the single channel configuration and a nonlinearity for multiple channel operation. This was traced to deflection of the test fixturing at the higher torque values achieved with multiple channels and not from interaction among the channels. Linear summing of torque is expected.

Waveforms and Harmonic Analysis

Motor voltage waveforms were recorded and their harmonic content analyzed. Tests were performed for both loaded and unloaded situations for several combinations of speeds, loads, channels and phases. Because of the extensive nature of these data, the following index of representative data is provided.

- Voltage Waveforms at No Load

  a) A comparison of line to neutral and line-to-line voltage waveforms as a function of speed can be obtained by reviewing the photographs listed in Table 6-3. These data were obtained from Channel "A".

  b) A comparison of the line to neutral voltage waveform for all four channels concurrently can be obtained as a function of speed by reviewing the photographs indicated in Table 6-4. A uniformity is noted among the individual channels.

Table 6-3 Voltage Waveforms at No Load
Motor Channel "A" Phases A, B, C

LOAD (Amps)	L-N	L-N PHOTO NUMBER	L-L	L-L PHOTO NUMBER
1) 1666 RPM DATA POINT				
0	A	5.4-A-1	A-B	5.4-D-1
	B	-2	B-C	-2
	C	-3	C-A	-3
2) 4333 RPM DATA POINT				
0	A	5.4-B-1	A-B	5.4-E-1
	B	-2	B-C	-2
	C	-3	C-A	-3
3) 10,000 RPM DATA POINT				
0	A	5.4-C-1	A-B	5.4-F-1
	B	-2	B-C	-2
	C	-3	C-A	-3

Motor Connections: Line to Neutral (L-N) & Line to Line (L-L)

Table 6-4 Voltage Waveforms at No Load
Motor Channels A, B, C, D

		QUADRANTS			
LOAD (Amps)	(L-N) MOTOR CONNECTION	MOTOR A PHOTO	MOTOR B PHOTO	MOTOR C PHOTO	MOTOR D PHOTO
1) 1666 RPM DATA POINT					
0	A-N	5.4-A-1	5.4-A-4	5.4-A-7	5.4-A-8
	B-N	-2	-5		
	C-N	-3	-6		
2) 4333 RPM DATA POINT					
0	A-N	5.4-B-1	5.4-B-4	5.4-B-7	5.4-B-8
	B-N	-2	-5		
	C-N	-3	-6		
3) 10,000 RPM DATA POINT					
0	A-N	5.4-C-1	5.4-C-4	5.4-C-7	5.4-C-8
	B-N	-2	-5		
	C-N	-3	-6		

- Voltage Waveforms at Load

    a) An indication of the effect of load on waveform can be obtained by examining the photos listed in Tables 6-5 and 6-6. Data in Table 6-5 are grouped as a function of speed. Data in Table 6-6 are grouped as a function of load current. All data were obtained from a loaded channel "A" with the remaining channels open circuited (unloaded).

    b) The effect on the waveform of a loaded channel on an unloaded channel can be obtained by reviewing the data listed in Table 6-7.

- Harmonic Analysis at No Load

    a) The harmonic content of the line to neutral and line-to-line waveforms of an unloaded channel can be obtained by reviewing the graphs listed in Table 6-8.

- Harmonic Analysis at Load

    a) The harmonic content of line to neutral and line-to-line waveforms for loaded channels can be obtained by reviewing the graphs listed in Tables 6-9 and 6-10. Table 6-9 presents the data as a function of speed. Table 6-10 presents the data by motor connection.

Table 6-5 Voltage Waveforms at Load
Motor Channel A

L-N	L-N PHOTO NUMBER	L-L	L-L PHOTO NUMBER	LOAD (Amps)
1) 1666 RPM DATA POINT				
A	5.5-A-20	A-B	5.5-A-21	6.1
2) 4333 RPM DATA POINT				
A	5.5-B-6	A-B	5.5-B-7	14.6
	-2		-3	17.8
3) 10,000 RPM DATA POINT				
A	5.5-C-2	A-B	5.5-C-3	10.2
	-4		-5	18.1
MOTOR CONNECTIONS: LINE TO NEUTRAL (L-N) & LINE TO LINE (L-L)				

Table 6-6 Voltage Waveforms at Load
Motor Channel A

LOAD (Amps)	SPEED (R.P.M.)	MOTOR CONNECTIONS	PHOTO NUMBER
6.0	1666	A-N	5.5-A-7
5.7	10K	A-N	5.5-C-1
10.1	1666	A-N	5.5-A-11
10.2	10K	A-N	5.5-C-2
10.2	10K	A-B	-3
14.8	1666	A-N	5.5-A-18
14.6	4333	A-N	5.5-B-6
14.6	4333	A-B	-7
17.8	4333	A-N	5.5-B-2
17.8	4333	A-B	-3
18.1	10K	A-N	5.5-C-4
18.1	10K	A-B	-5

Table 6-7 Voltage Waveforms Unloaded vs. Loaded
Motor Channels A & B

1) 4333 RPM DATA POINT

QUADRANT MOTOR	LOAD (Amps)	L-N	PHOTO NUMBER	L-L	PHOTO NUMBER
A	17.8	A	5.5-B-2	A-B	5.5-B-3
B	0		-4		-5

MOTOR CONNECTIONS: LINE TO NEUTRAL (L-N) & LINE TO LINE (L-L)

Table 6-8 Harmonic Analysis at No Load

A) 1666 RPM DATA POINT

LOAD (Amps)	CONSTANT	VARIABLE	H.A. GRAPH NUMBER
0	A-N	Y	5.4-A-1
		N	-9
0	N	A-N	5.4-A-9
		A-B	-10

MOTOR CONNECTIONS: LINE TO NEUTRAL (A-N) & LINE TO LINE (A-B)

Y = HARMONIC ANALYZER GROUNDED

N = HARMONIC ANALYZER UNGROUNDED

Table 6-9 Harmonic Analysis at Load

CONSTANT	VARIABLE	LOAD (Amps)	H.A. GRAPH NUMBER
1) 1666 RPM DATA POINT			
A-N	N	6.13	5.5-A-1
	Y	9.3	-3
	Y	14.1	-5
A-B	N	6.13	5.5-A-2
	Y	9.3	-4
	Y	14.1	-6
2) 4333 RPM DATA POINT			
A-N	N	14.6	5.5-B-1
	Y	14.4	-3
A-B	N	14.6	5.5-B-2
	Y	14.4	-4
N	A-N	14.6	5.5-B-1
	A-B	14.6	-2
Y	A-N	14.4	5.5-B-3
	A-B	14.4	-4
3) 10,000 RPM DATA POINT			
N	A-N	10.2	5.5-C-1
	A-B	10.2	-2

MOTOR CONNECTIONS: LINE TO NEUTRAL (A-N) & LINE TO LINE (A-B)

Y = HARMONIC ANALYZER GROUNDED

N = HARMONIC ANALYZER UNGROUNDED

Table 6-10 Harmonic Analysis at Load

CONSTANT	(R.P.M.) VARIABLE	LOAD (Amps)	H.A. GRAPH NUMBER
1) LINE TO NEUTRAL (A-N)			
N	1666	6.1	5.5-A-1
	4333	14.6	5.5-B-1
	10K	10.2	5.5-C-1
2) LINE TO LINE (A-B)			
N	1666	6.1	5.5-A-2
	4333	14.6	5.5-B-2
	10K	10.2	5.5-C-2
3) LINE TO NEUTRAL (A-N)			
Y	1666	9.3	5.5-A-3
	1666	14.1	5.5-A-5
	4333	14.4	5.5-B-3
4) LINE TO LINE (A-B)			
Y	1666	9.3	5.5-A-4
	1666	14.1	5.5-A-6
	4333	14.4	5.5-B-4

Y = HARMONIC ANALYZER GROUNDED

N = HARMONIC ANALYZER UNGROUNDED

6.3 MOTOR/CONTROLLER OPERATION

Modifications were made to a Sundstrand controller to allow it to drive a single channel. With the controller driving quadrant "A", no-load speeds up to 5,000 rpm were obtained with smooth acceleration and deceleration. Inability to drive the motor at speeds greater than 5,000 rpm was due to the controller. At this point testing was concluded.

6.4 WEIGHT SUMMARY AND DISTRIBUTION

WEIGHT SUMMARY

MOTOR ASSEMBLY (EP2758-10)		ACTUAL WEIGHT
a) Stator Inseparable Assembly (EP2758-94)		12.425 Lbs.
b) Rotor Balance Assembly (EP2758-210)		9.329 Lbs.
c) Other Motor Parts		11.56 Lbs.
d) Motor Assembly (EP2758-10)	TOTAL	33.31 Lbs.

WEIGHT DISTRIBUTION

	NOTE	LBS PREDICTED	LBS ACTUAL	LBS DIFFERENTIAL
A) STATOR INSEPARABLE ASSEMBLY (EP2758-94)				
1) Iron		6.853	7.020	+.167
2) Copper	(1)	4.337	5.230	+.893
3) Insulation, Tape	(2)			
Leadwire, Sleeving	(2)	—	.175	+.175
TOTAL		11.190	12.425	+1.235

NOTES:

(1) Stator coil form size had to be enlarged to allow for nesting and overlap clearance of coil end turns.

(2) These parts were not weight predicted.

	NOTE	LBS PREDICTED	LBS ACTUAL	LBS DIFFERENTIAL
B) ROTOR BALANCE ASSEMBLY (EP2758-211)				
1) SEPARABLE WEIGHTS				
a) Magnets		1.968	2.301	+.333
b) Containment feature	(3)	.182	.099	−.083
c) End plates	(4)	.165	.335	+.170
SUB-TOTAL		2.315	2.735	+.420

2) INSEPARABLE WEIGHTS					
a) Poles		(5)	1.855	—	—
b) Hub		(5)	.781	—	—
	SUB-TOTAL		2.636	—	—
3) NON-ELECTROMAGNETIC WEIGHTS					
a) Shaft (EP2758-213)		(6)	—	1.406	—
b) Rotor & Shaft Inseparable Assembly (EP2758-211), minus shaft (EP2758-213)		(6)	—	5.188	—
	TOTAL LBS.	(7)	4.951	9.329	—

NOTES:

(3) The containment feature was changed from a metallic sleeve to a graphite fiber-epoxy wrap.

(4) End plate material was changed from aluminum to stainless steel to allow for material removal during balancing.

(5) Rotor construction does not allow for individual weighing of rotor poles or the hub of the electromagnetic circuit prior to rotor assembly.

(6) These parts were not weight predicted.

(7) Weight difference due to notes (5) & (6).

7.0 CONCLUSION

7.0 CONCLUSION

It has been noted throughout this report that motor development is only one step in implementin a successful, electromagnetic summing, flight actuation system. Indeed, some of the more difficu work, the development of a viable redundancy management scheme, remains. Nevertheless, th completion of this project is considered an essential step toward an operational system.

The work accomplished demonstrates that competitive weight and performance are achievabl without difficult manufacturing methods. In addition, a data base has been developed providin validation of modeling techniques and the necessary background for preliminary controlle design.

The test simulation of failure effects and the development of the associated predictive models i viewed as the next logical step toward a functioning four channel controller and, ultimately, to a fully redundant demonstration system. The test motor is the tool available for this effort.

APPENDIX A

TEST DATA

APPENDIX A - TEST DATA

INDEX:

Data Sheets	Title
-	Test Procedure
-	Electromechanical Timing Schematics
5.1	Winding Resistance Data
5.2	Winding Inductance Data
5.3	Dielectric Strength Data
5.4	P.M.G. Speed vs. Voltage Output Data
5.5	P.M.G. Loading Data
5.6	Static Torque vs. Rotor Position Data
5.7	Static Torque Summing Data

TEST PROCEDURE

TEST PROCEDURE

QUAD REDUNDANT MOTOR EP 2758-10

CONTRACT NAS-9-16535

1.0 MOTOR TESTS

Motor assembly part number EP 2758-10

1.1 WINDING RESISTANCE

Record room ambient temperature. After allowing the motor to reach room ambient temperature, measure and record the individual phase resistances of each quadrant motor.

1.2 WINDING INDUCTANCE

a) Measure the winding phase inductance of each quadrant motor. Rotate the shaft in incremental steps measuring associated inductance. Locate rotor position with the centerline of the "sensor end shaft keyway" as the timing feature. Zero mechanical degrees rotor position occurs when the keyway centerline is aligned with the stator locking screw centerline.

b) Repeat readings for line to line winding connections.

1.3 DIELECTRIC STRENGTH

a) Motor Winding Test

1) Insulation Resistance Test

Apply 500 ± 50 VAC, 60 hertz for one minute between the neutral lead of quadrant motor "A" and ground. Record the insulation resistance value.

Repeat the test for the remaining quadrant motors.

Repeat the test between the neutral leads of quadrant motors "A" and "B". Record the insulation resistance value.

Repeat the test for the remaining quadrant motor combinations.

2) High Potential Test

Apply 1275 ± 25 VAC, 60 hertz for one minute or 1530 ± 25 VAC 60 hertz for one second between the netral lead of quadrant motor "A" and ground. Do not exceed a rate of 500 volts per second when applying this power. Record the leakage current value.

Repeat the test for the remaining quadrant motors.

Repeat the test between the neutral leads of quadrant motors "A" and "B". Record the leakage current value.

Repeat the test for the remaining quadrant motor combinations.

3) Insulation Resistance Retest

Repeat step 1.3-a-1

1.4 PERMANENT MAGNET GENERATOR (P.M.G.) SPEED VS. VOLTAGE OUTPUT

Drive the motor as a P.M.G. at indicated speeds. Measure the phase voltage output of all quadrants, and if possible, the torque input at each speed point. Obtain an oscilloscope voltage trace of all phases of quadrant motors "A" and "B" and phase "A" of the remaining quadrants at each of the motor speeds 1666, 4333 and 10,000 R.P.M.

If time permits, repeat above test on quadrant motor "A" measuring line to line voltage and obtaining waveforms.
If instrumentation is available, perform harmonic analysis on each quadrant during above test.

1.5 P.M.G. LOADING

Drive the motor as a P.M.G. at indicated speeds while loading quadrant motor "A" to desired values of phase current. Measure quadrant motor "A" watts, the phase voltage of all quadrants, and if possible, the torque input at each speed point. Maintain as near constant motor temperatures as possible for each reading. Obtain oscilloscope voltage traces of the loaded and unloaded quadrant motors at speeds of 1666, 4333 and 10,000 R.P.M.

If instrumentation is available, perform harmonic analysis on each quadrant during above test.

1.6 STATIC TORQUE VS. ROTOR POSITION

Apply D.C. power between phases "A" and "B" of quadrant motor "A" at one value of D.C. current. Record shaft torque output as a function of incremental rotor position.

Increase current in incremental steps at one rotor position. Record shaft torque, input current and voltage. Maintain as near constant motor temperatures as possible for each reading. Repeat for quadrant motors B, C & D.

1.7 STATIC TORQUE SUMMING

Apply D.C. power between phases "A" and "B" of quadrant motors "A" and "B" connected in series. Increase current in incremental steps at one rotor position. Record shaft torque, input current and voltage. Maintain as near constant motor temperatures as possible for each reading.

Repeat the test for phases "A" and "B" connected in series for quadrant motors A, B and C.

Repeat the test for phases "A" and "B" connected in series for quadrant motors A, B, C and D.

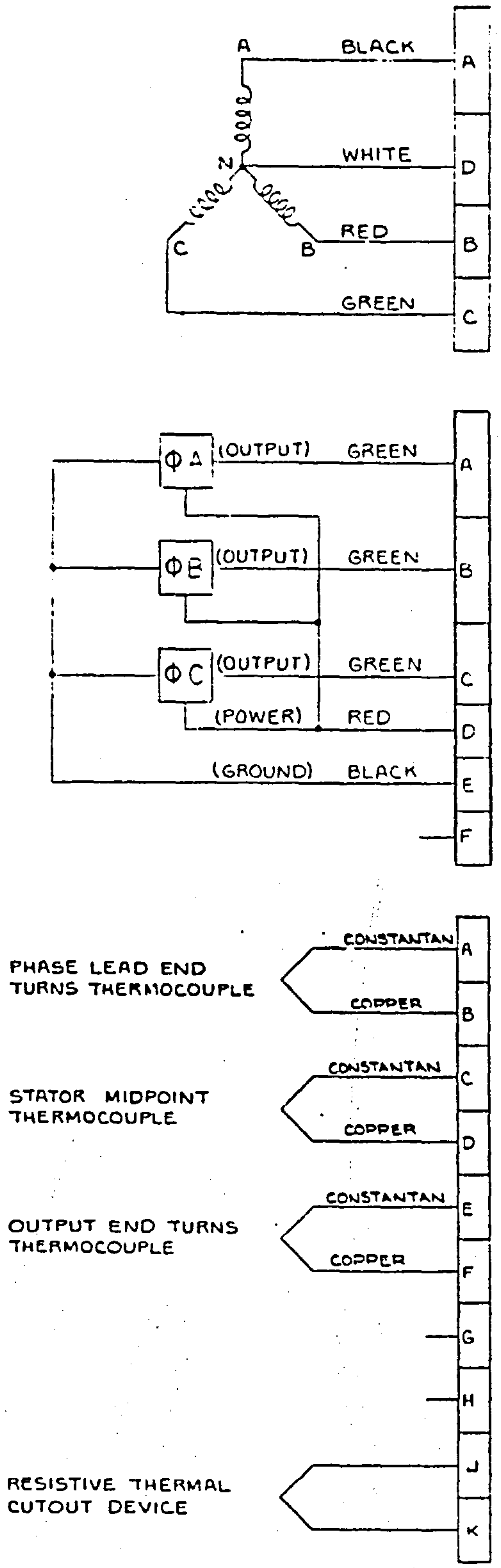

POWER CONNECTORS

male: MS3470L14-4P
female: MS3476L14-4S

SENSOR CONNECTORS

male: MS3470L10-6P
female: MS3476L10-6S

TEMPERATURE CONNECTORS

male: MS3470L12-10P
female: MS3476L12-10S

PINS A, C & E

male: DEUTSCH #105-371-01
female: DEUTSCH #105-372

MOTOR ELECTRICAL CONNECTOR LEGEND
FIGURE 1

S8308-R1

ZONING: 90 Mechanical degrees contains input/output for one quadrant motor

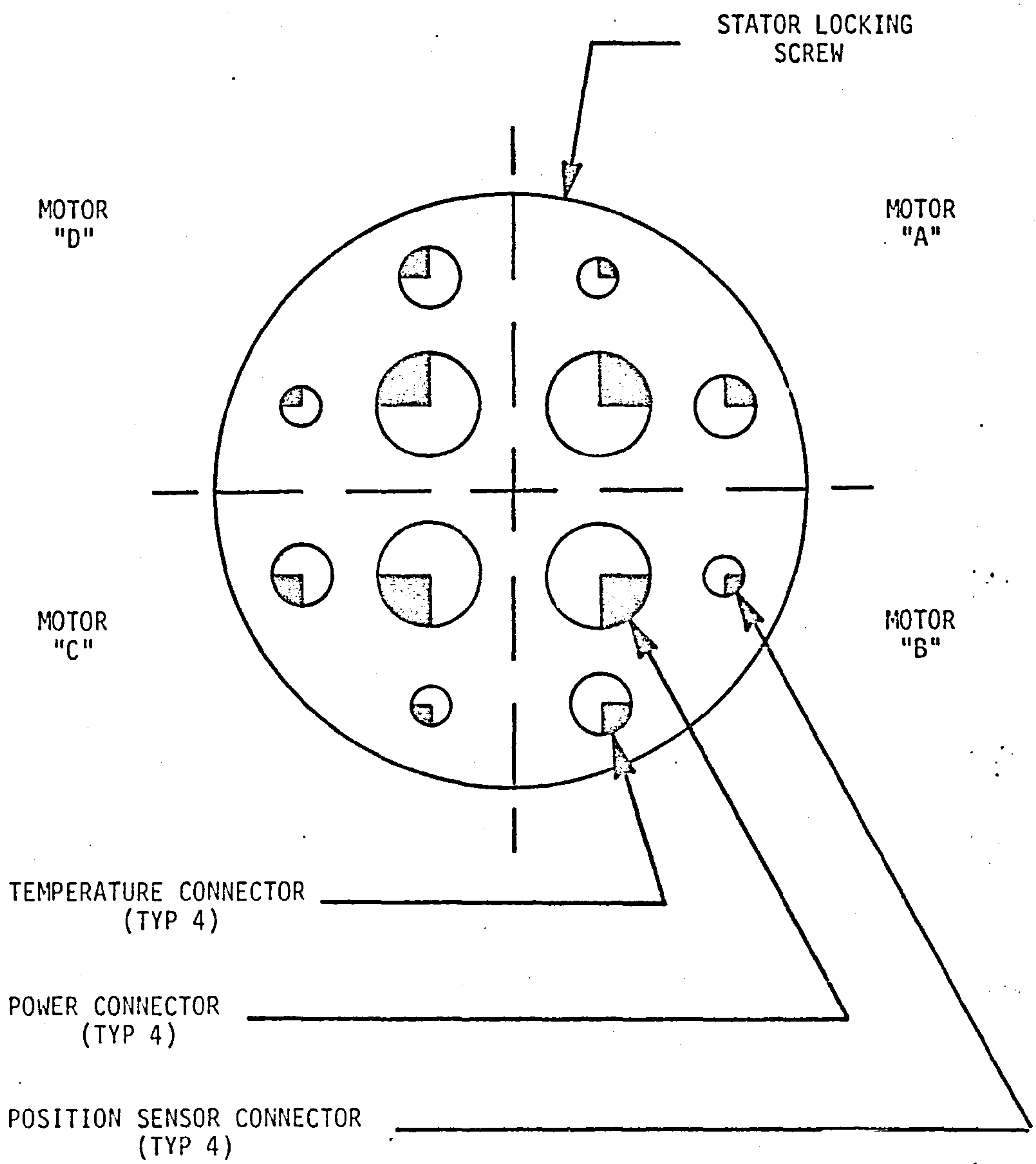

MOTOR ELECTRICAL CONNECTOR LOCATION LEGEND
FIGURE 2

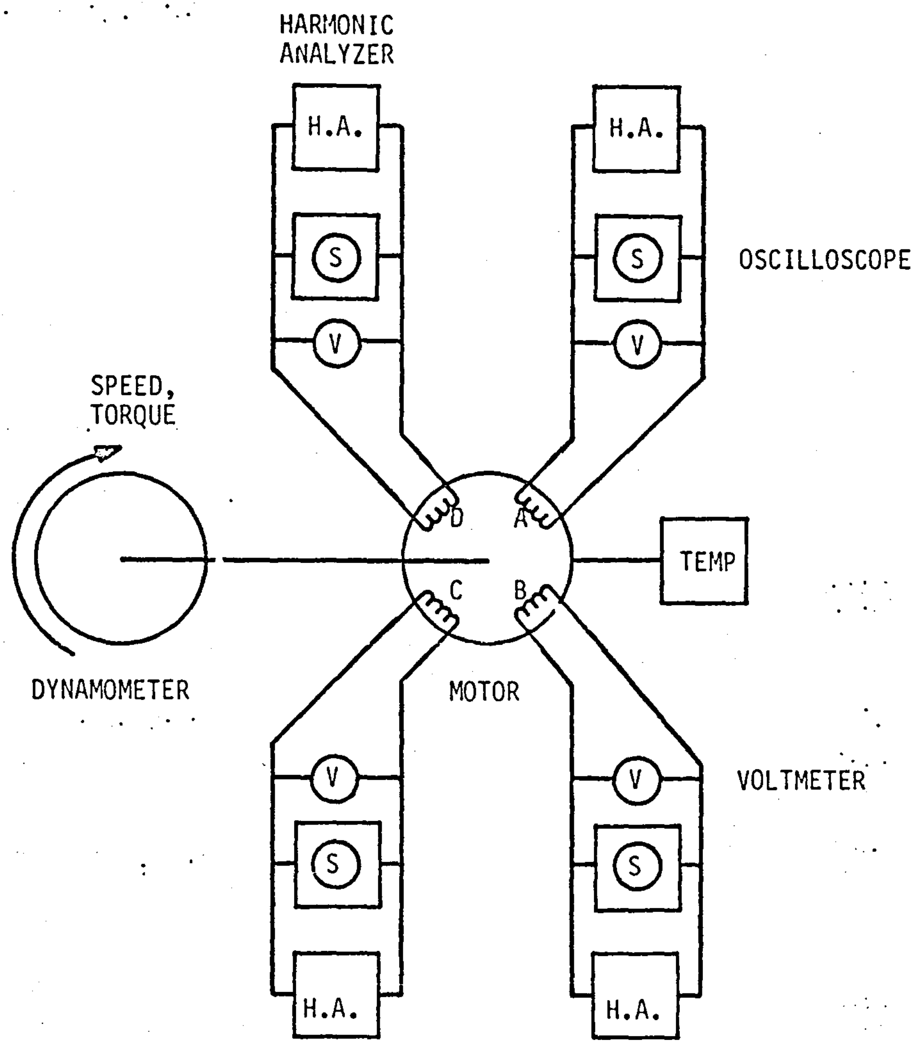

P.M.G. SPEED VS. VOLTAGE OUTPUT

FIGURE 3

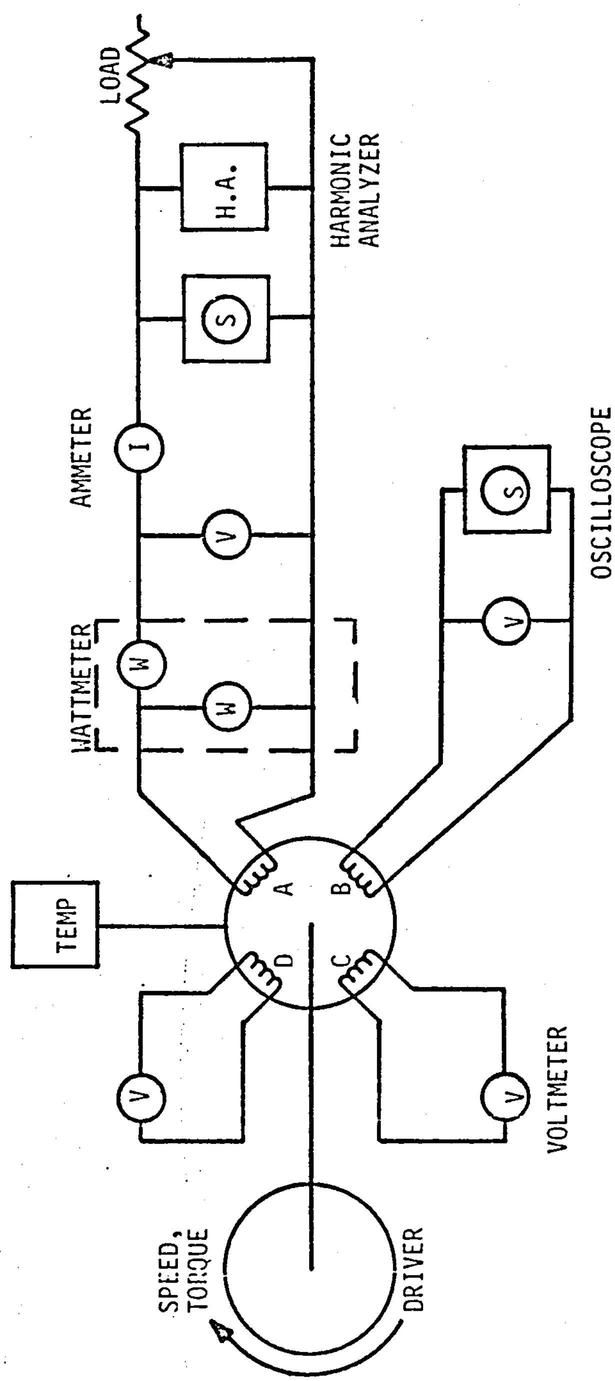

P.M.G. LOADING

FIGURE 4

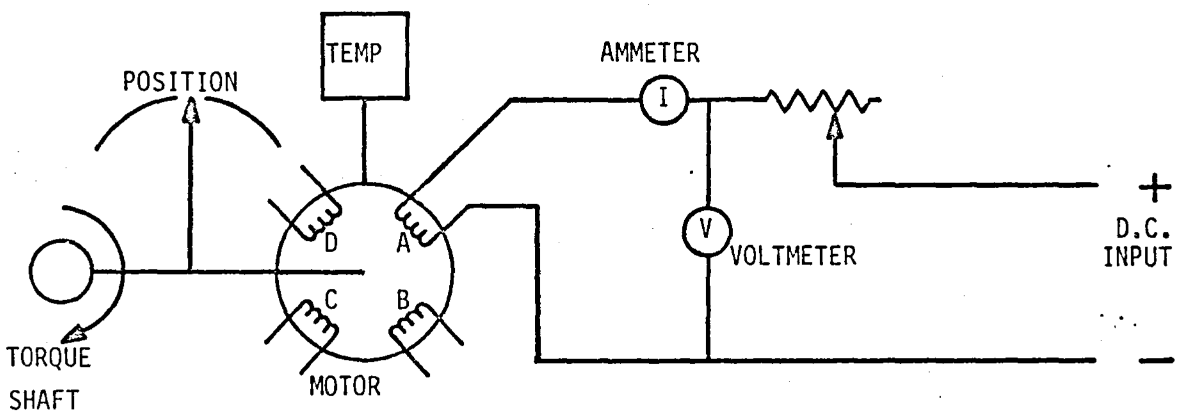

STATIC TORQUE VS. ROTOR POSITION

FIGURE 5

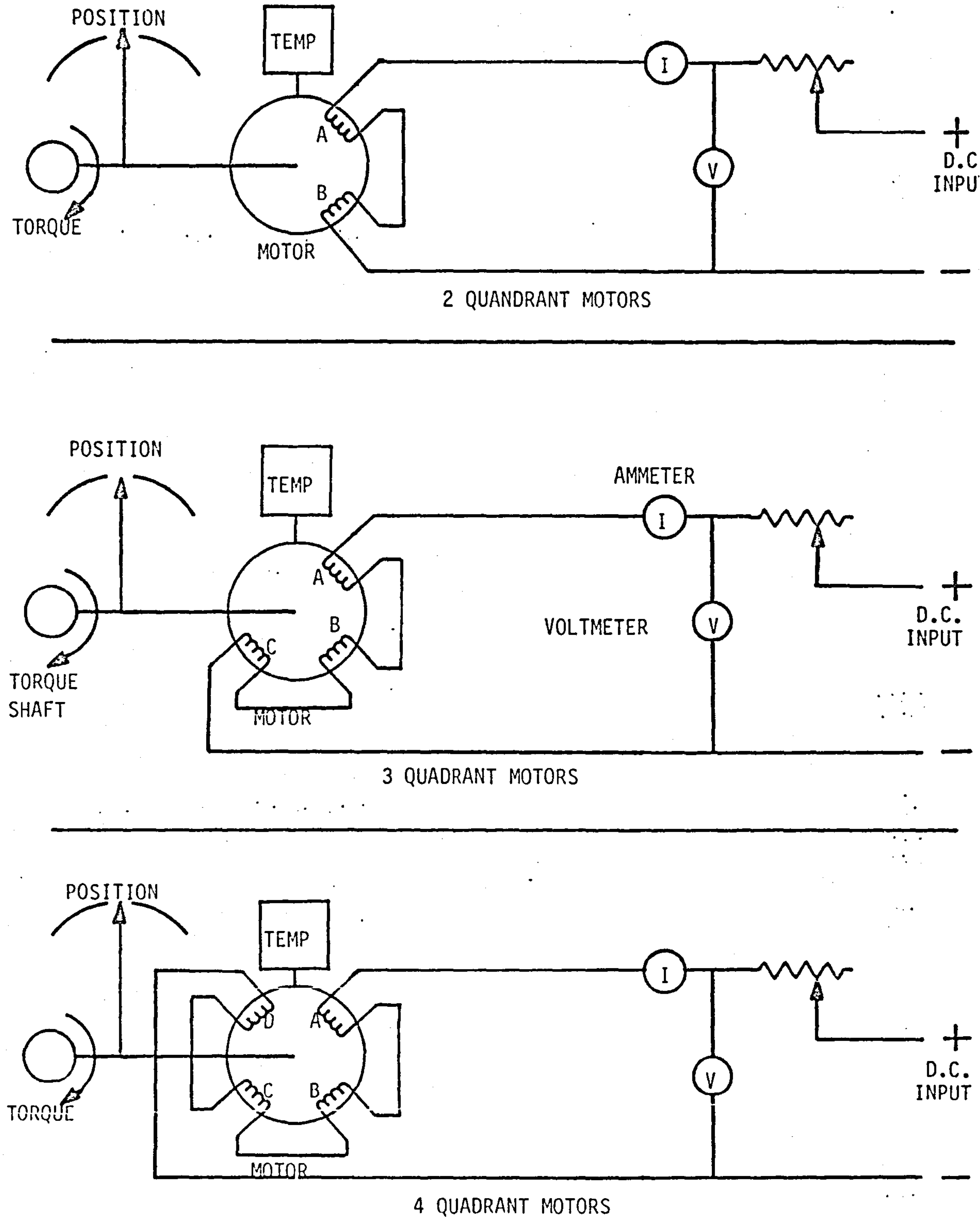

STATIC TORQUE SUMMING
FIGURE 6

ELECTROMECHANICAL TIMING SCHEMATICS

STATOR TIMING FEATURE DESCRIPTION

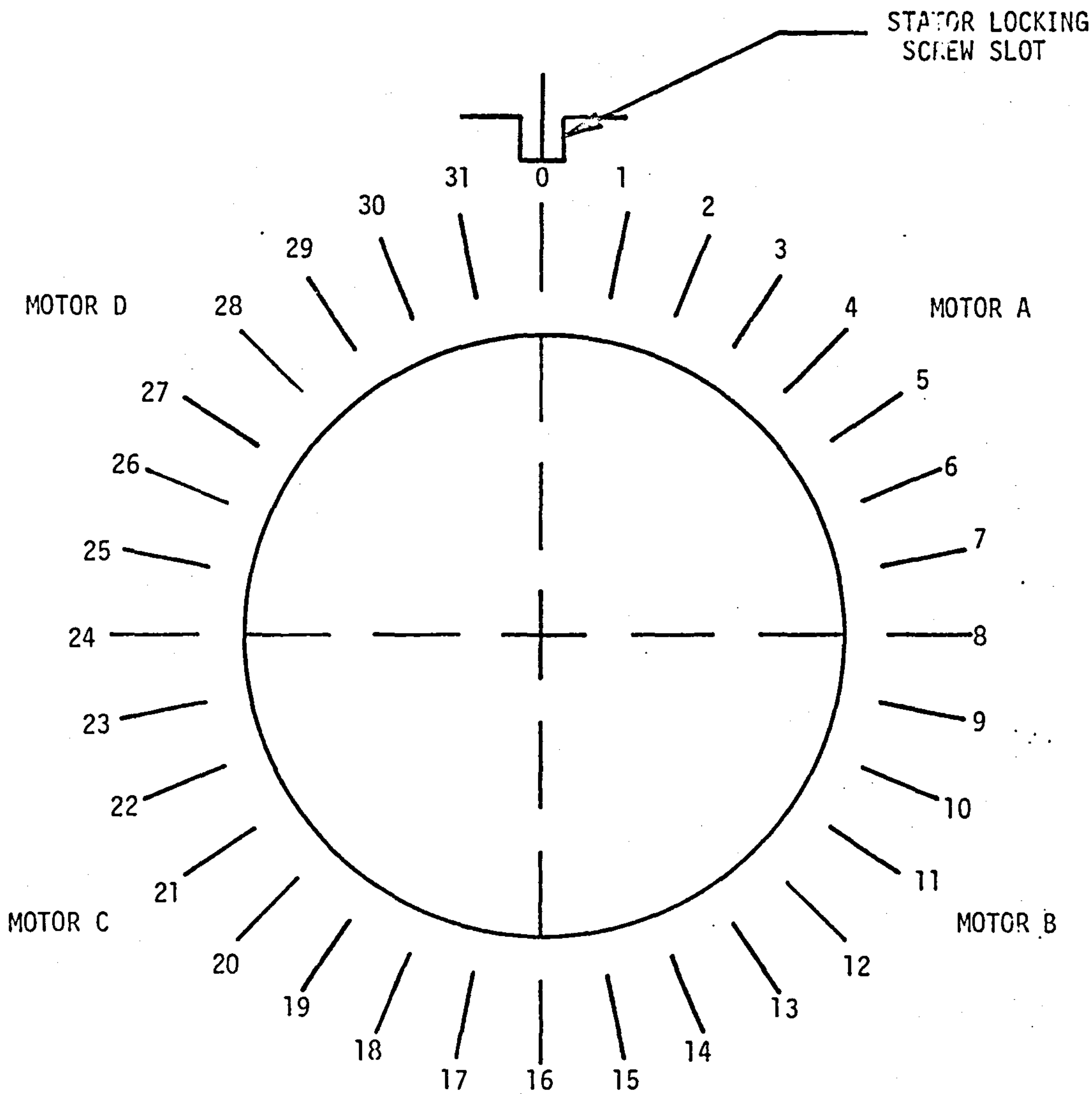

STATOR LOCKING SCREW SLOT TO QUADRANT MOTOR LOCATION

1) 8 timing positions = 90 mechanical degrees.

2) Timing position sequence viewed from motor connector end.

FIGURE 1

ROTOR TIMING FEATURE DESCRIPTION

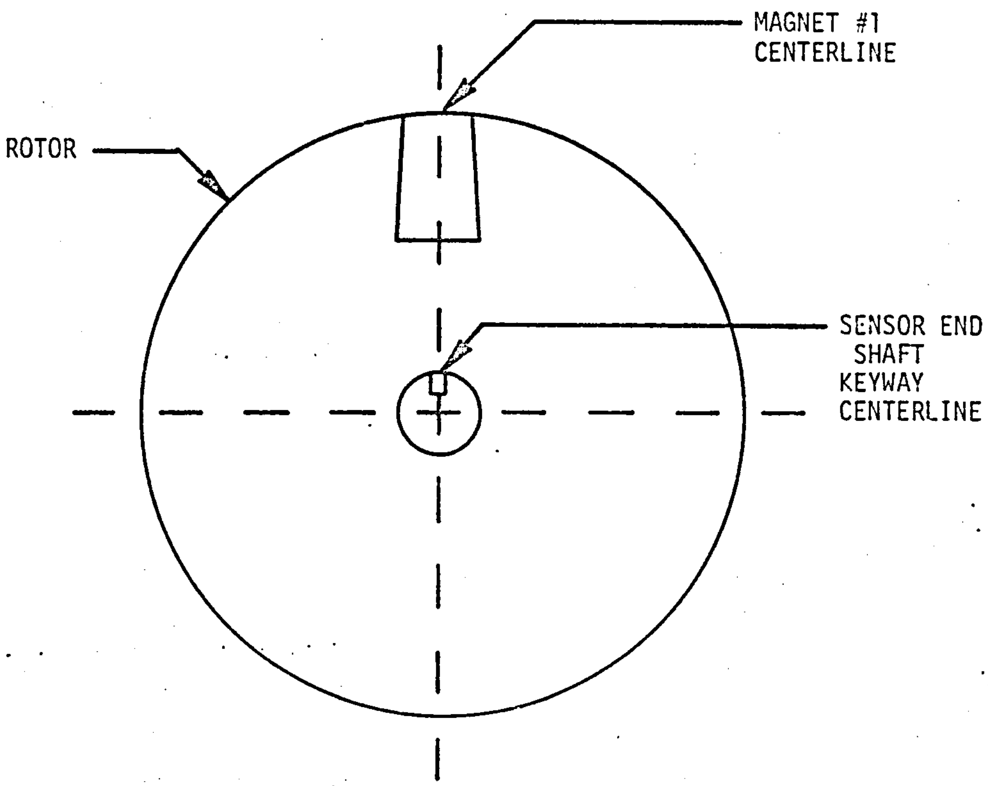

ROTOR SHAFT KEYWAY TO MAGNET LOCATION

1) Viewed from motor connector end.

2) ZERO REFERENCE POINT: Zero mechanical degrees rotor position equals magnet centerline (shaft keyway centerline) aligned with stator locking screw centerline.

FIGURE 2

WINDING RESISTANCE DATA

5.1) WINDING RESISTANCE

ROOM AMBIENT TEMPERATURE: 72°F

REF: PHASE RESISTANCE = .0872 TO .0936 ohms @ 77°F

RESISTANCE	PHASE A TO NEUTRAL	PHASE B TO NEUTRAL	PHASE C TO NEUTRAL
UNITS	OHMS	OHMS	OHMS
MOTOR A	.091	.092	.092
MOTOR B	.091	.090	.089
MOTOR C	.093	.092	.092
MOTOR D	.091	.092	.089

MEASUREMENTS TAKEN INCLUDE .002 Ω
OF MATING CONNECTOR AND LEADWIRE

TIM MAYER

WINDING INDUCTANCE DATA

5.2) WINDING INDUCTANCE

TEST SUMMARY

1) ROTOR #3 (10-26-83)

Inductance values were obtained using the first available rotor. Rotor #3 had some containment epoxy-wrap deficiencies, however it allowed obtaining preliminary inductance mapping values.

2) ROTOR #2 (11-17-83)

Inductance values were obtained using the final configuration rotor balance assembly. Additional stator winding combination tests were established to provide further data comparisons. These are series connected line to neutral and line to line lead combinations for all quadrant motors.

3) ROTOR #2 (12-9-83 to 12-13-83)

A runout of approximately .003 inches was observed on the lead end of the stator core I.D. The core was then ground to 3.180 inches concentric to the stator housing pilot diameter. Upon completion, the inductance test was rerun in portion for comparison purposes.

5.2) WINDING INDUCTANCE

TEST DATA SUMMARY

QUADRANT MOTOR	MOTOR CONNECTION	TEST #1 ROTOR #3 (uh)	TEST #2 ROTOR #2 (uh)	TEST #3 ROTOR #2 (uh)
	A-N	457	465	464
A	B-N	437	447	443
	C-N	431	438	438
	A-N	454		
B	B-N	445		
	C-N	451		
	A-N	450		
C	B-N	439		
	C-N	449		
	A-N	459		
D	B-N	447		
	C-N	450		
	A-B	1119	1146	
A	B-C	1216	1261	
	C-A	1227	1248	
	A-B	1111		
B	B-C	1228		
	C-A	1228		
	A-B	1113		
C	B-C	1232		
	C-A	1240		
	A-B	1117		
D	B-C	1240		
	C-A	1239		
A,B,C & D	A-N SERIES		2018	2012
A,B,C & D	B-N SERIES		2000	2013
A,B,C & D	A-B SERIES		4611	4613

5.2a) WINDING INDUCTANCE

QUADRANT MOTOR #A - PHASE A TO NEUTRAL

READING ROTATION: CW SENSOR END

ROTOR POSITION		UNITS	ROTOR POSITION		UNITS	ROTOR POSITION		UNITS	ROTOR POSITION		UNITS
#	DEGREES	uh	#	DEGREES	uh	#	DEGREES	uh	#	DEGREES	uh
0	0	452	8	90	464	16	180	461.5	24	270	417
½		483	½		[illegible]	½		[illegible]	½		472
1	11.25	452	9	101.25	494	17	191.25	[illegible]	25	281.25	473
½		420	½		435	½		[illegible]	½		418
2	22.5	452	10	112.5	[illegible]	18	202.25	[illegible]	26	292.5	446
½		485	½		511	½		[illegible]	½		475
3	33.75	451	11	123.75	469	19	213.75	474	27	303.75	472
½		422	½		432	½		420	½		420
4	45	423	12	135	471.5	20	225	444.5	28	315	448
½		487	½		507.5	½		475	½		478
5	56.25	456	13	146.25	468	21	236.25	470	29	326.25	472
½		425	½		431	½		417	½		422
6	67.5	454	14	157.5	466	22	247.5	418	30	337.5	451
½		488.5	½		504	½		471	½		482
7	78.75	452.5	15	168.75	469	23	258.75	472	31	348.75	482
½		424	½		431.5	½		417	½		423

AVERAGE VALUE: 456.98

MAXIMUM VALUE: 511

MINIMUM VALUE: 417.

L. KINTZ / B. ZELINSKI
10/26/83
ROTOR #3

5.2o) WINDING INDUCTANCE
QUADRANT MOTOR #A - PHASE B TO NEUTRAL
READING ROTATION: CW SENSOR END

ROTOR POSITION #	ROTOR POSITION DEGREES	UNITS uh	ROTOR POSITION #	ROTOR POSITION DEGREES	UNITS uh	ROTOR POSITION #	ROTOR POSITION DEGREES	UNITS uh	ROTOR POSITION #	ROTOR POSITION DEGREES	UNITS uh
0	0	464	8	90	[illegible]	16	180	483	24	270	454
½		431	½		408	½		415	½		423
1	11.25	406	9	101.25	411	17	191.25	414	25	281.25	402
½		433	½		[illegible]	½		459	½		420
2	22.5	464	10	112.5	[illegible]	18	202.25	472	26	292.5	455
½		433	½		[illegible]	½		407	½		427
3	33.75	405	11	123.75	417	19	213.75	404	27	303.75	404
½		435	½		[illegible]	½		458	½		428
4	45	462	12	135	[illegible]	20	225	[illegible]	28	315	457
½		405	½		[illegible]	½		404	½		447
5	56.25	407	13	146.25	[illegible]	21	236.25	[illegible]	29	326.25	403
½		446	½		[illegible]	½		440	½		429
6	67.5	465	14	157.5	[illegible]	22	247.5	[illegible]	30	337.5	459
½		408	½		[illegible]	½		[illegible]	½		[illegible]
7	78.75	409	15	168.75	[illegible]	23	258.75	402	31	348.75	405
½		464	½		[illegible]	½		[illegible]	½		433

AVERAGE VALUE: 437.33

MAXIMUM VALUE: 489

MINIMUM VALUE: 402

L. KINTZ / B. ZELINSKI
10/26/83
ROTOR # 3

5.2a) WINDING INDUCTANCE

QUADRANT MOTOR #A - PHASE C TO NEUTRAL

READING ROTATION: CW SENSOR END

ROTOR POSITION		UNITS	ROTOR POSITION		UNITS	ROTOR POSITION		UNITS	ROTOR POSITION		UNITS
#	DEGREES	uh	#	DEGREES	uh	#	DEGREES	uh	#	DEGREES	uh
0	0	400	8	90	402	16	180	407	24	270	395
½		400	½		405	½		427	½		396
1	11.25	445	9	101.25	457	17	191.25	468	25	281.25	449
½		457	½		474	½		433	½		444
2	22.5	398	10	112.5	410	18	202.25	400	26	292.5	397
½		426	½		413	½		423	½		422
3	33.75	458	11	123.75	482	19	213.75	455	27	303.75	452
½		453	½		479	½		452	½		425
4	45	398	12	135	410	20	225	397	28	315	398
½		429	½		444	½		396	½		423
5	56.25	461	13	146.25	483	21	236.25	436	29	326.25	455
½		457	½		443	½		449	½		449
6	67.5	401	14	157.5	408	22	247.5	396	30	337.5	399
½		402	½		440	½		395	½		400
7	78.75	451	15	168.75	479	23	258.75	431	31	348.75	458
½		403	½		443	½		445	½		458

AVERAGE VALUE: 431.42

MAXIMUM VALUE: 483

MINIMUM VALUE: 395

L. KINTZ / B. ZELINSKI

10/26/83

ROTOR # 3

5.2d WINDING INDUCTANCE

QUADRANT MOTOR #B - PHASE A TO NEUTRAL

READING ROTATION: CW SENSOR END

ROTOR POSITION		UNITS	ROTOR POSITION		UNITS	ROTOR POSITION		UNITS	ROTOR POSITION		UNITS
#	DEGREES	uh	#	DEGREES	uh	#	DEGREES	uh	#	DEGREES	uh
0	0	444	8	90	447	16	180	462	24	270	456
½		472	½		478	½		497	½		488
1	11.25	468	9	101.25	472	17	191.25	460	25	281.25	453
½		415	½		417	½		430	½		418
2	22.5	416	10	112.5	446	18	202.25	466	26	292.5	446
½		474	½		480	½		507	½		475
3	33.75	469	11	123.75	475	19	213.75	477	27	303.75	444
½		416	½		419	½		430	½		416
4	45	417	12	135	451	20	225	430	28	315	446
½		476	½		486	½		501	½		473
5	56.25	472	13	146.25	480	21	236.25	443	29	326.25	415
½		417	½		422	½		427	½		415
6	67.5	449	14	157.5	453	22	247.5	460	30	337.5	440
½		480	½		487	½		447	½		469
7	78.75	448	15	168.75	450	23	258.75	484	31	348.75	440
½		419	½		423	½		428	½		414

AVERAGE VALUE: 453.5

MAXIMUM VALUE: 507

MINIMUM VALUE: 414

L. KINTZ/B. ZELINSKI

10/27/83

ROTOR # 3

5.2a) WINDING INDUCTANCE

QUADRANT MOTOR #B - PHASE B TO NEUTRAL

READING ROTATION: CW SENSOR END

ROTOR POSITION		UNITS	ROTOR POSITION		UNITS	ROTOR POSITION		UNITS	ROTOR POSITION		UNITS
#	DEGREES	uh	#	DEGREES	uh	#	DEGREES	uh	#	DEGREES	uh
0	0	464	8	90	473	16	180	479	24	270	493
½		434	½		442	½		445	½		454
1	11.25	408	9	101.25	411	17	191.25	414	25	281.25	419
½		452	½		443	½		453	½		451
2	22.5	466	10	112.5	472	18	202.25	492	26	292.5	482
½		434	½		440	½		460	½		445
3	33.75	409	11	123.75	411	19	213.75	423	27	303.75	410
½		451	½		448	½		462	½		455
4	45	469	12	135	471	20	225	501	28	315	469
½		408	½		412	½		456	½		410
5	56.25	410	13	146.25	414	21	236.25	423	29	326.25	410
½		455	½		460	½		471	½		456
6	67.5	470	14	157.5	476	22	247.5	445	30	337.5	427
½		438	½		440	½		452	½		408
7	78.75	410	15	168.75	415	23	258.75	414	31	348.75	409
½		443	½		464	½		459	½		457

AVERAGE VALUE: 445.39

MAXIMUM VALUE: 501

MINIMUM VALUE: 408

L. KINTZ / B. ZELINSKI
10/27/83
ROTOR #3

5.2o) WINDING INDUCTANCE

QUADRANT MOTOR #B - PHASE C TO NEUTRAL

READING ROTATION: CW SENSOR END

ROTOR POSITION #	DEGREES	UNITS uh	ROTOR POSITION #	DEGREES	UNITS uh	ROTOR POSITION #	DEGREES	UNITS uh	ROTOR POSITION #	DEGREES	UNITS uh
0	0	410	8	90	415	16	180	418	24	270	423
½		438	½		416	½		421	½		423
1	11.25	468	9	101.25	432	17	191.25	473	25	281.25	485
½		463	½		470	½		475	½		480
2	22.5	413	10	112.5	413	18	202.25	426	26	292.5	415
½		440	½		415	½		460	½		440
3	33.75	471	11	123.75	461	19	213.75	503	27	303.75	473
½		466	½		470	½		492	½		470
4	45	412	12	135	415	20	225	426	28	315	413
½		441	½		447	½		458	½		438
5	56.25	472	13	146.25	482	21	236.25	491	29	326.25	470
½		468	½		478	½		497	½		466
6	67.5	413	14	157.5	418	22	247.5	424	30	337.5	411
½		415	½		420	½		424	½		412
7	78.75	462	15	168.75	483	23	258.75	445	31	348.75	452
½		474	½		482	½		444	½		465

AVERAGE VALUE: 450.53

MAXIMUM VALUE: 503

MINIMUM VALUE: 411

L. KINTZ/B. ZELINSKI

10/27/83

ROTOR #3

5.2b) WINDING INDUCTANCE

QUADRANT MOTOR #C - PHASE A TO NEUTRAL

READING ROTATION: CW SENSOR END

ROTOR POSITION #	DEGREES	UNITS uh	ROTOR POSITION #	DEGREES	UNITS uh	ROTOR POSITION #	DEGREES	UNITS uh	ROTOR POSITION #	DEGREES	UNITS uh
0	0	453	8	90	411	16	180	443	24	270	458
½		487	½		460	½		476	½		495
1	11.25	451	9	101.25	464	17	191.25	475	25	281.25	489
½		413	½		412	½		413	½		426
2	22.5	441	10	112.5	422	18	202.25	414	26	292.5	462
½		477	½		473	½		455	½		505
3	33.75	470	11	123.75	461	19	213.75	477	27	303.75	462
½		414	½		413	½		444	½		425
4	45	441	12	135	414	20	225	417	28	315	461
½		474	½		472	½		482	½		500
5	56.25	470	13	146.25	440	21	236.25	454	29	326.25	461
½		413	½		413	½		419	½		422
6	67.5	439	14	157.5	414	22	247.5	452	30	337.5	455
½		472	½		475	½		486	½		498
7	78.75	441	15	168.75	467	23	258.75	476	31	348.75	460
½		412	½		414	½		417	½		423

AVERAGE VALUE: 450.33

MAXIMUM VALUE: 505

MINIMUM VALUE: 411

L. KINTZ / B. ZELINSKI

10/27/83

ROTOR #3

5.2a) WINDING INDUCTANCE

QUADRANT MOTOR #C - PHASE B TO NEUTRAL

READING ROTATION: CW SENSOR END

ROTOR POSITION		UNITS	ROTOR POSITION		UNITS	ROTOR POSITION		UNITS	ROTOR POSITION		UNITS
#	DEGREES	uh	#	DEGREES	uh	#	DEGREES	uh	#	DEGREES	uh
0	0	484	8	90	463	16	180	465	24	270	478
½		416	½		431	½		406	½		440
1	11.25	415	9	101.25	403	17	191.25	407	25	281.25	411
½		462	½		438	½		439	½		451
2	22.5	479	10	112.5	464	18	202.25	[illegible]	26	292.5	496
½		409	½		405	½		434	½		[illegible]
3	33.75	407	11	123.75	404	19	213.75	407	27	303.75	418
½		467	½		448	½		456	½		475
4	45	469	12	135	463	20	225	471	28	315	[illegible]
½		407	½		406	½		436	½		418
5	56.25	406	13	146.25	405	21	236.25	408	29	326.25	417
½		444	½		465	½		441	½		467
6	67.5	418	14	157.5	466	22	247.5	477	30	337.5	[illegible]
½		406	½		406	½		[illegible]	½		449
7	78.75	405	15	168.75	406	23	258.75	411	31	348.75	414
½		443	½		468	½		446	½		[illegible]

AVERAGE VALUE: 439.41

MAXIMUM VALUE: 495

MINIMUM VALUE: 403

L. KINTZ / B. ZELINSKI
10/27/83
ROTOR #3

5.2o) WINDING INDUCTANCE
QUADRANT MOTOR #C - PHASE C TO NEUTRAL
READING ROTATION: CW SENSOR END

ROTOR POSITION #	ROTOR POSITION DEGREES	UNITS uh	ROTOR POSITION #	ROTOR POSITION DEGREES	UNITS uh	ROTOR POSITION #	ROTOR POSITION DEGREES	UNITS uh	ROTOR POSITION #	ROTOR POSITION DEGREES	UNITS uh
0	0	421	8	90	437	16	180	413	24	270	417
½		449	½		411	½		414	½		452
1	11.25	485	9	101.25	[illegible]	17	191.25	475	25	281.25	493
½		483	½		469	½		475	½		486
2	22.5	415	10	112.5	[illegible]	18	202.25	412	26	292.5	425
½		412	½		411	½		414	½		461
3	33.75	475	11	123.75	456	19	213.75	464	27	303.75	501
½		473	½		441	½		477	½		497
4	45	413	12	135	411	20	225	415	28	315	424
½		413	½		439	½		416	½		456
5	56.25	458	13	146.25	413	21	236.25	481	29	326.25	497
½		472	½		471.	½		481	½		492
6	67.5	411	14	157.5	412	22	247.5	419	30	337.5	423
½		411	½		412	½		419	½		422
7	78.75	458	15	168.75	476	23	258.75	484	31	348.75	479
½		468	½		475	½		478	½		495

AVERAGE VALUE: 449.2

MAXIMUM VALUE: 501

MINIMUM VALUE: 411

L. KINTZ / B. ZELINSKI
10/27/83
ROTOR # 3

5.2b) WINDING INDUCTANCE

QUADRANT MOTOR # D - PHASE C TO A

READING ROTATION: CW SENSOR END

ROTOR POSITION		UNITS	ROTOR POSITION		UNITS	ROTOR POSITION		UNITS	ROTOR POSITION		UNITS
#	DEGREES	uh	#	DEGREES	uh	#	DEGREES	uh	#	DEGREES	uh
0	0	1145	8	90	1150	16	180	1105	24	270	1125
½		1235	½		1230	½		1140	½		1215
1	11.25	1410	9	101.25	1345	17	191.25	1360	25	281.25	1390
½		1240	½		1195	½		1140	½		1195
2	22.5	1175	10	112.5	1115	18	202.25	1105	26	292.5	1125
½		1260	½		1200	½		1200	½		1360
3	33.75	1430	11	123.75	1365	19	213.75	1340	27	303.75	1360
½		1240	½		1200	½		1180	½		1130
4	45	1165	12	135	1120	20	225	1105	28	315	1150
½		1390	½		1200	½		1195	½		1370
5	56.25	1380	13	146.25	1355	21	236.25	1340	29	326.25	1370
½		1200	½		1155	½		1185	½		1195
6	67.5	1160	14	157.5	1100	22	247.5	1120	30	337.5	1135
½		1235	½		1180	½		1215	½		1230
7	78.75	1410	15	168.75	1370	23	258.75	1400	31	348.75	1310
½		1230	½		1180	½		1190	½		1215

AVERAGE VALUE: 1238.75

MAXIMUM VALUE: 1430

MINIMUM VALUE: 1100

L. KINTZ / B. ZELINSKI

11/7/83

ROTOR #3

5.2a) WINDING INDUCTANCE
QUADRANT MOTOR #A - PHASE A TO NEUTRAL
READING ROTATION: CW SENSOR END

ROTOR POSITION		UNITS	ROTOR POSITION		UNITS	ROTOR POSITION		UNITS	ROTOR POSITION		UNITS
#	DEGREES	uh	#	DEGREES	uh	#	DEGREES	uh	#	DEGREES	uh
0	0	434	8	90	430	16	180	435	24	270	442
½		490	½		488	½		465	½		510
1	11.25	492	9	101.25	489	17	191.25	502	25	281.25	470
½		430	½		433	½		466	½		440
2	22.5	449	10	112.5	455	18	202.25	436	26	292.5	442
½		485	½		460	½		465	½		508
3	33.75	452	11	123.75	495	19	213.75	504	27	303.75	468
½		426	½		457	½		439	½		440
4	45	427	12	135	434	20	225	465	28	315	441
½		480	½		463	½		509	½		507
5	56.25	481	13	146.25	497	21	236.25	509	29	326.25	502
½		426	½		434	½		439	½		439
6	67.5	428	14	157.5	436	22	247.5	441	30	337.5	464
½		481	½		464	½		510	½		501
7	78.75	483	15	168.75	501	23	258.75	510	31	348.75	501
½		430	½		460	½		440	½		434

AVERAGE VALUE: 464.67

MAXIMUM VALUE: 510

MINIMUM VALUE: 426

L. KINTZ
11/17/83
ROTOR #2

5.2a) **WINDING INDUCTANCE**
QUADRANT MOTOR #A - PHASE B TO NEUTRAL
READING ROTATION: CW SENSOR END

ROTOR POSITION #	ROTOR POSITION DEGREES	UNITS uh	ROTOR POSITION #	ROTOR POSITION DEGREES	UNITS uh	ROTOR POSITION #	ROTOR POSITION DEGREES	UNITS uh	ROTOR POSITION #	ROTOR POSITION DEGREES	UNITS uh
0	0	478	8	90	447	16	180	477	24	270	487
½		443	½		461	½		478	½		447
1	11.25	415	9	101.25	429	17	191.25	439	25	281.25	423
½		436	½		412	½		416	½		454
2	22.5	470	10	112.5	438	18	202.25	478	26	292.5	488
½		438	½		466	½		478	½		447
3	33.75	412	11	123.75	433	19	213.75	417	27	303.75	422
½		434	½		414	½		443	½		452
4	45	464	12	135	472	20	225	481	28	315	487
½		463	½		472	½		446	½		446
5	56.25	431	13	146.25	415	21	236.25	421	29	326.25	421
½		411	½		416	½		485	½		450
6	67.5	452	14	157.5	475	22	247.5	486	30	337.5	484
½		458	½		474	½		446	½		447
7	78.75	428	15	168.75	416	23	258.75	422	31	348.75	420
½		409	½		440	½		475	½		446

AVERAGE VALUE: 447.36
MAXIMUM VALUE: 488
MINIMUM VALUE: 409

L. KINTZ
11/17/83
ROTOR # 2

5.2o) WINDING INDUCTANCE
QUADRANT MOTOR #A - PHASE C TO NEUTRAL
READING ROTATION: CW SENSOR END

ROTOR POSITION		UNITS	ROTOR POSITION		UNITS	ROTOR POSITION		UNITS	ROTOR POSITION		UNITS
#	DEGREES	uh	#	DEGREES	uh	#	DEGREES	uh	#	DEGREES	uh
0	0	433	8	90	422	16	180	431	24	270	439
½		409	½		405	½		411	½		417
1	11.25	434	9	101.25	429	17	191.25	439	25	281.25	444
½		465	½		462	½		474	½		482
2	22.5	428	10	112.5	426	18	202.25	433	26	292.5	416
½		406	½		407	½		410	½		416
3	33.75	429	11	123.75	434	19	213.75	440	27	303.75	482
½		461	½		468	½		476	½		480
4	45	425	12	135	430	20	225	413	28	315	414
½		403	½		409	½		415	½		438
5	56.25	426	13	146.25	409	21	236.25	482	29	326.25	480
½		455	½		472	½		481	½		479
6	67.5	402	14	157.5	470	22	247.5	438	30	337.5	414
½		403	½		409	½		416	½		414
7	78.75	426	15	168.75	439	23	258.75	446	31	348.75	441
½		456	½		474	½		481	½		474

AVERAGE VALUE: 438.16

MAXIMUM VALUE: 482

MINIMUM VALUE: 402

L. KINTZ
11/17/83
ROTOR # 2

5.2b) WINDING INDUCTANCE

QUADRANT MOTOR #A - PHASE A TO B

READING ROTATION: CW SENSOR END

ROTOR POSITION		UNITS	ROTOR POSITION		UNITS	ROTOR POSITION		UNITS	ROTOR POSITION		UNITS
#	DEGREES	uh	#	DEGREES	uh	#	DEGREES	uh	#	DEGREES	uh
0	0	1135	8	90	1110	16	180	1085	24	270	1260
½		1245	½		1235	½		1270	½		1255
1	11.25	1130	9	101.25	1110	17	191.25	1150	25	281.25	1070
½		1040	½		1035	½		1055	½		1070
2	22.5	1120	10	112.5	1120	18	202.25	1160	26	292.5	1260
½		1230	½		1240	½		1280	½		1255
3	33.75	1110	11	123.75	1245	19	213.75	1155	27	303.75	1020
½		1030	½		1040	½		1060	½		1070
4	45	1120	12	135	1135	20	225	1145	28	315	1150
½		1220	½		1235	½		1270	½		1250
5	56.25	1100	13	146.25	1240	21	236.25	1150	29	326.25	1065
½		1020	½		1040	½		1070	½		1100
6	67.5	1205	14	157.5	1095	22	247.5	1160	30	337.5	1150
½		1215	½		1280	½		1250	½		1245
7	78.75	1105	15	168.75	1235	23	258.75	1075	31	348.75	1140
½		1025	½		1050	½		1080	½		1055

AVERAGE VALUE: 1146.48

MAXIMUM VALUE: 1280

MINIMUM VALUE: 1020

L. KINTZ
11/17/83
ROTOR #2

5.2b) WINDING INDUCTANCE
QUADRANT ROTOR # A - PHASE B TO C
READING ROTATION: CW SENSOR END

ROTOR POSITION #	DEGREES	UNITS uh	ROTOR POSITION #	DEGREES	UNITS uh	ROTOR POSITION #	DEGREES	UNITS uh	ROTOR POSITION #	DEGREES	UNITS uh
0	0	1365	8	90	1340	16	180	1440	24	270	1380
½		1140	½		1115	½		1240	½		1170
1	11.25	1145	9	101.25	1120	17	191.25	1160	25	281.25	1170
½		1370	½		1355	½		1290	½		1400
2	22.5	1350	10	112.5	1360	18	202.25	1445	26	292.5	1260
½		1125	½		1135	½		1245	½		1175
3	33.75	1125	11	123.75	1140	19	213.75	1150	27	303.75	1170
½		1365	½		1375	½		1395	½		1395
4	45	1350	12	135	1245	20	225	1275	28	315	1370
½		1115	½		1140	½		1165	½		1170
5	56.25	1110	13	146.25	1140	21	236.25	1255	29	326.25	1220
½		1370	½		1370	½		1395	½		1400
6	67.5	1340	14	157.5	1375	22	247.5	1380	30	337.5	1265
½		1100	½		1245	½		1170	½		1155
7	78.75	1210	15	168.75	1145	23	258.75	1170	31	348.75	1155
½		1365	½		1260	½		1405	½		1375

AVERAGE VALUE: 1260.7

MAXIMUM VALUE: 1445

MINIMUM VALUE: 1100

L. KINTZ
11/17/83
ROTOR # 2

5.2b) WINDING INDUCTANCE

QUADRANT MOTOR # A - PHASE C TO A

READING ROTATION: CW SENSOR END

ROTOR POSITION		UNITS	ROTOR POSITION		UNITS	ROTOR POSITION		UNITS	ROTOR POSITION		UNITS
#	DEGREES	uh	#	DEGREES	uh	#	DEGREES	uh	#	DEGREES	uh
0	0	1135	8	90	1115	16	180	1140	24	270	1170
½		1230	½		1230	½		1155	½		1270
1	11.25	1360	9	101.25	1375	17	191.25	1420	25	281.25	1400
½		1220	½		1220	½		1385	½		1260
2	22.5	1125	10	112.5	1120	18	202.25	1140	26	292.5	1170
½		1210	½		1235	½		1150	½		1270
3	33.75	1360	11	123.75	1380	19	213.75	1415	27	303.75	1380
½		1205	½		1230	½		1260	½		1240
4	45	1105	12	135	1135	20	225	1160	28	315	1160
½		1210	½		1235	½		1270	½		1250
5	56.25	1390	13	146.25	1380	21	236.25	1385	29	326.25	1380
½		1195	½		1245	½		1250	½		1245
6	67.5	1095	14	157.5	1150	22	247.5	1160	30	337.5	1155
½		1210	½		1150	½		1265	½		1250
7	78.75	1355	15	168.75	1405	23	258.75	1390	31	348.75	1390
½		1200	½		1250	½		1260	½		1230

AVERAGE VALUE: 1248.2

MAXIMUM VALUE: 1420

MINIMUM VALUE: 1095

L. KINTZ
11/17/83
ROTOR #2

5.2) WINDING INDUCTANCE
QUADRANT MOTORS A, B, C & D. PHASE "A" WINDINGS
SERIES CONNECTED.

ROTOR POSITION		UNITS	ROTOR POSITION		UNITS	ROTOR POSITION		UNITS	ROTOR POSITION		UNITS
#	DEGREES	uh	#	DEGREES	uh	#	DEGREES	uh	#	DEGREES	uh
0	0	1880	8	90	1955	16	180	1890	24	270	1885
½		2180	½		2180	½		2280	½		2180
1	11.25	2100	9	101.25	2175	17	191.25	2150	25	281.25	1980
½		1870	½		1875	½		1880	½		1880
2	22.5	1890	10	112.5	1950	18	202.25	2050	26	292.5	1960
½		2165	½		2170	½		2255	½		2180
3	33.75	1955	11	123.75	2170	19	213.75	1955	27	303.75	1950
½		1880	½		1880	½		1890	½		1880
4	45	1950	12	135	1885	20	225	2035	28	315	1965
½		2165	½		2175	½		2290	½		2180
5	56.25	1975	13	146.25	2165	21	236.25	2075	29	326.25	1960
½		1885	½		1875	½		1880	½		1880
6	67.5	1885	14	157.5	1890	22	247.5	1955	30	337.5	1945
½		2175	½		1950	½		2180	½		2175
7	78.75	1950	15	168.75	2275	23	258.75	2185	31	348.75	2175
½		1875	½		1885	½		1880	½		1880

AVERAGE VALUE: 2017.5

MAXIMUM VALUE: 2290

MINIMUM VALUE: 1870

L. KINTZ
11/18/83
ROTOR #2

5.2) WINDING INDUCTANCE

QUADRANT MOTORS A, B, C & D. PHASE "B" WINDINGS SERIES CONNECTED.

ROTOR POSITION		UNITS	ROTOR POSITION		UNITS	ROTOR POSITION		UNITS	ROTOR POSITION		UNITS
#	DEGREES	uh	#	DEGREES	uh	#	DEGREES	uh	#	DEGREES	uh
0	0	2180	8	90	2170	16	180	2250	24	270	2170
½		1990	½		1950	½		2045	½		1950
1	11.25	1875	9	101.25	1870	17	191.25	1875	25	281.25	1880
½		1965	½		1960	½		1880	½		1960
2	22.5	2175	10	112.5	2165	18	202.25	2255	26	292.5	2170
½		1975	½		1945	½		2035	½		1955
3	33.75	1880	11	123.75	1880	19	213.75	1870	27	303.75	1880
½		1965	½		1955	½		2050	½		1980
4	45	2175	12	135	2175	20	225	2170	28	315	2175
½		1950	½		1960	½		2040	½		1950
5	56.25	1880	13	146.25	1880	21	236.25	1880	29	326.25	1875
½		1970	½		1950	½		1975	½		1980
6	67.5	2180	14	157.5	2230	22	247.5	2175	30	337.5	2175
½		1955	½		1970	½		1950	½		1960
7	78.75	1880	15	168.75	1880	23	258.75	1875	31	348.75	1880
½		1965	½		1890	½		1980	½		1950

AVERAGE VALUE: 1999.77 L. KINTZ

MAXIMUM VALUE: 2255 11/18/83

MINIMUM VALUE: 1870 ROTOR #2

5.2) WINDING INDUCTANCE
QUADRANT MOTORS A, B, C & D. PHASE "A" & "B" WINDINGS
SERIES CONNECTED.

ROTOR POSITION		UNITS	ROTOR POSITION		UNITS	ROTOR POSITION		UNITS	ROTOR POSITION		UNITS
#	DEGREES	uh	#	DEGREES	uh	#	DEGREES	uh	#	DEGREES	uh
0	0	4540	8	90	4550	16	180	4720	24	270	4920
½		4920	½		4920	½		5450	½		4940
1	11.25	4525	9	101.25	4395	17	191.25	4695	25	281.25	4255
½		4265	½		4255	½		4280	½		4355
2	22.5	4530	10	112.5	4550	18	202.25	4720	26	292.5	4930
½		4920	½		4930	½		5260	½		4580
3	33.75	4520	11	123.75	4530	19	213.75	4260	27	303.75	4270
½		4250	½		4260	½		4290	½		4320
4	45	4910	12	135	4550	20	225	5260	28	315	4935
½		4925	½		4970	½		5315	½		4970
5	56.25	4260	13	146.25	4550	21	236.25	4345	29	326.25	4275
½		4255	½		4260	½		4260	½		4275
6	67.5	4545	14	157.5	4545	22	247.5	4925	30	337.5	4920
½		4935	½		4930	½		4940	½		4955
7	78.75	4520	15	168.75	4625	23	258.75	4260	31	348.75	4535
½		4255	½		4285	½		4260	½		4270

AVERAGE VALUE: 4611.33 L. KINTZ
MAXIMUM VALUE: 5450 11/18/83
MINIMUM VALUE: 4250 ROTOR #2

5.2a) WINDING INDUCTANCE

QUADRANT MOTOR #A - PHASE A TO NEUTRAL

READING ROTATION: CW SENSOR END

ROTOR POSITION		UNITS	ROTOR POSITION		UNITS	ROTOR POSITION		UNITS	ROTOR POSITION		UNITS
#	DEGREES	uh	#	DEGREES	uh	#	DEGREES	uh	#	DEGREES	uh
0	0	457	8	90	454	16	180	464	24	270	506
½		494	½		488	½		500	½		498
1	11.25	457	9	101.25	428	17	191.25	460	25	281.25	440
½		432	½		434	½		437	½		441
2	22.5	453	10	112.5	435	18	202.25	466	26	292.5	489
½		488	½		486	½		501	½		504
3	33.75	455	11	123.75	494	19	213.75	463	27	303.75	439
½		430	½		435	½		440	½		439
4	45	454	12	135	436	20	225	507	28	315	471
½		483	½		496	½		505	½		503
5	56.25	450	13	146.25	496	21	236.25	439	29	326.25	440
½		428	½		460	½		440	½		439
6	67.5	452	14	157.5	434	22	247.5	506	30	337.5	467
½		483	½		499	½		506	½		499
7	78.75	456	15	168.75	467	23	258.75	440	31	348.75	460
½		429	½		436	½		440	½		434

AVERAGE VALUE: 464.25

MAXIMUM VALUE: 507

MINIMUM VALUE: 428

L. KINTZ / B. ZELINSKI

12/9/83

ROTOR #2

NOTE: STATOR BORED TO 3.180

5.2o) WINDING INDUCTANCE

QUADRANT MOTOR #A - PHASE B TO NEUTRAL

READING ROTATION: CW SENSOR END

ROTOR POSITION #	ROTOR POSITION DEGREES	UNITS uh	ROTOR POSITION #	ROTOR POSITION DEGREES	UNITS uh	ROTOR POSITION #	ROTOR POSITION DEGREES	UNITS uh	ROTOR POSITION #	ROTOR POSITION DEGREES	UNITS uh
0	0	477	8	90	462	16	180	475	24	270	476
½		417	½		437	½		450	½		420
1	11.25	417	9	101.25	411	17	191.25	416	25	281.25	421
½		470	½		433	½		440	½		484
2	22.5	471	10	112.5	468	18	202.25	477	26	292.5	476
½		414	½		437	½		440	½		419
3	33.75	412	11	123.75	413	19	213.75	417	27	303.75	443
½		451	½		436	½		459	½		483
4	45	466	12	135	472	20	225	479	28	315	469
½		430	½		436	½		418	½		419
5	56.25	410	13	146.25	414	21	236.25	419	29	326.25	421
½		429	½		439	½		465	½		469
6	67.5	462	14	157.5	474	22	247.5	482	30	337.5	480
½		431	½		464	½		420	½		420
7	78.75	409	15	168.75	416	23	258.75	420	31	348.75	418
½		431	½		439	½		484	½		447

AVERAGE VALUE: 443.34

MAXIMUM VALUE: 484

MINIMUM VALUE: 409

L. KINTZ / B. ZELINSKI

12/13/83

ROTOR #2

NOTE: STATOR BORED TO 3.180

5.2d) WINDING INDUCTANCE

QUADRANT MOTOR #A - PHASE C TO NEUTRAL

READING ROTATION: CW SENSOR END

ROTOR POSITION		UNITS	ROTOR POSITION		UNITS	ROTOR POSITION		UNITS	ROTOR POSITION		UNITS
#	DEGREES	uh	#	DEGREES	uh	#	DEGREES	uh	#	DEGREES	uh
0	0	409	8	90	425	16	180	434	24	270	413
½		431	½		405	½		409	½		445
1	11.25	467	9	101.25	431	17	191.25	437	25	281.25	478
½		432	½		464	½		472	½		440
2	22.5	407	10	112.5	427	18	202.25	410	26	292.5	414
½		428	½		407	½		411	½		443
3	33.75	461	11	123.75	434	19	213.75	474	27	303.75	479
½		460	½		468	½		435	½		440
4	45	406	12	135	436	20	225	412	28	315	413
½		422	½		409	½		444	½		436
5	56.25	457	13	146.25	433	21	236.25	479	29	326.25	476
½		457	½		469	½		436	½		440
6	67.5	423	14	157.5	438	22	247.5	413	30	337.5	413
½		404	½		409	½		442	½		436
7	78.75	428	15	168.75	437	23	258.75	479	31	348.75	473
½		458	½		472	½		441	½		465

AVERAGE VALUE: 438.22

MAXIMUM VALUE: 479

MINIMUM VALUE: 404

L. KINTZ / B. ZELINSKI

12/13/83

ROTOR #2

NOTE: STATOR BORED TO 3.180

5.2) WINDING INDUCTANCE

QUADRANT ROTORS A, B, C & D. PHASE "A" WINDINGS SERIES CONNECTED.

ROTOR POSITION #	ROTOR POSITION DEGREES	UNITS uh	ROTOR POSITION #	ROTOR POSITION DEGREES	UNITS uh	ROTOR POSITION #	ROTOR POSITION DEGREES	UNITS uh	ROTOR POSITION #	ROTOR POSITION DEGREES	UNITS uh
0	0	1965	8	90	1880	16	180	1975	24	270	2180
½		2190	½		1970	½		2200	½		2180
1	11.25	1950	9	101.25	2170	17	191.25	2090	25	281.25	1880
½		1880	½		1960	½		1885	½		1890
2	22.5	1960	10	112.5	1885	18	202.25	1880	26	292.5	2075
½		2180	½		2080	½		2175	½		2185
3	33.75	1960	11	123.75	2180	19	213.75	1995	27	303.75	1970
½		1880	½		1880	½		1890	½		1890
4	45	1965	12	135	1880	20	225	1980	28	315	1980
½		2175	½		2180	½		2190	½		2185
5	56.25	2090	13	146.25	2115	21	236.25	1970	29	326.25	1960
½		1885	½		1895	½		1890	½		1880
6	67.5	1895	14	157.5	1890	22	247.5	1960	30	337.5	1970
½		2180	½		2115	½		2185	½		2190
7	78.75	2160	15	168.75	2180	23	258.75	1960	31	348.75	1970
½		1950	½		1890	½		1880	½		1880

AVERAGE VALUE: 2012.27

MAXIMUM VALUE: 2200

MINIMUM VALUE: 1880

L. KINTZ / B. ZELINSKI

12/13/83

ROTOR #2

NOTE: STATOR BORED TO 3.180

5.2) WINDING INDUCTANCE

QUADRANT MOTORS A, B, C & D. PHASE "B" WINDINGS SERIES CONNECTED.

ROTOR POSITION		UNITS	ROTOR POSITION		UNITS	ROTOR POSITION		UNITS	ROTOR POSITION		UNITS
#	DEGREES	uh	#	DEGREES	uh	#	DEGREES	uh	#	DEGREES	uh
0	0	2180	8	90	1880	16	180	1960	24	270	2170
½		1980	½		2170	½		2190	½		1880
1	11.25	1880	9	101.25	2180	17	191.25	1970	25	281.25	1870
½		1945	½		1870	½		1890	½		2180
2	22.5	2185	10	112.5	1890	18	202.25	2170	26	292.5	2200
½		2090	½		2170	½		2160	½		1880
3	33.75	1880	11	123.75	2105	19	213.75	1870	27	303.75	1895
½		1875	½		1875	½		1960	½		2200
4	45	2080	12	135	1880	20	225	2180	28	315	2185
½		2185	½		2100	½		1960	½		1950
5	56.25	1960	13	146.25	2180	21	236.25	1880	29	326.25	1880
½		1880	½		1870	½		1960	½		1960
6	67.5	1960	14	157.5	1880	22	247.5	2190	30	337.5	2170
½		2155	½		2160	½		1960	½		1995
7	78.75	2065	15	168.75	2105	23	258.75	1825	31	348.75	1870
½		1825	½		1880	½		1990	½		1980

AVERAGE VALUE: 2012.81

MAXIMUM VALUE: 2200

MINIMUM VALUE: 1870

L. KINTZ / B. ZELINSKI

12/13/83

ROTOR #2

NOTE: STATOR BORED TO 3.180

5.2) WINDING INDUCTANCE

QUADRANT MOTORS A, B, C & D. PHASE "A" & "B" WINDINGS SERIES CONNECTED.

ROTOR POSITION		UNITS	ROTOR POSITION		UNITS	ROTOR POSITION		UNITS	ROTOR POSITION		UNITS
#	DEGREES	uh	#	DEGREES	uh	#	DEGREES	uh	#	DEGREES	uh
0	0	4555	8	90	4290	16	180	4290	24	270	4985
½		5060	½		4585	½		4850	½		4600
1	11.25	4565	9	101.25	5075	17	191.25	4590	25	281.25	4280
½		4270	½		4540	½		4280	½		4600
2	22.5	4575	10	112.5	4280	18	202.25	4580	26	292.5	5080
½		4975	½		4570	½		4980	½		4595
3	33.75	4555	11	123.75	4970	19	213.75	4585	27	303.75	4280
½		4275	½		4600	½		4285	½		4290
4	45	4575	12	135	4270	20	225	4950	28	315	4960
½		4990	½		4545	½		4960	½		4965
5	56.25	4570	13	146.25	5090	21	236.25	4290	29	326.25	4400
½		4285	½		4585	½		4290	½		4285
6	67.5	4575	14	157.5	4280	22	247.5	4950	30	337.5	4590
½		4965	½		4575	½		4965	½		4965
7	78.75	4965	15	168.75	4990	23	258.75	4300	31	348.75	4600
½		4415	½		4370	½		4550	½		4280

AVERAGE VALUE: 4612.89

MAXIMUM VALUE: 5090

MINIMUM VALUE: 4270

L. KINTZ / B. ZELINSKI
12/13/83
ROTOR #2

NOTE: STATOR BORED TO 3.180

DIELECTRIC STRENGTH DATA

5.3) DIELECTRIC STRENGTH

a) Motor Winding Test

Quadrant motors A,B,C & D neutral leads are designated below as A,B,C & D.

1) INSULATION RESISTANCE TEST

TEST POINTS	MEG OHMS	TEST POINTS	MEG OHMS	TEST POINTS	MEG OHMS	TEST POINTS	MEG OHMS
A-GND	30K	A - B	68 K	B - C	30 K	C - D	33 K
B-GND	23.8K	A - C	35K	B - D	65K	---	---
C-GND	24 K	A - D	35K	---	---	---	---
D-GND	75K	---	---	---	---	---	---

2) HIGH POTENTIAL TEST

TEST POINTS	m a	TEST POINTS	m a	TEST POINTS	m a	TEST POINTS	m a
A-GND	1.25	A - B	0.78	B - C	0.72	C - D	0.77
B-GND	1.2	A - C	0.78	B - D	0.75	---	---
C-GND	1.25	A - D	0.79	---	---	---	---
D-GND	1.25	---	---	---	---	---	---

3) INSULATION RESISTANCE RETEST

TEST POINTS	MEG OHMS	TEST POINTS	MEG OHMS	TEST POINTS	MEG OHMS	TEST POINTS	MEG OHMS
A-GND	70K	A - B	125K	B - C	35K	C - D	20K
B-GND	25K	A - C	100K	B - D	19K	---	---
C-GND	25K	A - D	90K	---	---	---	---
D-GND	100K	---	---	---	---	---	---

P.M.G. SPEED VS. VOLTAG OUTPUT DATA

5.4) P.M.G. SPEED VS. VOLTAGE OUTPUT

TEST SUMMARY

1) ROTOR #3 (11-14-83)

P.M.G. voltage values were obtained using the first available rotor. Rotor #3 had some containment epoxy-wrap deficiencies, however it allowed obtaining preliminary speed vs. voltage values.

2) ROTOR #2 (12-7-83)

A runout of approximately .003 inches was observed on the lead end of the stator core I.D. The core was then ground to 3.180 inches concentric to the stator housing pilot diameter. Upon completion, the generated voltage test was run using the final configuration rotor balance assembly.

All photographs and harmonic analysis data pertain to this rotor configuration only.

5.4) P.M.G. SPEED VS. VOLTAGE OUTPUT

PHOTOGRAPH VS. HARMONIC ANALYSIS CROSS REFERENCE TABLE

PHOTO NUMBER	SPEED (R.P.M.)	LOAD (AMPS)	QUADRANT MOTOR	MOTOR CONNECTION	HARMONIC ANALYSIS GRAPH NUMBER
5.4-A-1	1667	0	A	A-N	5.4-A-1, -9
-2	1640	↓	↓	B-N	-2
-3	1661			C-N	-3
-4	1667		B	A-N	-4
-5	1655		↓	B-N	-5
-6	1645			C-N	-6
-7	1668		C	A-N	-7
-8	1671		D	A-N	-8
5.4-B-1	4333	0	A	A-N	5.4-B-1
-2	4337	↓	↓	B-N	
-3	4335			C-N	
5.4-B-4	4336		B	A-N	5.4-B-2
-5	4347		↓	B-N	
-6	4329			C-N	
-7	4346		C	A-N	5.4-B-3
-8	4338		D	A-N	5.4-B-4
5.4-C-1	10008	0	A	A-N	5.4-C-1
-2	10001	↓	↓	B-N	
-3	9998			C-N	
5.4-C-4	9930		B	A-N	5.4-C-2
-5	9938		↓	B-N	
-6	9960			C-N	
-7	10080		C	A-N	5.4-C-3
-8	10024		D	A-N	5.4-C-4
5.4-D-1	1665	0	A	A-B	5.4-A-10
-2	1664	↓	↓	B-C	
-3	1674			C-A	
5.4-E-1	4342	0	A	A-B	
-2	4352	↓	↓	B-C	
-3	4365			C-A	
5.4-F-1	9210	0	A	A-B	
-2	9178	↓	↓	B-C	
-3	9170			C-A	

5.4) P.M.G. SPEED VS. VOLTAGE OUTPUT

HARMONIC ANALYSIS MAGNITUDE SUMMARY

N = ungrounded harmonic analyzer

Y = grounded harmonic analyzer

GRAPH NUMBER	SPEED (R.P.M.)	LOAD (AMPS)	QUADRANT MOTOR	MOTOR CONNECTION	GND	(HARMONIC) 3rd	5th	7th
A) 1666 RPM DATA POINT								
5.4-A-1	1645	0	A	A-N	Y	8.4	10.5	.8
-2	1650	↓	↓	B-N	↓	8.2	10	.78
-3	1660			C-N		8.0		.78
-4	1660		B	A-N		8.2	↓	.76
-5	1650		↓	B-N		8.2		.73
-6	1650			C-N		8.4		.74
-7	1665		C	A-N		8.2		.70
-8	1660		D	↓		8.2		.76
-9	1663		A		N	8.2		.72
-10	1674		A	A-B	N	.076		.78
B) 4333 RPM DATA POINT								
5.4-B-1	4335	0	A	A-N	Y	8.6	10	.90
-2	4333	↓	B	↓	↓	8.8	10	.88
-3	4325		C			8.2	9.8	.73
-4	4372		D			8.4	10	.78
C) 10,000 RPM DATA POINT								
5.4-C-1	10020	0	A	A-N	Y	7.8	10	.89
-2	9930	↓	B	↓	↓	8.8	9.8	.97
-3	10087		C			8.8	9.9	.85
-4	10024		D			8.0	10	.85

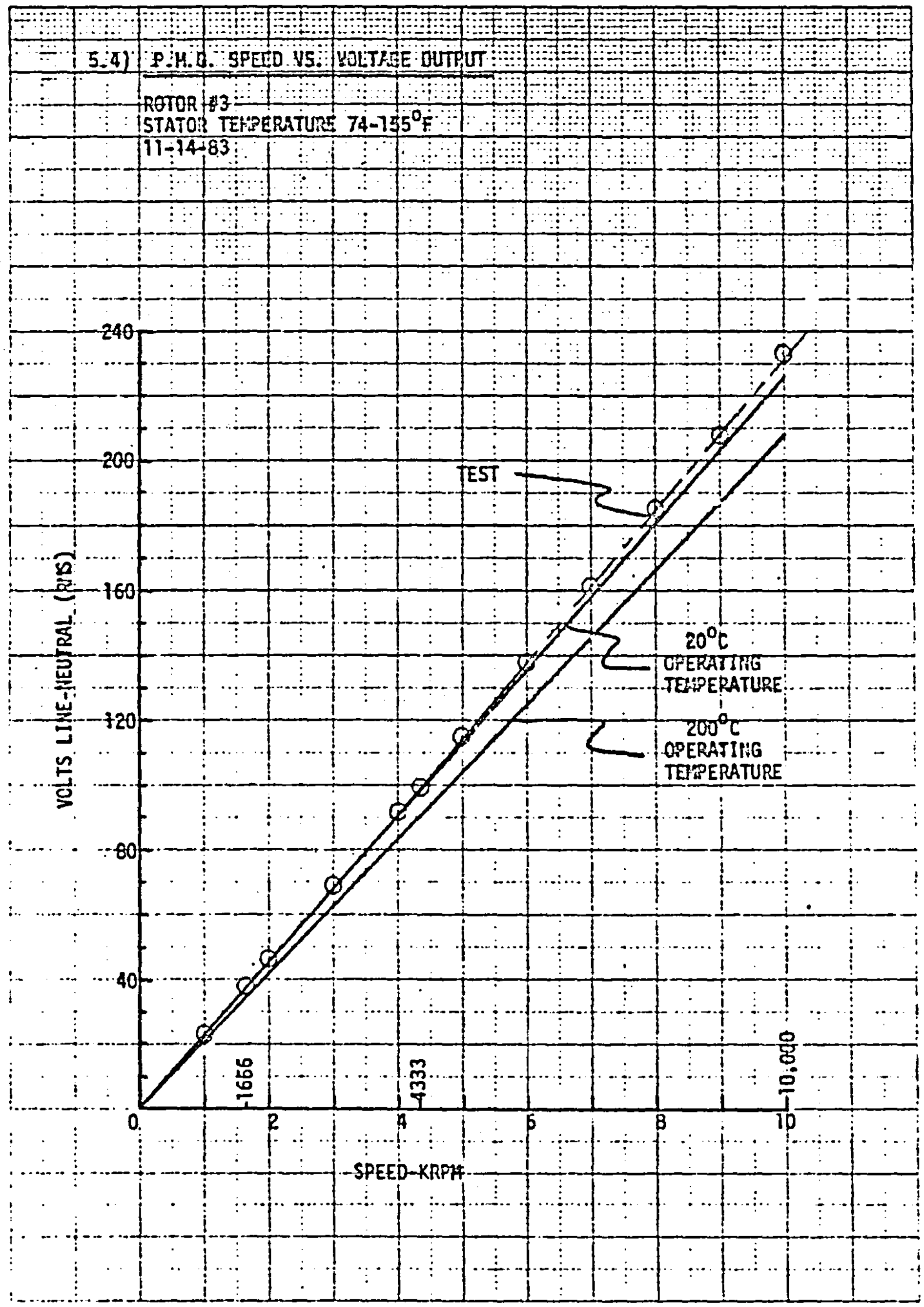

5.4) P.M.G. SPEED VS. VOLTAGE OUTPUT
ROTOR #3
STATOR TEMPERATURE 74-155°F
11-14-83
240
200
160
120
80
40
0
VOLTS LINE-NEUTRAL (RMS)
TEST
20°C
OPERATING
TEMPERATURE
200°C
OPERATING
TEMPERATURE
1666
4333
10,000
2
4
6
8
10
SPEED-KRPM

5.4) P.M.G. SPEED V.S. VOLTAGE OUTPUT

a) Phase Voltage Output

L. KINTZ, K. GARC
11/4/83
ROTOR #3 (6'10")

SPEED (r.p.m.)		TEMP	TORQUE	MOTOR A				SPEED r.p.m.	TEMP	TORQUE	MOTOR B			
DESIRED	ACTUAL	°F	IN-LBS	Van	Vbn	Vcn	Vave	ACTUAL	°F	IN-LBS	Van	Vbn	Vcn	Vave
1665	1666	—	5.425	38	38	38	38	1666	77	4.625	38	38	38	38
2000	2K	—	5.7	46	46	46	46	2K	78	5.	46	46	46	46
4000	4K	—	7.2	91	92	92	92	4K	86	6.8	91	91	91	91
4333	4333	—	7.45	98	99	99	99	4333	90	7.	99	99	99	99
6000	6K	119	8.525	137	138	138	138	6K	107	8.15	136	136	137	136
8000	8K	125	10.3	184	185	185	185	8K	126	9.5	183	184	184	184
10,000	10K	151	11.4	232	233	233	233	10K	153	10.7	231	231	232	231
1K	1K	—	4.7	23	23	23	23	1K	74	4.	23	23	23	23
3K	3K	—	6.55	69	69	69	69	3K	81	5.95	68	68	69	68
5K	5K	—	7.85	115	115	116	115	5K	99	7.35	114	114	114	114
7K	7K	113	9.8	160	161	161	161	7K	113	8.8	159	[illegible]	159	159
9K	9K	137	10.625	207	208	[illegible]	208	9K	138	10.1	207	208	208	208

TEMP. BY WINDING T.C.

5.4) P.M.G. SPEED V.S. VOLTAGE OUTPUT

a) Phase Voltage Output

SPEED (r.p.m.)		TEMP	TORQUE	MOTOR C				SPEED r.p.m.	TEMP	TORQUE	MOTOR D			
DESIRED	ACTUAL	°F	IN-LBS	Van	Vbn	Vcn	Vave	ACTUAL	°F	IN-LBS	Van	Vbn	Vcn	Vave
1666	1666	93	4.475	38	38	38	38	1666	93	4.25	38	38	38	38
2000	2K	93	4.75	45	45	45	45	2K	95	4.5	45	45	45	45
4000	4K	97	6.55	91	91	91	91	4K	101	6.2	91	91	91	91
4333	4333	101	6.75	99	99	99	99	4333	107	6.45	98	98	98	98
6000	6K	111	8.	136	136	137	136	6K	118	7.55	135	136	136	136
8000	8K	126	9.35	183	183	183	183	8K	136	8.9	182	183	183	183
10,000	10K	147	10.575	230	230	230	230	10K	155	10.2	230	230	230	230
1K	1K	92	3.8	23	23	23	23	1K	92	3.6	22	22	22	22
3K	3K	96	5.7	68	68	68	68	3K	96	5.35	68	68	68	68
5K	5K	105	7.275	114	114	114	114	5K	111	6.8	113	114	114	114
7K	7K	117	8.75	158	159	159	159	7K	128	8.2	158	159	159	159
9K	9K	137	9.85	206	207	207	207	9K	147	9.45	206	207	207	207

TEMP. BY WINDING T.C.

L. KINTZ / K. GABE
11/14/83
ROTOR # 3 (6'10')

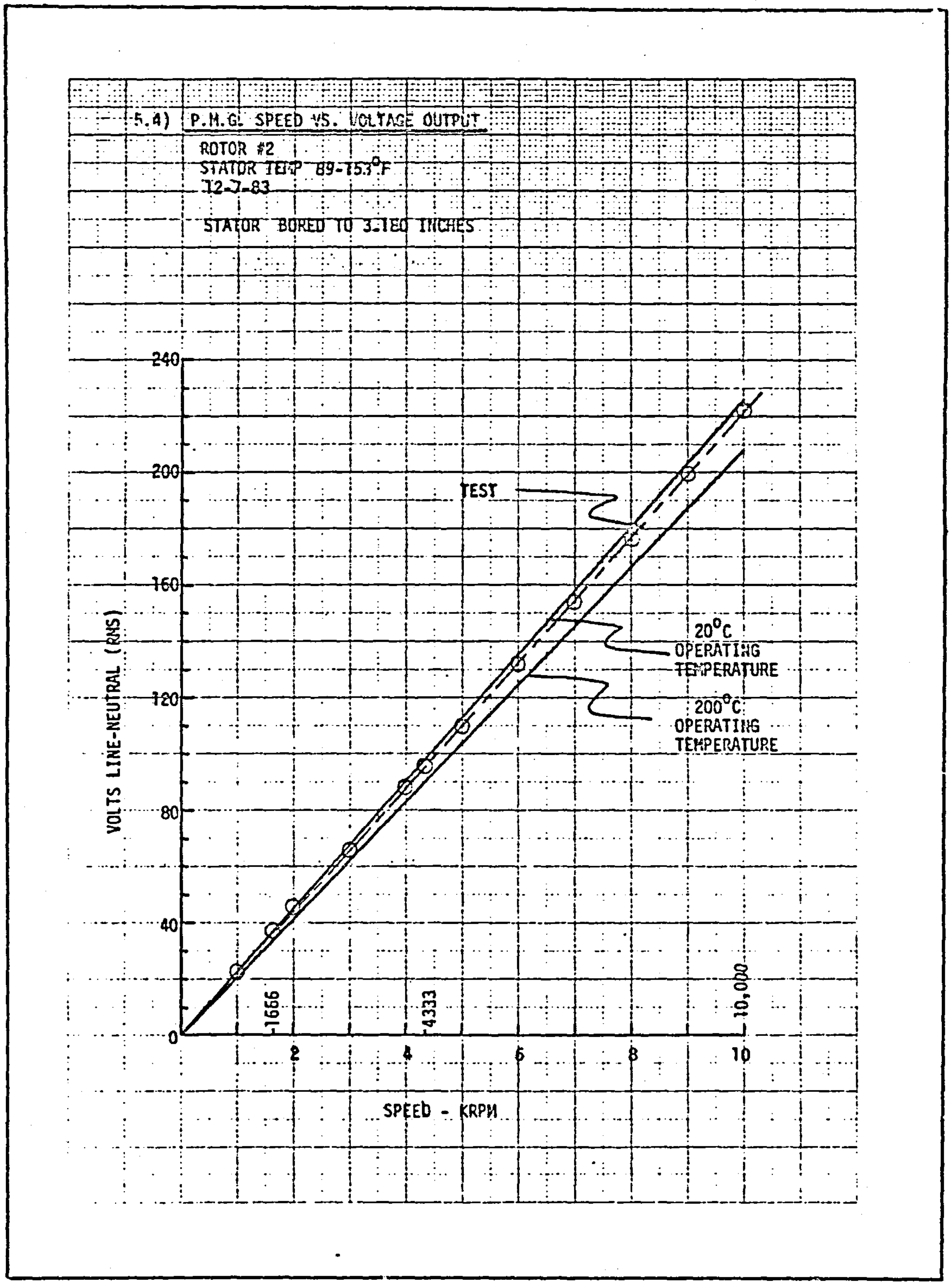
5.4) P.M.G. SPEED VS. VOLTAGE OUTPUT
ROTOR #2
STATOR TEMP 89-153°F
12-7-83
STATOR BORED TO 3.160 INCHES
240
200
160
120
80
40
0
VOLTS LINE-NEUTRAL (RMS)
TEST
20°C
OPERATING
TEMPERATURE
200°C
OPERATING
TEMPERATURE
1666
4333
10,000
2
4
6
8
10
SPEED - KRPM

5.4) P.M.G. SPEED V.S. VOLTAGE OUTPUT

a) Phase Voltage Output

L. KINTZ / B. ZELINSKI
ROTOR #2
12/7/83

SPEED (r.p.m.)		TEMP	TORQUE	MOTOR A				SPEED r.p.m.	TEMP	TORQUE	MOTOR B			
DESIRED	ACTUAL	°F	IN-LBS	Van	Vbn	Vcn	Vave	ACTUAL	°F	IN-LBS	Van	Vbn	Vcn	Vave
1666	1660	89.1	5.15	37	37	37	37	1670	90.1	4.7	37	37	37	37
2000	2004	89.8	5.5	45	45	45	45	2005	91.	5.35	45	45	45	45
4000	4K	94.3	7.15	87	88	88	88	4K	96.1	7.	87	88	88	88
4333	4335	97.3	7.5	95	95	95	95	4333	99.3	7.35	95	95	95	95
6000	6005	106.2	8.85	132	132	132	132	6K	106.9	8.65	132	132	132	132
8000	7998	119.7	10.25	176	176	177	176	7990	119.1	10.	175	176	176	176
10,000	10K	135.5	11.65	221	222	222	222	10K	136.8	11.4	[illegible]	[illegible]21	221	221
1K	1009	88.3	4.35	22	22	22	22	1010	88.9	4.13	22	22	22	22
3K	3004	91.4	6.35	66	66	66	66	2995	92.8	6.2	66	66	66	66
5K	5K	102.4	7.95	109	110	110	110	5010	103.8	7.9	110	110	11[illegible]	110
7K	6995	112.5	9.6	154	154	154	154	6984	112.1	9.35	153	154	154	154
9K	91.	127.2	10.7	198	199	199	199	8990	128.5	10.6	198	198	198	198

TEMP BY WINDING T.C.
STATOR BORED TO 3.180

5.4) P.M.G. SPEED V.S. VOLTAGE OUTPUT

a) Phase Voltage Output

SPEED (r.p.m.)		TEMP	TORQUE	MOTOR C				SPEED r.p.m.	TEMP	TORQUE	MOTOR D			
DESIRED	ACTUAL	°F	IN-LBS	Van	Vbn	Vcn	Vave	ACTUAL	°F	IN-LBS	Van	Vbn	Vcn	Vave
1666	1665	89.8	4.63	38	38	38	38	1660	89.8	5.3	37	37	37	37
2000	2K	90.5	5.05	45	45	45	45	2K	90.7	5.65	45	45	45	45
4000	3995	95.2	6.85	88	88	88	88	4K	99.3	7.5	87	88	88	88
4333	4336	100.	7.1	95	95	95	95	4336	103.8	7.8	95	95	95	95
6000	6K	110.8	8.3	132	133	133	133	6K	112.1	9.	131	132	132	132
8000	8K	121.1	9.63	177	177	177	177	8K	124.7	10.35	176	177	177	177
10,000	10K	133.8	11.	222	222	222	222	9996	153	11.7	222	222	222	222
1K	1K	89.2	3.85	22	22	22	22	1K	88.7	4.5	22	22	22	22
3K	3006	92.7	6.	66	66	66	66	2995	93.2	6.65	65	65	66	65
5K	5K	103.5	7.65	110	110	110	110	4995	107.4	8.15	109	110	110	110
7K	6995	117.1	9.05	154	155	155	155	7K	117.5	9.7	153	154	154	154
9K	9005	129.7	10.25	199	200	200	200	9K	136.8	11.05	199	200	200	200

TEMP BY WINDING T.C.
STATOR BORED TO 3.180

L. KINTZ & ZELINSKI
ROTOR #2
12/7/83

S8308-R1

ORIGINAL PAGE
BLACK AND WHITE PHOTOGRAPH

5.4) P.M.G. SPEED VS. VOLTAGE OUTPUT

A) 1666 RPM DATA POINT

VERTICAL SCALE: 2 VOLTS/DIVISION
TRANSFORMER RATIO: 8.05/1
HORIZONTAL SCALE: 500 μSEC/DIVISION

1) MOTOR A, PHASE A
VRMS 34.1
PERIOD 4.5 msec
FREQ 222 Hz
SPEED 1665 RPM

XFMR RATIO 8.05:1 12-21-83

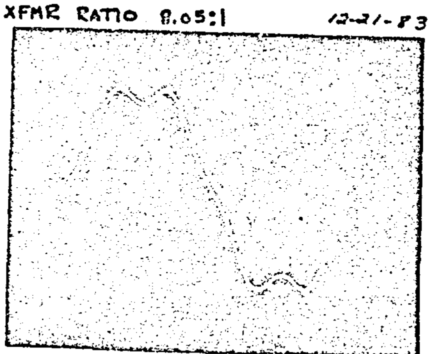

MOTOR A, ΦA, 1667 RPM DYNE NO LOAD

2) MOTOR A, PHASE B
VRMS 33.9
PERIOD 4.6 msec
FREQ 217 Hz
SPEED 1627 RPM

XFMR RATIO 8.05:1 12-21-83

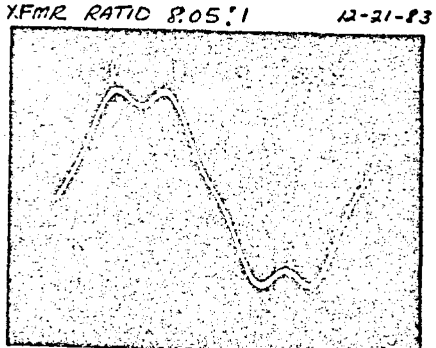

MOTOR A, ΦB, 1640 RPM DYNE NO LOAD

3) MOTOR A, PHASE C
VRMS 34.1
PERIOD 4.5 msec
FREQ 222 Hz
SPEED 1665 RPM

XFMR RATIO 8.05:1 12-21-83

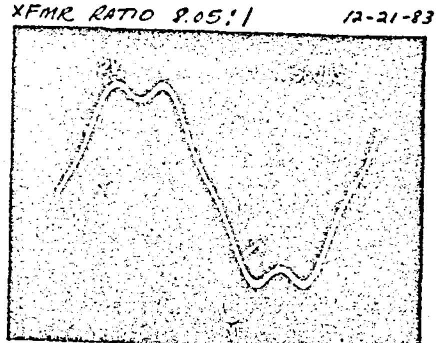

MOTOR A, ΦC, 1661 RPM DYNE NO LOAD

BLACK AND WHITE PHOTOGRAPH

5.4) P.M.G. SPEED VS. VOLTAGE OUTPUT

A) 1666 RPM DATA POINT

VERTICAL SCALE: 2 VOLTS/DIVISION

TRANSFORMER RATIO: 8.05/1

HORIZONTAL SCALE: 500 µSEC/DIVISION

4) MOTOR B, PHASE A

VRMS 34.1

PERIOD 4.5 msec

FREQ 222 Hz

SPEED 1665 RPM

XFMR RATIO 8.05:1 12-21-83

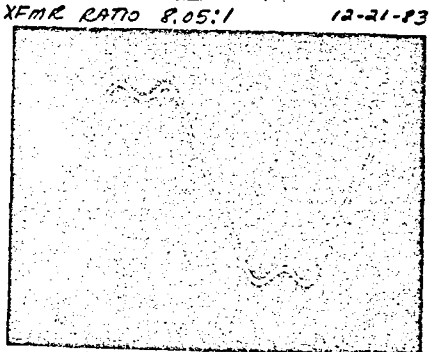

MOTOR B ΦA, 1667 RPM DYNE NO LOAD

5) MOTOR B, PHASE B

VRMS 34.1

PERIOD 4.5 msec

FREQ 222 Hz

SPEED 1665 RPM

XFMR RATIO 8.05:1 12-21-83

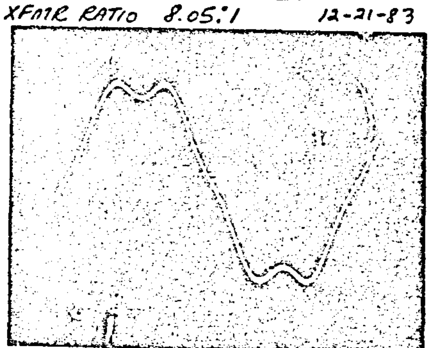

MOTOR B, ΦB, 1655 RPM DYNE NO LOAD

6) MOTOR B, PHASE C

VRMS 34.1

PERIOD 4.53 msec

FREQ 221 Hz

SPEED 1658 RPM

XFMR RATIO 8.05:1 12-21-83

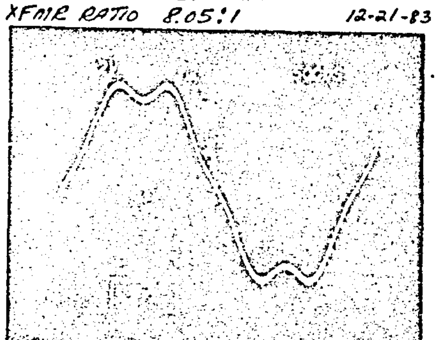

MOTOR B, ΦC, 1645 RPM DYNE NO LOAD

ORIGINAL PAGE
BLACK AND WHITE PHOTOGRAPH

5.4) P.M.G. SPEED VS. VOLTAGE OUTPUT

A) 1666 RPM DATA POINT

VERTICAL SCALE: 2 VOLTS/DIVISION
TRANSFORMER RATIO: 8.05/1
HORIZONTAL SCALE: 500 μSEC/DIVISION

7) MOTOR C, PHASE A
VRMS 34.1
PERIOD 4.5 msec
FREQ 222 Hz
SPEED 1665 RPM

XFMR RATIO 8.05:1 12-21-83

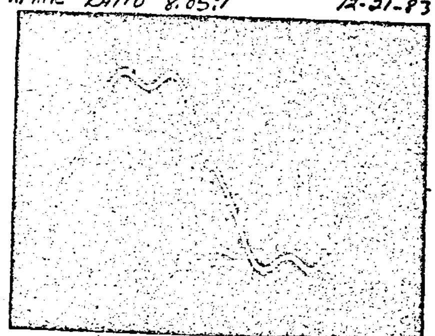

MOTOR C, ΦA, 1668 RPM DYNE NO LOAD

8) MOTOR D, PHASE A
VRMS 34.1
PERIOD 4.48 msec
FREQ 223 Hz
SPEED 1673 RPM

XFMR RATIO 8.05:1 12-21-83

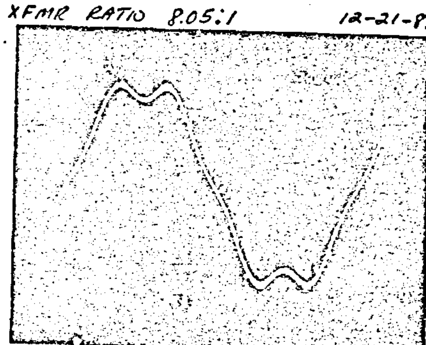

MOTOR D, ΦA, 1671 RPM DYNE NO LOAD

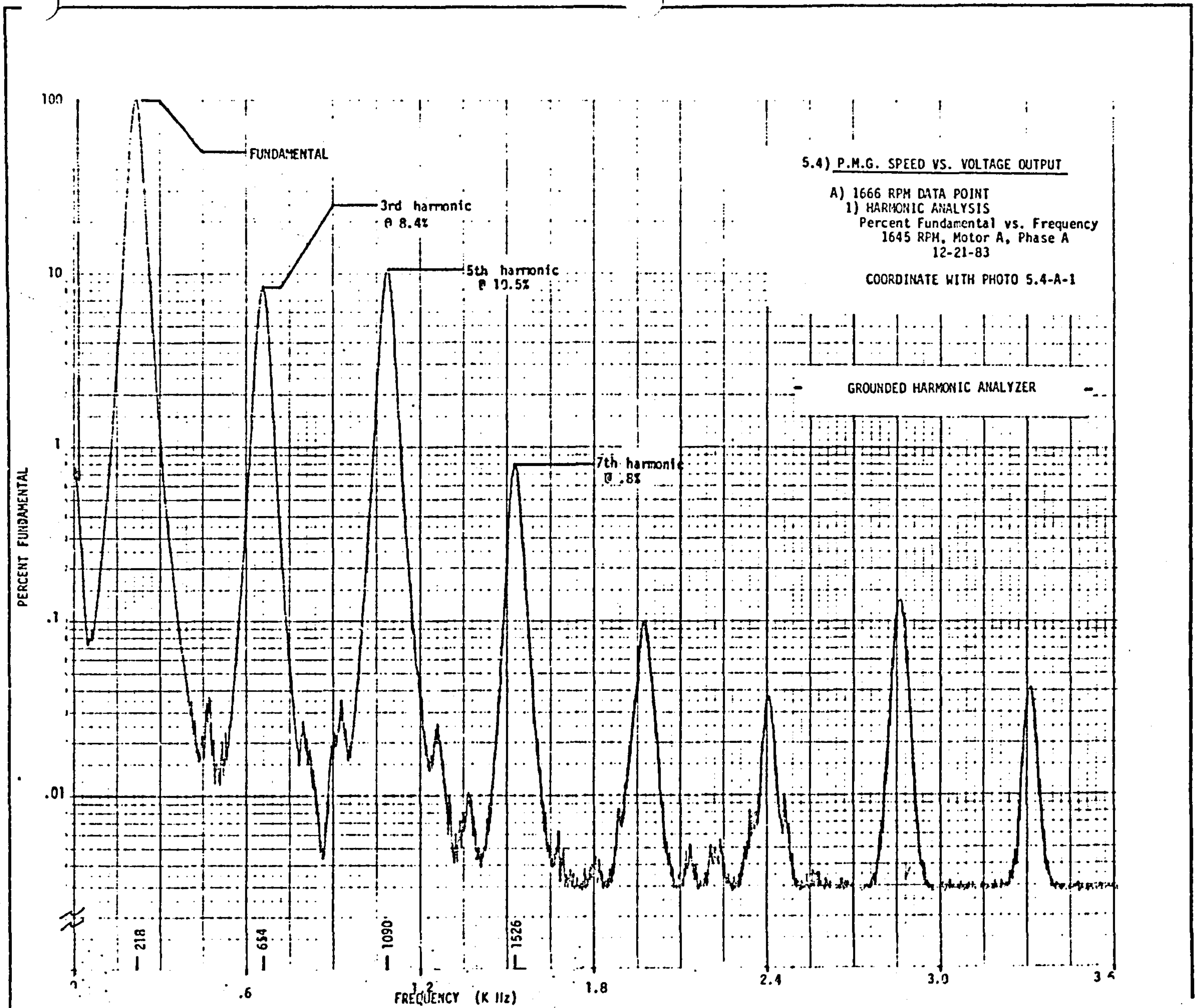
5.4) P.M.G. SPEED VS. VOLTAGE OUTPUT
A) 1666 RPM DATA POINT
1) HARMONIC ANALYSIS
Percent Fundamental vs. Frequency
1645 RPM, Motor A, Phase A
12-21-83
COORDINATE WITH PHOTO 5.4-A-1
GROUNDED HARMONIC ANALYZER
FUNDAMENTAL
3rd harmonic @ 8.4%
5th harmonic @ 10.5%
7th harmonic @ .8%
PERCENT FUNDAMENTAL
100
10
1
.1
.01
218
654
1090
1526
.6
1.2
1.8
2.4
3.0
FREQUENCY (K Hz)

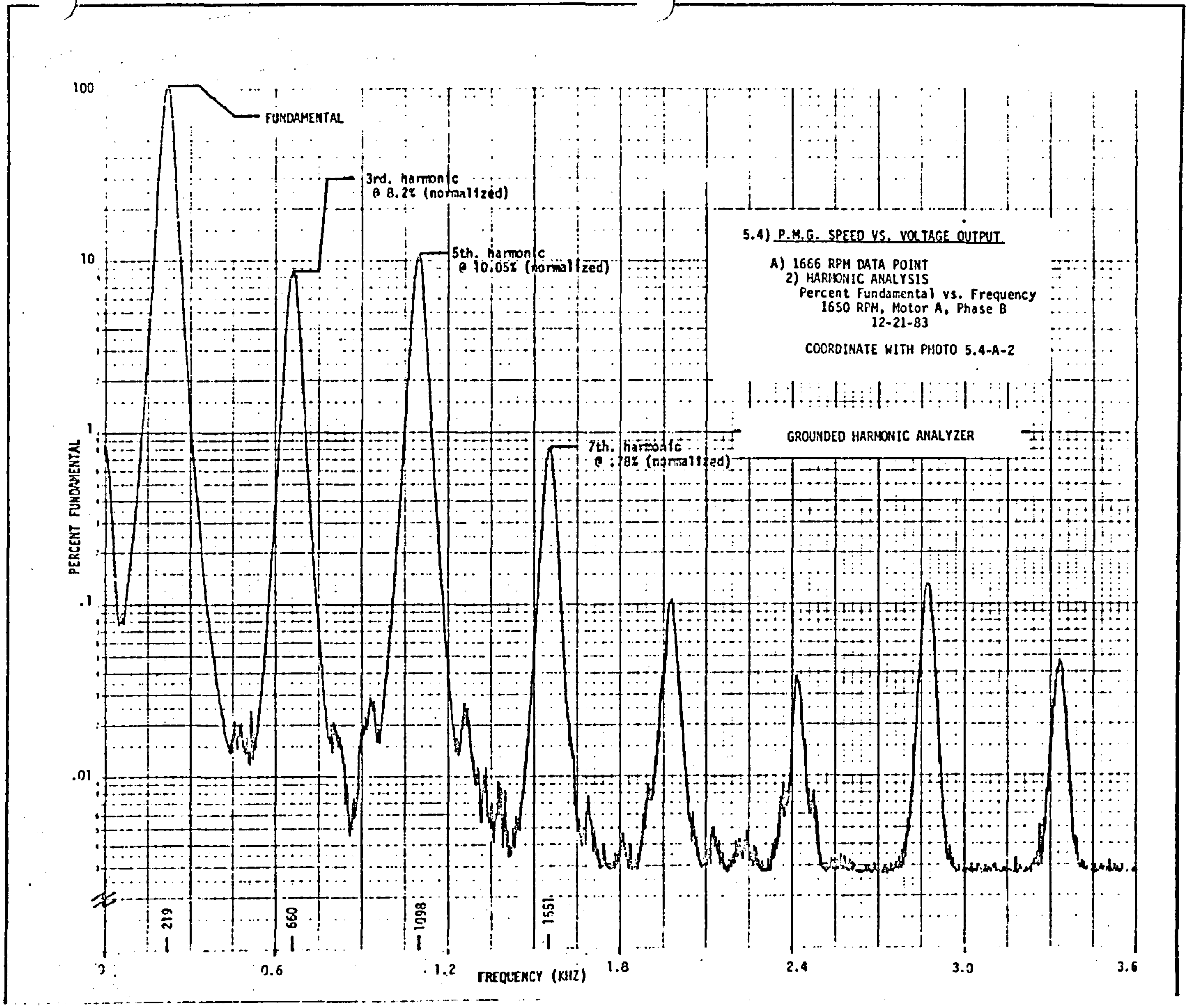
5.4) P.M.G. SPEED VS. VOLTAGE OUTPUT
A) 1666 RPM DATA POINT
2) HARMONIC ANALYSIS
Percent Fundamental vs. Frequency
1650 RPM, Motor A, Phase B
12-21-83
COORDINATE WITH PHOTO 5.4-A-2
GROUNDED HARMONIC ANALYZER
FUNDAMENTAL
3rd. harmonic
@ 8.2% (normalized)
5th. harmonic
@ 10.05% (normalized)
7th. harmonic
@ .78% (normalized)
PERCENT FUNDAMENTAL
100
10
1
.1
.01
219
660
1098
1551
0
0.6
1.2
1.8
2.4
3.0
3.6
FREQUENCY (KHZ)

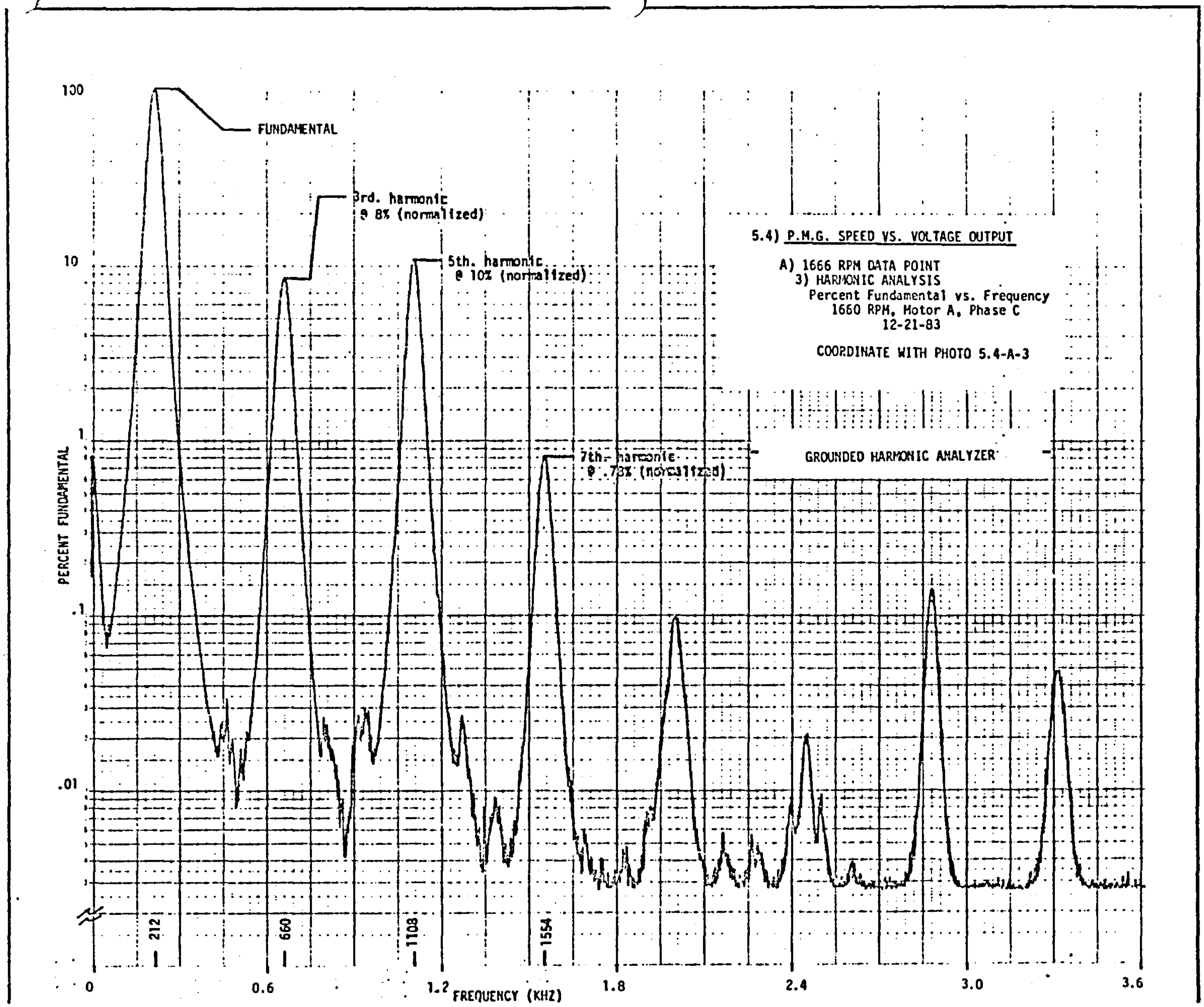

5.4) P.M.G. SPEED VS. VOLTAGE OUTPUT
A) 1666 RPM DATA POINT
3) HARMONIC ANALYSIS
Percent Fundamental vs. Frequency
1660 RPM, Motor A, Phase C
12-21-83
COORDINATE WITH PHOTO 5.4-A-3
GROUNDED HARMONIC ANALYZER
FUNDAMENTAL
3rd. harmonic
@ 8% (normalized)
5th. harmonic
@ 10% (normalized)
7th. harmonic
@ .73% (normalized)
PERCENT FUNDAMENTAL
100
10
1
.1
.01
212
660
1108
1554
0
0.6
1.2
1.8
2.4
3.0
3.6
FREQUENCY (KHZ)

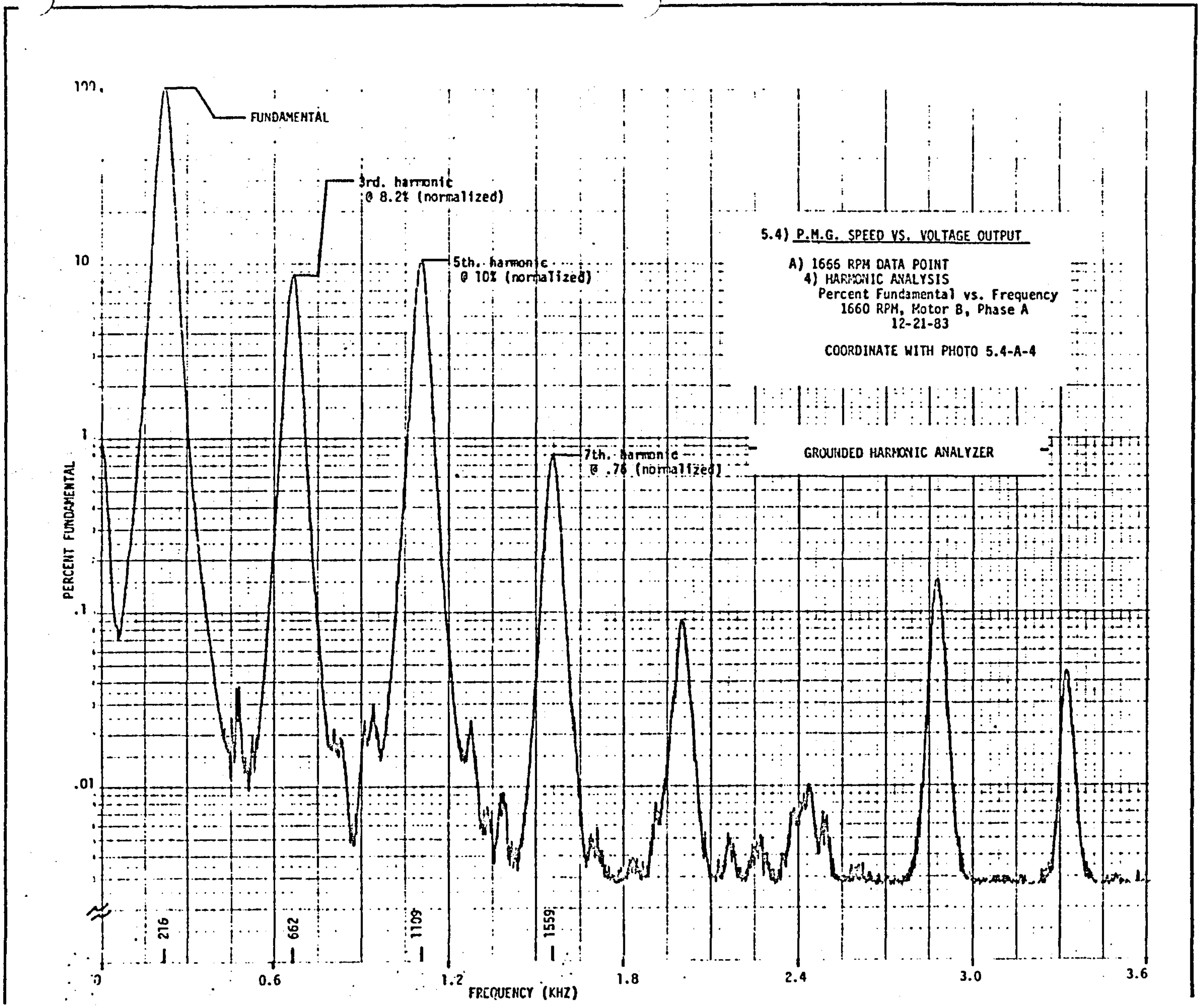
5.4) P.M.G. SPEED VS. VOLTAGE OUTPUT
A) 1666 RPM DATA POINT
4) HARMONIC ANALYSIS
Percent Fundamental vs. Frequency
1660 RPM, Motor B, Phase A
12-21-83
COORDINATE WITH PHOTO 5.4-A-4
GROUNDED HARMONIC ANALYZER
FUNDAMENTAL
3rd. harmonic @ 8.2% (normalized)
5th. harmonic @ 10% (normalized)
7th. harmonic @ .7% (normalized)
PERCENT FUNDAMENTAL
100.
10
1
.1
.01
216
662
1109
1559
0
0.6
1.2
1.8
2.4
3.0
3.6
FREQUENCY (KHZ)

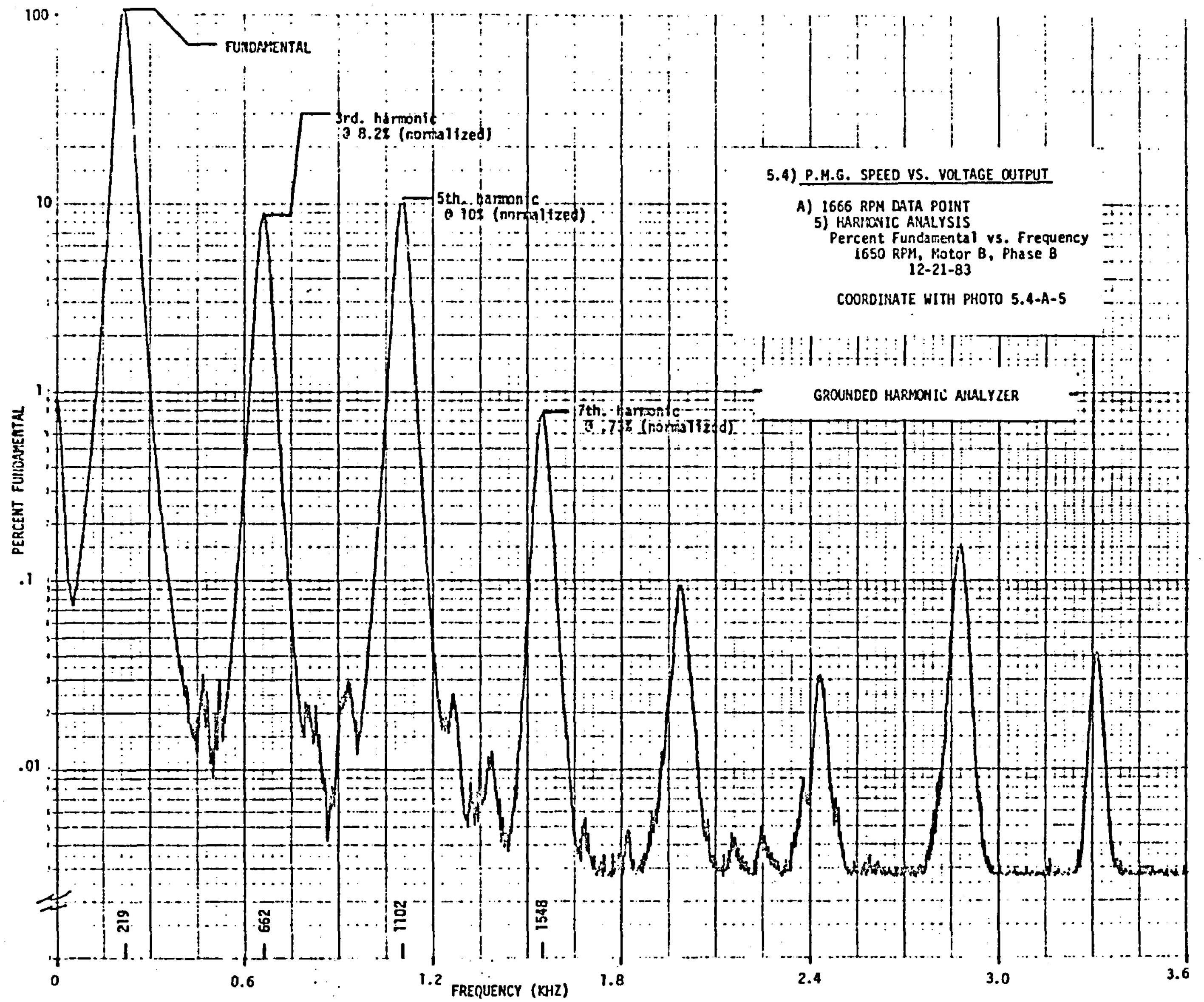

5.4) P.M.G. SPEED VS. VOLTAGE OUTPUT
A) 1666 RPM DATA POINT
5) HARMONIC ANALYSIS
Percent Fundamental vs. Frequency
1650 RPM, Motor B, Phase B
12-21-83
COORDINATE WITH PHOTO 5.4-A-5
GROUNDED HARMONIC ANALYZER
FUNDAMENTAL
3rd. harmonic
@ 8.2% (normalized)
5th. harmonic
@ 10% (normalized)
7th. harmonic
@ .73% (normalized)
PERCENT FUNDAMENTAL
100
10
1
.1
.01
219
662
1102
1548
0
0.6
1.2
1.8
2.4
3.0
3.6
FREQUENCY (KHZ)

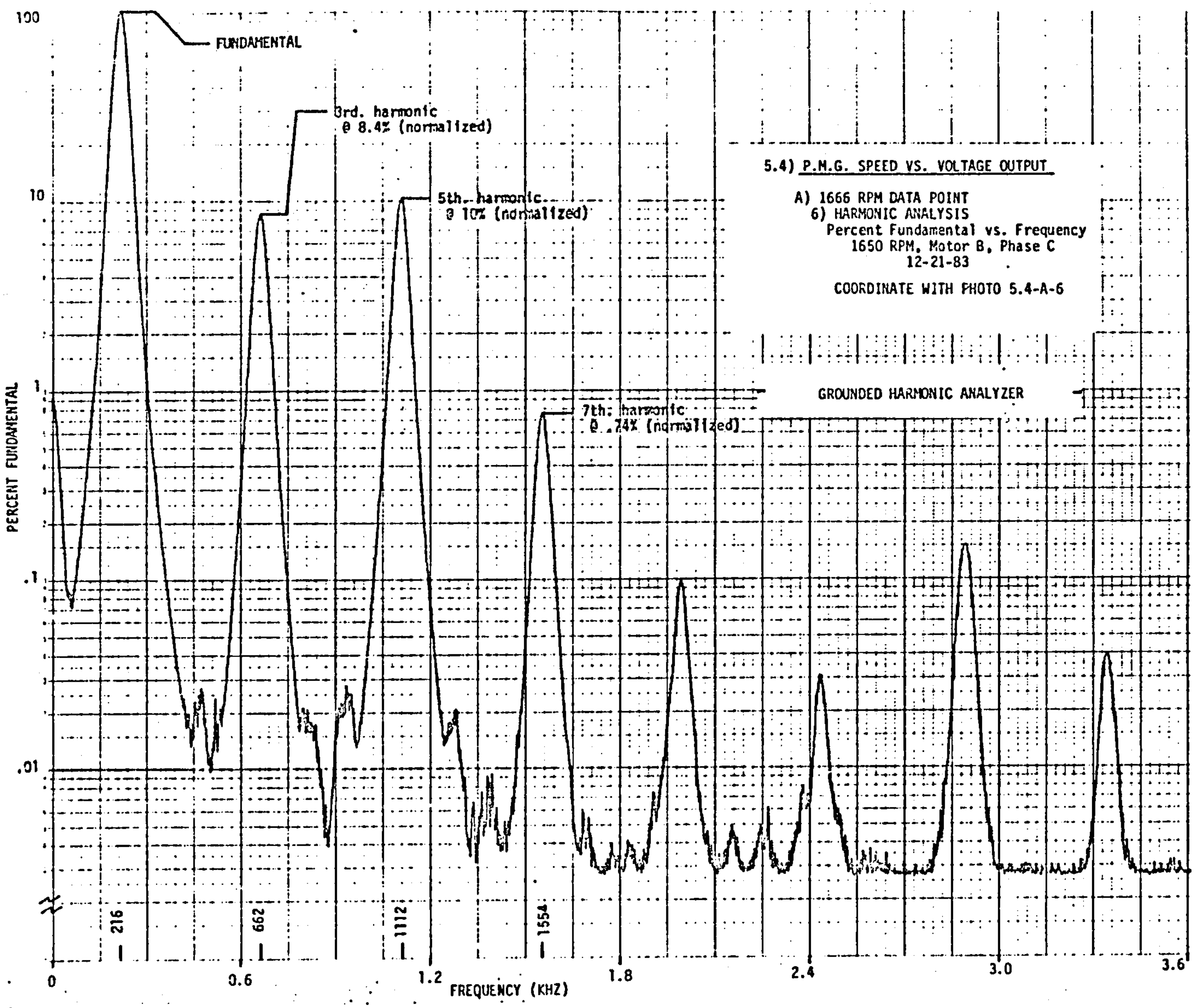

5.4) P.M.G. SPEED VS. VOLTAGE OUTPUT
A) 1666 RPM DATA POINT
6) HARMONIC ANALYSIS
Percent Fundamental vs. Frequency
1650 RPM, Motor B, Phase C
12-21-83
COORDINATE WITH PHOTO 5.4-A-6
GROUNDED HARMONIC ANALYZER
FUNDAMENTAL
3rd. harmonic
@ 8.4% (normalized)
5th. harmonic
@ 10% (normalized)
7th. harmonic
@ .74% (normalized)
PERCENT FUNDAMENTAL
100
10
1
.1
.01
216
662
1112
1554
0
0.6
1.2
1.8
2.4
3.0
3.6
FREQUENCY (KHZ)

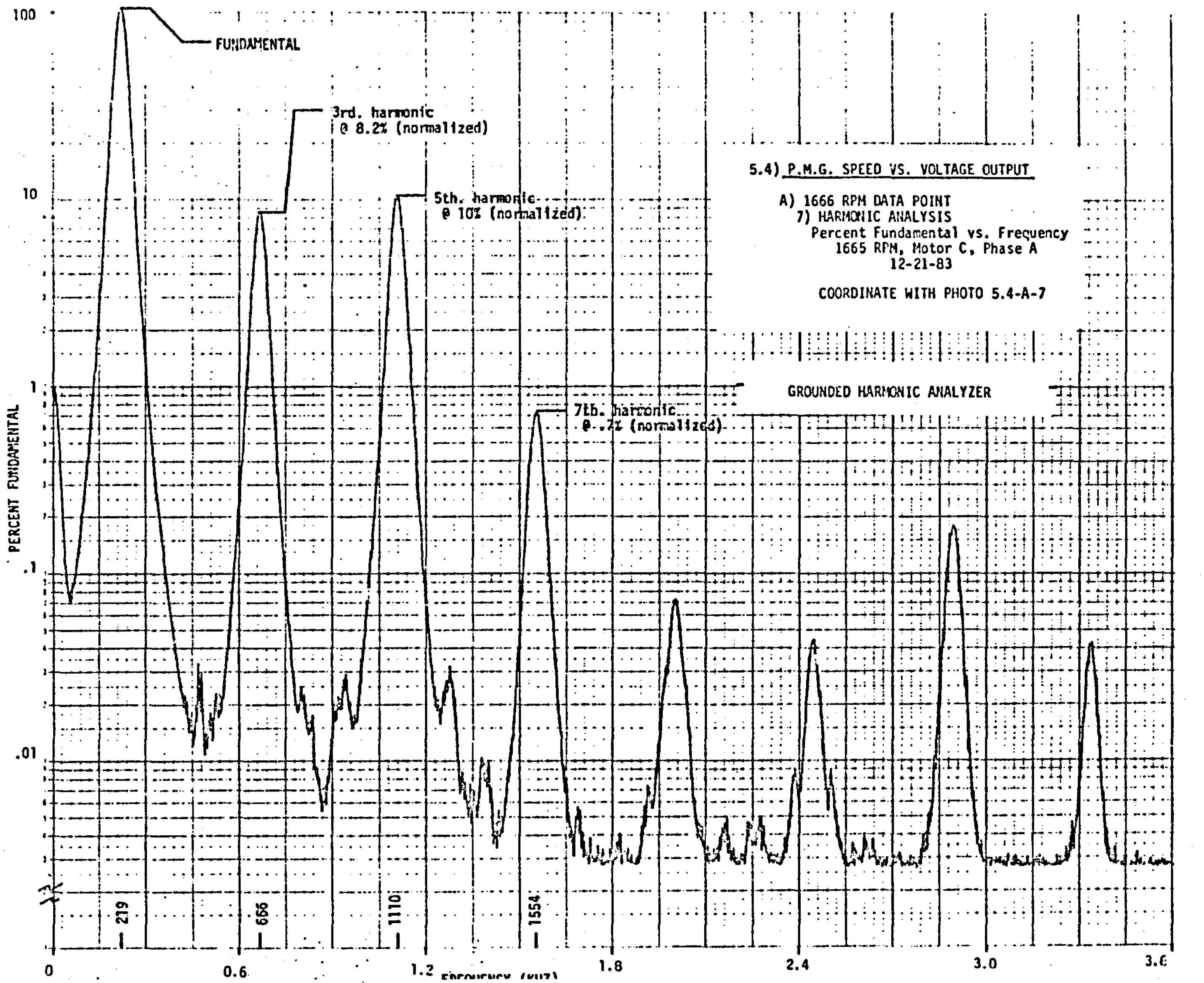
5.4) P.M.G. SPEED VS. VOLTAGE OUTPUT
A) 1666 RPM DATA POINT
7) HARMONIC ANALYSIS
Percent Fundamental vs. Frequency
1665 RPM, Motor C, Phase A
12-21-83
COORDINATE WITH PHOTO 5.4-A-7
GROUNDED HARMONIC ANALYZER
FUNDAMENTAL
3rd. harmonic
@ 8.2% (normalized)
5th. harmonic
@ 10% (normalized)
PERCENT FUNDAMENTAL
100
10
1
.1
.01
219
666
1110
1554
0
0.6
1.2
1.8
2.4
3.0

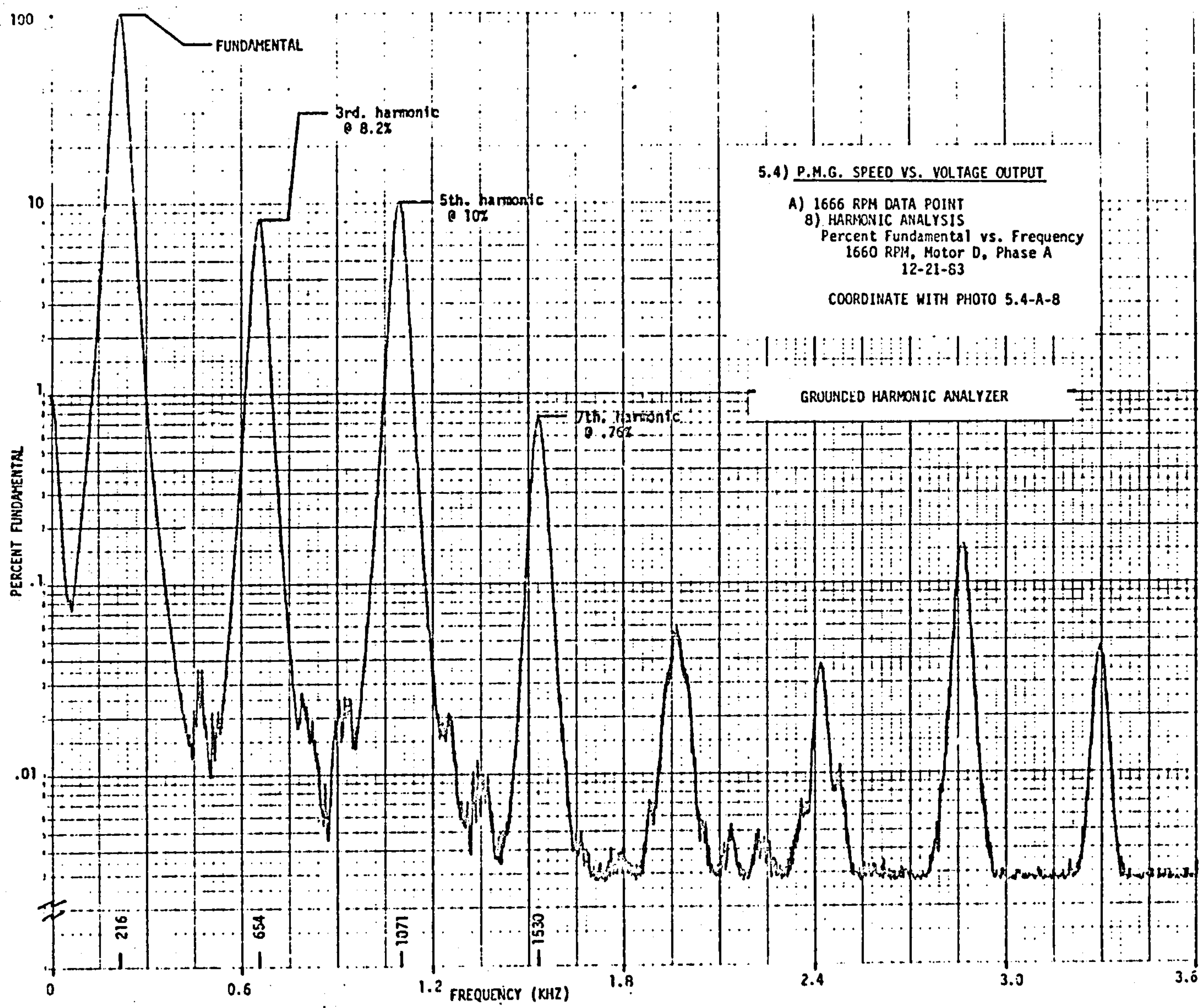
FUNDAMENTAL
3rd. harmonic
@ 8.2%
5th. harmonic
@ 10%
7th. harmonic
@ .76%
5.4) P.M.G. SPEED VS. VOLTAGE OUTPUT
A) 1666 RPM DATA POINT
8) HARMONIC ANALYSIS
Percent Fundamental vs. Frequency
1660 RPM, Motor D, Phase A
12-21-83
COORDINATE WITH PHOTO 5.4-A-8
GROUNDED HARMONIC ANALYZER
PERCENT FUNDAMENTAL
100
10
1
.1
.01
216
654
1071
1530
0
0.6
1.2
FREQUENCY (KHZ)
1.8
2.4
3.0
3.6

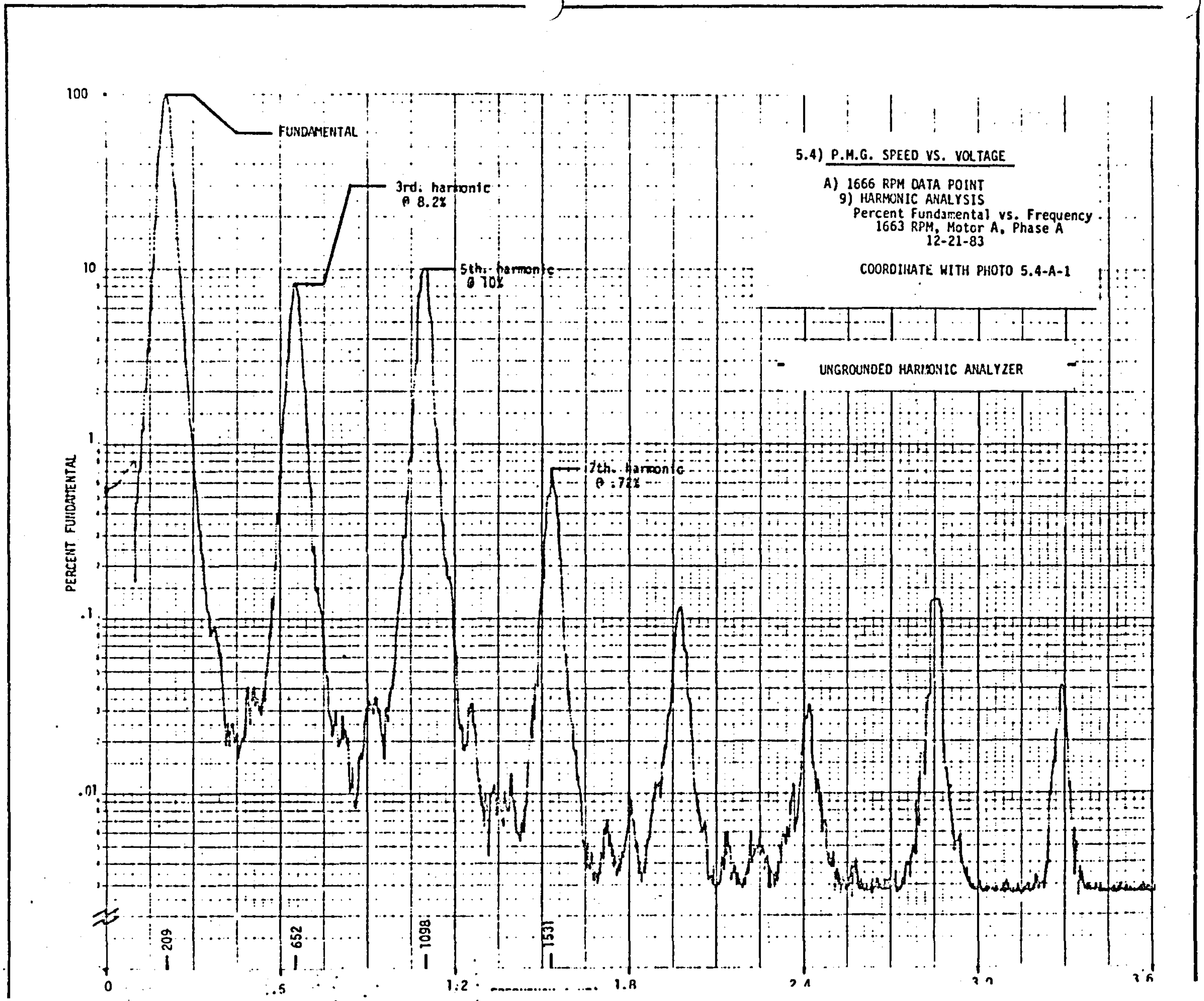

5.4) P.M.G. SPEED VS. VOLTAGE
A) 1666 RPM DATA POINT
9) HARMONIC ANALYSIS
Percent Fundamental vs. Frequency
1663 RPM, Motor A, Phase A
12-21-83
COORDINATE WITH PHOTO 5.4-A-1
UNGROUNDED HARMONIC ANALYZER
FUNDAMENTAL
3rd. harmonic @ 8.2%
5th. harmonic @ 10%
7th. harmonic @ .72%
PERCENT FUNDAMENTAL
100
10
1
.1
.01
209
652
1098
1531
0
.5
1.2
1.8
2.4
3.0
3.6

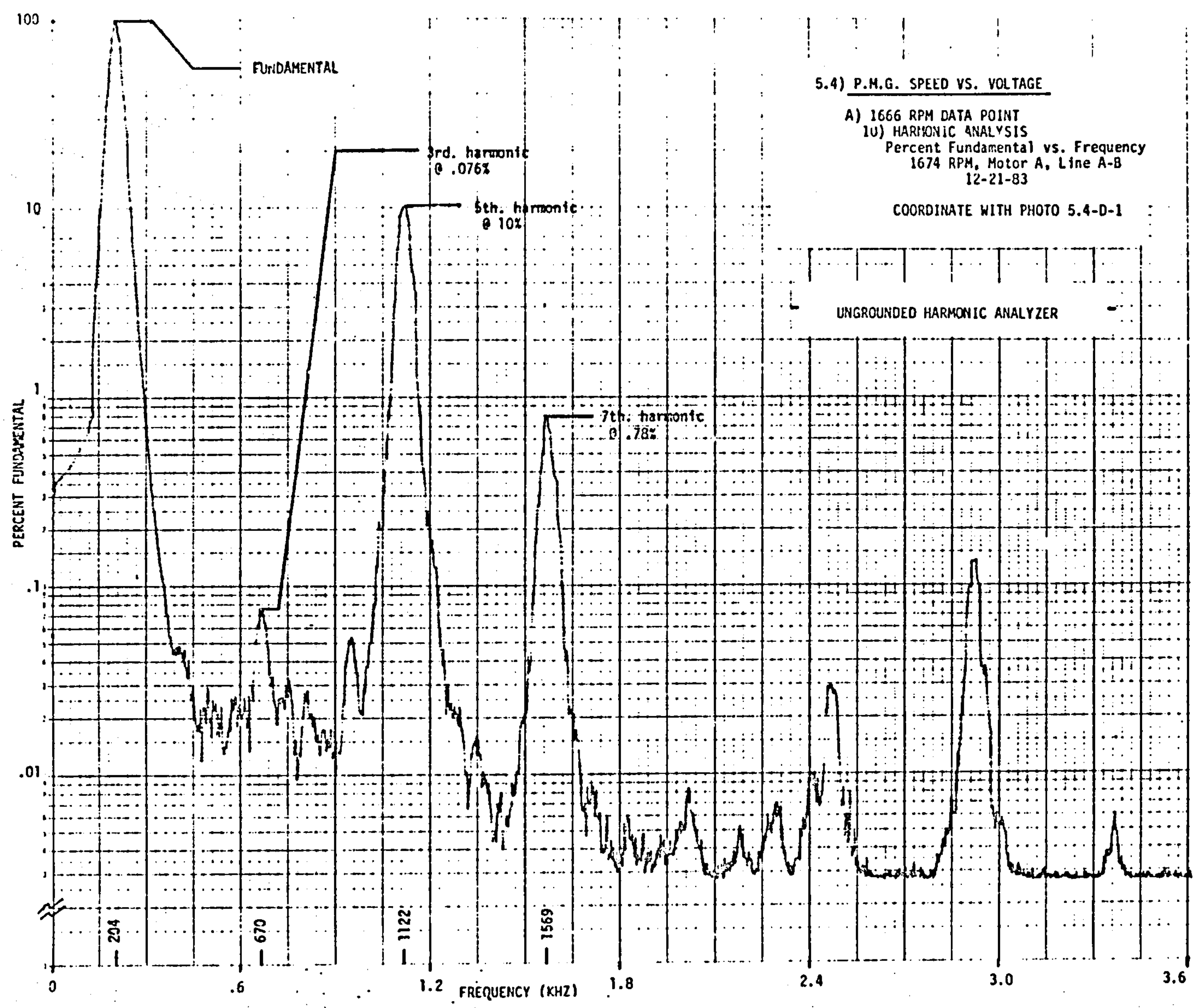
5.4) P.M.G. SPEED VS. VOLTAGE
A) 1666 RPM DATA POINT
10) HARMONIC ANALYSIS
Percent Fundamental vs. Frequency
1674 RPM, Motor A, Line A-B
12-21-83
COORDINATE WITH PHOTO 5.4-D-1
UNGROUNDED HARMONIC ANALYZER
FUNDAMENTAL
3rd. harmonic
@ .076%
5th. harmonic
@ 10%
7th. harmonic
@ .78%
PERCENT FUNDAMENTAL
100
10
1
.1
.01
204
670
1122
1569
0
.6
1.2
1.8
2.4
3.0
3.6
FREQUENCY (KHZ)

ORIGINAL PAGE
BLACK AND WHITE PHOTOGRAPH

5.4) P.M.G. SPEED VS. VOLTAGE OUTPUT

B) 4333 RPM DATA POINT

VERTICAL SCALE: 5 VOLTS/DIVISION
TRANSFORMER RATIO: 8.05/1
HORIZONTAL SCALE: 200 USEC/DIVISION

1) MOTOR A, PHASE A
VRMS 93.9
PERIOD 1.69 msec
FREQ 592 Hz
SPEED 4438 RPM

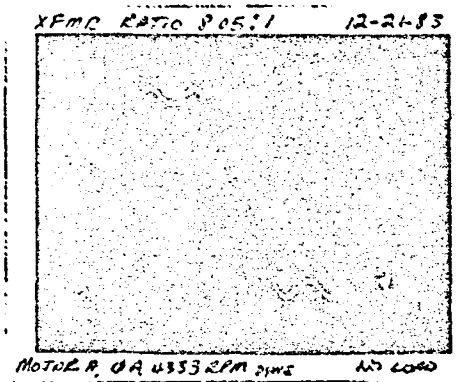

2) MOTOR A, PHASE B
VRMS 93.9
PERIOD 1.69 msec
FREQ 592 Hz
SPEED 4438 RPM

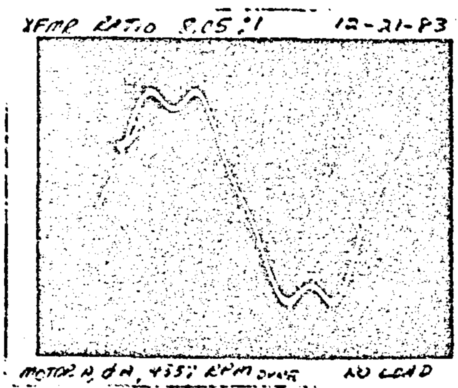

3) MOTOR A, PHASE C
VRMS 91.8
PERIOD 1.7 msec
FREQ 583 Hz
SPEED 4412 RPM

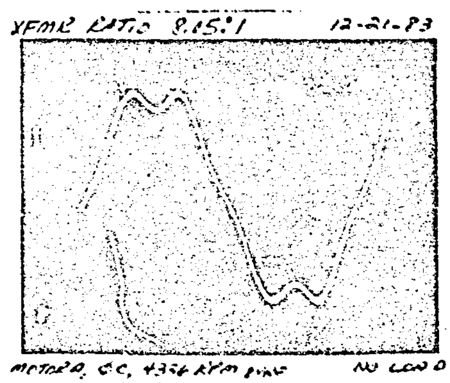

ORIGINAL PAGE
BLACK AND WHITE PHOTOGRAPH

5.4) P.M.G. SPEED VS. VOLTAGE OUTPUT

B) 4333 RPM DATA POINT

VERTICAL SCALE: 5 VOLTS/DIVISION
TRANSFORMER RATIO: 8.05/1
HORIZONTAL SCALE: 200 μSEC/DIVISION

4) MOTOR B, PHASE A
VRMS 91.8
PERIOD 1.7 msec
FREQ 588 Hz
SPEED 4412 RPM

XFMR RATIO 8.05:1 12-21-83

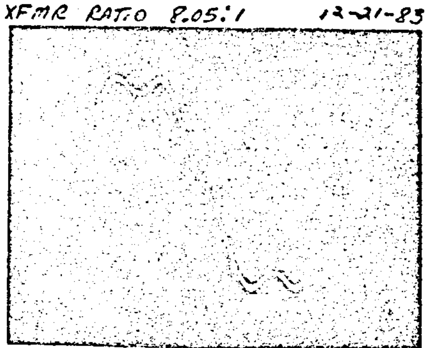

MOTOR B ØA, 4336 RPM DYNE NO LOAD

5) MOTOR B, PHASE B
VRMS 91.8
PERIOD 1.7 msec
FREQ 588 Hz
SPEED 4412 RPM

XFMR RATIO 8.05:1 12-21-83

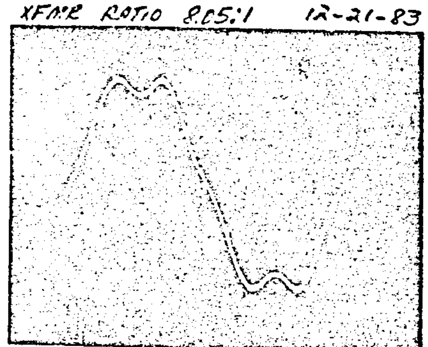

MOTOR B, ØB, 4347 RPM DYNE NO LOAD

6) MOTOR B, PHASE C
VRMS 91.8
PERIOD 1.7 msec
FREQ 588 Hz
SPEED 4412 RPM

XFMR RATIO 8.05:1 12-21-83

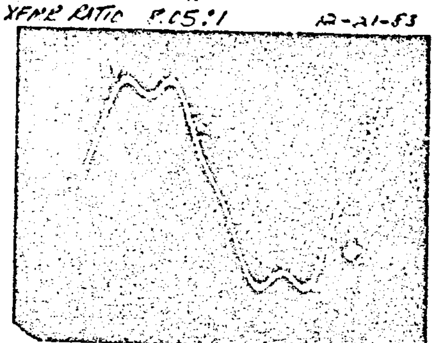

MOTOR B ØC, 4329 RPM DYNE NO LOAD

5.4) P.M.G. SPEED VS. VOLTAGE OUTPUT

B) 4333 RPM DATA POINT

VERTICAL SCALE: 5 VOLTS/DIVISION
TRANSFORMER RATIO: 8.05/1
HORIZONTAL SCALE: 200 μSEC/DIVISION

7) MOTOR C, PHASE A
VRMS 92.5
PERIOD 1.7 msec
FREQ 588 Hz
SPEED 4412 RPM

XFMR RATIO 8.05:1 12-21-83

MOTOR C, ΦA, 4546 RPM DYN NO LOAD

8) MOTOR D, PHASE A
VRMS 91.8
PERIOD 1.7 msec
FREQ 588 Hz
SPEED 4412 RPM

XFMR RATIO 8.05:1 12-21-83

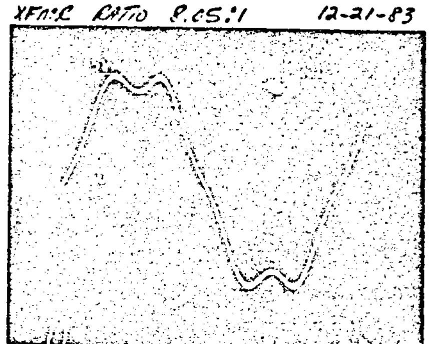

MOTOR D, ΦA, 4333 RPM DYNE NO LOAD

ORIGINAL PAGE
BLACK AND WHITE PHOTOGRAPH

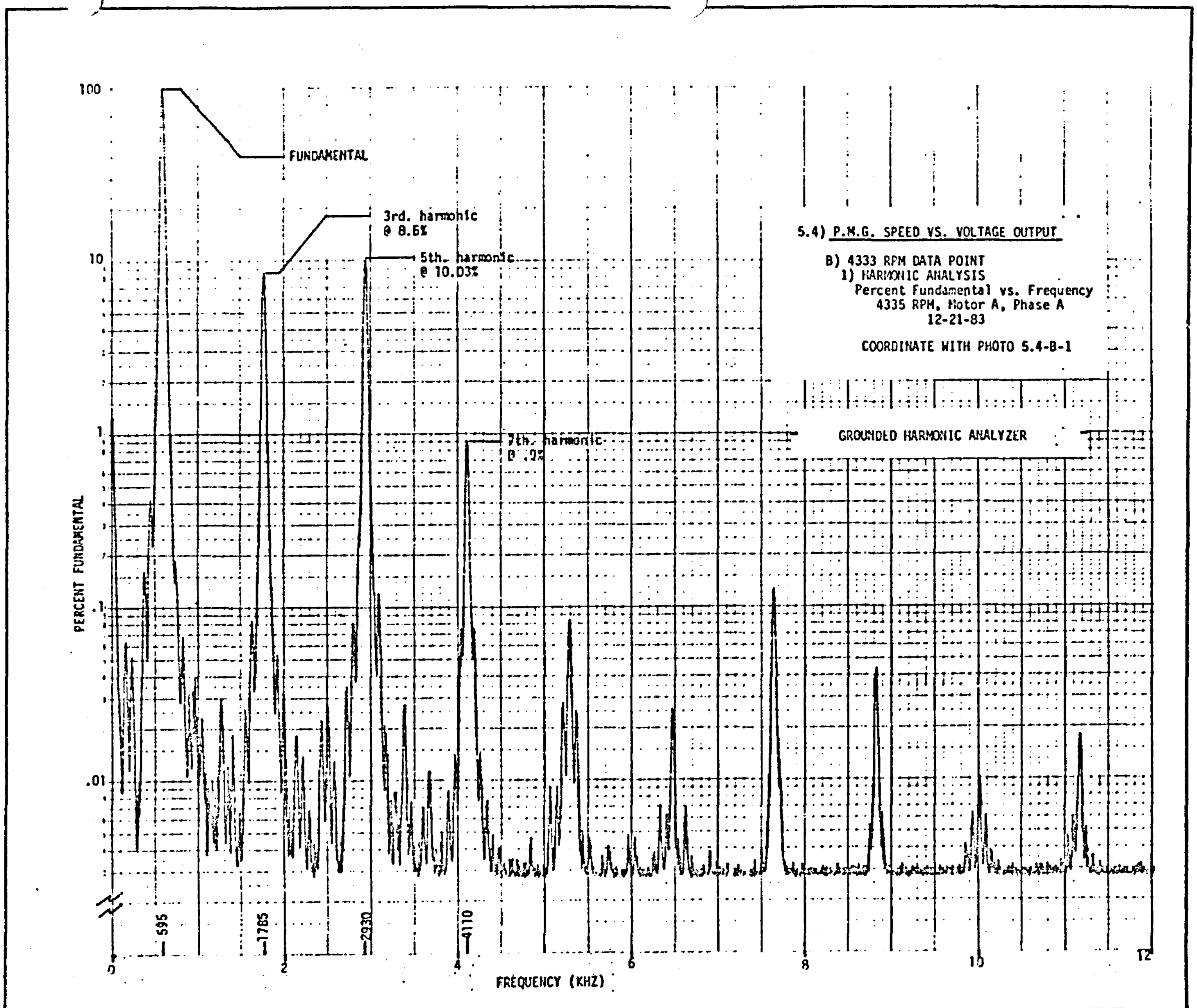

FUNDAMENTAL
3rd. harmonic
@ 8.6%
5th. harmonic
@ 10.03%
7th. harmonic
@ .9%
5.4) P.M.G. SPEED VS. VOLTAGE OUTPUT
B) 4333 RPM DATA POINT
1) HARMONIC ANALYSIS
Percent Fundamental vs. Frequency
4335 RPM, Motor A, Phase A
12-21-83
COORDINATE WITH PHOTO 5.4-B-1
GROUNDED HARMONIC ANALYZER
PERCENT FUNDAMENTAL
FREQUENCY (KHZ)
100
10
1
.1
.01
595
1785
2930
4110
0
2
4
6
8
10
12

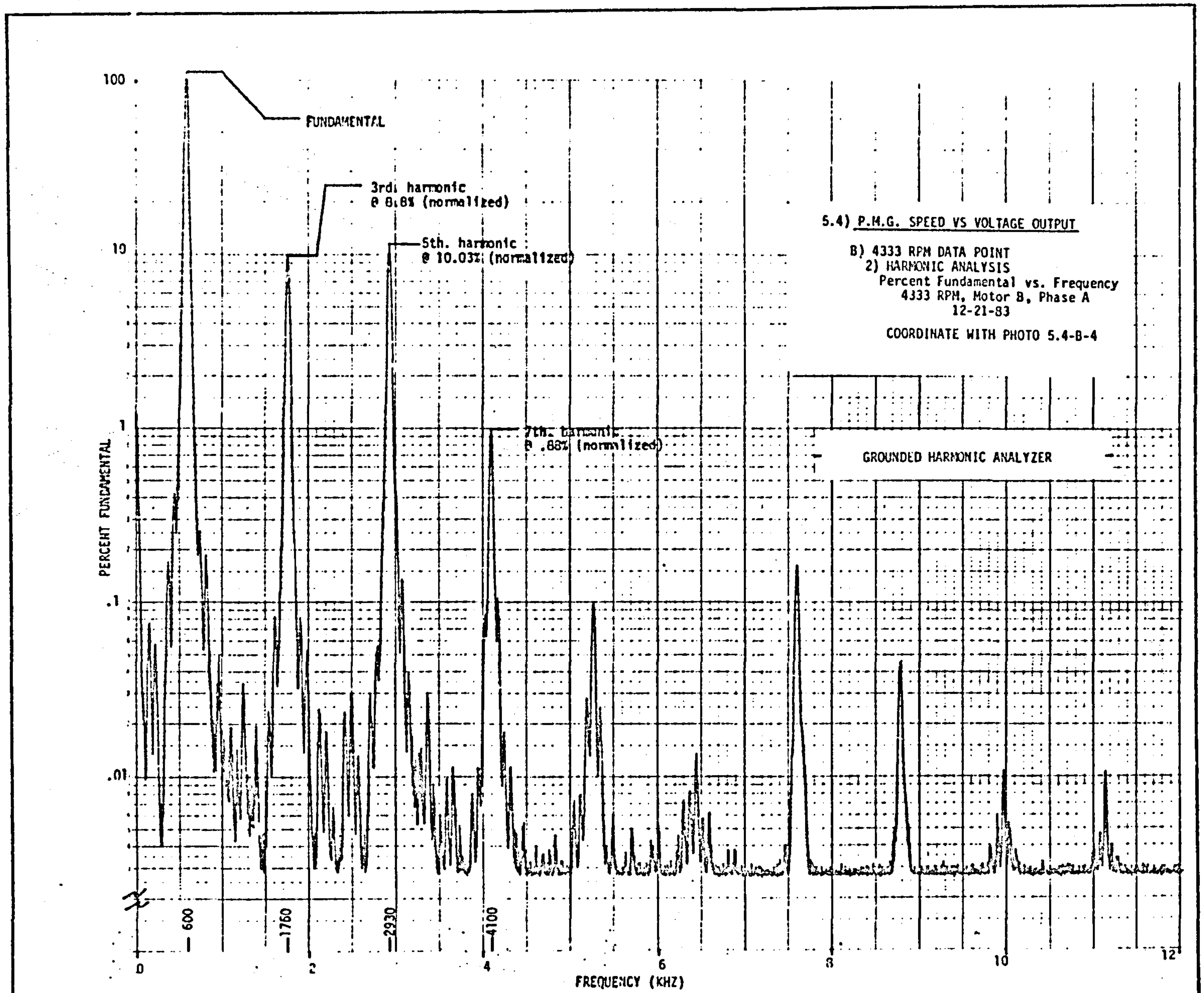

FUNDAMENTAL
3rd harmonic
@ 8.8% (normalized)
5th. harmonic
@ 10.03% (normalized)
7th. harmonic
@ .88% (normalized)
5.4) P.M.G. SPEED VS VOLTAGE OUTPUT
B) 4333 RPM DATA POINT
2) HARMONIC ANALYSIS
Percent Fundamental vs. Frequency
4333 RPM, Motor B, Phase A
12-21-83
COORDINATE WITH PHOTO 5.4-B-4
GROUNDED HARMONIC ANALYZER
PERCENT FUNDAMENTAL
100
10
1
.1
.01
600
1760
2930
4100
0
2
4
6
8
10
12
FREQUENCY (KHZ)

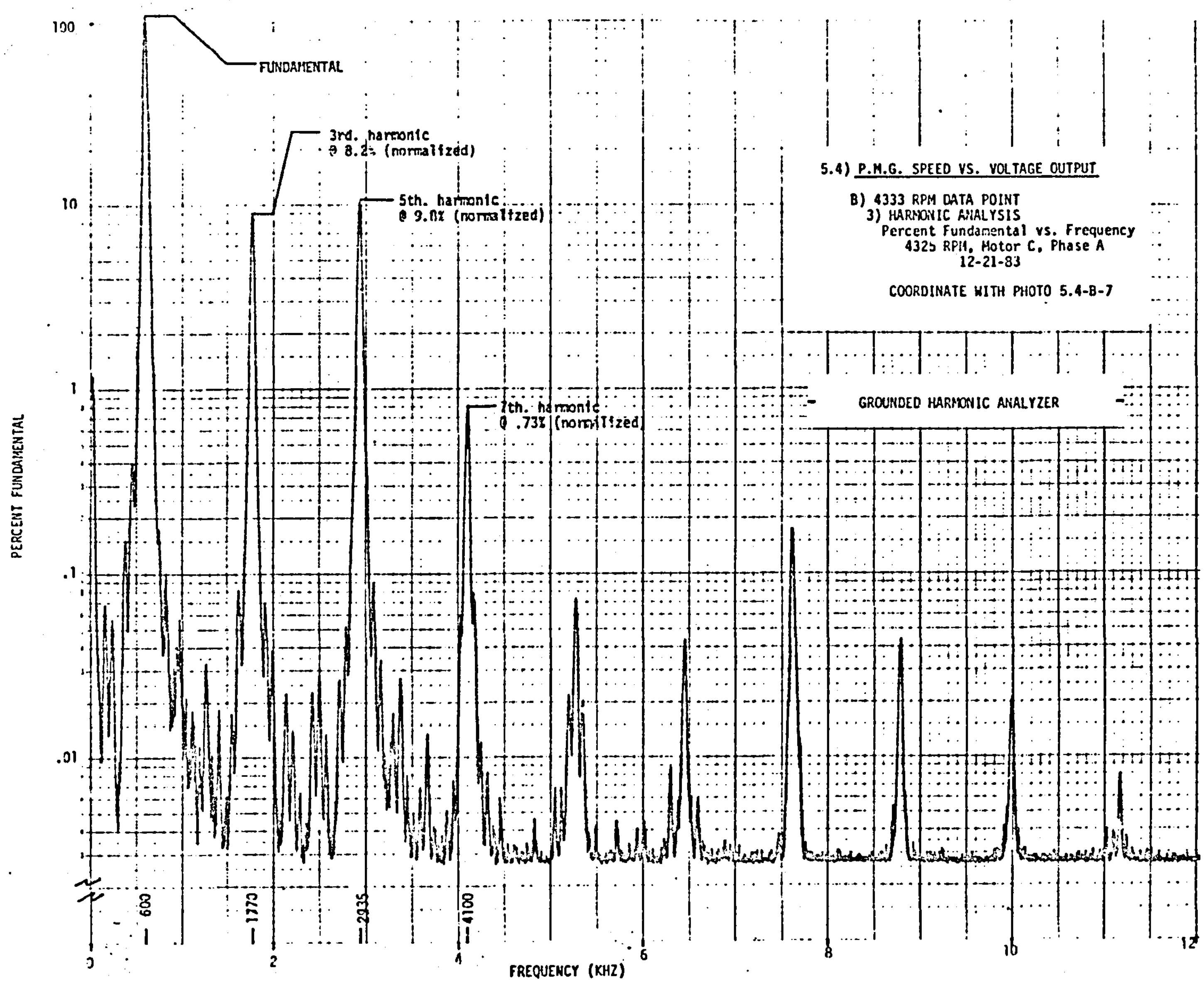

FUNDAMENTAL
3rd. harmonic
@ 8.2% (normalized)
5th. harmonic
@ 9.8% (normalized)
7th. harmonic
@ .73% (normalized)
5.4) P.M.G. SPEED VS. VOLTAGE OUTPUT
B) 4333 RPM DATA POINT
3) HARMONIC ANALYSIS
Percent Fundamental vs. Frequency
4325 RPM, Motor C, Phase A
12-21-83
COORDINATE WITH PHOTO 5.4-B-7
GROUNDED HARMONIC ANALYZER
PERCENT FUNDAMENTAL
100
10
1
.1
.01
600
1770
2935
4100
0
2
4
6
8
10
12
FREQUENCY (KHZ)

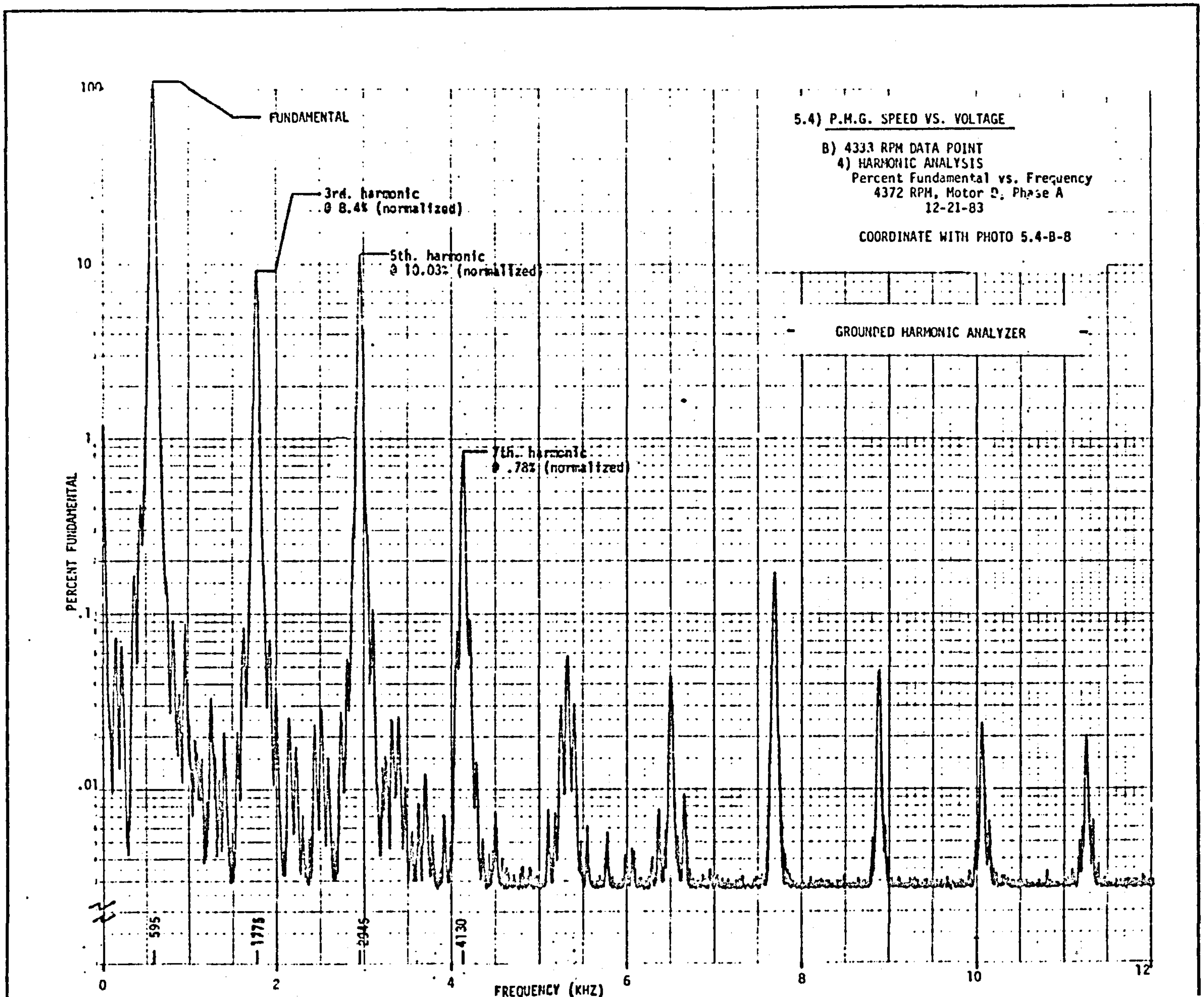

5.4) P.M.G. SPEED VS. VOLTAGE
B) 4333 RPM DATA POINT
4) HARMONIC ANALYSIS
Percent Fundamental vs. Frequency
4372 RPM, Motor D, Phase A
12-21-83
COORDINATE WITH PHOTO 5.4-B-8
GROUNDED HARMONIC ANALYZER
FUNDAMENTAL
3rd. harmonic
@ 8.4% (normalized)
5th. harmonic
@ 10.03% (normalized)
7th. harmonic
@ .78% (normalized)
PERCENT FUNDAMENTAL
100
10
1
.1
.01
595
1778
2945
4130
0
2
4
6
8
10
12
FREQUENCY (KHZ)

5.4) P.M.G. SPEED VS. VOLTAGE OUTPUT

C) 10,000 RPM DATA POINT

VERTICAL SCALE: 20 VOLTS/DIVISION
TRANSFORMER RATIO: 8.05/1
HORIZONTAL SCALE: 100 µSEC/DIVISION

1) MOTOR A, PHASE A
VRMS 216
PERIOD 720 usec
FREQ 1389 Hz
SPEED 10417 RPM

XFMR RATIO 8.05:1 12-21-83

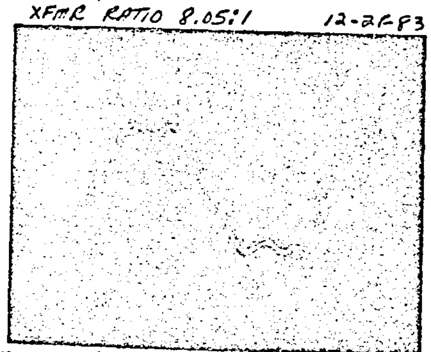

MOTOR A, ΦA, 10008 RPM DYNE NO LOAD

2) MOTOR A, PHASE B
VRMS 216
PERIOD 720 usec
FREQ 1389 Hz
SPEED 10417 RPM

XFMR RATIO 8.05:1 12-21-83

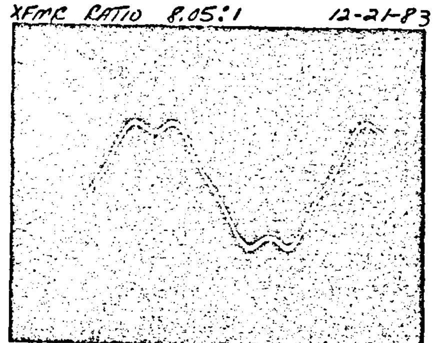

MOTOR A, ΦA, 10001 RPM DYNE NO LOAD

3) MOTOR A, PHASE C
VRMS 216
PERIOD 720 usec
FREQ 1389 Hz
SPEED 10417 RPM

XFMR RATIO 8.05:1 12-21-83

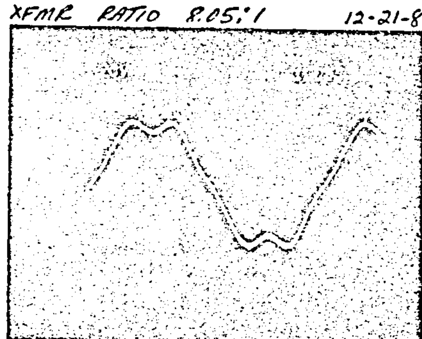

MOTOR A ΦC, 9998 RPM DYNE NO LOAD

ORIGINAL PAGE
BLACK AND WHITE PHOTOGRAPH

5.4) P.M.G. SPEED VS. VOLTAGE OUTPUT

C) 10,000 RPM DATA POINT

VERTICAL SCALE: 20 VOLTS/DIVISION
TRANSFORMER RATIO: 8.05/1
HORIZONTAL SCALE: 100 μSEC/DIVISION

4) MOTOR B, PHASE A
VRMS 216
PERIOD 725 usec
FREQ 1379 Hz
SPEED 10343 RPM

XFMR RATIO 8.05:1 12-21-83

MOTOR B, ΦA, 9930 RPM DYNE NO LOAD

5) MOTOR B, PHASE B
VRMS 216
PERIOD 720 usec
FREQ 1389 Hz
SPEED 10417 RPM

XFMR RATIO 8.05:1 12-21-83

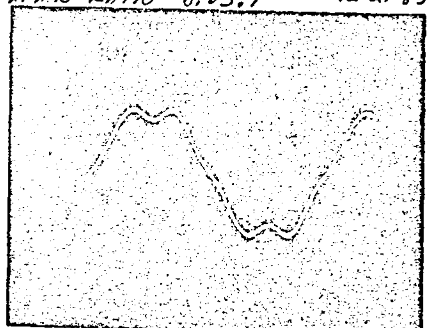

MOTOR B, ΦB, 9938 RPM DYNE NO LOAD

6) MOTOR B, PHASE C
VRMS 216
PERIOD 720 usec
FREQ 1389 Hz
SPEED 10417 RPM

XFMR RATIO 8.05:1 12-21-83

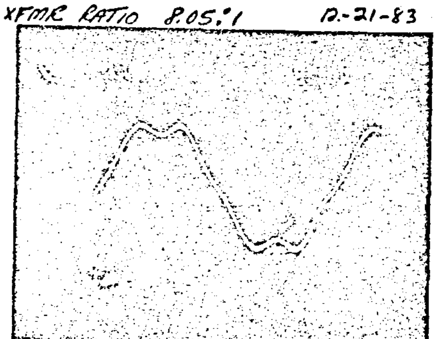

MOTOR B ΦC, 9960 RPM DYNE NO LOAD

ORIGINAL PAGE
BLACK AND WHITE PHOTOGRAPH

5.4) P.M.G. SPEED VS. VOLTAGE OUTPUT

C) 10,000 RPM DATA POINT

VERTICAL SCALE: 20 VOLTS/DIVISION
TRANSFORMER RATIO: 8.05/1
HORIZONTAL SCALE: 100 μSEC/DIVISION

7) MOTOR C, PHASE A
VRMS 216
PERIOD 715 usec
FREQ 1399 Hz
SPEED 10490 RPM

XFMR RATIO 8.05:1 12-21-83

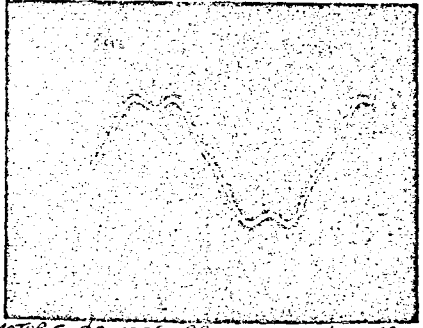

MOTOR C, ΦA, 10080RPM DYNE NO LOAD

8) MOTOR D, PHASE A
VRMS 216
PERIOD 715 usec
FREQ 1399 Hz
SPEED 10490 RPM

XFMR RATIO 8.05:1 12-21-83

MOTOR D, ΦA, 10024RPM DYNE NO LOAD

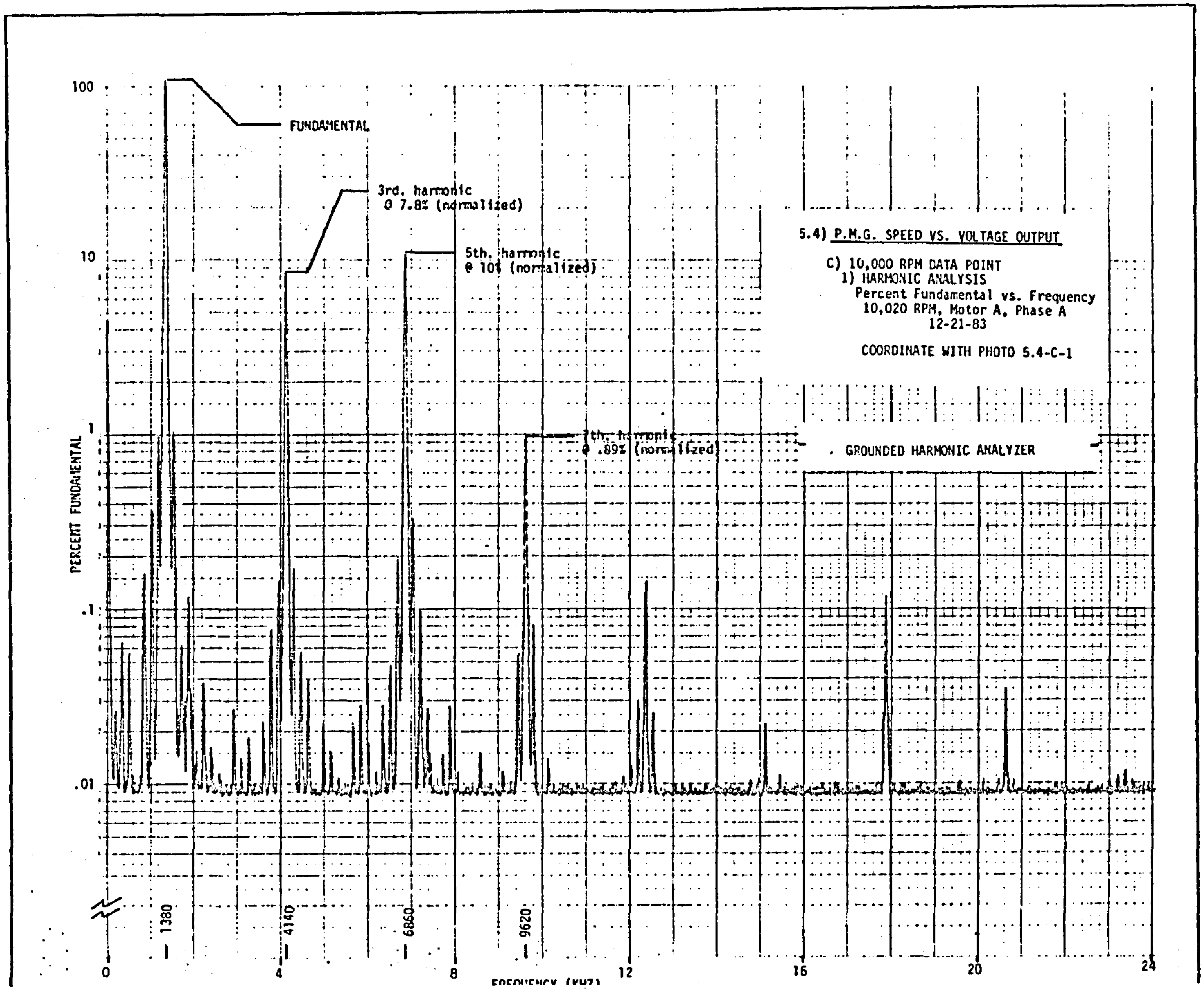

5.4) P.M.G. SPEED VS. VOLTAGE OUTPUT
C) 10,000 RPM DATA POINT
1) HARMONIC ANALYSIS
Percent Fundamental vs. Frequency
10,020 RPM, Motor A, Phase A
12-21-83
COORDINATE WITH PHOTO 5.4-C-1
GROUNDED HARMONIC ANALYZER
FUNDAMENTAL
3rd. harmonic
@ 7.8% (normalized)
5th. harmonic
@ 10% (normalized)
7th. harmonic
@ .89% (normalized)
PERCENT FUNDAMENTAL
100
10
1
.1
.01
1380
4140
6860
9620
0
4
8
12
16
20
24

S8308-
Page

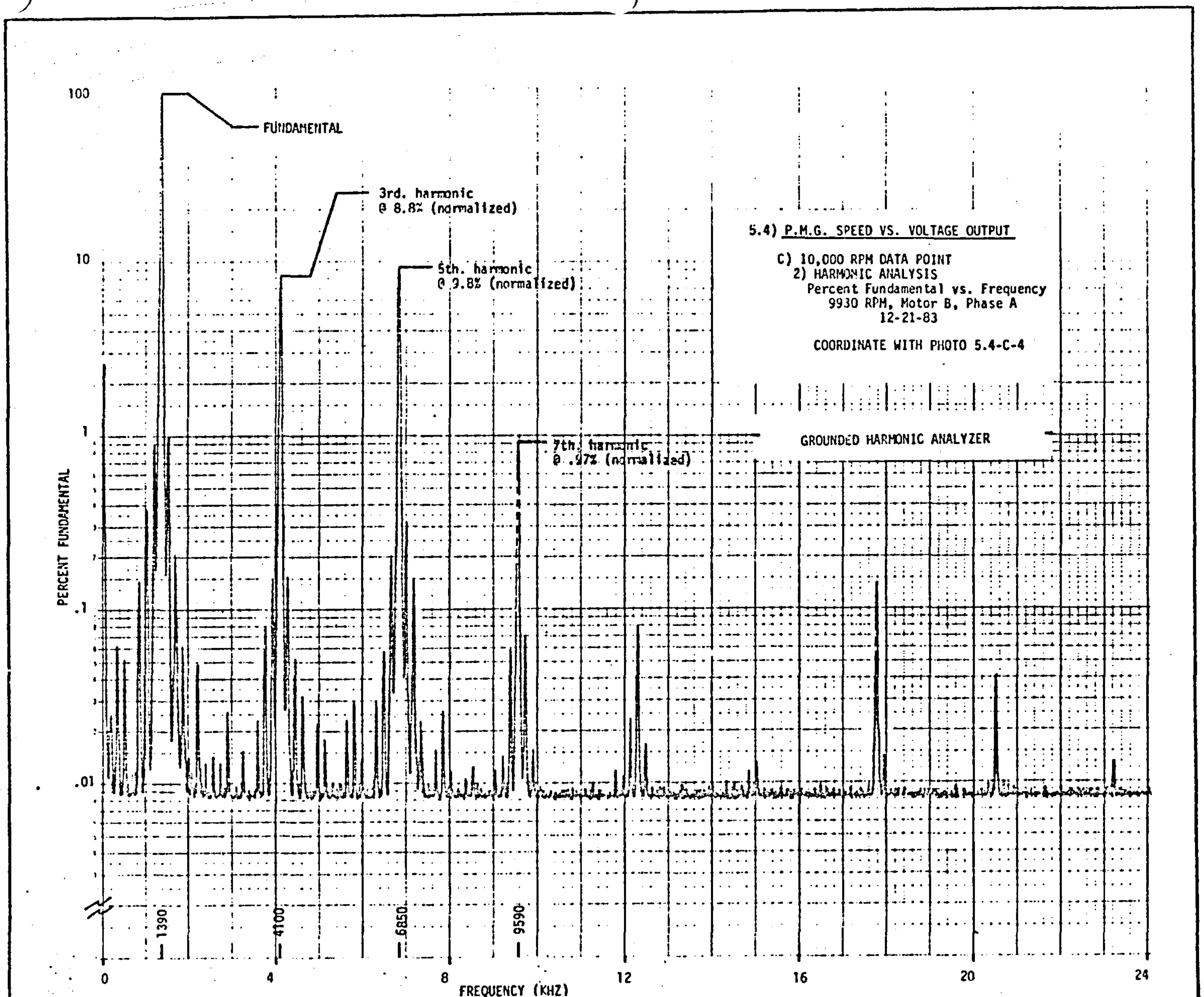
5.4) P.M.G. SPEED VS. VOLTAGE OUTPUT
C) 10,000 RPM DATA POINT
2) HARMONIC ANALYSIS
Percent Fundamental vs. Frequency
9930 RPM, Motor B, Phase A
12-21-83
COORDINATE WITH PHOTO 5.4-C-4
GROUNDED HARMONIC ANALYZER
FUNDAMENTAL
3rd. harmonic
@ 8.8% (normalized)
5th. harmonic
@ 9.8% (normalized)
7th. harmonic
@ .97% (normalized)
PERCENT FUNDAMENTAL
100
10
1
.1
.01
1390
4100
6850
9590
0
4
8
12
16
20
24
FREQUENCY (KHZ)

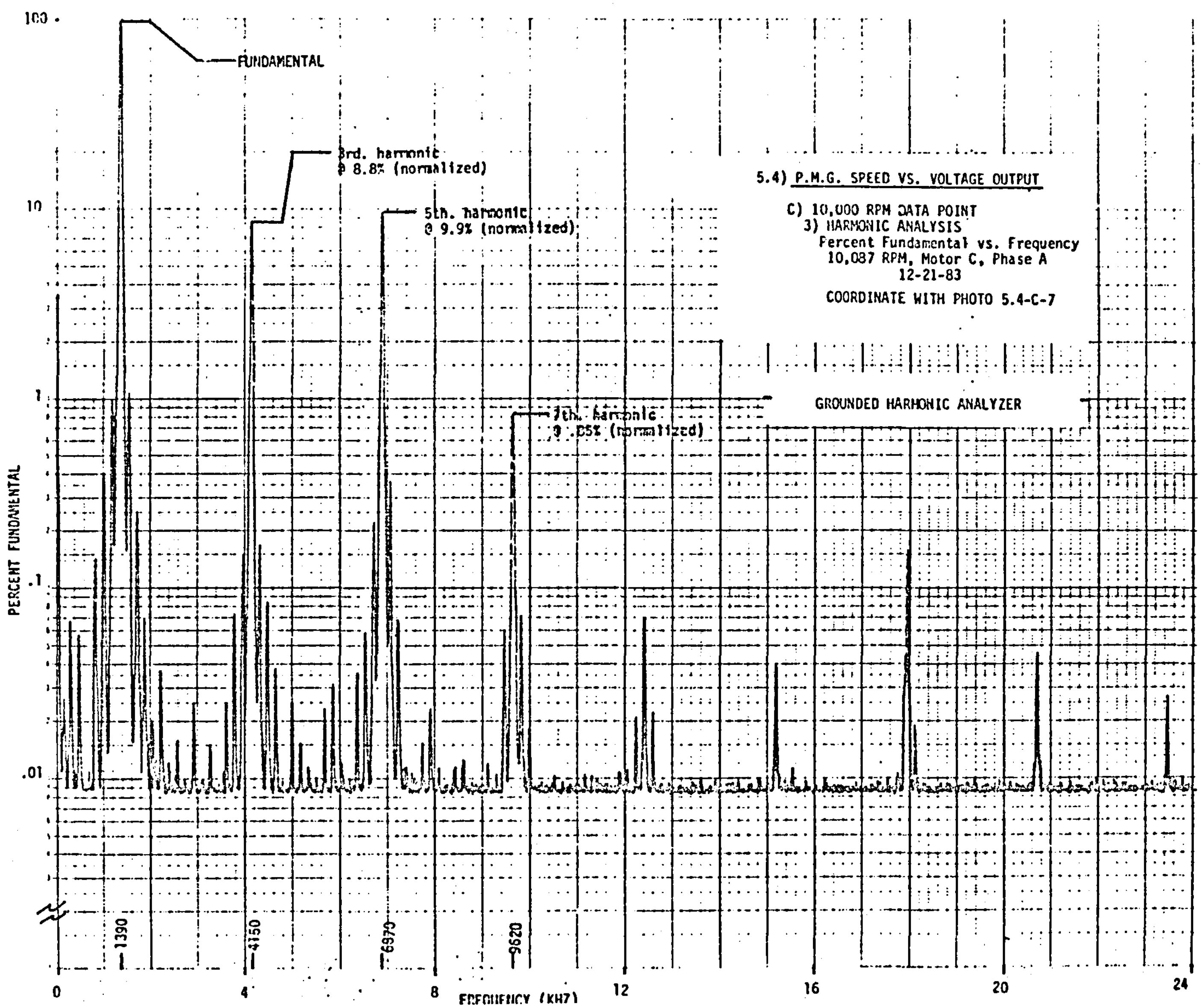

5.4) P.M.G. SPEED VS. VOLTAGE OUTPUT
C) 10,000 RPM DATA POINT
3) HARMONIC ANALYSIS
Percent Fundamental vs. Frequency
10,087 RPM, Motor C, Phase A
12-21-83
COORDINATE WITH PHOTO 5.4-C-7
GROUNDED HARMONIC ANALYZER
FUNDAMENTAL
3rd. harmonic
@ 8.8% (normalized)
5th. harmonic
@ 9.9% (normalized)
7th. harmonic
@ .85% (normalized)
PERCENT FUNDAMENTAL
100
10
1
.1
.01
1390
4150
6970
9620
0
4
8
12
16
20
24
FREQUENCY (KHZ)

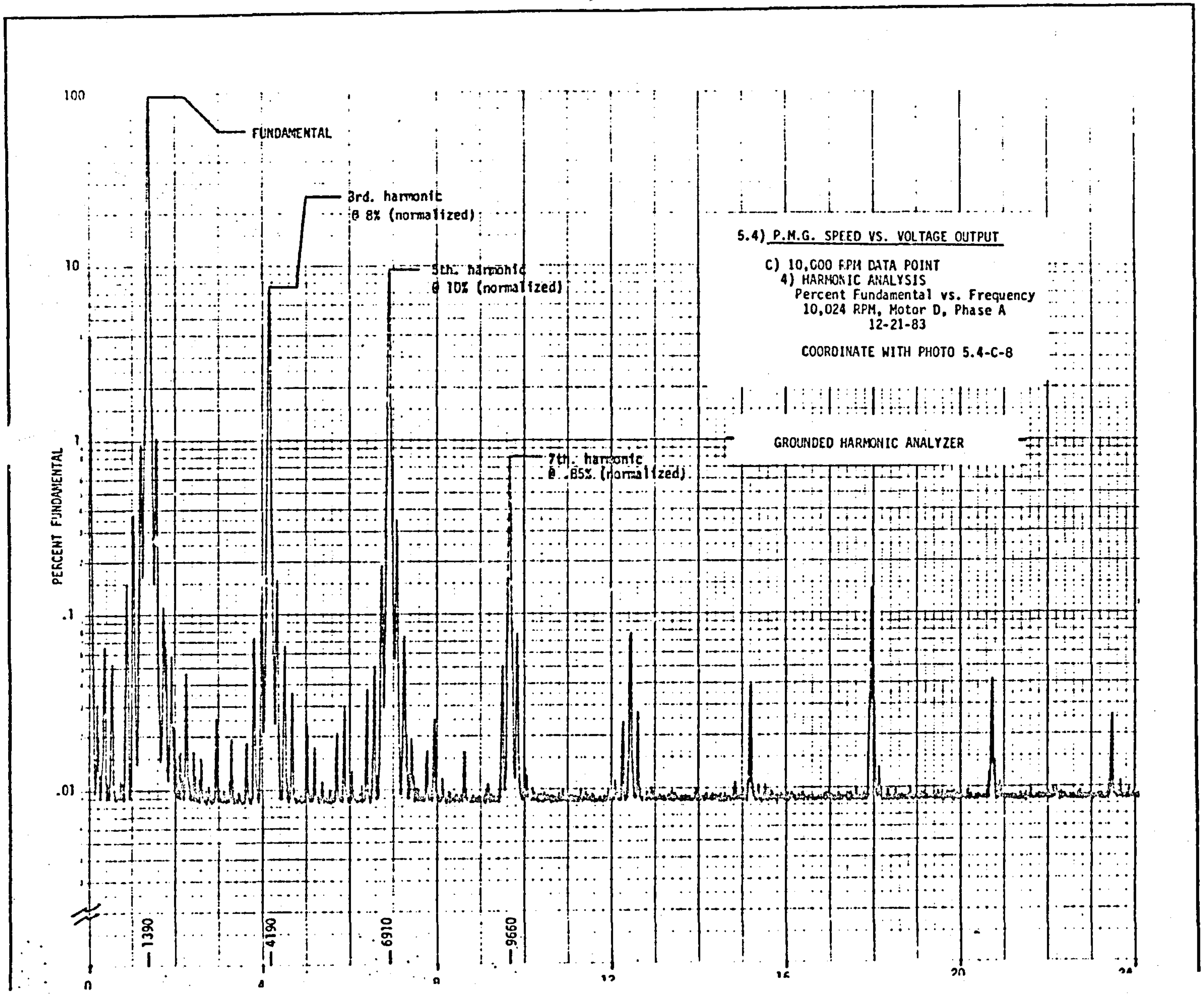
100
10
1
.1
.01
PERCENT FUNDAMENTAL
FUNDAMENTAL
3rd. harmonic
@ 8% (normalized)
5th. harmonic
@ 10% (normalized)
7th. harmonic
@ .85% (normalized)
5.4) P.M.G. SPEED VS. VOLTAGE OUTPUT
C) 10,000 RPM DATA POINT
4) HARMONIC ANALYSIS
Percent Fundamental vs. Frequency
10,024 RPM, Motor D, Phase A
12-21-83
COORDINATE WITH PHOTO 5.4-C-8
GROUNDED HARMONIC ANALYZER
1390
4190
6910
9660
0
4
8
12
16
20
24

ORIGINAL PAGE
BLACK AND WHITE PHOTOGRAPH

5.4) P.M.G. SPEED VS. VOLTAGE OUTPUT

D) 1666 RPM DATA POINT

VERTICAL SCALE: 5 VOLTS/DIVISION
PROBE RATIO: X 10
HORIZONTAL SCALE: 500 μSEC/DIVISION

1) MOTOR A, LINE A TO B
VRMS 70.7
PERIOD 4.4 msec
FREQ 227 Hz
SPEED 1703 RPM

D-5 TEST STAND 1-10-84

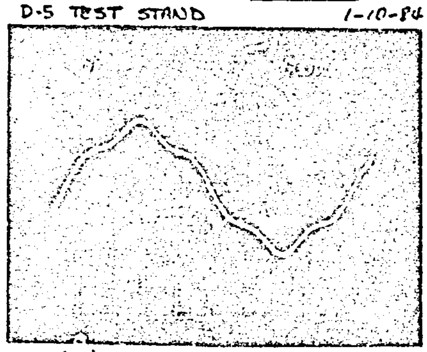

MOTOR A, ΦA-B 1665 RPM NO LOAD

2) MOTOR A, LINE B TO C
VRMS 70.7
PERIOD 4.4 msec
FREQ 227 Hz
SPEED 1703 RPM

D-5 TEST STAND 1-10-84

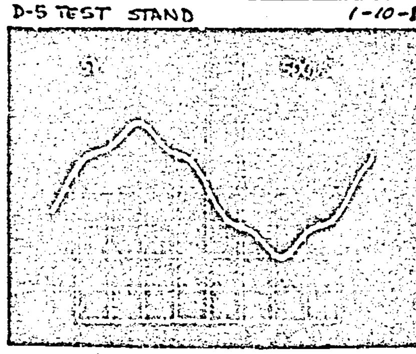

MOTOR A, ΦB-C 1664 RPM NO LOAD

3) MOTOR A, LINE C TO A
VRMS 70.3
PERIOD 4.4 msec
FREQ 227 Hz
SPEED 1703 RPM

D-5 TEST STAND 1-10-84

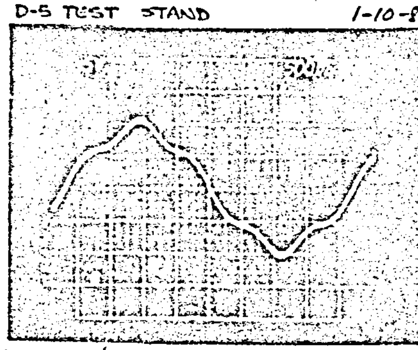

MOTOR A, ΦC-A 1674 RPM NO LOAD

ORIGINAL PAGE
BLACK AND WHITE PHOTOGRAPH

5.4) P.M.G. SPEED VS. VOLTAGE OUTPUT

E) 4333 RPM DATA POINT

VERTICAL SCALE: 2 VOLTS/DIVISION
PROBE RATIO: X 100
HORIZONTAL SCALE: 200 μSEC/DIVISION

1) MOTOR A, LINE A TO B
VRMS 184
PERIOD 1.68 msec
FREQ 595 Hz
SPEED 4462 RPM

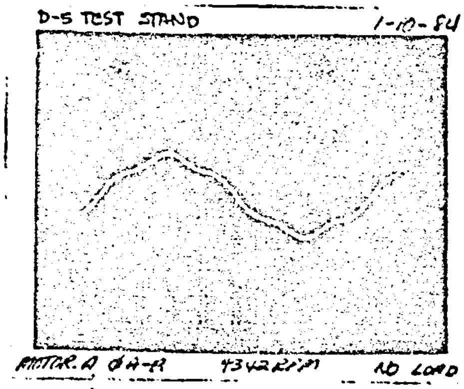

2) MOTOR A, LINE B TO C
VRMS 184
PERIOD 1.68 msec
FREQ 595 Hz
SPEED 4462 RPM

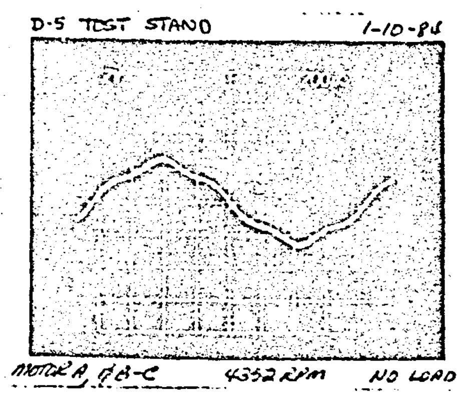

3) MOTOR A, LINE C TO A
VRMS 184
PERIOD 1.68 msec
FREQ 595 Hz
SPEED 4462 RPM

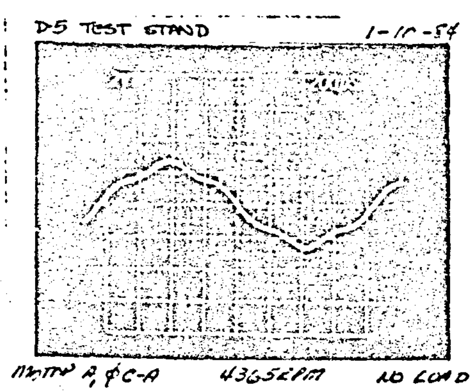

ORIGINAL PAGE
BLACK AND WHITE PHOTOGRAPH

5.4) P.M.G. SPEED VS. VOLTAGE OUTPUT

F) 10,000 RPM DATA POINT

VERTICAL SCALE: 2 VOLTS/DIVISION
PROBE RATIO: X 100
HORIZONTAL SCALE: 100 μSEC/DIVISION

1) MOTOR A, LINE A TO B
VRMS 382
PERIOD .8 msec
FREQ 1250 Hz
SPEED 9375 RPM

D-5 TEST STAND 1-10-84

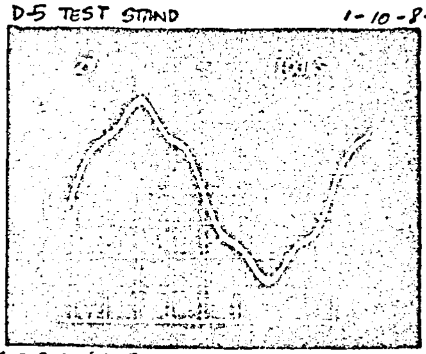

MOTOR A, ΦA-B 9280 RPM NO LOAD

2) MOTOR A, LINE B TO C
VRMS 382
PERIOD .8 msec
FREQ 1250 Hz
SPEED 9375 RPM

D-5 TEST STAND 1-10-84

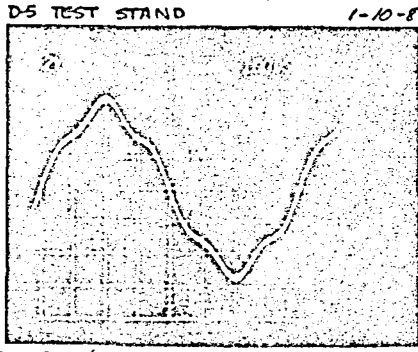

MOTOR A, ΦB-C 9178 RPM NO LOAD

3) MOTOR A, LINE C TO A
VRMS 382
PERIOD .8 msec
FREQ 1250 Hz
SPEED 9375 RPM

D-5 TEST STAND 1-10-84

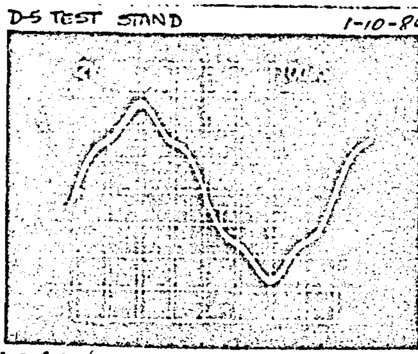

MOTOR A, ΦC-A 9170 RPM NO LOAD

P.M.G. LOADING DATA

5.5) P.M.G. LOADING

PHOTOGRAPH VS. HARMONIC ANALYSIS CROSS REFERENCE TABLE

PHOTO NUMBER	SPEED (R.P.M.)	LOAD (AMPS)	QUADRANT MOTORS	MOTOR CONNECTION	HARMONIC ANALYSIS GRAPH NUMBER
5.5-A-1	1690	.93	A	A-N	
-2	1685	.93		B-N	
-3	1686	.93		C-N	
-4	1676	1.74		A-N	
-5	1660	3.5			
-6	1648	5.2			
-7	1665	6			
-8	1672	7			
-9	1671	7.9			
5.5-A -10	1697	9.3			5.5-A-3
-11	1675	10.1			
-12	1684	10.7			
-13	1678	11.5			
-14	1670	12.3			
-15	1671	13			
-16	1660	13.4			
5.5-A -17	1663	14.1			5.5-A-5
-18	1671	14.8			
-19	1668	15.4			
-20	1656	6.1			5,5-A-1
-21	1647	6.1		A-B	5.5-A-2
5.5-B-1	4362	2.4	A	A-N	
-2	4323	17.8			
-3	4325	17.8		A-B	
-4	4312	0	B	A-N	
-5	4315	0	B	A-B	
-6	4325	14.6	A	A-N	5.5-B-1, -3
-7	4333	14.6		A-B	5.5-B-2, -4
5.5-C-1	10081	5.7	A	A-N	
-2	10014	10.2			5.5-C-1
-3	9968	10.2		A-B	5.5-C-2
-4	10034	18.1		A-N	
-5	9990	18.1		A-B	

5.5) P.M.G. LOADING

HARMONIC ANALYSIS MAGNITUDE SUMMARY

N = ungrounded harmonic analyzer

Y = grounded harmonic analyzer

GRAPH NUMBER	SPEED (R.P.M.)	LOAD (AMPS)	QUADRANT MOTOR	MOTOR CONNECTION	GND	(HARMONIC) 3rd	5th	7th
A) 1666 RPM DATA POINT								
5.5-A-1	1660	6.1	A	A-N	N	7.9	7.3	.72
-2	1647	6.1	↓	A-B	N	.6	7.2	.74
-3	1671	9.3	↓	A-N	Y	6.9	5.6	.53
-4	1684	9.3	↓	A-B	Y	8.3	5.6	.53
-5	1639	14.1	↓	A-N	Y	6.5	3.9	.45
-6	1647	14.1	↓	A-B	Y	7.8	3.9	.43
B) 4333 RPM DATA POINT								
5.5-B-1	4325	14.6	A	A-N	N	6.3	3.4	.44
-2	4333	14.6	↓	A-B	N	1.0	3.4	.42
-3	4316	14.4	↓	A-N	Y	6.2	3.5	.46
-4	4310	14.4	↓	A-B	Y	7.6	3.5	.48
C) 10,000 RPM DATA POINT								
5.5-C-1	10K	10.2	A	A-N	N	5.9	3.0	.46
-2	10K	10.2	↓	A-B	N	1.1	3.0	.39

5.5) P.M.G. LOADING

A) 1666 RPM DATA POINT

LOAD	SPEED 1666 r.p.m.	TEMP	TORQUE	MOTOR A				MOTOR A				MOTOR A			
ACTUAL	ACTUAL	°F	IN-LBS	Ia	Ib	Ic	Iave	Van	Vbn	Vcn	Vave	Wa	Wb	Wc	Wtot
350	1666	95	11.4	.92	.93	.94	.93	37.1	36.9	37.1	37	34.9	35.6	35.7	106
700	1662	96	15.9	1.67	1.82	1.73	1.74	36.2	36.5	36.5	36.4	60.5	66.5	62	189
1400	1652	97	25.7	3.46	3.55	3.55	3.52	35.6	36.2	36	35.9	123	129	128	380
2100	1647	98	34.5	5.01	5.29	5.15	5.15	34.9	35.7	35.4	35.3	176	190	183	549
2450	1662	99	39.3	5.87	6.21	6.04	6.04	35	35.9	35.4	35.4	206	224	215	645
2800	1664	100	44.5	6.87	7.07	7.06	7.0	34.5	35.7	35.1	35.1	238	253	249	740
3150	1670	105	48.9	7.69	7.95	7.91	7.85	34.4	35.6	35.	35.	265	284	277	826
3500	1676	83	56.1	9.08	9.44	9.36	9.29	33.7	35.1	34.4	34.4	310	336	326	972
3850	1670	95	60	9.82	10.25	10.11	10.1	33.4	34.9	34.1	34.1	329	360	347	1036
4200	1670	98	63.2	10.4	11.	10.7	10.7	33.1	34.7	33.8	33.9	347	386	366	1099
4550	1669	107	66.7	11.1	11.8	11.5	11.5	32.8	34.4	33.5	33.6	364	408	384	1156
4900	1668	113	70.3	12.	12.5	12.3	12.3	32.3	34.1	33.	33.1	385	430	406	1221

B. ZELINSKI / L. KINTZ

1/11/84

5.5) P.M.G. LOADING

A) 1666 RPM DATA POINT

LOAD	SPEED 1666 r.p.m.	TEMP	TORQUE	MOTOR A				MOTOR A				MOTOR A			
ACTUAL	ACTUAL	°F	IN-LBS	Ia	Ib	Ic	Iave	Van	Vbn	Vcn	Vave	Wa	Wb	Wc	Wtot
5250	1670	117	73.6	12.6	13.3	13.	13.	31.9	33.8	32.7	32.8	402	451	425	1278
5600	1662	122	75.6	13.	13.9	13.4	13.4	31.5	33.5	32.3	32.4	409	465	432	1306
5950	1664	126	78.6	13.6	14.6	14.1	14.1	31.2	33.2	32.	32.1	425	486	450	1361
6300	1665	123	81.6	14.3	15.3	14.9	14.8	30.8	32.9	31.6	31.8	441	505	472	1418
6650	1662	132	84.	14.9	15.9	15.5	15.4	30.4	32.6	31.2	31.4	455	525	482	1462

B. ZELINSKI/L. KINTZ
1/11/84

5.5) P.M.G. LOADING

A) 1666 RPM DATA POINT

LOAD	SPEED 1666 R.P.M.			MOTOR B				MOTOR C				MOTOR D			
ACTUAL	ACTUAL			Van	Vbn	Vcn	Vave	Van	Vbn	Vcn	Vave	Van	Vbn	Vcn	Vave
350	1687			36.6	36.6	36.7	36.6	36.6	36.6	36.7	36.6	36.5	36.5	36.5	36.5
700	1669			36.1	36.0	36.1	36.1	36.0	36.0	36.1	36.0	36.0	36.1	36.1	36.1
1400	1658			36.0	35.9	36.0	36.0	35.8	35.7	35.9	35.8	35.7	35.5	35.6	35.6
2100	1651			36.1	35.8	35.9	35.9	35.7	35.7	35.7	35.7	35.5	35.2	35.5	35.4
2450	1676			36.7	36.3	36.3	36.4	36.3	36.3	36.3	36.3	36.1	35.8	36.1	36.0
2800	1669			37.1	36.7	36.9	36.9	36.8	36.8	36.8	36.8	36.7	36.2	36.6	36.5
3150	1670			37.3	36.8	37.1	37.1	36.9	36.9	37.0	36.9	36.8	36.2	36.8	36.6
3500	1685			37.4	36.9	37.2	37.2	37.1	37.6	37.1	37.1	37.0	36.4	37.0	36.8
3850	1674			37.3	36.8	37.1	37.1	36.9	36.8	36.9	36.9	36.8	36.1	36.7	36.5
4200	1681			37.5	36.9	37.2	37.2	37.0	37.0	37.1	37.0	37.0	36.3	37.0	36.8
4550	1675			37.4	36.8	37.2	37.1	37.0	36.9	37.0	37.0	36.9	36.1	36.8	36.6
4900	1669			37.4	36.7	37.1	37.1	36.9	36.8	36.9	36.9	36.9	36.0	36.8	36.6

B. ZELINSKI / L. KINTZ
1/11/84

5.5) P.M.G. LOADING

A) 1666 RPM DATA POINT

LOAD	SPEED 1666 R.P.M.			MOTOR B				MOTOR C				MOTOR D			
ACTUAL	ACTUAL			Van	Vbn	Vcn	Vave	Van	Vbn	Vcn	Vave	Van	Vbn	Vcn	Vave
5250	1669			37.4	36.7	37.1	37.1	36.9	36.9	36.9	36.9	36.9	36.0	36.8	36.6
5600	1660			37.3	36.6	37.0	37.0	36.7	36.7	36.8	36.7	36.7	35.7	36.6	36.3
5950	1664			37.4	36.7	37.1	37.1	36.9	37.8	36.9	37.2	36.8	35.8	36.7	36.4
6300	1670			37.6	36.7	37.2	37.2	37.1	36.9	37.0	37.0	37.1	35.9	36.9	36.6
6650	1671			37.7	36.8	37.2	37.2	37.0	36.9	37.1	37.0	37.1	35.9	36.9	36.6

B. ZELINSKI / L. KINTZ
1/11/84

5.5) P.M.G. LOADING

A) 1666 RPM DATA POINT

QUADRANT MOTOR A: RESISTIVE LOADED

VERTICAL SCALE: .2 VOLTS/DIVISION
PROBE RATIO: X 100
HORIZONTAL SCALE: 500 μSEC/DIVISION

1) MOTOR A, PHASE A
VRMS 35.4
PERIOD 4.3 msec
FREQ 233 Hz
SPEED 1748 RPM
LOAD .93 amps
TEMP (F) 95

D5 TEST STAND 1-10-84

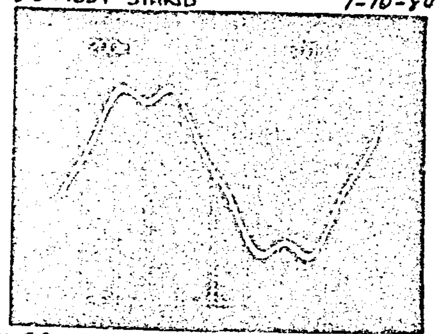

MOTOR A, φA 1690RPM 350W

2) MOTOR A, PHASE B
VRMS 35.4
PERIOD 4.4 msec
FREQ 227 Hz
SPEED 1703 RPM
LOAD .93 amps
TEMP (F) 95

D-5 TEST STAND 1-10-84

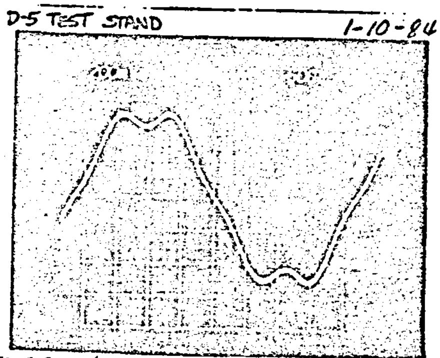

MOTOR A, φB 1685RPM 350W

3) MOTOR A, PHASE C
VRMS 35.4
PERIOD 4.4 msec
FREQ 227 Hz
SPEED 1703 RPM
LOAD .93 amps
TEMP (F) 95

D5 TEST STAND 1-10-84

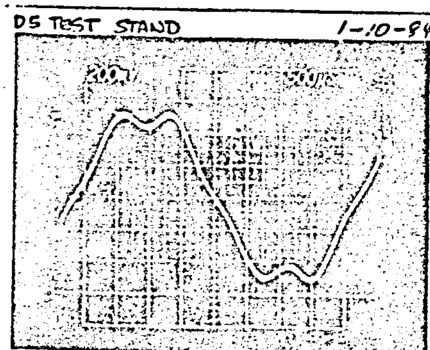

MOTOR A, φC 1686 RPM 350W

ORIGINAL PAGE
BLACK AND WHITE PHOTOGRAPH

5.5) P.M.G. LOADING

A) 1666 RPM DATA POINT

QUADRANT MOTOR A: RESISTIVE LOADED

VERTICAL SCALE: .2 VOLTS/DIVISION
PROBE RATIO: X 100
HORIZONTAL SCALE: 500 µSEC/DIVISION

4) MOTOR A, PHASE A
- VRMS 33.9
- PERIOD 4.4 msec
- FREQ 227 Hz
- SPEED 1703 RPM
- LOAD 1.74 amps
- TEMP (F) 83

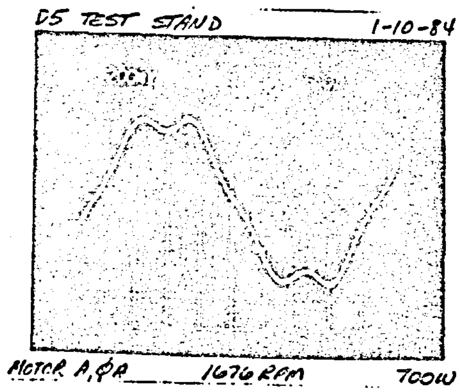

5) MOTOR A, PHASE A
- VRMS 33.2
- PERIOD 4.4 msec
- FREQ 227 Hz
- SPEED 1703 RPM
- LOAD 3.5 amps
- TEMP (F) 83

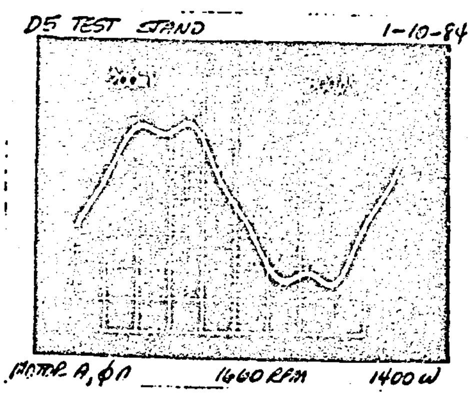

6) MOTOR A, PHASE A
- VRMS 33.2
- PERIOD 4.5 msec
- FREQ 222 Hz
- SPEED 1665 RPM
- LOAD 5.2 amps
- TEMP (F) 86

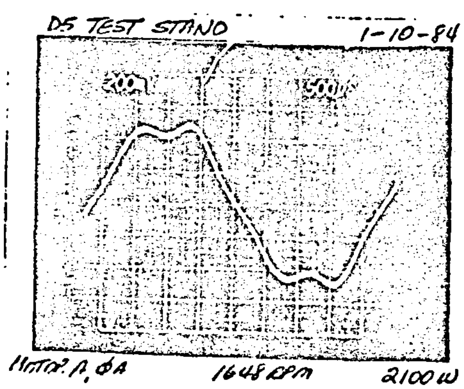

BLACK AND WHITE PHOTOGRAPH

ORIGINAL PAGE
BLACK AND WHITE PHOTOGRAPH

5.5) P.M.G. LOADING

A) 1666 RPM DATA POINT

QUADRANT MOTOR A: RESISTIVE LOADED

VERTICAL SCALE: .2 VOLTS/DIVISION
PROBE RATIO: X 100
HORIZONTAL SCALE: 500 µSEC/DIVISION

7) MOTOR A, PHASE A
VRMS 33.2
PERIOD 4.4 msec
FREQ 227 Hz
SPEED 1703 RPM
LOAD 6 amps
TEMP (F) 84

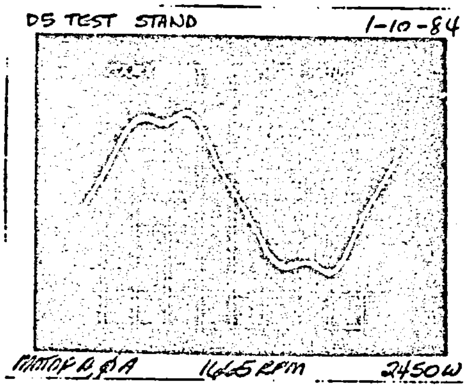

8) MOTOR A, PHASE A
VRMS 32.5
PERIOD 4.4 msec
FREQ 227 Hz
SPEED 1703 RPM
LOAD 7 amps
TEMP (F) 102

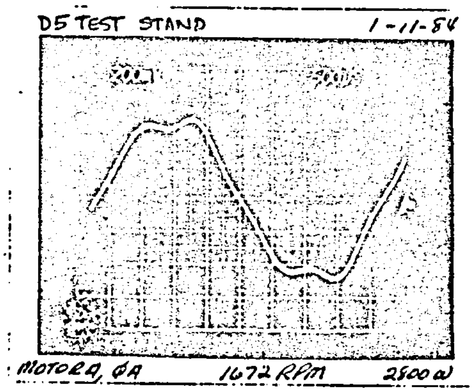

9) MOTOR A, PHASE A
VRMS 32.5
PERIOD 4.4 msec
FREQ 227 Hz
SPEED 1703 RPM
LOAD 7.9 amps
TEMP (F) 103

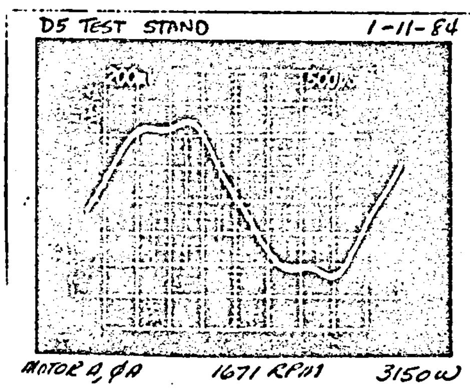

ORIGINAL PAGE
BLACK AND WHITE PHOTOGRAPH

5.5) P.M.G. LOADING

A) 1656 RPM DATA POINT

QUADRANT MOTOR A: RESISTIVE LOADED

VERTICAL SCALE: .2 VOLTS/DIVISION
PROBE RATIO: X 100
HORIZONTAL SCALE: 500 μSEC/DIVISION

10) MOTOR A, PHASE A
VRMS 31.8
PERIOD 4.3 msec
FREQ 233 Hz
SPEED 1748 RPM
LOAD 9.3 amps
TEMP (F) 91

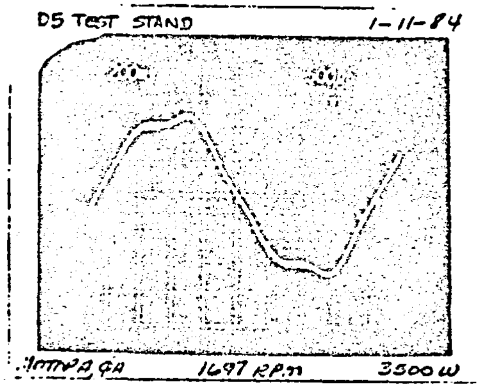

11) MOTOR A, PHASE A
VRMS 31.1
PERIOD 4.4 msec
FREQ 227 Hz
SPEED 1703 RPM
LOAD 10.1 amps
TEMP (F) 99

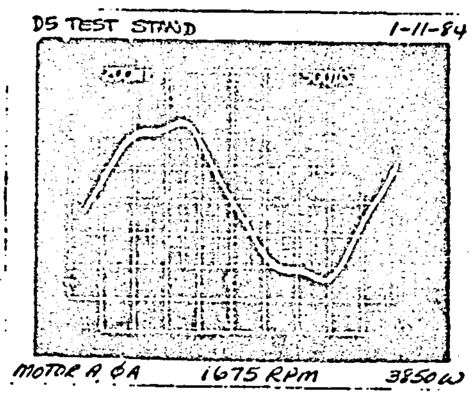

12) MOTOR A, PHASE A
VRMS 31.1
PERIOD 4.4 msec
FREQ 227 Hz
SPEED 1703 RPM
LOAD 10.7 amps
TEMP (F) 104

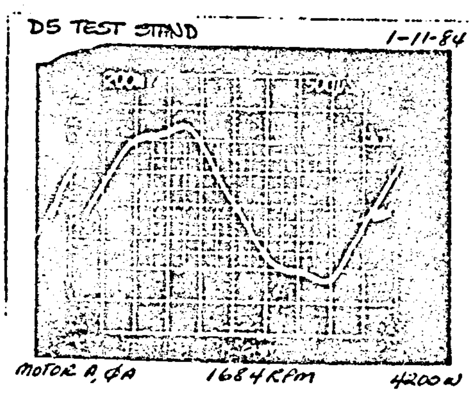

ORIGINAL PAGE
BLACK AND WHITE PHOTOGRAPH

5.5) P.M.G. LOADING

A) 1666 RPM DATA POINT

QUADRANT MOTOR A: RESISTIVE LOADED

VERTICAL SCALE: .2 VOLTS/DIVISION
PROBE RATIO: X 100
HORIZONTAL SCALE: 500 μSEC/DIVISION

13) MOTOR A, PHASE A
VRMS 31.1
PERIOD 4.4 msec
FREQ 227 Hz
SPEED 1703 RPM
LOAD 11.5 amps
TEMP (F) 111

D5 TEST STAND 1-11-84

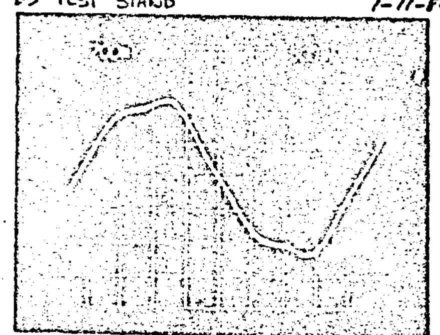

MOTOR A, ØA 1678 RPM 4550 W

14) MOTOR A, PHASE A
VRMS 30.4
PERIOD 4.4 msec
FREQ 227 Hz
SPEED 1703 RPM
LOAD 12.3 amps
TEMP (F) 116

D5 TEST STAND 1-11-84

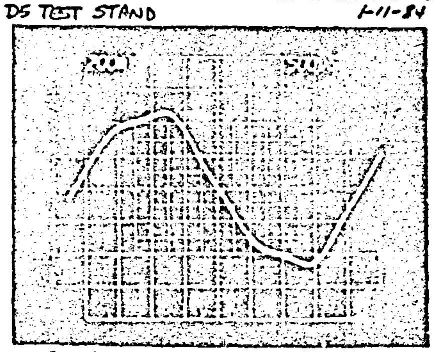

MOTOR A, ØA 1670 RPM 4900 W

15) MOTOR A, PHASE A
VRMS 30.4
PERIOD 4.4 msec
FREQ 227 Hz
SPEED 1703 RPM
LOAD 13 amps
TEMP (F) 120

D5 TEST STAND 1-11-84

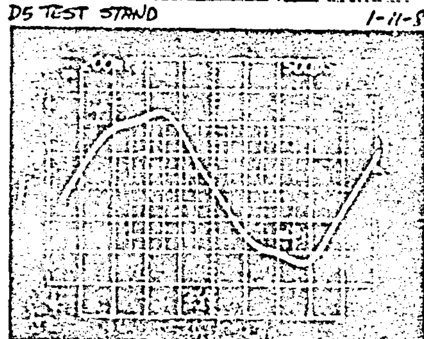

MOTOR A, ØA 1671 RPM 5250 W

ORIGINAL PAGE
BLACK AND WHITE PHOTOGRAPH

5.5) P.M.G. LOADING

A) 1666 RPM DATA POINT

QUADRANT MOTOR A: RESISTIVE LOADED

VERTICAL SCALE: .2 VOLTS/DIVISION
PROBE RATIO: X 100
HORIZONTAL SCALE: 500 μSEC/DIVISION

16) MOTOR A, PHASE A
VRMS 29.7
PERIOD 4.4 msec
FREQ 227 Hz
SPEED 1703 RPM
LOAD 13.4 amps
TEMP (F) 124

DS TEST STAND 1-11-84

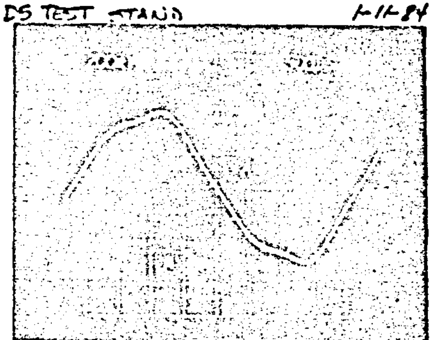

MOTOR A, φA 1660 RPM 5600W

17) MOTOR A, PHASE A
VRMS 29.7
PERIOD 4.4 msec
FREQ 227 Hz
SPEED 1703 RPM
LOAD 14.1 amps
TEMP (F) 128

DS TEST STAND 1-11-84

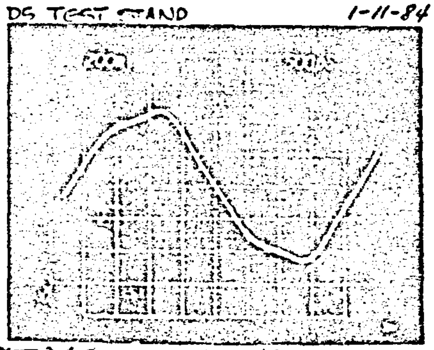

MOTOR A, φA 1663 RPM 5450W

18) MOTOR A, PHASE A
VRMS 29.7
PERIOD 4.4 msec
FREQ 227 Hz
SPEED 1703 RPM
LOAD 14.8 amps
TEMP (F) 130

DS TEST STAND 1-11-84

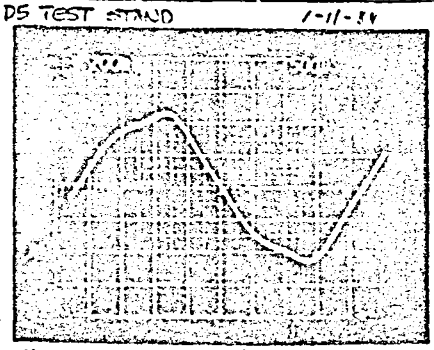

MOTOR A, φA 1671 RPM 6300 W

ORIGINAL PAGE
BLACK AND WHITE PHOTOGRAPH

5.5) P.M.G. LOADING

A) 1666 RPM DATA POINT

QUADRANT MOTOR A: RESISTIVE LOADED

VERTICAL SCALE: .2 VOLTS/DIVISION
PROBE RATIO: X 100
HORIZONTAL SCALE: 500 μSEC/DIVISION

19) MOTOR A, PHASE A

VRMS 29.7
PERIOD 4.4 msec
FREQ 227 Hz
SPEED 1703 RPM
LOAD 15.4 amps
TEMP (F) 135

D5 TEST STAND 1-11-84

Motor A, ΦA 1668 RPM 6650W

5.5) P.M.G. LOADING

A) 1666 RPM DATA POINT

COMPARISON OF 'PHASE' AND 'LINE TO LINE' VOLTAGE WAVEFORMS FOR RESISTANCE LOADED QUADRANT MOTOR 'A'

.2 VOLT/DIVISION:	VERTICAL SCALE:	.5 VOLT/DIVISION
X100:	PROBE RATIO:	X100
500 μSEC/DIVISION:	HORIZONTAL SCALE:	500 μSEC/DIVISION

20) MOTOR A, PHASE A

VRMS 31.1

PERIOD 4.5 msec

FREQ 222 Hz

SPEED 1665 RPM

LOAD 6.1 amps

TEMP (F) 90

21) MOTOR A, LINE A TO B

VRMS 61.9

PERIOD 4.5 msec

FREQ 222 Hz

SPEED 1665 RPM

LOAD 6.1 amps

TEMP (F) 90

1-16-84

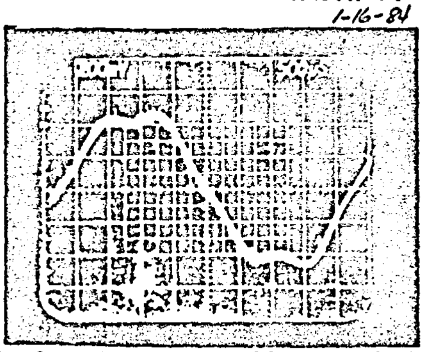

MOTOR A, ΦA 1656 RPM 8250 W

1-13-84

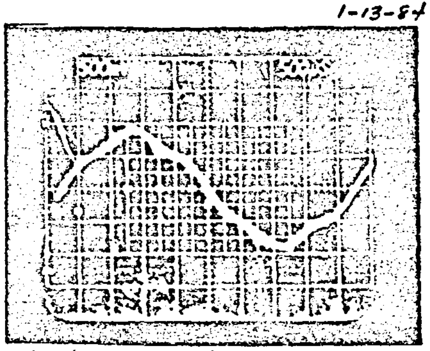

MOTOR A, ΦA-B 1647 RPM 8250 W

ORIGINAL PAGE
BLACK AND WHITE PHOTOGRAPH

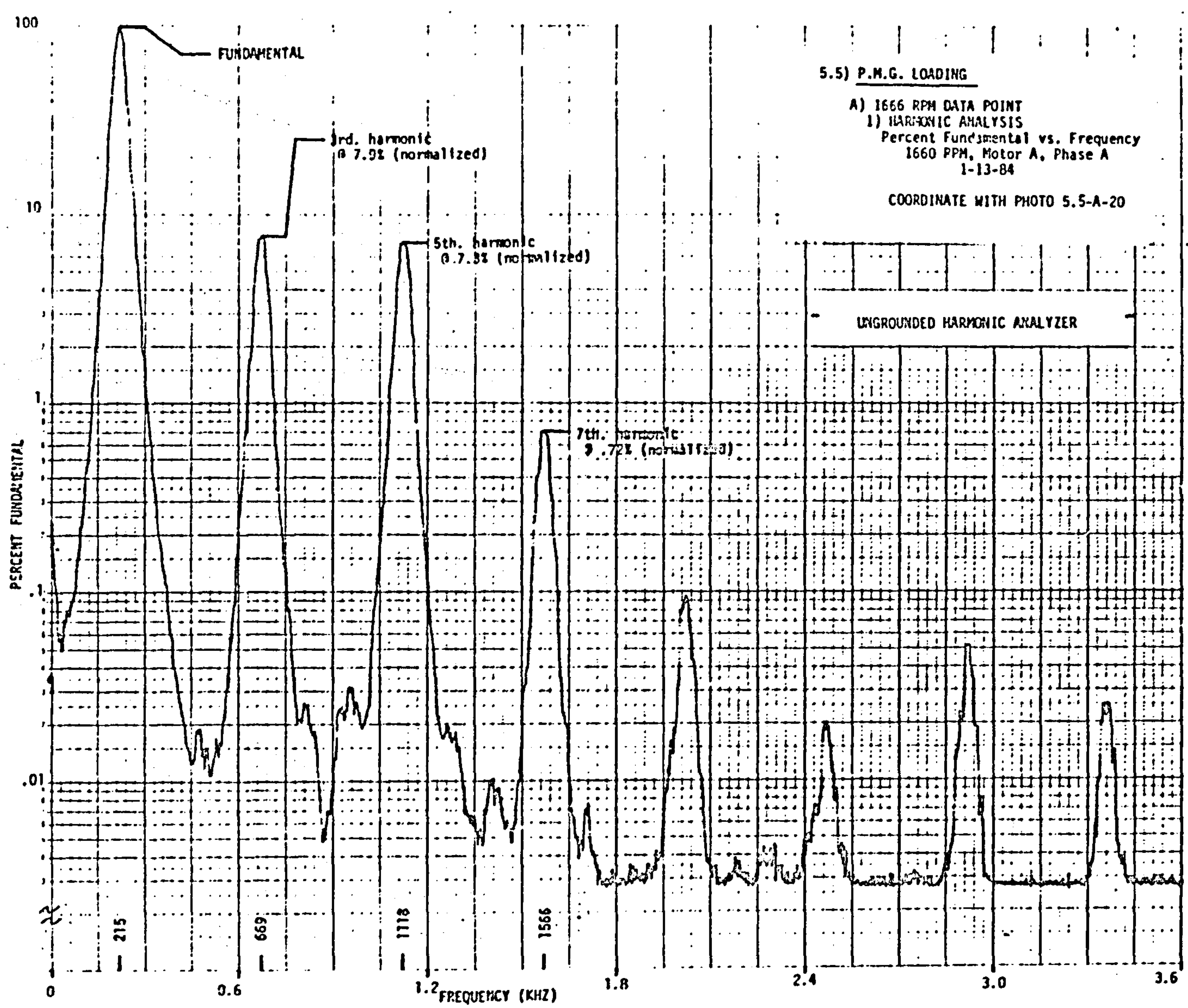
5.5) P.M.G. LOADING
A) 1666 RPM DATA POINT
1) HARMONIC ANALYSIS
Percent Fundamental vs. Frequency
1660 PPM, Motor A, Phase A
1-13-84
COORDINATE WITH PHOTO 5.5-A-20
UNGROUNDED HARMONIC ANALYZER
FUNDAMENTAL
3rd. harmonic
@ 7.9% (normalized)
5th. harmonic
@ 7.3% (normalized)
7th. harmonic
@ .72% (normalized)
PERCENT FUNDAMENTAL
100
10
1
.1
.01
215
669
1118
1566
0
0.6
1.2
1.8
2.4
3.0
3.6
FREQUENCY (KHZ)

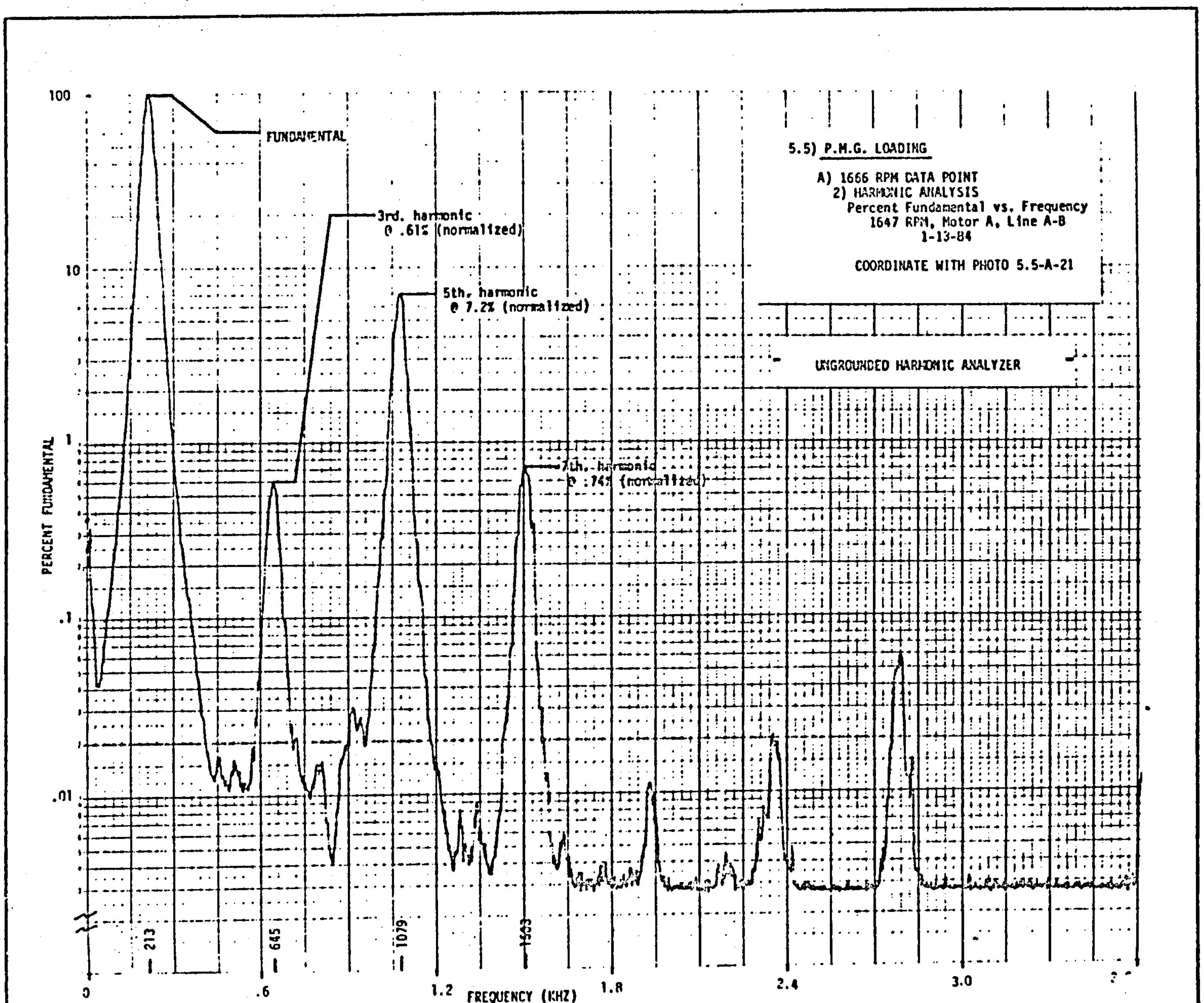
5.5) P.M.G. LOADING
A) 1666 RPM DATA POINT
2) HARMONIC ANALYSIS
Percent Fundamental vs. Frequency
1647 RPM, Motor A, Line A-B
1-13-84
COORDINATE WITH PHOTO 5.5-A-21
UNGROUNDED HARMONIC ANALYZER
FUNDAMENTAL
3rd. harmonic
@ .61% (normalized)
5th. harmonic
@ 7.2% (normalized)
7th. harmonic
@ .74% (normalized)
PERCENT FUNDAMENTAL
100
10
1
.1
.01
FREQUENCY (KHZ)
0
.6
1.2
1.8
2.4
3.0
213
645
1079
1503

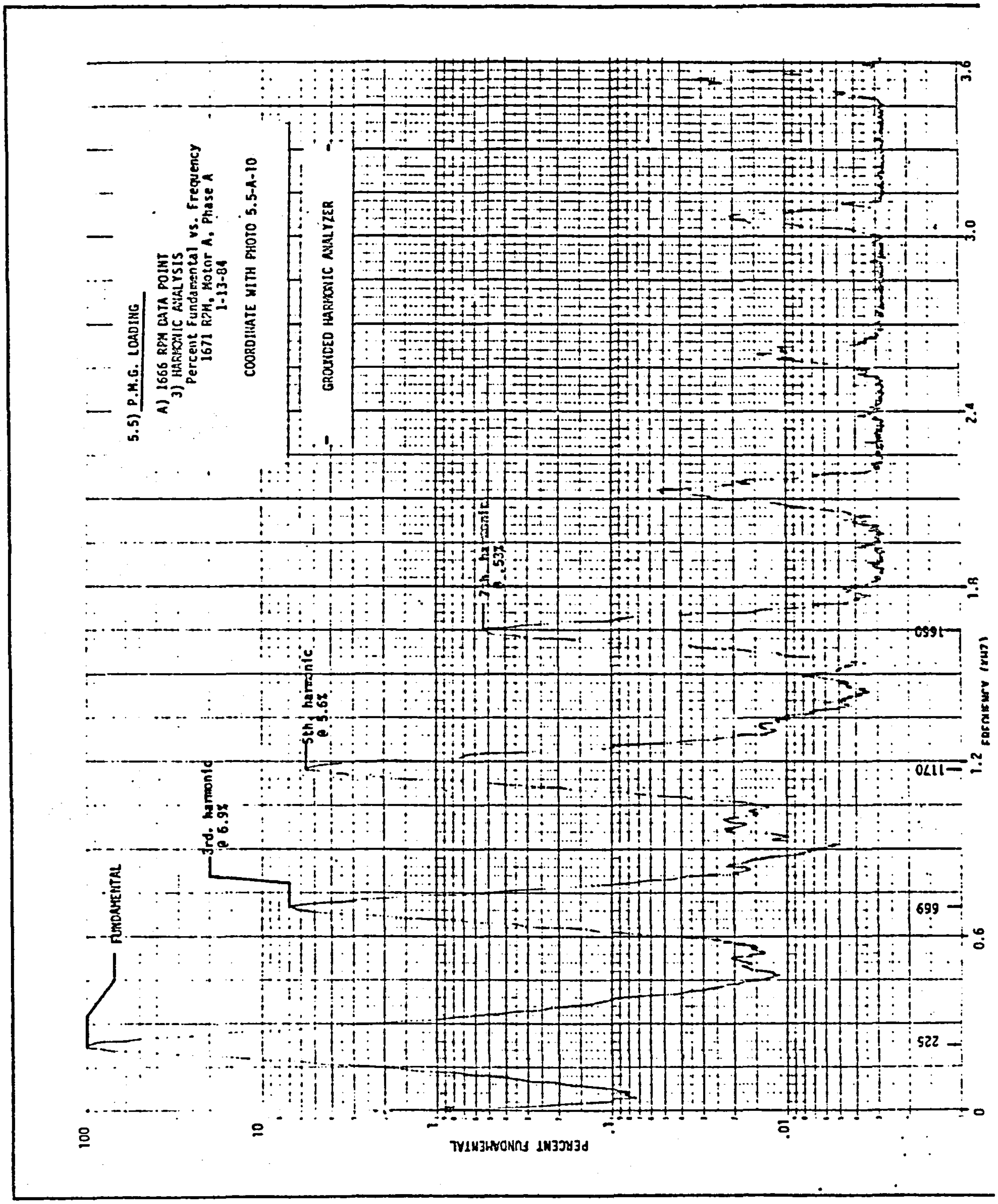
5.5) P.M.G. LOADING
A) 1666 RPM DATA POINT
3) HARMONIC ANALYSIS
Percent Fundamental vs. Frequency
1671 RPM, Motor A, Phase A
1-13-84
COORDINATE WITH PHOTO 5.5-A-10
GROUNDED HARMONIC ANALYZER
FUNDAMENTAL
3rd. harmonic @ 6.9%
5th harmonic @ 5.6%
7th harmonic @ .53%
100
10
1.
.1
.01
PERCENT FUNDAMENTAL
0
225
669
0.6
1170
1.2
1660
1.8
2.4
3.0
3.6
FREQUENCY (KHZ)

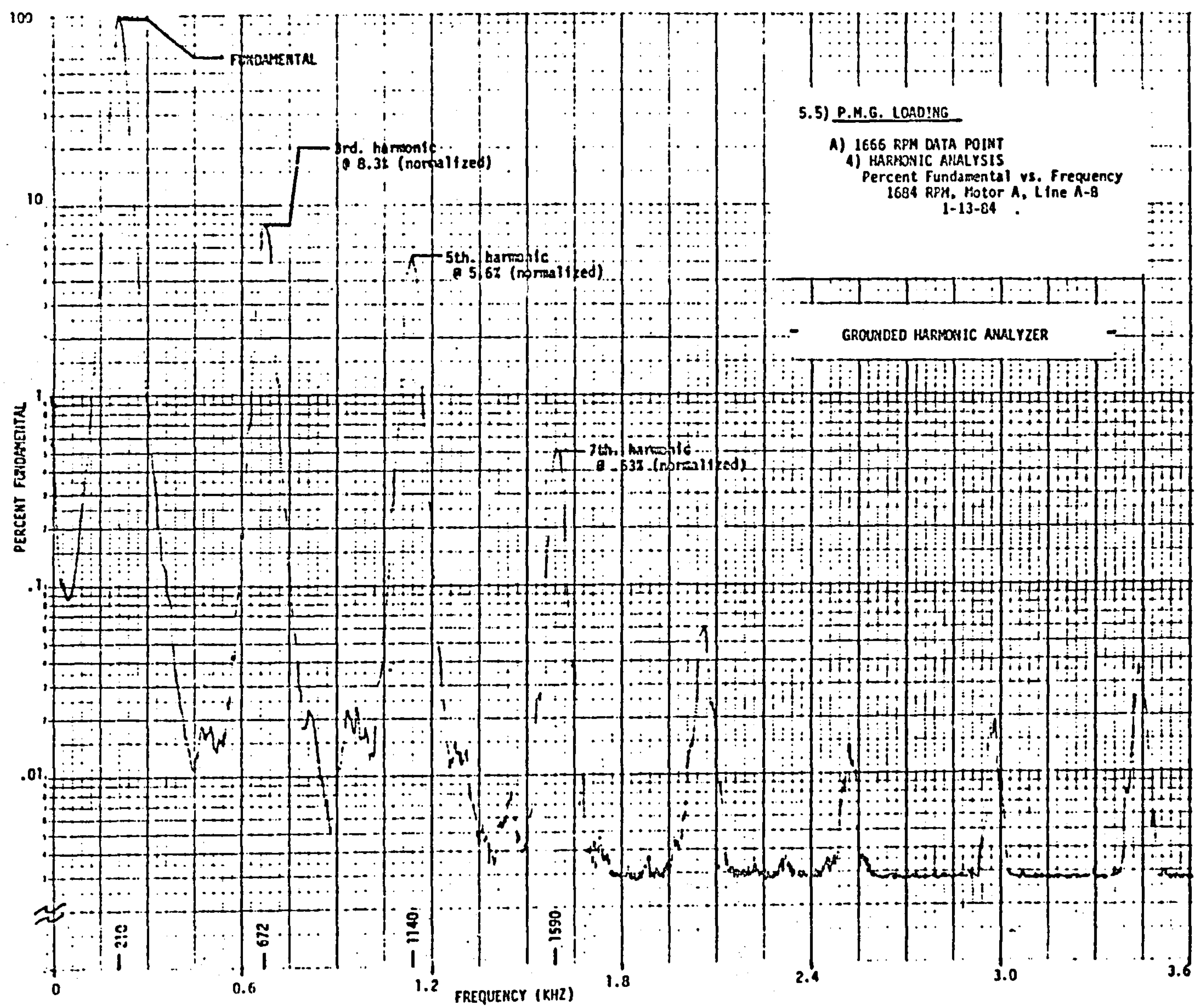
5.5) P.M.G. LOADING
A) 1666 RPM DATA POINT
4) HARMONIC ANALYSIS
Percent Fundamental vs. Frequency
1684 RPM, Motor A, Line A-B
1-13-84
GROUNDED HARMONIC ANALYZER
FUNDAMENTAL
3rd. harmonic
@ 8.3% (normalized)
5th. harmonic
@ 5.6% (normalized)
7th. harmonic
@ .63% (normalized)
PERCENT FUNDAMENTAL
100
10
1
.1
.01
FREQUENCY (KHZ)
0
0.6
1.2
1.8
2.4
3.0
3.6
210
672
1140
1590

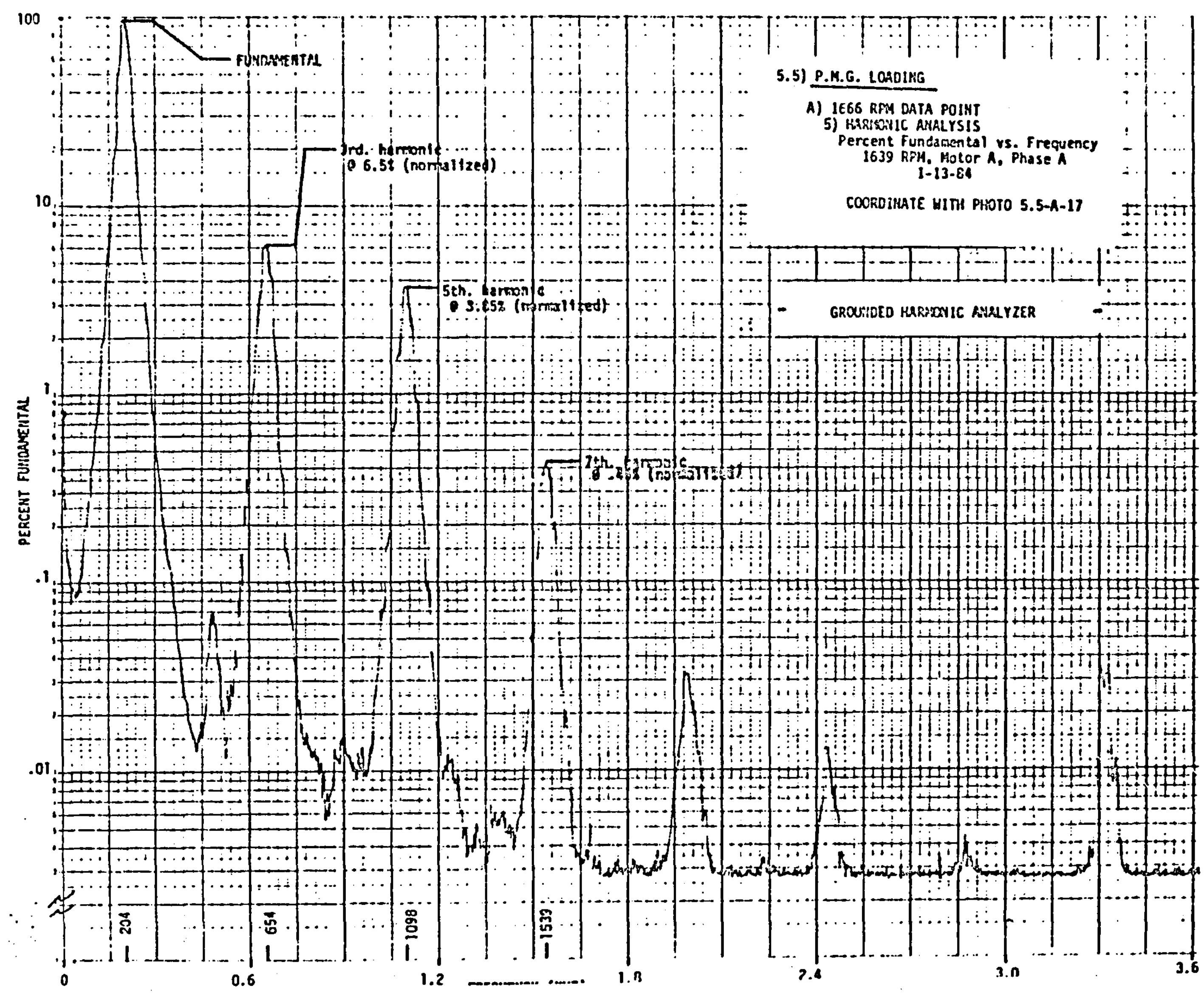
5.5) P.M.G. LOADING
A) 1666 RPM DATA POINT
5) HARMONIC ANALYSIS
Percent Fundamental vs. Frequency
1639 RPM, Motor A, Phase A
1-13-84
COORDINATE WITH PHOTO 5.5-A-17
GROUNDED HARMONIC ANALYZER
FUNDAMENTAL
3rd. harmonic
@ 6.5% (normalized)
5th. harmonic
@ 3.85% (normalized)
7th. harmonic
PERCENT FUNDAMENTAL
100
10
1
.1
.01
204
654
1098
1533
0
0.6
1.2
1.8
2.4
3.0
3.6

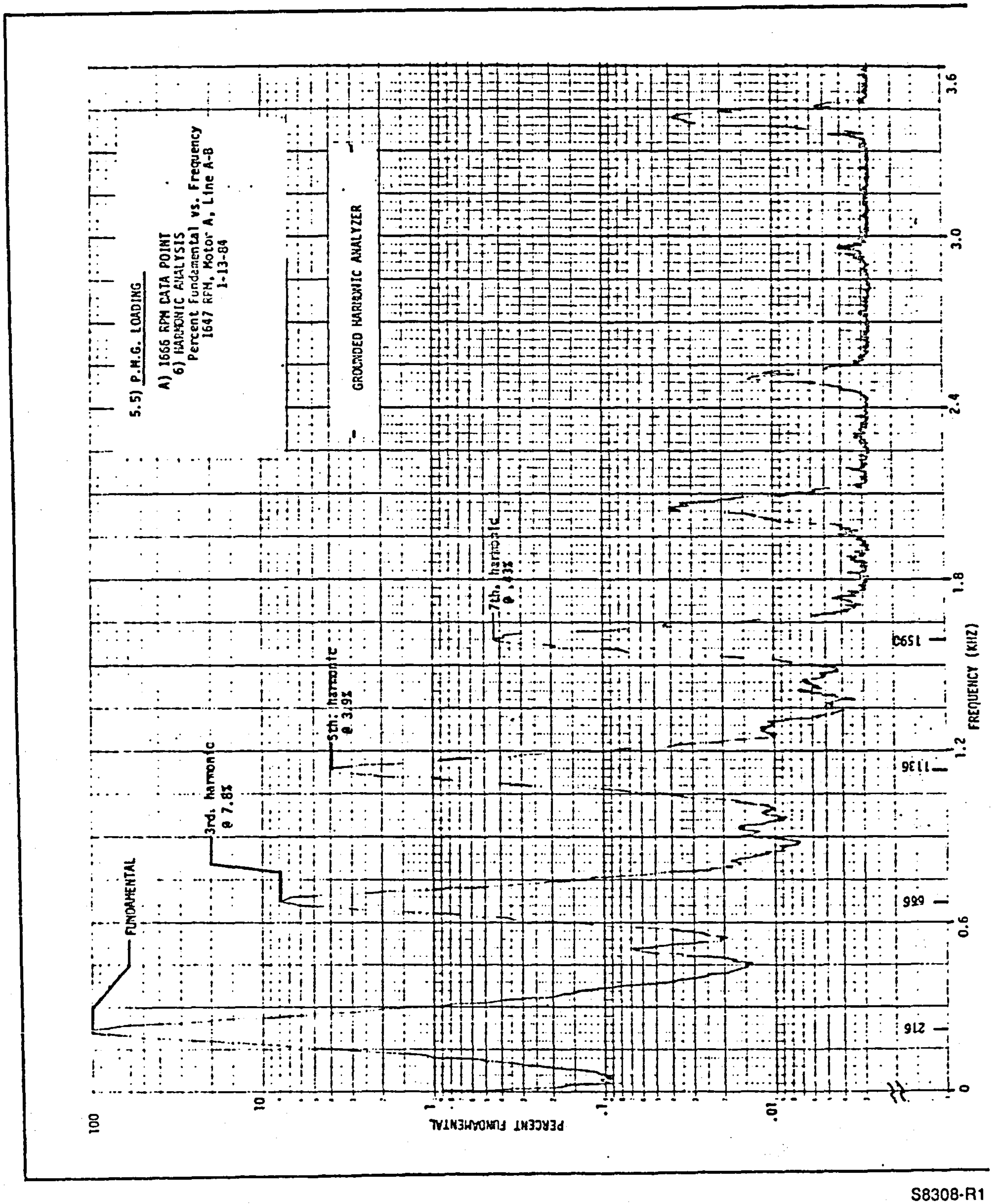
5.5) P.M.G. LOADING
A) 1666 RPM DATA POINT
6) HARMONIC ANALYSIS
Percent Fundamental vs. Frequency
1647 RPM, Motor A, Line A-B
1-13-84
GROUNDED HARMONIC ANALYZER
FUNDAMENTAL
3rd. harmonic @ 7.8%
5th. harmonic @ 3.9%
7th. harmonic @ .43%
PERCENT FUNDAMENTAL
100
10
1
.1
.01
FREQUENCY (KHZ)
0
216
0.6
666
1.2
1136
1590
1.8
2.4
3.0
3.6

5.5) P.M.G. LOADING

B) 4333 RPM DATA POINT

LOAD	SPEED 4333 r.p.m.	TEMP	TORQUE	MOTOR A				MOTOR A				MOTOR A			
ACTUAL	ACTUAL	°F	IN-LBS	Ia	Ib	Ic	Iave	Van	Vbn	Vcn	Vave	Wa	Wb	Wc	Wtot
350	4334	114	21.9	2.33	2.38	2.38	2.36	94.9	95.9	95.7	95.5	222	229	229	680
700	4319	140	33.3	4.3	4.7	4.4	4.5	93.7	95.4	94.7	94.6	403	449	415	1267
1400	4322	147	45.4	6.5	7.0	6.6	6.7	92.	94.7	93.3	93.3	597	666	620	1883
2100	4340	121	74.6	12.2	13.2	12.6	12.7	86.	90.7	88	88.2	1053	1206	1117	3376
2450	4326	143	82.2	13.8	15.1	14.4	14.4	83.2	88.3	85.2	85.6	1151	1336	1225	3712
2800	4334	163	89.8	15.8	16.9	16.4	16.4	80.2	86.4	82.6	83.1	1268	1462	1354	4084
3150	4313	152	94.7	17.1	18.4	17.8	17.8	77.5	83.7	79.7	80.3	1330	1549	1422	4301
3850	4331	180	104.2	20.6	22.4	21.4	21.5	70.6	77	72	73.2	1451	1729	1554	4734
4550	4326	170	105.2	22.4	24.5	23.2	23.4	66.3	71.9	67.8	68.7	1463	1746	1559	4768
5250	4329	205	105.3	23.9	26.2	24.8	25.0	61.8	67.6	63.3	64.2	1479	1779	1580	4838
5950	4310	238	103.5	25.2	27.4	26.1	26.2	57.0	62.8	58.4	59.4	1435	1726	1527	4688
6650	4381	252	100.9	26.2	28.6	27.1	27.3	53.9	59.1	55.2	56.1	1420	1702	1505	4627

B. ZELINSKI / L. KINTZ

1/12/84

5.5) P.M.G. LOADING

B) 4333 RPM DATA POINT

LOAD	SPEED 1666 R.P.M.			MOTOR B				MOTOR C				MOTOR D			
ACTUAL	ACTUAL			Van	Vbn	Vcn	Vave	Van	Vbn	Vcn	Vave	Van	Vbn	Vcn	Vave
350	4351			96.9	96.2	96.4	96.5	96.3	96.3	94.6	95.7	96.9	95.6	96.1	96.2
700	4321			96.7	96.0	96.5	96.4	96.3	96.2	96.4	96.3	96.0	95.2	95.9	95.7
1400	4320			97.2	96.1	96.7	96.7	96.5	96.3	96.5	96.4	96.2	94.9	96.1	95.7
2100	4350			97.6	95.9	97	96.8	96.4	96.3	96.6	96.4	96.5	94.1	96.2	95.6
2450	4331			97.6	95.8	97	96.8	96.4	96.2	96.5	96.4	96.5	93.7	96.2	95.5
2800	4338			98.2	96.1	97.5	97.3	96.9	96.6	97	96.8	97	93.1	96.7	95.6
3150	4324			97.6	95.6	96.9	96.7	96.3	96	96.4	96.2	96.5	93.2	96.1	95.3
3850	4279			98	95.7	97.4	97	96	95.3	95.4	95.6	95.6	91.9	95.2	94.2
4550	4322			97.7	95.7	97.3	96.9	96.3	96.1	96.5	96.3	96.7	92.9	96.5	95.4
5250	4379			98.8	97.1	98.8	98.2	98	97	98.3	97.8	98.6	94.7	98.6	97.3
5950	4497			99.2	98	99.9	99	99.8	100.8	101.6	100.7	102.1	98.4	102.7	101.1
6650	4662			103.8	103.1	105.4	104.1	105.9	105.7	106.9	106.2	107.9	104.5	109.7	107.4

B. ZELINSKI / L. KINTZ
1/2/84

5.5) P.M.G. LOADING

B) 4333 RPM DATA POINT

VERTICAL SCALE: .5 VOLTS/DIVISION
PROBE RATIO: X 100
HORIZONTAL SCALE: 200 μSEC/DIVISION

1) MOTOR A, PHASE A

VRMS 91.9
PERIOD 1.68 msec
FREQ 595 Hz
SPEED 4463 RPM
LOAD 2.4 amps
TEMP (F) 124

1-11-84

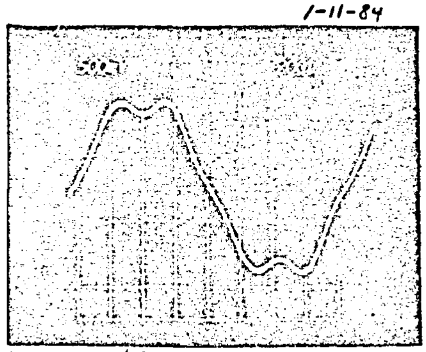

Motor A, ØA 4362 RPM 350W

ORIGINAL PAGE
BLACK AND WHITE PHOTOGRAPH

5.5) P.M.G. LOADING

B) 4333 RPM DATA POINT

COMPARISON OF 'PHASE' AND 'LINE TO LINE' VOLTAGE WAVEFORMS FOR RESISTANCE LOADED QUAD 'A' & UNLOADED QUAD 'B' MOTORS AT ONE LOAD POINT.

.5 VOLT/DIVISION:	VERTICAL SCALE:	1 VOLT/DIVISION
X100:	PROBE RATIO:	X100
200 μSEC/DIVISION:	HORIZONTAL SCALE:	200 μSEC/DIVISION

2) MOTOR A, PHASE A

VRMS 81.3 SPEED 4462 RPM
PERIOD 1.68 msec LOAD 17.8 amps
FREQ 595 Hz TEMP (F) 152

LOADED 1-11-84

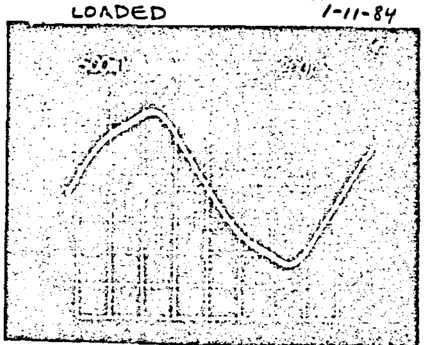

Motor A, ØA 4323 RPM 3150 W

3) MOTOR A, LINE A TO B

VRMS 134.3 SPEED 4462 RPM
PERIOD 1.68 msec LOAD 17.8 amps
FREQ 595 Hz TEMP (F) 152

LOADED 1-11-84

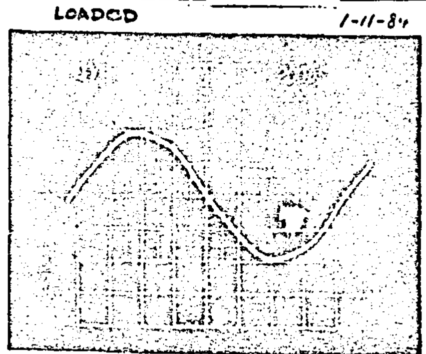

MOTOR A, ØA-B 4325 RPM 3150 W

4) MOTOR B, PHASE A

VRMS 91.9 SPEED 4410
PERIOD 1.7 msec LOAD 0
FREQ 588 Hz TEMP (F) 152

UNLOADED 1-11-84

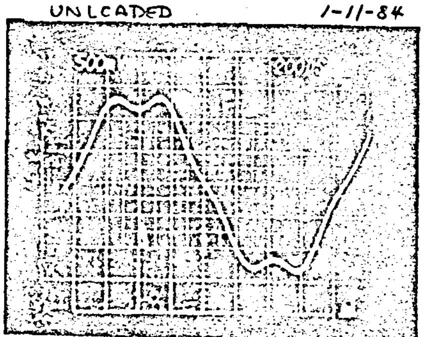

Motor B. ØA 4312 RPM 3150 W ON MOTOR A

5) MOTOR B, LINE A TO B

VRMS 184 SPEED 4462 RPM
PERIOD 1.68 msec LOAD 0
FREQ 595 Hz TEMP (F) 152

3150W ON MOTOR A 1-11-84

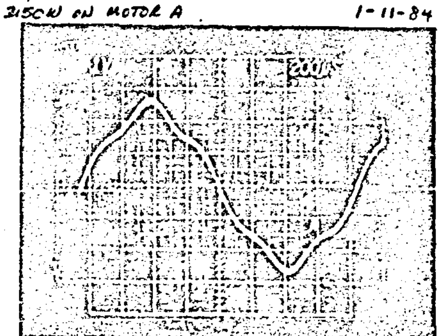

Motor B, ØA - ØB 4315 RPM

ORIGINAL PAGE
BLACK AND WHITE PHOTOGRAPH

5.5) P.M.G. LOADING

B) 4333 RPM DATA POINT

COMPARISON OF 'PHASE' AND 'LINE TO LINE' VOLTAGE
WAVEFORMS FOR RESISTANCE LOADED QUADRANT MOTOR 'A'

.5 VOLT/DIVISION:	VERTICAL	SCALE:	1 VOLT/DIVISION
X100:	PROBE	RATIO:	X100
200 μSEC/DIVISION:	HORIZONTAL	SCALE:	200 μSEC/DIVISION

6) MOTOR A, PHASE A
VRMS 81.3
PERIOD 1.68 msec
FREQ 595 Hz
SPEED 4463 RPM
LOAD 14.6 amps
TEMP (F) 170

7) MOTOR A, LINE A TO B
VRMS 148.5
PERIOD 1.68 msec
FREQ 595 Hz
SPEED 4463 RPM
LOAD 14.6 amps
TEMP (F) 174

1-16-84

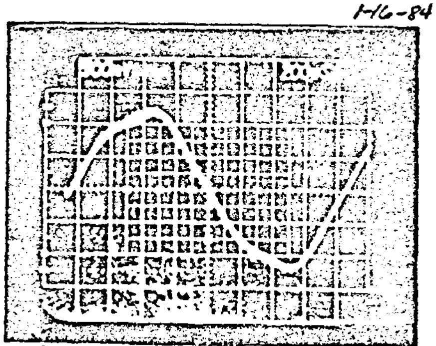

MOTOR A, ΦA 4325 RPM 8250 W

1-16-84

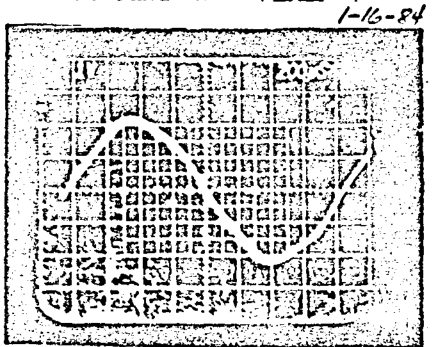

MOTOR A, ΦA-B 4333 RPM 8250 W

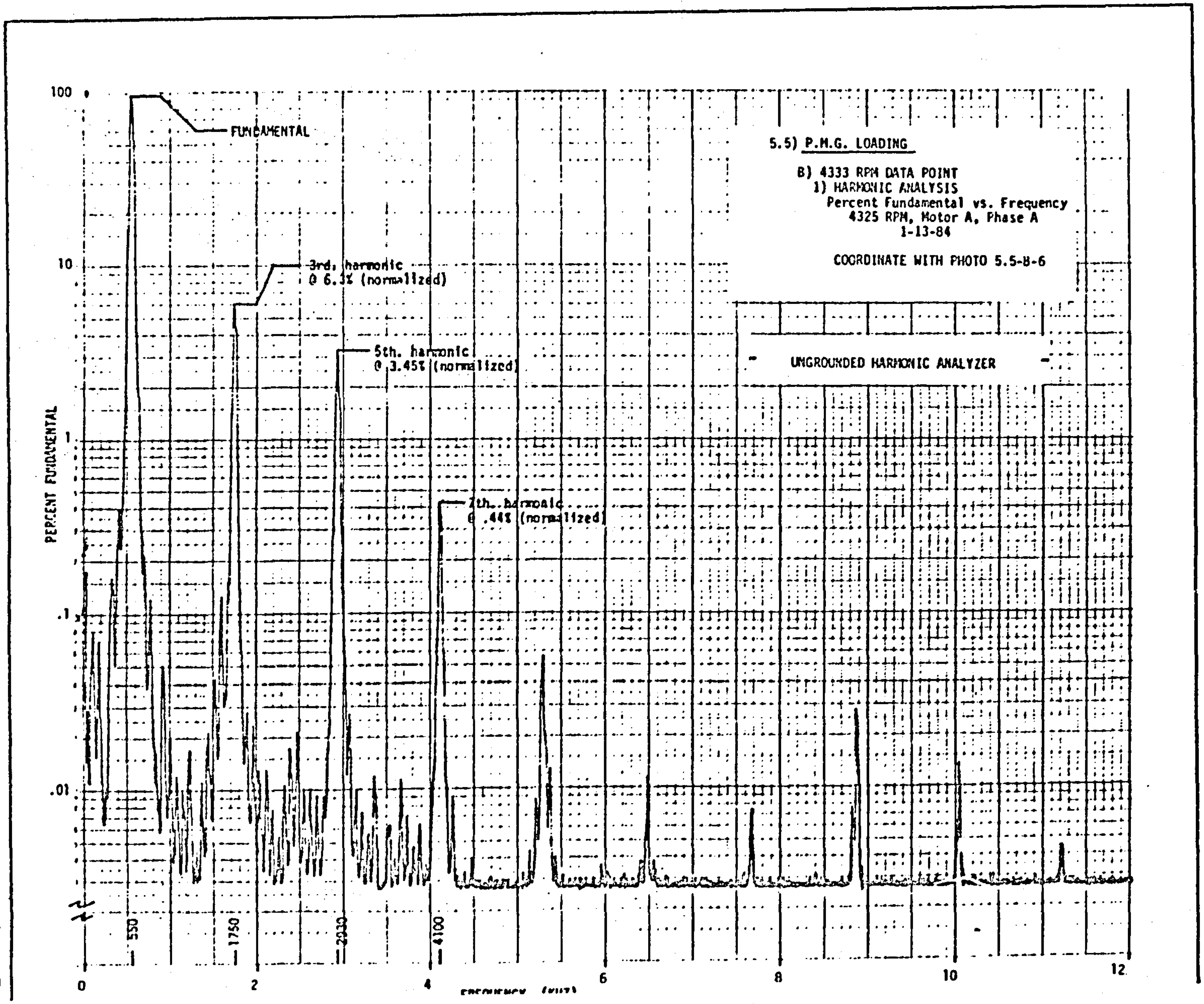

5.5) P.M.G. LOADING
B) 4333 RPM DATA POINT
1) HARMONIC ANALYSIS
Percent Fundamental vs. Frequency
4325 RPM, Motor A, Phase A
1-13-84
COORDINATE WITH PHOTO 5.5-B-6
UNGROUNDED HARMONIC ANALYZER
FUNDAMENTAL
3rd. harmonic
@ 6.3% (normalized)
5th. harmonic
@ 3.45% (normalized)
7th. harmonic
@ .44% (normalized)
PERCENT FUNDAMENTAL
100
10
1
.1
.01
550
1750
2930
4100
0
2
4
6
8
10
12

S8308-R1

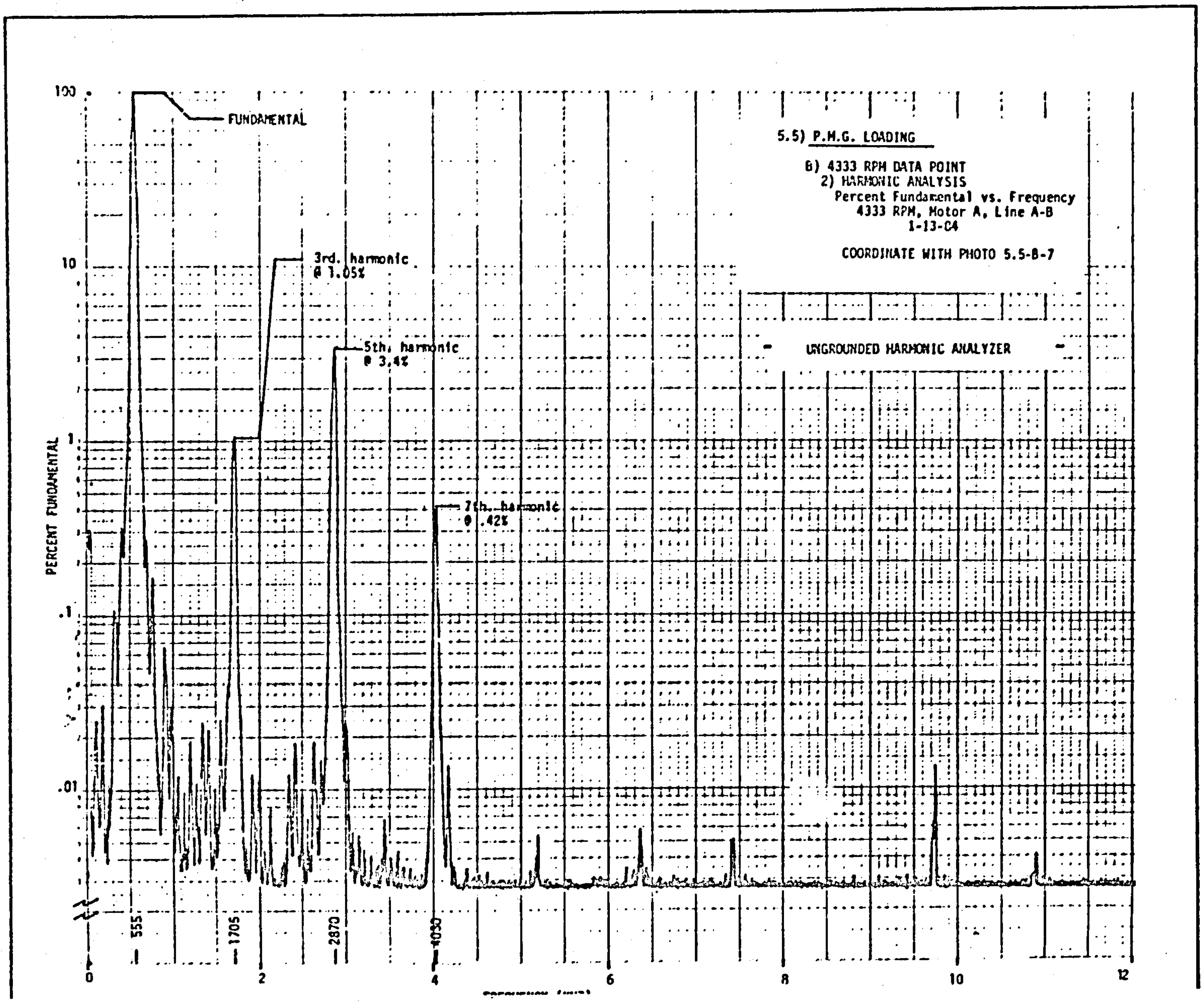

5.5) P.M.G. LOADING
6) 4333 RPM DATA POINT
2) HARMONIC ANALYSIS
Percent Fundamental vs. Frequency
4333 RPM, Motor A, Line A-B
1-13-C4
COORDINATE WITH PHOTO 5.5-B-7
UNGROUNDED HARMONIC ANALYZER
FUNDAMENTAL
3rd. harmonic @ 1.05%
5th. harmonic @ 3.4%
7th. harmonic @ .42%
PERCENT FUNDAMENTAL
100
10
1
.1
.01
0
2
4
6
8
10
12
555
1705
2870
4030

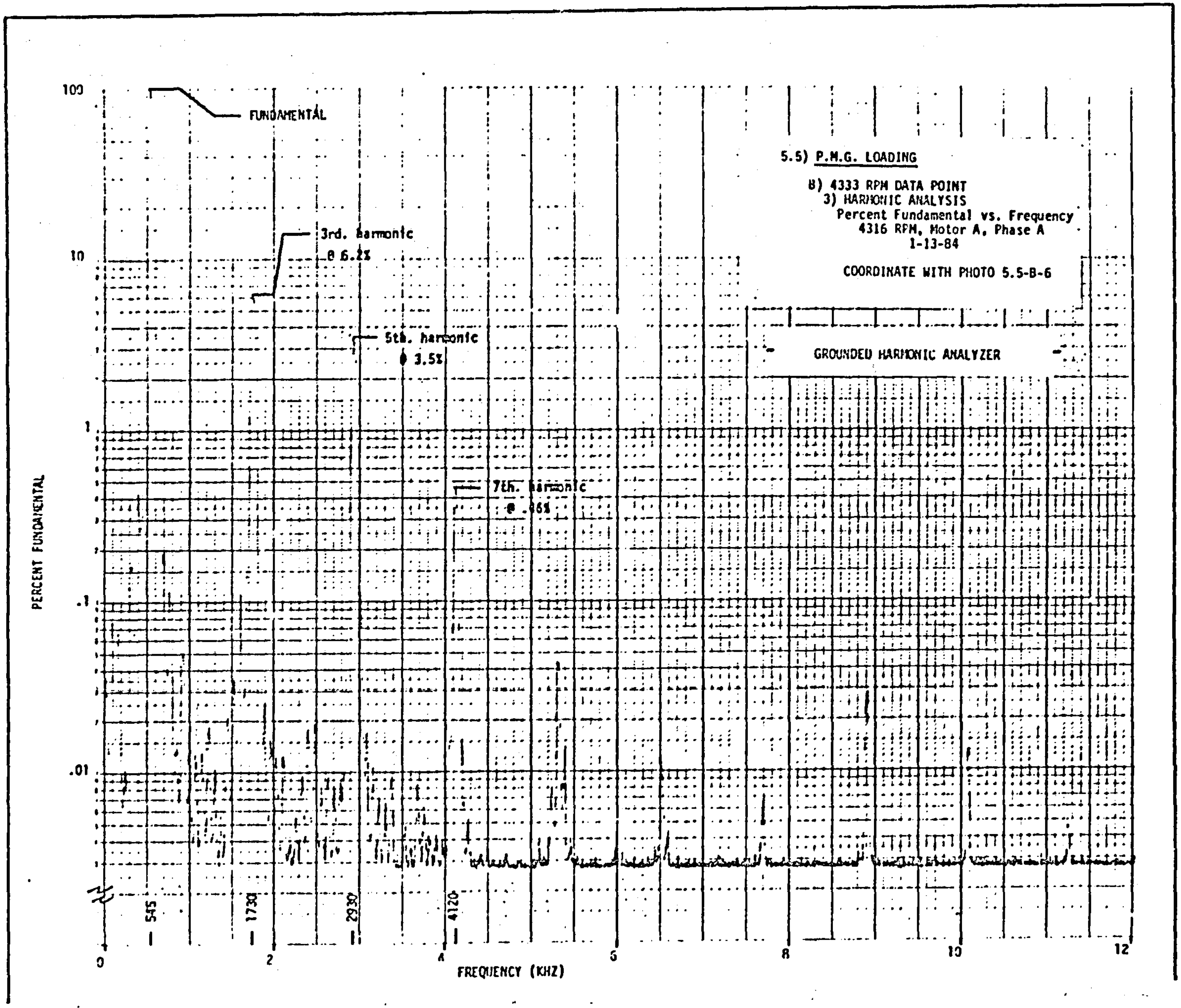

5.5) P.M.G. LOADING
B) 4333 RPM DATA POINT
3) HARMONIC ANALYSIS
Percent Fundamental vs. Frequency
4316 RPM, Motor A, Phase A
1-13-84
COORDINATE WITH PHOTO 5.5-B-6
GROUNDED HARMONIC ANALYZER
FUNDAMENTAL
3rd. harmonic
@ 6.2%
5th. harmonic
@ 3.5%
7th. harmonic
@ .46%
PERCENT FUNDAMENTAL
FREQUENCY (KHZ)
100
10
1
.1
.01
545
1730
2930
4120
0
2
4
6
8
10
12

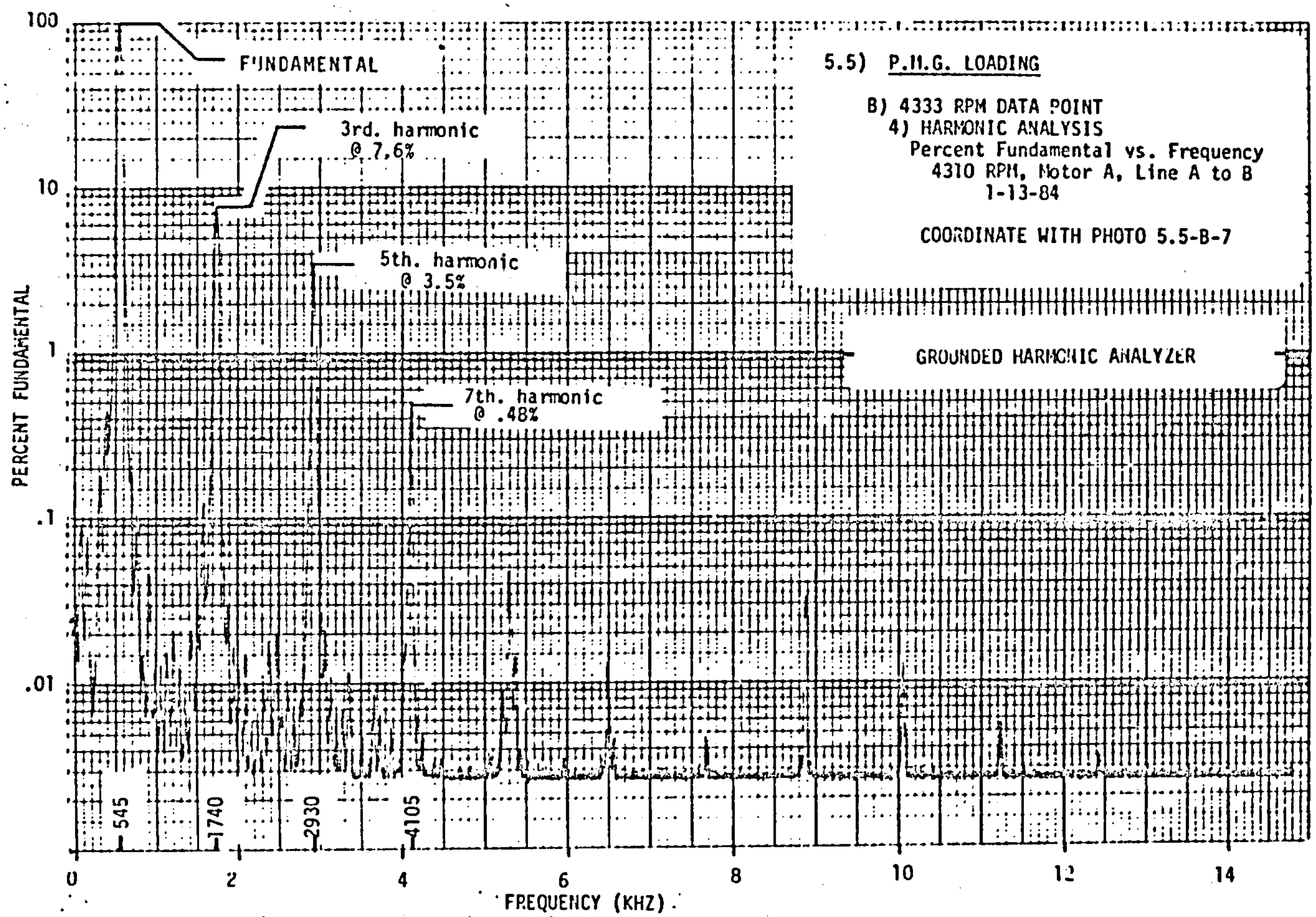

5.5) P.M.G. LOADING
B) 4333 RPM DATA POINT
4) HARMONIC ANALYSIS
Percent Fundamental vs. Frequency
4310 RPM, Motor A, Line A to B
1-13-84
COORDINATE WITH PHOTO 5.5-B-7
GROUNDED HARMONIC ANALYZER
FUNDAMENTAL
3rd. harmonic
@ 7.6%
5th. harmonic
@ 3.5%
7th. harmonic
@ .48%
PERCENT FUNDAMENTAL
100
10
1
.1
.01
545
1740
2930
4105
0
2
4
6
8
10
12
14
FREQUENCY (KHZ)

5.5) P.M.G. LOADING

C) 10,000 RPM DATA POINT

L. KINTZ / B. ZELINSKI

1/13 - 1/16

LOAD	SPEED 10,000 r.p.m.	TEMP	TORQUE	MOTOR A				MOTOR A				MOTOR A			
ACTUAL	ACTUAL	°F	IN-LBS	Ia	Ib	Ic	Iave	Van	Vbn	Vcn	Vave	Wa	Wb	Wc	Wtot
1375	9983	136	42.6	6.6	5.2	5.4	5.7	214	220	219	218	1409	1160	1184	3753
2750	9978	236	65.5	9.9	10.5	10.2	10.2	205	215	209	210	2035	2278	2138	6451
4125	10020	274	84.5	15	14.9	14.4	14.8	188	204	196	196	2819	3036	2838	8693
5500	10005	292	95.3	18.1	18.5	17.8	18.1	173	189	180	181	3021	3510	3198	9729
6875	9992	195	106	20.2	21.8	20.8	20.9	166.7	180.4	170.6	173	3041	3935	3544	10520
8250	9990	258	107.6	22.8	24.1	22.9	23.3	149.2	165.8	155.3	157	2788	3988	3555	10431

L. KINTZ / B. ZELINSKY
1/13 - 1/16

5.5) P.M.G. LOADING

C) 10,000 RPM DATA POINT

LOAD	SPEED 10,000 R.P.M.			MOTOR B				MOTOR C				MOTOR D			
ACTUAL	ACTUAL			Van	Vbn	Vcn	Vave	Van	Vbn	Vcn	Vave	Van	Vbn	Vcn	Vave
1375	9987			223	222	222	222	223	223	224	223	223	220	223	222
2750	10035			226	222	224	224	224	224	225	224	225	220	225	223
4125	10043			226	222	224	224	224	224	224	224	226	218	225	222
5500	10016			224	220	223	222	223	224	224	224	226	217	225	223
6845	9944			220	221	224	222	222	223	224	223	224	216	223	221
8250	9951			226	222	226	225	224	224	225	224	225	216	224	222

5.5) P.M.G. LOADING

C) 10,000 RPM DATA POINT

QUADRANT MOTOR A: RESISTIVE LOADED

VERTICAL SCALE: 1 VOLTS/DIVISION
PROBE RATIO: X 100
HORIZONTAL SCALE: 100 USEC/DIVISION

1) MOTOR A, PHASE A

VRMS 198

PERIOD .73 msec

FREQ 1370 Hz

SPEED 10275 RPM

LOAD 5.7 amps

TEMP (F) 160

1-16-84

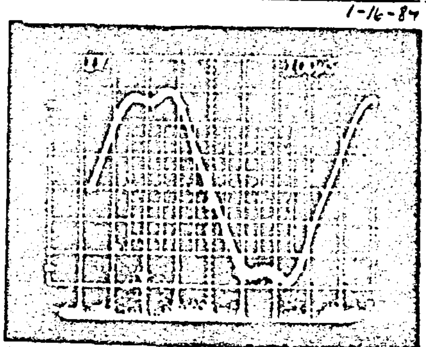

Motor A, ФA 10081 RPM 1375W

ORIGINAL PAGE
BLACK AND WHITE PHOTOGRAPH

ORIGINAL PAGE
BLACK AND WHITE PHOTOGRAPH

5.5) P.M.G. LOADING

C) 10,000 RPM DATA POINT

COMPARISON OF 'PHASE' AND 'LINE TO LINE' VOLTAGE WAVEFORMS FOR RESISTANCE LOADED QUADRANT MOTOR 'A' AT TWO LOAD POINTS.

1 VOLT/DIVISION:	VERTICAL SCALE:	2 VOLTS/DIVISION
X100:	PROBE RATIO:	X100
100 μSEC/DIVISION:	HORIZONTAL SCALE:	100 μSEC/DIVISION

2) MOTOR A, PHASE A

VRMS 198 SPEED 10275 RPM
PERIOD .73 msec LOAD 10.2 amps
FREQ 1370 Hz TEMP (F) 180

1-16-84

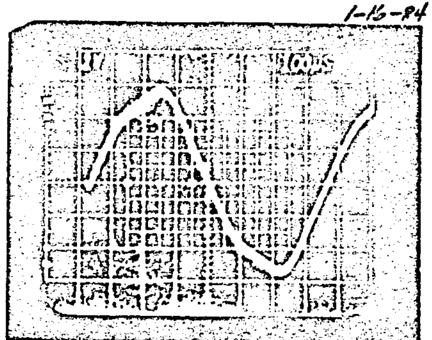

MOTOR A, ΦA 10014 RPM 2750W

3) MOTOR A, LINE A TO B

VRMS 368 SPEED 10275 RPM
PERIOD .73 msec LOAD 10.2 amps
FREQ 1370 Hz TEMP (F) 184

1-16-84

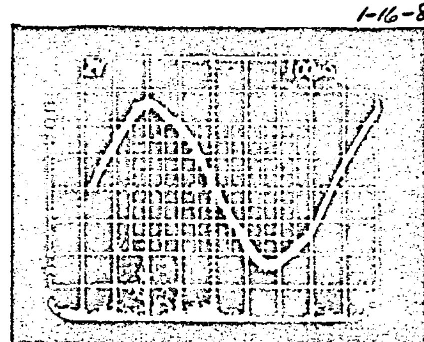

MOTOR A, ΦA-B 9968 RPM 2750W

4) MOTOR A, PHASE A

VRMS 184 SPEED 10275 RPM
PERIOD .73 msec LOAD 18.1 amps
FREQ 1370 Hz TEMP (F) 220

1-16-84

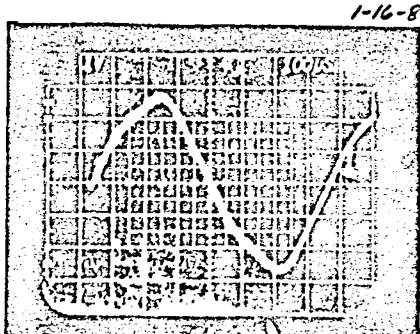

MOTOR A. ΦA 10034 RPM 5500W

5) MOTOR A, LINE A TO B

VRMS 325 SPEED 10275 RPM
PERIOD .73 msec LOAD 18.1 amps
FREQ 1370 Hz TEMP (F) 190

1-16-84

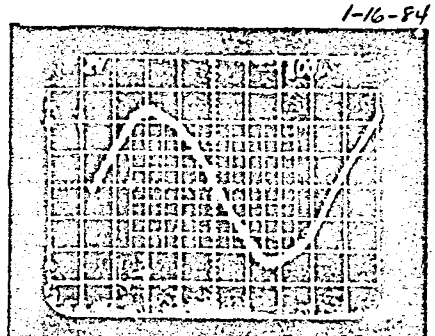

MOTOR A, ΦA-B 9990 RPM 5500W

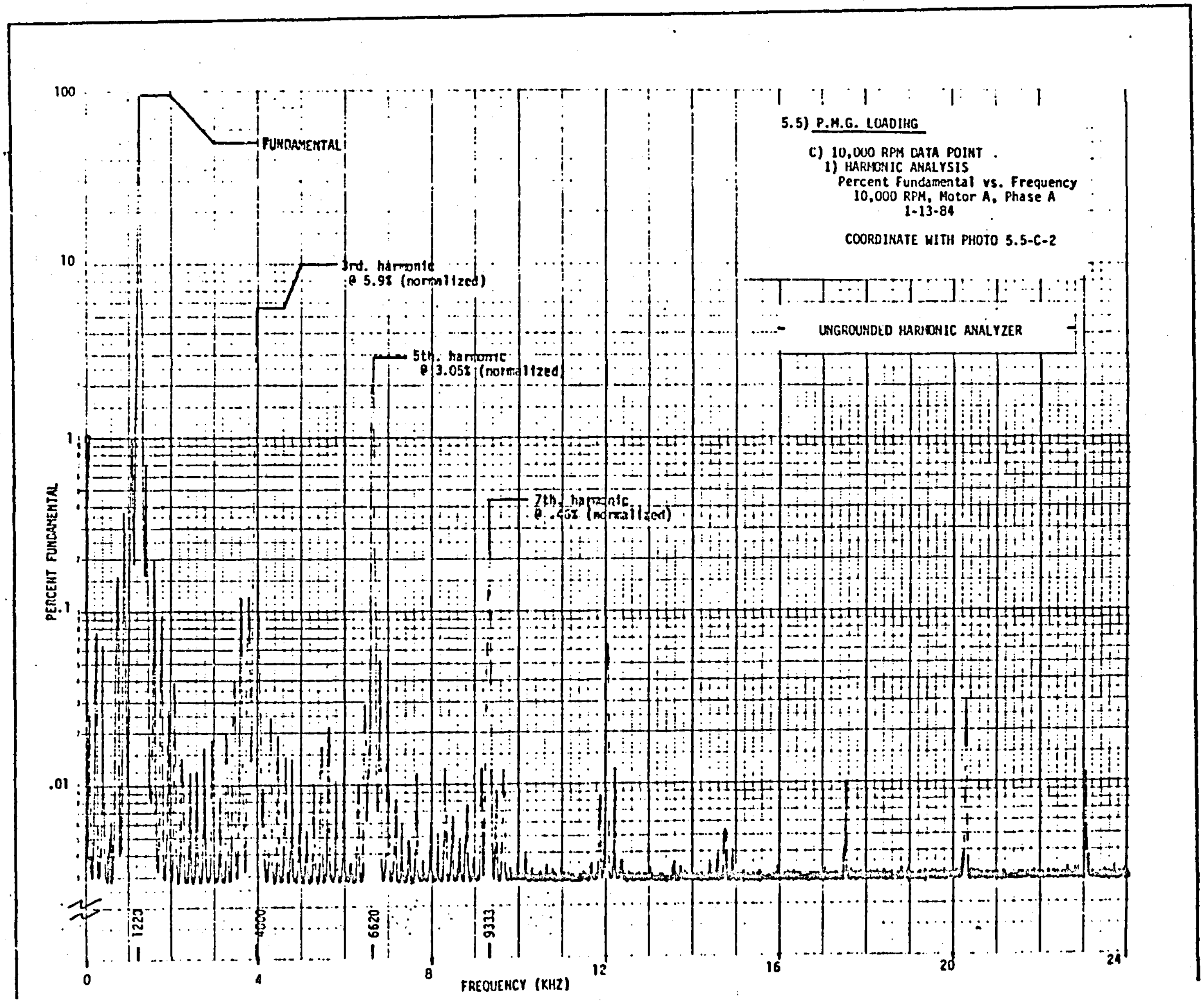
5.5) P.M.G. LOADING
C) 10,000 RPM DATA POINT
1) HARMONIC ANALYSIS
Percent Fundamental vs. Frequency
10,000 RPM, Motor A, Phase A
1-13-84
COORDINATE WITH PHOTO 5.5-C-2
UNGROUNDED HARMONIC ANALYZER
FUNDAMENTAL
3rd. harmonic
@ 5.9% (normalized)
5th. harmonic
@ 3.05% (normalized)
7th. harmonic
PERCENT FUNDAMENTAL
100
10
1
.1
.01
1220
4000
6620
9333
0
4
8
12
16
20
24
FREQUENCY (KHZ)

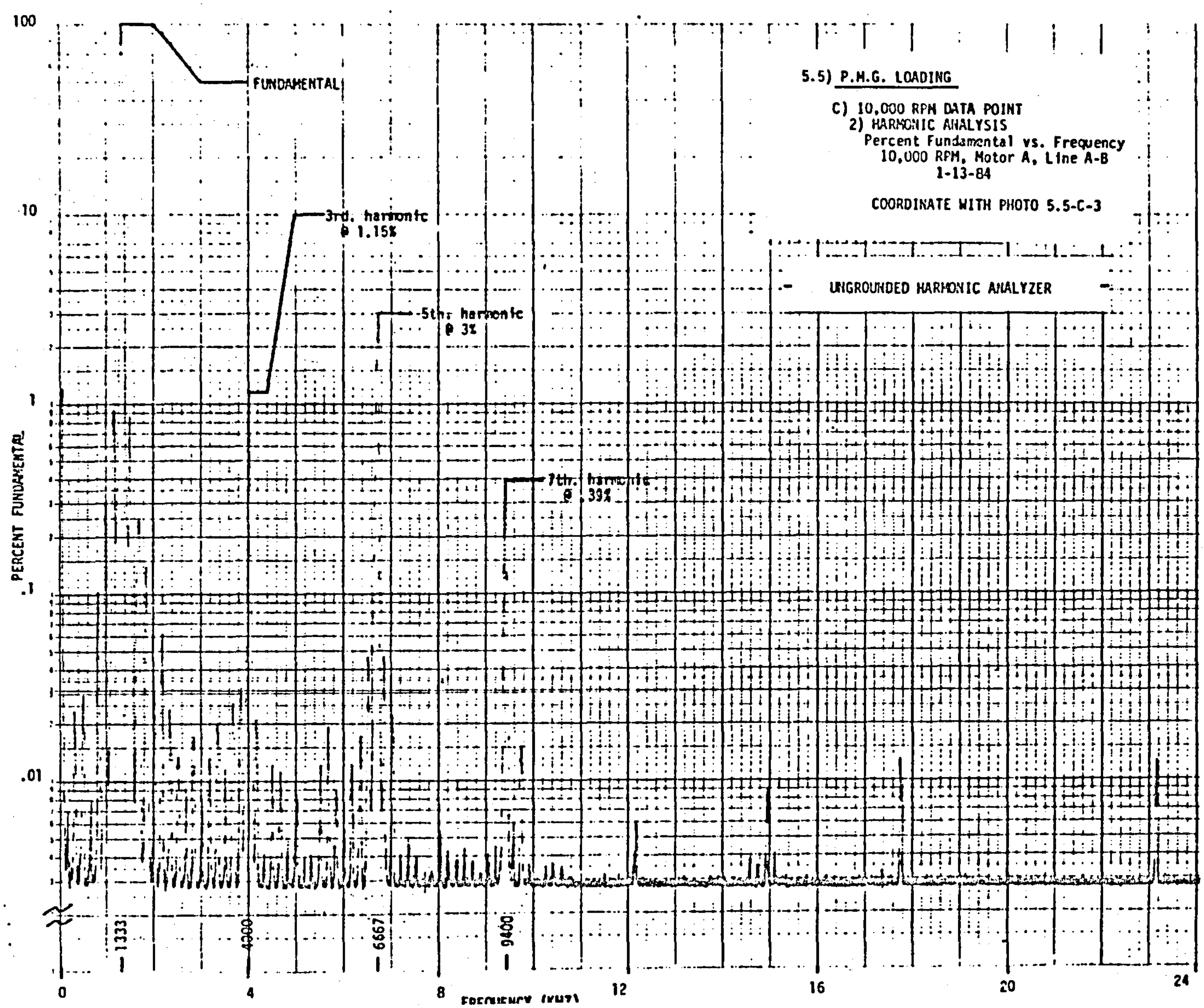
5.5) P.M.G. LOADING
C) 10,000 RPM DATA POINT
2) HARMONIC ANALYSIS
Percent Fundamental vs. Frequency
10,000 RPM, Motor A, Line A-B
1-13-84
COORDINATE WITH PHOTO 5.5-C-3
UNGROUNDED HARMONIC ANALYZER
FUNDAMENTAL
3rd. harmonic @ 1.15%
5th. harmonic @ 3%
7th. harmonic @ .39%
PERCENT FUNDAMENTAL
100
10
1
.1
.01
1333
4000
6667
9400
0
4
8
12
16
20
24
FREQUENCY (KHZ)

STATIC TORQUE VS. ROTOR POSITION DATA

5.6) STATIC TORQUE VS. ROTOR POSITION

TEST SUMMARY

a) TORQUE VS. ROTOR POSITION

1) Quadrant Motor A
2) 3' Lever
3) 500 in-lb Torque Shaft (TS173)
4) Jan 18, 1984

b) TORQUE VS. CURRENT

1) Quadrant Motor A
2) Rotor Position: 30.94 Mechanical Degrees (#2.75)
3) 3' Lever
4) 500 in-lb Torque Shaft (TS173)
5) Jan 18, 1984

c) AVERAGE TORQUE VS. CURRENT

1) Quadrant Motors A, B, C & D
2) Rotor Position: 91.13 Mechanical Degrees (#8.1)
3) Locked Shaft
4) 200 in-lb Torque Shaft (TS179)
5) Jan 19, 1984

REPEAT C

c) AVERAGE TORQUE VS. CURRENT

1) Quadrant Motors A, B, C & D
2) Rotor Position: Indeterminate due to motor assembly level
3) Locked Shaft
4) 500 in-lb Torque Shaft (TS173)
5) Feb 7, 1984

5.6) STATIC TORQUE VS. ROTOR POSITION

a) TORQUE VS. ROTOR POSITION

Quadrant Motor A
Reading rotation: Clockwise sensor end

ROTOR POSITION		UNITS	ROTOR POSITION		UNITS	ROTOR POSITION		UNITS	ROTOR POSITION		UNITS
#	DEGREES	IN-LBS	#	DEGREES	IN-LBS	#	DEGREES	IN-LBS	#	DEGREES	IN-LBS
0	0	11.0	8	90	4.0	16	180	9.0	24	270	8.0
½		17.0	½		17.0	½		18.0	½		16.0
1	11.25	15.0	9	101.25	13.0	17	191.25	11.0	25	281.25	12.0
½		6.0	½		1.0	½		3.0	½		0.0
2	22.5	9.0	10	112.5	16.0	18	202.25	25.0	26	292.5	15.0
* ½		18.0	½		27.0	½		22.0	½		24.0
3	33.75	23.0	11	123.75	15.0	19	213.75	10.0	27	303.75	17.0
½		14.0	½		3.0	½		5.0	½		9.0
4	45	5.0	12	135	9.0	20	225	16.0	28	315	6.0
½		16.0	½		18.0	½		17.0	½		16.0
5	56.25	18.0	13	146.25	8.0	21	236.25	7.0	29	326.25	13.0
½		4.0	½		2.0	½		2.0	½		1.0
6	67.5	12.0	14	157.5	18.0	22	247.5	16.0	30	337.5	13.0
½		19.0	½		26.0	½		23.0	½		25.0
7	78.75	23.0	15	168.75	17.0	23	258.75	16.0	31	348.75	23.0
½		12.0	½		9.0	½		9.0	½		9.0

AVERAGE VALUE: 13.14

MAXIMUM VALUE: 27.0

MINIMUM VALUE: 0.0

1-18-84

INPUT CURRENT: 5 A.D.C.

(1) * 2.75 (30.94 DEGREES) @ 25 IN-LBS

(2) READINGS TAKEN WITH 500 IN-LB TORQUE SHAFT (TS 173)

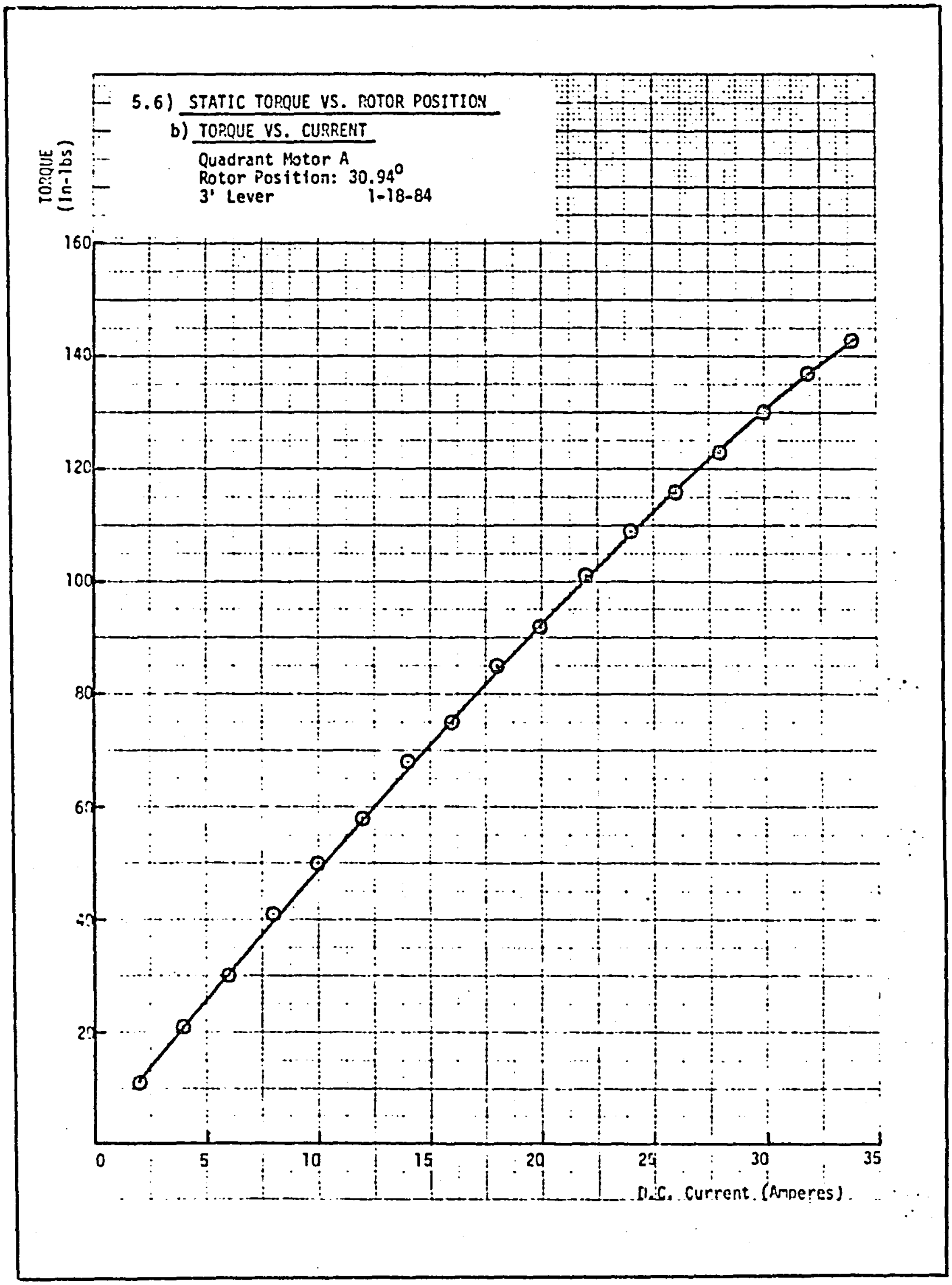
5.6) STATIC TORQUE VS. ROTOR POSITION
b) TORQUE VS. CURRENT
Quadrant Motor A
Rotor Position: 30.94°
3' Lever 1-18-84
TORQUE (In-lbs)
160
140
120
100
80
60
40
20
0
5
10
15
20
25
30
35
D.C. Current (Amperes)

C-2

5.6) STATIC TORQUE VS. ROTOR POSITION

b) TORQUE VS. CURRENT

Quadrant Motor A
Rotor position: 30.94° (#2.75)

INPUT CURRENT	INPUT VOLTAGE	STATOR TEMP.	QUAD A TORQUE
amperes	volts	°F	in-lbs
2	0.3	72	11.0
4	0.7	72	21.0
6	1.0	72	30.0
8	1.4	73	41.0
10	1.8	74	50.0
12	2.1	75	58.0
14	2.4	76	68.0
16	2.8	77	75.0
18	3.2	78	85.0
20	3.5	79	95.0
22	3.9	80	101.0
24	4.3	81	109.0
26	4.7	82	116.0
28	5.1	83	123.0
30	5.5	84	130.0
32	5.9	85	137.0
34	6.4	86	143.0

C. ZELINSKI / L. KINTZ 1/18/84
(1) 500 IN-LB TORQUE SHAFT (TS 173)
(2) 3' LEVER

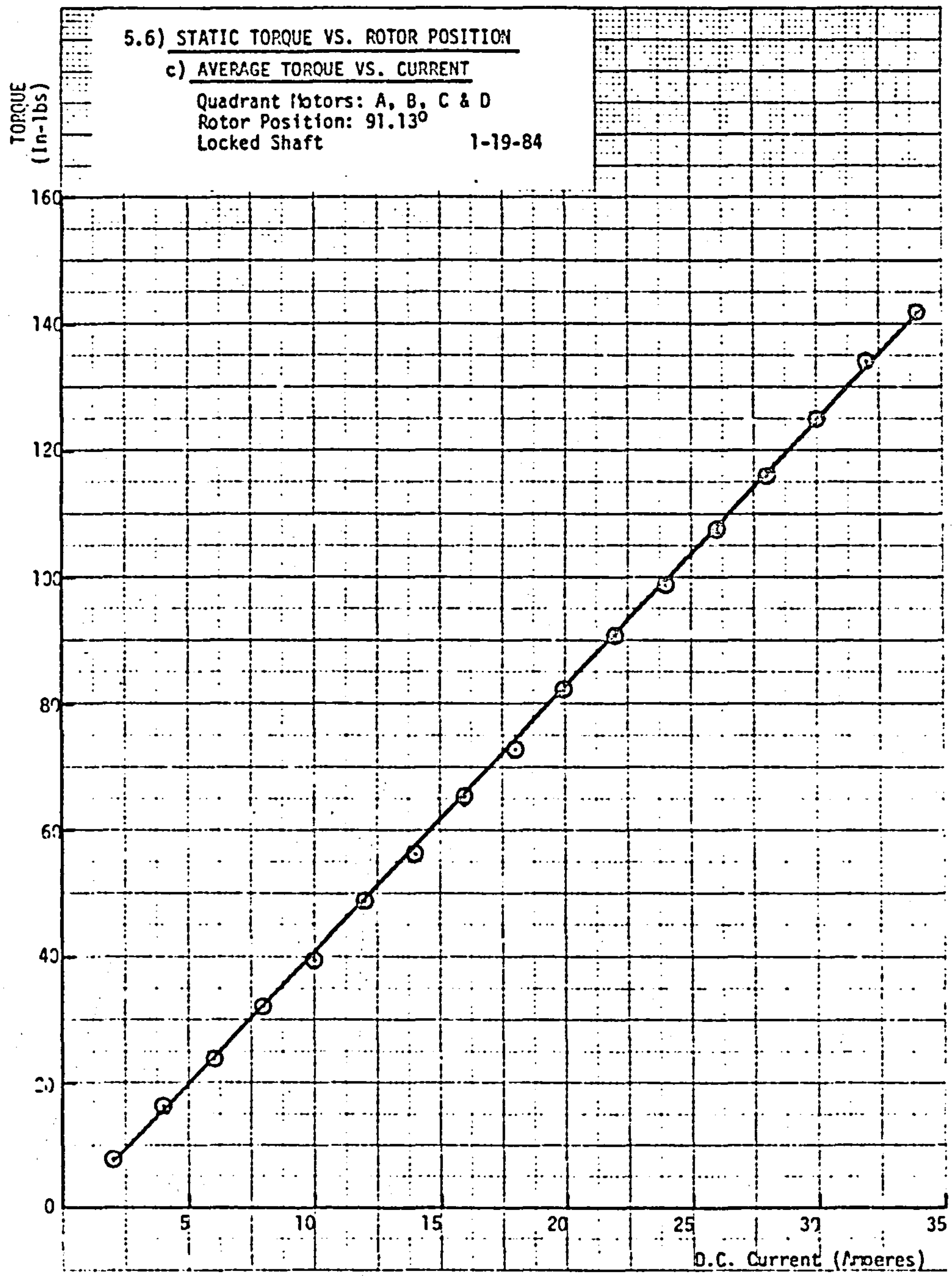

5.6) STATIC TORQUE VS. ROTOR POSITION
c) AVERAGE TORQUE VS. CURRENT
Quadrant Motors: A, B, C & D
Rotor Position: 91.13°
Locked Shaft
1-19-84
TORQUE (In-lbs)
160
140
120
100
80
60
40
20
0
5
10
15
20
25
30
35
D.C. Current (Amperes)

5.6) STATIC TORQUE VS. ROTOR POSITION

c) AVERAGE TORQUE VS. CURRENT

Quadrant Motors A, B, C & D
Rotor position: 91.13° (#8.1)

INPUT CURRENT	INPUT VOLTAGE	QUAD A TORQUE	QUAD B TORQUE	QUAD C TORQUE	QUAD D TORQUE	AVERAGE TORQUE
amperes	volts	in-lbs	in-lbs	in-lbs	in-lbs	in-lbs
2	0.3	7.9	9.4	8.9	9.6	9.0
4	0.7	16.2	16.1	16.1	17.5	16.5
6	1.0	23.8	24.2	23.6	25.4	24.3
8	1.4	31.6	32.5	31.8	33.2	32.3
10	1.7	39.2	39.8	40.2	40.7	40.0
12	2.1	48.8	48.5	48.5	50.4	49.1
14	2.4	56.3	55.6	55.5	58.1	56.4
16	2.8	65.2	64.0	63.2	65.3	64.4
18	3.1	72.8	71.9	71.4	73.5	72.4
20	3.5	82.1	80.2	79.1	82.0	80.9
22	3.9	90.9	87.6	87.5	89.6	88.9
24	4.2	98.8	96.7	95.8	98.2	97.4
26	4.6	107.5	105.0	104.0	107.5	106.0
28	5.1	115.9	113.0	112.0	115.3	114.1
30	5.4	125.0	122.0	120.3	123.7	122.8
32	5.9	134.0	130.0	129.1	131.0	131.0
34	6.3	141.7	137.0	137.0	140.4	139.0

B. ZELINSKI / L. KINTZ 1/19/84

(1) 200 IN-LB TORQUE SHAFT (TS 179)

(2) LOCKED SHAFT

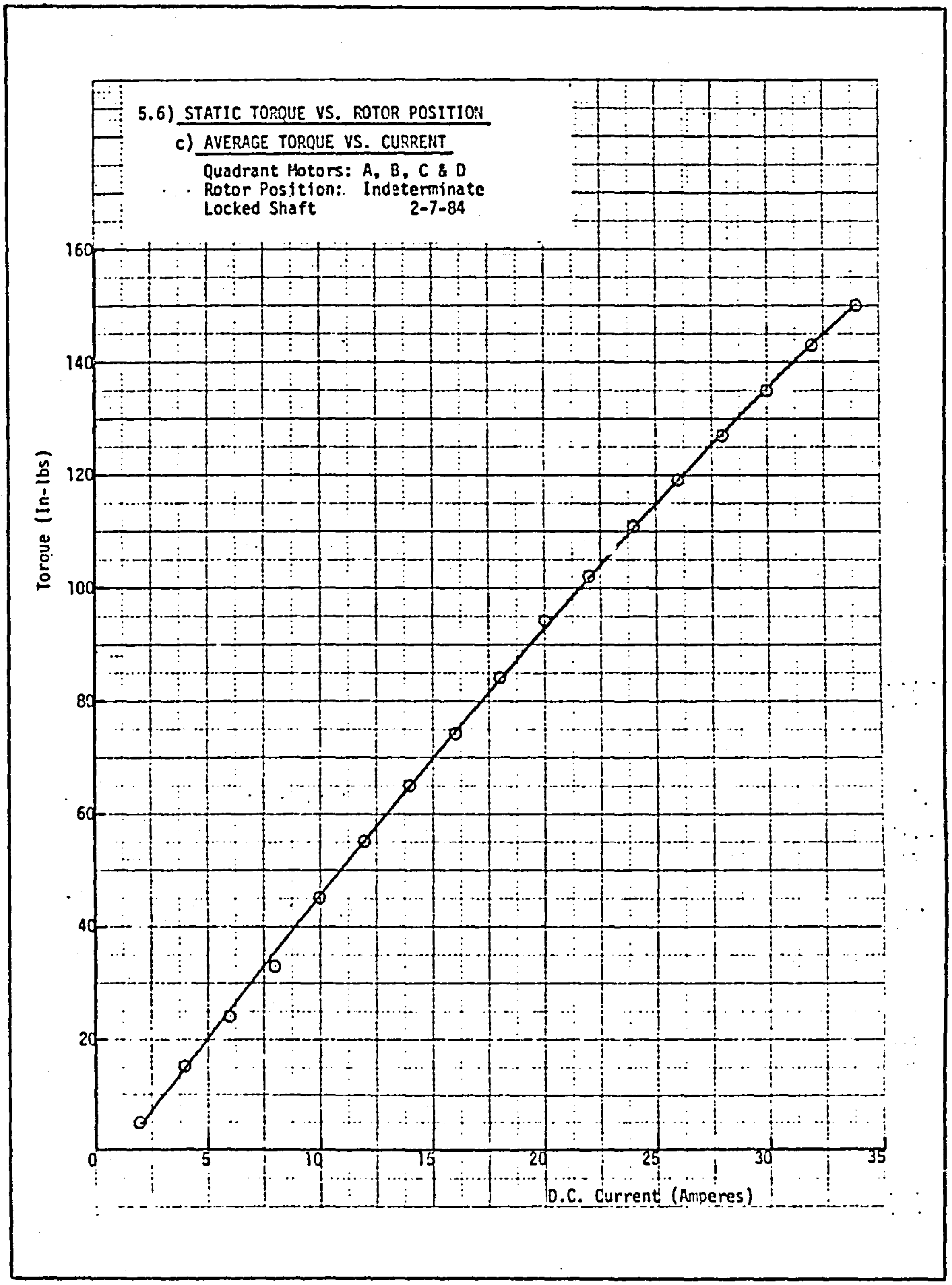
5.6) STATIC TORQUE VS. ROTOR POSITION
c) AVERAGE TORQUE VS. CURRENT
Quadrant Motors: A, B, C & D
Rotor Position: Indeterminate
Locked Shaft 2-7-84
Torque (In-lbs)
160
140
120
100
80
60
40
20
0
5
10
15
20
25
30
35
D.C. Current (Amperes)

5.6) STATIC TORQUE VS. ROTOR POSITION

c) AVERAGE TORQUE VS. CURRENT

Quadrant Motors A, B, C & D
Rotor position: INDETERMINATE

INPUT CURRENT amperes	INPUT VOLTAGE volts	QUAD A TORQUE in-lbs	QUAD B TORQUE in-lbs	QUAD C TORQUE in-lbs	QUAD D TORQUE in-lbs	AVERAGE TORQUE in-lbs
2	0.3	5	5	6	6	5.5
4	0.7	15	13	14	15	14.3
6	[illegible]	24	23	24	24	23.8
8	1.4	33	33	33	34	33.3
10	1.7	45	43	45	45	44.5
12	2.1	55	53	54	55	54.5
14	2.4	65	62	63	64	63.5
16	2.8	74	71	72	73	72.5
18	3.1	84	81	81	83	82.[illegible]
20	3.5	94	89	91	92	91.5
[illegible]	3.9	102	98	98	100	99.5
24	4.2	111	107	107	109	108.5
26	4.6	119	114	115	117	116.3
28	5.1	127	123	123	125	124.5
30	5.4	135	131	131	133	132.5
32	5.9	143	137	137	140	139.3
34	6.3	150	145	144	147	146.5

L. KINTZ 2/7/84

(1) 500 IN-LB TORQUE SHAFT (TS173)

(2) LOCKED SHAFT

STATIC TORQUE SUMMING DATA

5.7) STATIC TORQUE SUMMING

TEST SUMMARY

TORQUE VS. CURRENT

a) Quadrant Motors A & B

b) Quadrant Motors A, B & C

c) Quadrant Motors A, B, C & D

SERIES 1

1) Jan 18, 1984
2) Rotor Position: 30.94 Mechanical Degrees (#2.75)
3) 3' Lever
4) 500 in-lb Torque Shaft (TS173)

SERIES 2

1) Jan 19, 1984
2) Rotor Position: 91.13 Mechanical Degrees (#8.1)
3) Locked Shaft
4) 200 in-lb Torque Shaft (TS179)

SERIES 3

1) Jan 19, 1984
2) Rotor Position: 93.38 Mechanical Degrees (#8.3)
3) Locked Shaft
4) 500 in-lb Torque Shaft (TS173)

SERIES 4

1) Feb 7, 1984
2) Rotor Position: Indeterminate due to motor assembly level
3) Locked Shaft
4) 500 in-lb Torque Shaft (TS173)

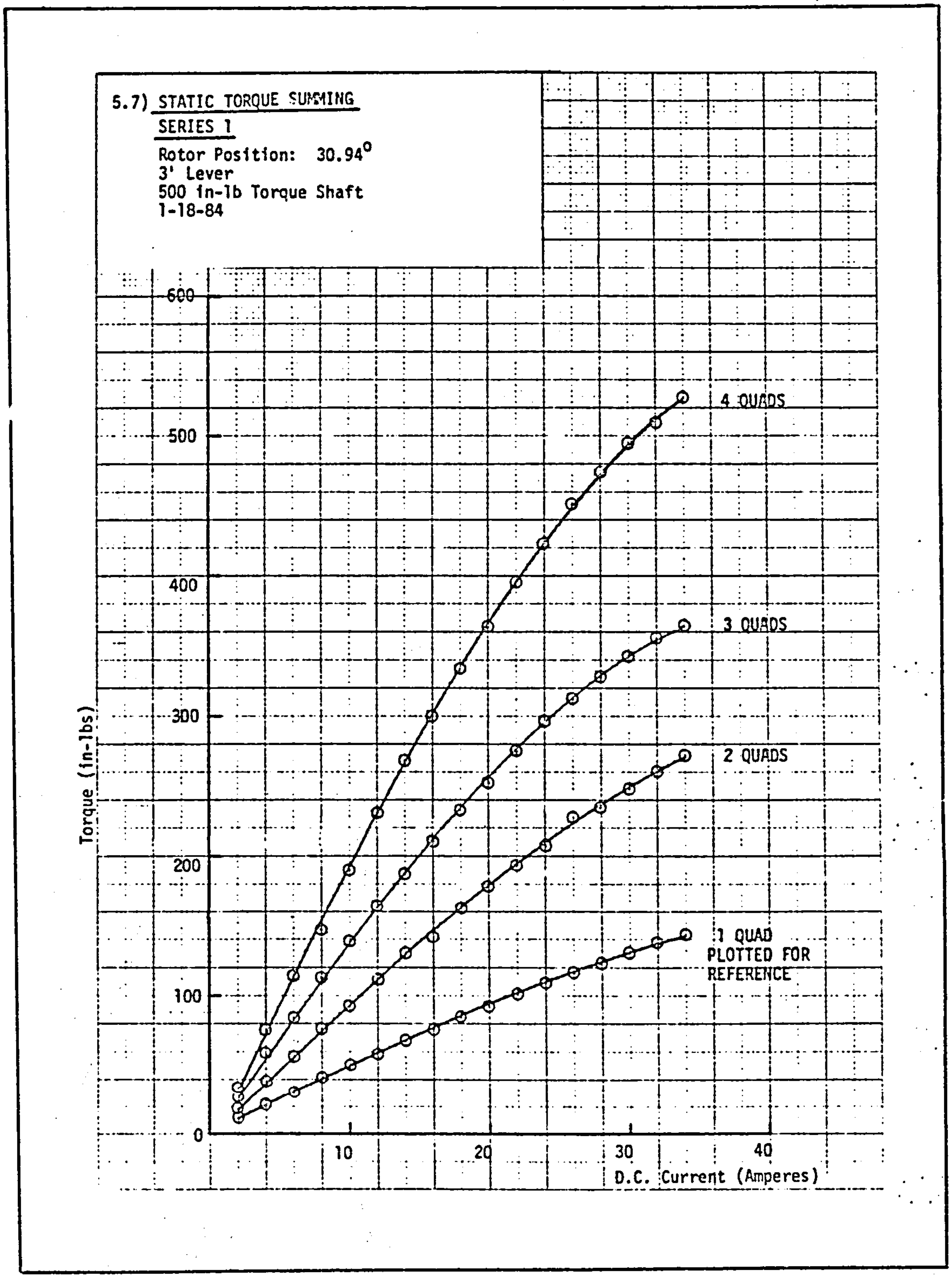
5.7) STATIC TORQUE SUMMING
SERIES 1
Rotor Position: 30.94°
3' Lever
500 in-lb Torque Shaft
1-18-84
Torque (in-lbs)
0
100
200
300
400
500
600
10
20
30
40
D.C. Current (Amperes)
4 QUADS
3 QUADS
2 QUADS
1 QUAD PLOTTED FOR REFERENCE

5.7) STATIC TORQUE SUMMING

a) Quadrant Motors A & B

SERIES 1

INPUT CURRENT	INPUT VOLTAGE	STATOR TEMP.	MAX TORQUE	SHAFT POSITION
amperes	volts	°F	in-lbs	degrees
2	0.6	75	19.0	30.94
4	1.3	75	39.0	
6	2.0	75	56.0	
8	2.7	75	76.0	
10	3.3	75	92.0	
12	4.1	75	111.0	
14	4.8	75	130.0	
16	5.4	76	141.0	
18	6.3	77	163.0	
20	6.9	78	178.0	
22	7.6	79	193.0	
24	8.4	80	207.0	
26	9.2	81	227.0	
28	10.0	82	235.0	
30	10.8	83	248.0	
32	11.6	84	260.0	
34	12.7	85	272.0	30.94

B. ZELINSKI / L. KINTZ 1/18/84

(1) 500 IN-LB TORQUE SHAFT (TS 173)

(2) 3' LEVER

5.7) STATIC TORQUE SUMMING

b) Quadrant Motors A & B & C

SERIES 1

INPUT CURRENT	INPUT VOLTAGE	STATOR TEMP.	MAX TORQUE	SHAFT POSITION
amperes	volts	°F	in-lbs	degrees
2	0.9	83	26	30.94
4	2.0	83	58	
6	3.0	83	84	
8	4.1	83	113	
10	5.1	83	138	
12	6.2	83	164	
14	7.2	83	187	
16	8.2	83	210	
18	9.5	83	233	
20	10.4	84	252	
22	11.5	85	274	
24	12.7	86	296	
26	13.9	87	312	
28	15.0	88	327	
30	16.2	89	342	
32	17.5	90	355	
34	18.8	91	364	30.94

B. ZELINSKI / L. KINTZ 1/18/84

(1) 500 IN-LB TORQUE SHAFT (TS173)

(2) 3' LEVER

5.7) STATIC TORQUE SUMMING

c) Quadrant Motors A & B & C & D

SERIES 1

INPUT CURRENT	INPUT VOLTAGE	STATOR TEMP.	MAX TORQUE	SHAFT POSITION
amperes	volts	°F	in-lbs	degrees
2	1.2	87	33	30.94
4	2.8	87	75	
6	4.2	87	114	
8	5.4	87	147	
10	6.8	87	170	
12	8.4	87	231	
14	9.8	87	268	
16	11.0	87	300	
18	12.4	87	333	
20	13.9	87	364	
22	15.3	88	395	
24	17.0	89	422	
26	18.8	90	451	
28	20.0	91	474	
30	21.7	92	495	
32	23.4	93	508	
34	25.0	94	527	30.94

B. ZELINSKI / L. KINTZ 1/18/84

(1) 500 IN-LB TORQUE SHAFT (TS173)

(2) 3' LEVER

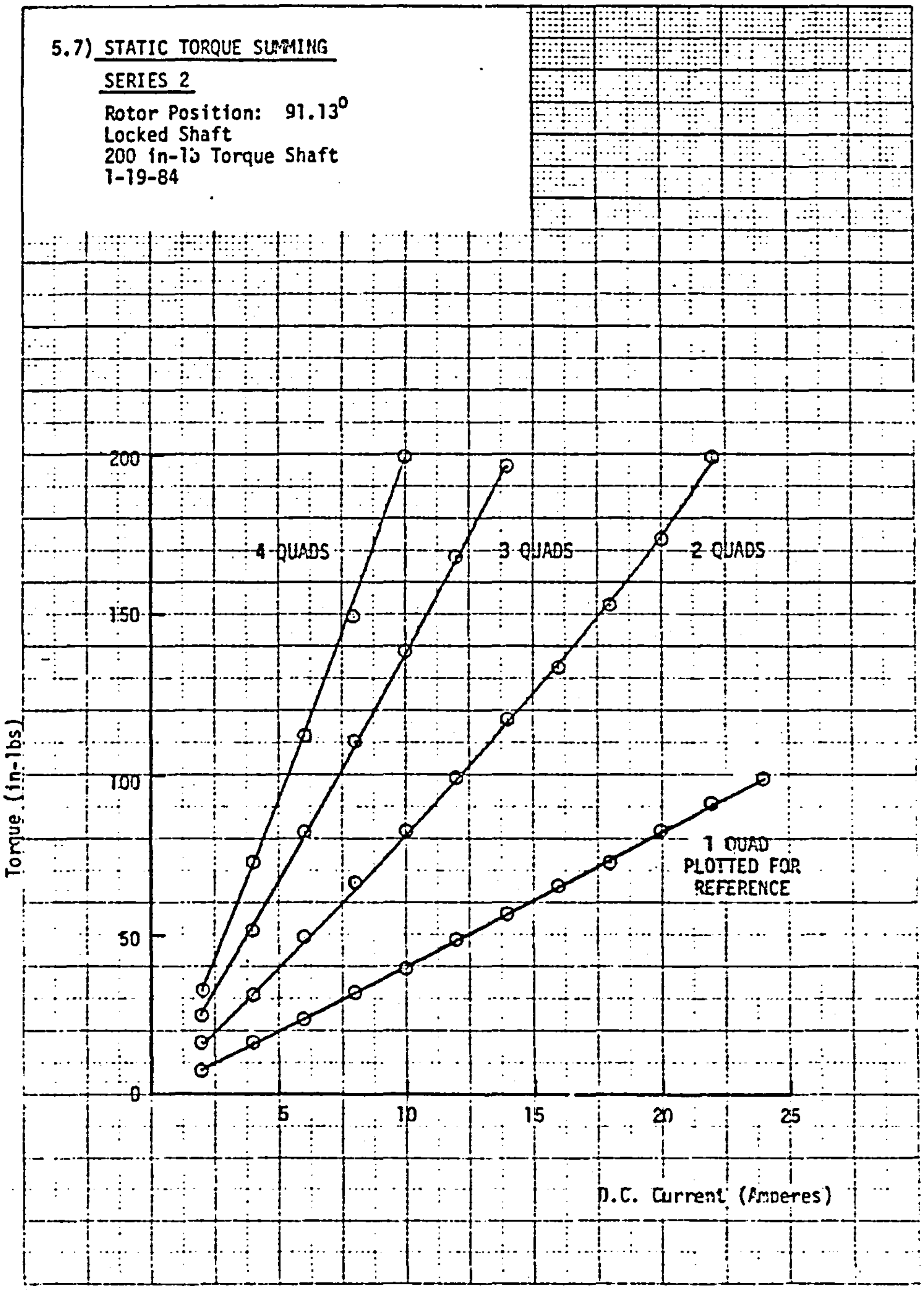

5.7) STATIC TORQUE SUMMING
SERIES 2
Rotor Position: 91.13°
Locked Shaft
200 in-lb Torque Shaft
1-19-84
4 QUADS
3 QUADS
2 QUADS
1 QUAD
PLOTTED FOR
REFERENCE
Torque (in-lbs)
200
150
100
50
0
5
10
15
20
25
D.C. Current (Amperes)

5.7) <u>STATIC TORQUE SUMMING</u>

a) Quadrant Motors A & B

SERIES 2

INPUT CURRENT	INPUT VOLTAGE	STATOR TEMP.	MAX TORQUE	SHAFT POSITION
amperes	volts	°F	in-lbs	degrees
2	0.64	76	16.2	91.13
4	1.4	76	31.4	
6	2.1	76	[illegible]	
8	2.8	76	66.1	
10	3.5	76	82.5	
12	4.2	76	98.6	
14	4.9	76	116.5	
16	5.7	77	133	
18	6.4	78	152.7	
20	7.5	79	173.8	
22	7.9	80	199	91.13

B. ZELINSKI / L. KINTZ 1/19/84

(1) 200 IN-LB TORQUE SHAFT (TS 179)

(2) LOCKED SHAFT

5.7) <u>STATIC TORQUE SUMMING</u>

b) Quadrant Motors A & B & C

SERIES 2

INPUT CURRENT	INPUT VOLTAGE	STATOR TEMP.	MAX TORQUE	SHAFT POSITION
amperes	volts	°F	in-lbs	degrees
2	0.99	80	24.7	91.13
4	2.0	80	52.6	
6	3.1	80	82.3	
8	4.1	80	109.6	
10	5.1	80	137.7	
12	6.2	80	168	
14	7.1	80	196.1	91.13

B. ZELINSKI / L. KINTZ 1/19/84

(1) 200 IN-LB TORQUE SHAFT (TS 179)

(2) LOCKED SHAFT

5.7) STATIC TORQUE SUMMING

c) Quadrant Motors A & B & C & D

SERIES 2

INPUT CURRENT	INPUT VOLTAGE	STATOR TEMP.	MAX TORQUE	SHAFT POSITION
amperes	volts	°F	in-lbs	degrees
2	1.3	81	31.7	91.13
4	2.7	81	72.9	
6	3.9	81	112.4	
8	5.2	81	149.3	
10	6.7	81	197.8	91.13

B. ZELINSKI / L. KINTZ 1/19/84

(1) 200 IN-LB TORQUE SHAFT (TS179)

(2) LOCKED SHAFT

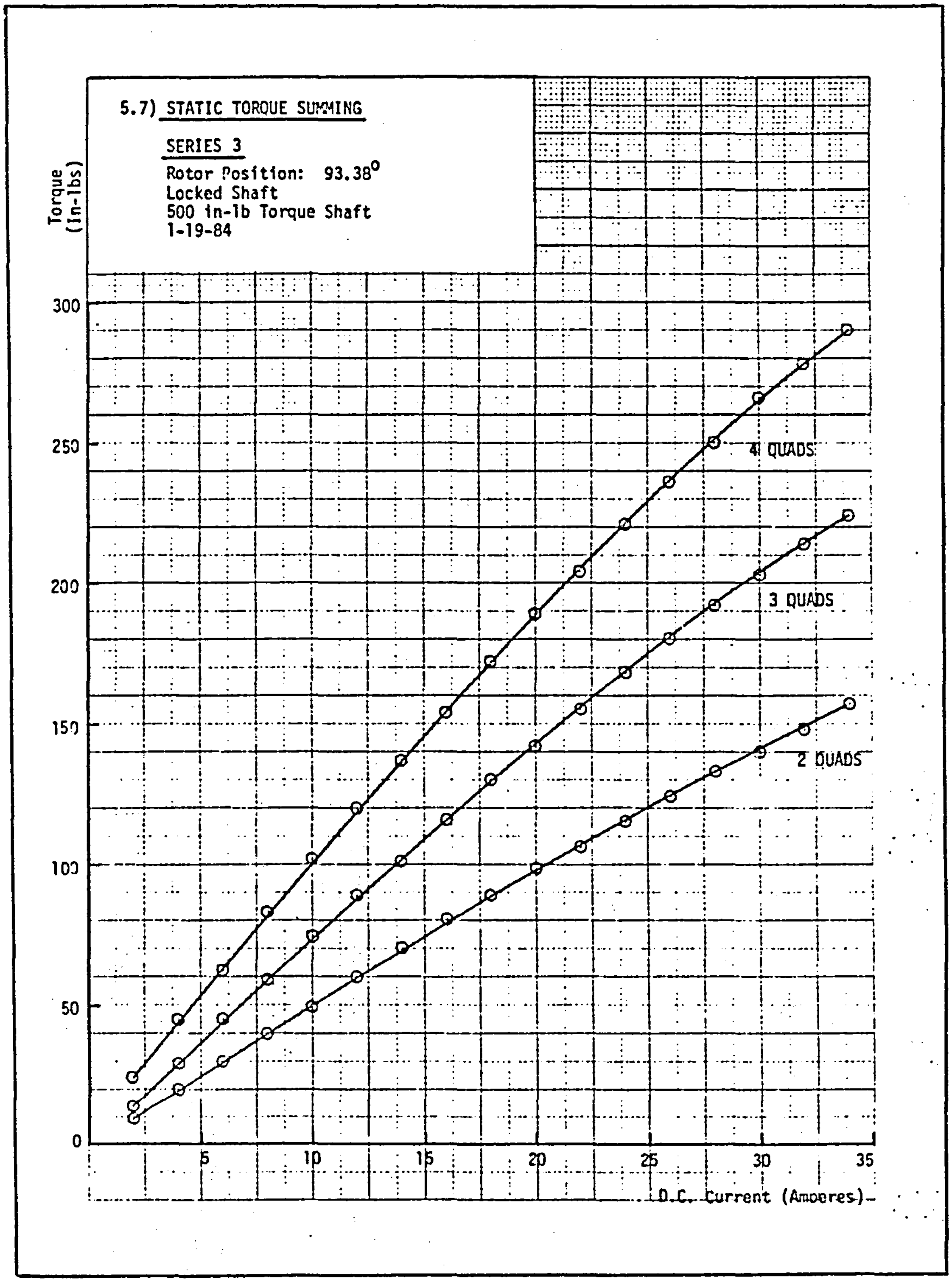
5.7) STATIC TORQUE SUMMING
SERIES 3
Rotor Position: 93.38°
Locked Shaft
500 in-lb Torque Shaft
1-19-84
Torque (In-lbs)
0
50
100
150
200
250
300
5
10
15
20
25
30
35
D.C. Current (Amperes)
4 QUADS
3 QUADS
2 QUADS

5.7) STATIC TORQUE SUMMING

a) Quadrant Motors A & B
SERIES 3

INPUT CURRENT	INPUT VOLTAGE	STATOR TEMP.	MAX TORQUE	SHAFT POSITION
amperes	volts	°F	in-lbs	degrees
2	0.64	76	9	93.37
4	1.4		20	
6	2.1		30	
8	2.8		40	
10	3.5		49	
12	4.2		60	
14	4.9		70	
16	5.7		80	
18	6.4		89	
20	7.5		98	
22	7.9		106	
24	8.7		115	
26	9.4		124	
28	10.2		133	
30	11.1		140	
32	11.9		148	
34	12.9		157	93.38

B. ZELINSKI / L. KINTZ 1/19/84

(1) 500 IN-LB TORQUE SHAFT (TS173)

(2) LOCKED SHAFT

5.7) STATIC TORQUE SUMMING

b) Quadrant Motors A & B & C

SERIES 3

INPUT CURRENT	INPUT VOLTAGE	STATOR TEMP.	MAX TORQUE	SHAFT POSITION
amperes	volts	°F	in-lbs	degrees
2	0.99	80	14	93.38
4	2.0		29	
6	3.1		45	
8	4.1		59	
10	5.1		74	
12	6.2		89	
14	7.1		101	
16	8.3		116	
18	9.3		130	
20	10.4		142	
22	11.4		155	
24	12.7		168	
26	13.8		180	
28	14.9		192	
30	16.2		203	
32	17.5		214	
34	18.8		224	93.38

B. ZELINSKI / L. KINTZ 1/19/84

(1) 500 IN-LB TORQUE SHAFT (TS 173)

(2) LOCKED SHAFT

5.7) STATIC TORQUE SUMMING

c) Quadrant Motors A & B & C & D

SERIES 3

INPUT CURRENT	INPUT VOLTAGE	STATOR TEMP.	MAX TORQUE	SHAFT POSITION
amperes	volts	°F	in-lbs	degrees
2	1.3	81	24	93.38
4	2.7		45	
6	3.9		62	
8	5.2		83	
10	6.7		102	
12	7.9		120	
14	9.3		137	
16	10.7		154	
18	12.1		172	
20	13.5		189	
22	14.9		204	
24	16.5		221	
26	17.9		236	
28	19.4		250	
30	21.3		266	
32	22.9		278	
34	24.5		290	93.38

B. ZELINSKI / L. KINTZ 1/19/84

(1) 500 IN-LB TORQUE SHAFT (TS 173)

(2) LOCKED SHAFT

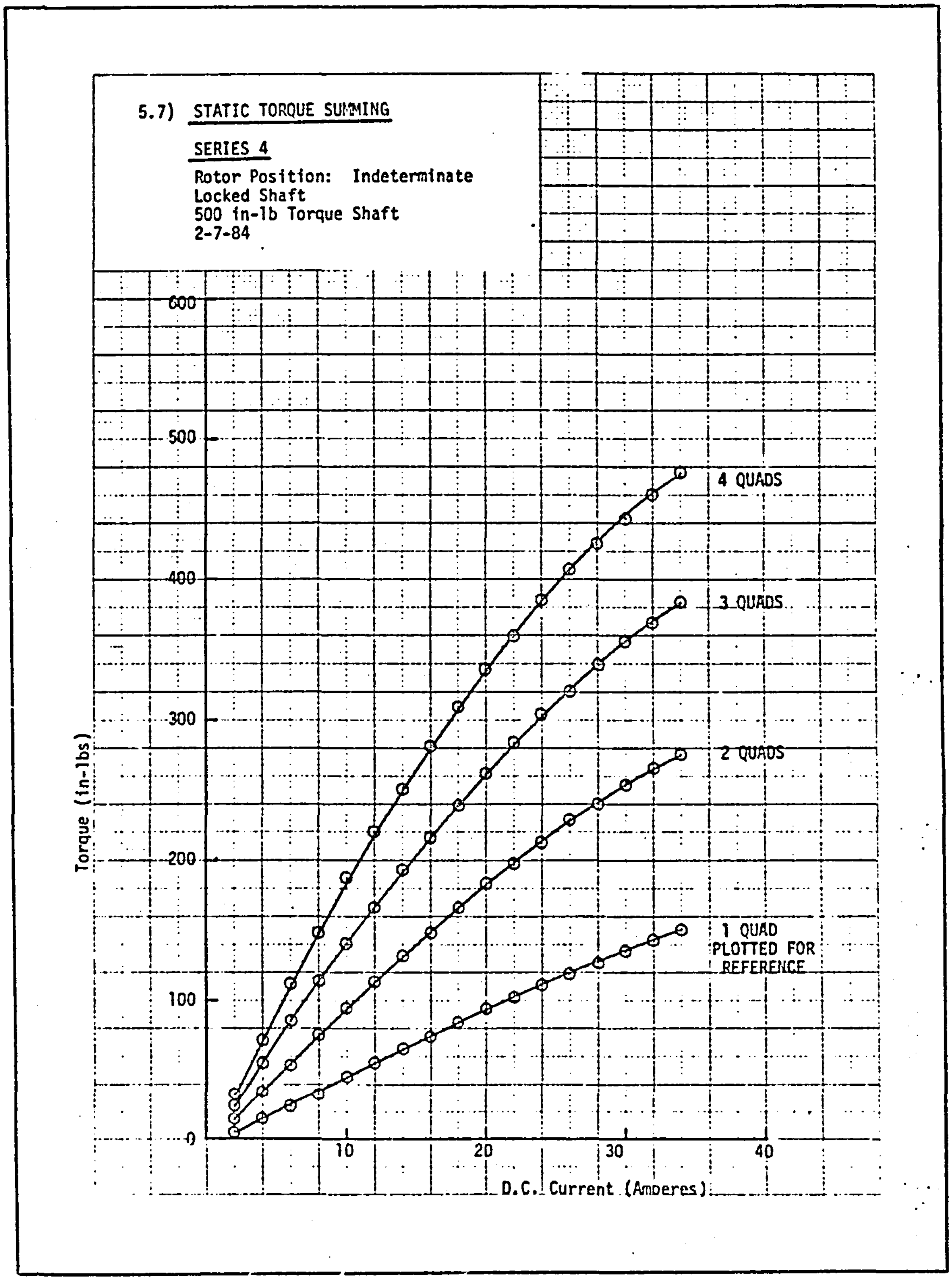
5.7) STATIC TORQUE SUMMING
SERIES 4
Rotor Position: Indeterminate
Locked Shaft
500 in-lb Torque Shaft
2-7-84
600
500
400
300
200
100
0
Torque (in-lbs)
10
20
30
40
D.C. Current (Amperes)
4 QUADS
3 QUADS
2 QUADS
1 QUAD
PLOTTED FOR
REFERENCE

5.7) STATIC TORQUE SUMMING

a) Quadrant Motors A & B
SERIES 4

INPUT CURRENT	INPUT VOLTAGE	STATOR TEMP.	MAX TORQUE	SHAFT POSITION
amperes	volts	°F	in-lbs	degrees
2	NOT MEASURED	NOT MEASURED	14	RANDOM
4			34	
6			54	
8			75	
10			95	
12			113	
14			131	
16			148	
18			166	
20			183	
22			197	
24			213	
26			227	
28			240	
30			254	
32			265	
34			275	

L. KINTZ 2/7/84

(1) 500 IN-LB TORQUE SHAFT (TS173)

(2) LOCKED SHAFT

5.7) STATIC TORQUE SUMMING

b) Quadrant Motors A & B & C

SERIES 4

INPUT CURRENT	INPUT VOLTAGE	STATOR TEMP.	MAX TORQUE	SHAFT POSITION
amperes	volts	°F	in-lbs	degrees
2	NOT MEASURED	NOT MEASURED	24	RANDOM
4			55	
6			85	
8			112	
10			140	
12			166	
14			193	
16			216	
18			239	
20			262	
22			283	
24			304	
26			320	
28			339	
30			355	
32			369	
34			383	

L. KINTZ 2/7/84

(1) 500 IN-LB TORQUE SHAFT (TS173)

(2) LOCKED SHAFT

5.7) STATIC TORQUE SUMMING

c) Quadrant Motors A & B & C & D

SERIES 4

INPUT CURRENT	INPUT VOLTAGE	STATOR TEMP.	MAX TORQUE	SHAFT POSITION
amperes	volts	°F	in-lbs	degrees
2	NOT MEASURED	NOT MEASURED	33	RANDOM
4			72	
6			112	
8			148	
10			187	
12			220	
14			250	
16			281	
18			310	
20			336	
22			359	
24			385	
26			407	
28			425	
30			443	
32			460	
34			476	

L. KINTZ 2/7/84

(1) 500 IN-LB TORQUE SHAFT (TS173)

(2) LOCKED SHAFT

APPENDIX B

CONTROL STRATEGY

Optimization of Brushless DC Motor Design

By
Jayant G. Vaidya, Sr. Research Engineer
Sundstrand Corporation, Advanced Technology Operations
Rockford, IL 61101

Introduction

Brushless dc motors are generally required to operate under widely varying conditions of load. These varying conditions include: changes in torque, changes in speed, and resulting changes in power output. On the other hand there are changes of input voltage and commutation angle that are optional and can be selected to suit the performance capabilities of the brushless dc motor. The back e.m.f. and the winding inductance per phase of a multi-phase brushless dc motor are the two design parameters that must be selected to obtain an optimum design. It is the purpose of this article to present techniques for optimizing the performance of brushless dc motors by selecting the design parameters and the optional operating points for input voltage and commutation angle for specific load characteristics.

A simplified model representing one phase of a multi-phase, permanet magnet field brushless dc motor is employed. It is proposed that such a model is an extremely convenient tool for evaluating performance under a variety of operating conditions. It is indicated how this simplified model can be applied to optimization of the brushless dc motor design. It is then shown how the technique of optimization can be applied to different types of designs for specific load characteristics such as constant torque, constant speed, constant power, and combinations thereof.

The Simplified Model of Brushless DC Motor

Consider one phase of a permanent magnet field brushless dc motor having an n-phase winding. If the winding resistance is neglected, this phase can be represented schematically as shown in Figure 1. The applied voltage is V volts r.m.s. per phase and the back e.m.f. is E volts r.m.s. per phase. Let us assume that both V and E are sinusoidal. The winding inductance is L henry. Let us assume that there is no magnetic saturation in the armature iron so that the value of L remains constant regardless of changes in current. Since most of the machines to which this analysis is applied are likely to use permanent magnets with the relative permeability close to one (such as ceramic or samarium cobalt magnets), it is safe to assume that the winding inductance L remains practically constant regardless of the angular position of the field with respect to the armature winding.

Defining the r.m.s. value of the current in the phase under consideration as I amperes,

$$\bar{I} = \frac{\bar{V} - \bar{E}}{2\pi fL}, \tag{1}$$

where $\bar{I}$, $\bar{V}$, $\bar{E}$ are phasor quantities and f equa' . ..e frequency in Hertz. Defining the commutation angle as δ radians and the power factor angle as ϕ radians, the phaso diagrams with all the quantities can be drawn as shown in Figure 2. The power input to the motor is given by

$$P = n\ VI\ \cos\phi \tag{2}$$

This is also the power output if all the losses such as iron losses and windage and friction losses are neglected for our simplified model. By examination of the phasor diagram,

$$I = \frac{E\sin\delta}{2\pi fL\ (\cos\phi\ )} \tag{3}$$

Combining equations (2) and (3) above,

$$P = \frac{nVE\sin\delta}{2\pi fL} \tag{4}$$

This is the well-known power equation for the cylindrical rotor synchronous machines.

Using the Simplified Model for Design Optimization

Certain general comments can be made regarding the brushless dc ..otor on the basis of equations (2), (3), and (4). These are as follows:

a) The power is proportional to the back e.m.f. E. This can be increased at the cost of increased weight of the permanent magnet field as well as the armature.

b) The power is inversely proportional to the inductance L. Thus if the number of turns in the armature is increased to increase the back E.M.F., the inductance increases in proportion to the square of the number of turns. This will in fact reduce the power.

c) To keep the motor current as low as possible, the power factor, $\cos\phi$ must be kept close to 1. However any attempt to increase $\cos\phi$ requires changes in the back e.m.f. E and the commutation angle δ.

To clarify these points, let us consider the case of a fixed power, constant speed brushless dc motor, operating from a fixed input voltage. Although such a simple requirement may not occur in practical situations, it will help illustrate the optimization procedure. In order to keep the armature current to a minimum, let us assume that the power factor is restricted to 1. Then applying equation (4), the power

$$P \propto \frac{E\sin\delta}{L} \qquad (5)$$

Once a certain configuration of the motor is determined the value of E can be increased by increasing the stack length of the motor. However, the inductance L also increases with the stack length. Then

$$P \propto \sin\delta \qquad (6)$$

However, from the phasor diagram of Figure 2,

$$E \cos\delta = V, \text{ for } \cos\phi = 1$$

or $$\sin\delta = \sqrt{1-V^2/E^2}$$

If we define a variable $e = E/V$,

$$\sin\delta = \sqrt{1 - 1/e^2}$$

then $$P \propto \sqrt{1- 1/e^2}$$

Now the weight of the motor is a function of the back e.m.f. and we can express,

$$\text{Weight, } W \propto e^x,$$

where x is variable dependent on the total weight increase caused by the increase of back e.m.f. E. Then we can define the power per unit weight as

$$P/W = \sqrt{1 - 1/e^2}/e^x \qquad (7)$$

This equation is plotted in Figure 3 for several values of x to illustrate how an optimum power to weight ratio can be obtained. From the curve for any specific value of x, the optimum value of e and the optimum value of the back e.m.f. E can be selected where the ratio P/W reaches its peak. Any further increase in the back e.m.f. E will in fact result in a less than optimum design. Similar curves can be plotted for power factors other than 1.

Let us consider another case where the value of E is fixed as a percentage of the applied voltage V, and the power factor must be otimized. Two independent situations arise in this case: One where E is less than V, and the other where E is greater than V. Figure 4 shows the phasor diagram for the situation where E is less than V. Here the maximum value of the power factor $\cos\phi$ is attained when the power factor angle ϕ is smallest. This occurs when the phasor $(\bar{V}-\bar{E})$ is tangential to the locus of E as shown in Figure 4. At this point the power factor angle and the commutation angle are equal and

$$\cos\phi = \cos\delta = E/V \tag{8-a}$$

And the power equation (4) for the optimum power factor becomes,

$$P = \frac{nE\sqrt{V^2-E^2}}{2\pi fL} \tag{9-a}$$

In the second situation where E is greater than V, the maximum value of the power factor that can be attained is 1 as shown in the phasor diagram. The commutation angle δ is given by

$$\cos\delta = V/E \tag{8-b}$$

And the power equation (4) for the power factor of 1, becomes,

$$P = \frac{nV\sqrt{E^2-V^2}}{2\pi fL} \tag{9-b}$$

Using equations (9-a) and (9-b), optimum values of the winding inductance per phase, L can be determined for given applied voltage V and back e.m.f. E. The optimum value of commutation angle δ can be determined using equations (8-a) and (8-b).

Constant Torque Operation

The procedure for optimization of the power factor as discussed above can be extended to the constant torque load characteristics shown in Figure 6. First the design parameters may be optimized at the highest operating speed of N_2 R.P.M. where maximum power occurs. At this point the input voltage should be held at its maximum value V. As the operating speed of the motor is reduced, the back e.m.f. E as well as the reactance $2\pi fL$ reduce in proportion to the speed. The power factor can be held constant at its optimum value if the applied voltage V is reduced in proportion to the speed. The commutation angle δ is also held at its original value throughout the operating range. The power as in equation (4) falls in proportion to the reduction of the applied voltage V as the speed is reduced.

Two cases, one with the back e.m.f. E less than the applied voltage V, and the other with the back e.m.f. greater than the applied voltage V are shown in Figures 7 and 8. Equations (8-a) and (9-a) and (8-b) and (9-b) apply to the two cases at the peak speed of N_2 R.P.M. At any lower speed N, the power is reduced by the factor N/N_2 as required by the load.

Constant Speed Operation

The constant speed characteristic is shown in Figure 10. One approach would be to optimize the power factor at the peak torque load keeping the back e.m.f. E below the value of the applied voltage V as shown in Figure 4. Then as the torque is reduced from its peak value, the applied voltage can be reduced, holding the commutation angle constant so that the power factor increases until it reaches the value of 1. This is shown by means of a phasor diagram in Figure 11. At the peak torque point, the relationships of equations (8-a) and (9-a) are valid for the optimum power factor. The minimum torque level that can be then reached for the power factor of 1 is then given the following equation,

$$T_1 = T_2 \frac{E\cos\delta}{V}$$

$$= T_2\left(\frac{E^2}{V^2}\right), \tag{10}$$

where,

T_1 = Torque at power factor of 1

T_2 = Peak torque.

Any further reduction in the torque can be obtained by reducing the commutation angle and simultaneously increasing the applied voltage to main-

tain the power facotr at 1. This procedure will allow unlimited reduction in the torque right down to zero.

Constant Power Operation

Consider the load characteristics shown in Figure 11, where the power requirement remains constant over the speed range from N_1 r.p.m. to N_2 r.p.m. In this case to get the optimum design, it is best to restric the current at the maximum and minimum speeds to a certain value, consistent with highest possible power factor. Here once again the ratio of E to $2\pi fL$ remains constant over the speed range, and if we keep the applied voltage constant, then the power

$$P \propto \sin\delta \tag{11}$$

Since the power is constant throughout the operating range, the commutation angle δ should remain constant. Now let us set the back e.m.f. E_1 at speed N_1 such that at the required power level, the optimum conditions of Figure 4 and equations (8-a) and (9-a) are attained. Then at the highest speed of N_2,

$$E_2 = \frac{N_2}{N_1} E_1 \tag{12}$$

This will result in a shift in the power factor angle from ϕ_1 lagging to ϕ_2 leading. In order to keep the currents for the two speeds equal, ϕ_1 and ϕ_2 must be equal as can be readily seen by applying equation (2). Phasor diagram for these two speed conditions is shown in Figure 12. Then from the phasor diagram, for the optimum condition of $\phi_1 = \phi_2 = \phi$,

$$E_2 \cos 2\phi = E_1 \tag{13}$$

Combining equations (12) and (13)

$$\cos 2\phi = N_1/N_2 \tag{14}$$

From equation (14) it can be seen that the optimum power factor for constant power operation at the extreme speeds of N_1 R.P.M. and N_2 R.P.M. is given by

$$\cos\phi = \cos\left[\frac{1}{2}\cos^{-1}\frac{N_1}{N_2}\right] \tag{15}$$

As the speed range is widened, the power factor at the extreme speeds gets lower. The power factor at all intermediate speeds is always above the value reached at the extreme speed conditions.

If it is desired to improve the power factor beyond the value obtained using equation (15), it will be necessary to arrange switching of winding connections from star to delta or from parallel to series at a predetermined speed between the upper and lower speed limits.

Combinations of Different Load Characteristics

In practical design applications combinations of two or more types of speed torque characteristic curves may occur. Figure 13 illustrates one such case. Here the entire load characteristic can be split into two parts: one constant torque operation from the speed N_1 R.P.M. to the speed N_2 R.P.M. and another constant power operation from the speed N_2 R.P.M. to N_3 R.P.M. Each part can be treated individually as already discussed. Thus during the constant power operation, the power factor may be optimized at the extreme speeds of N_2 R.P.M. and N_3 R.P.M. The applied voltage V and the commutation angle δ are held constant throughout this speed range. On the other hand, during the constant torque operation, the applied voltage may be reduced as the speed is reduced and the commutation angle is held constant. Similar approach of dealing with the load characteristics in parts may be taken where other combinations of speed torque curves occur.

Conclusion

An approach to the optimization of the design parameters for permanent magnet field brushless dc motors is presented in this article. Certain assumptions have been made so that specific goals for the design parameters such as the back e.m.f., the winding inductance and the commutation angle can be established for any specific speed torque curve. Once this is done, the basic electromagnetic design of the brushless dc motor can be established. After this a detailed analysis of the design at specific load points of interest will require inclusion of other parameters such as winding resistance, saturation of iron, variation of inductance, harmonics in applied voltage and back e.m.f., and various losses which were neglected in the model employed in this article.

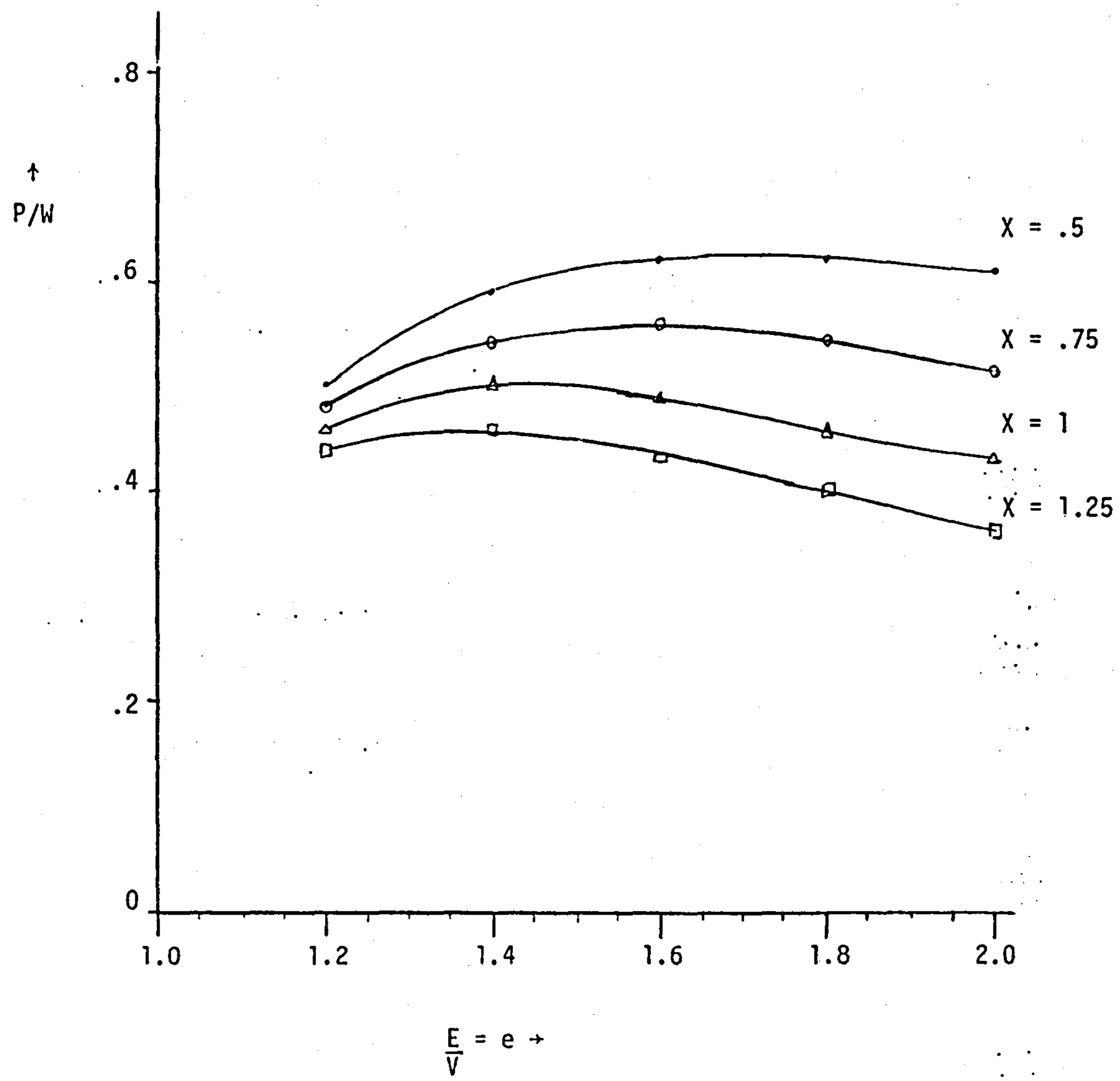

Figure 3: Power to Weight Ratio as a Function of Back E.M.F. to Applied Voltage Ratio, with Power Factor, cosϕ = 1.

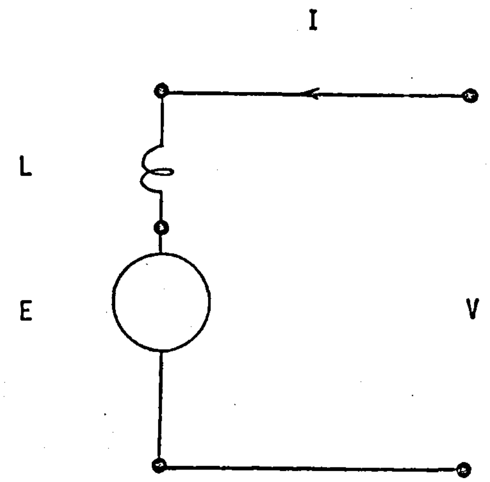

Figure 1 : Schematic Showing One Phase

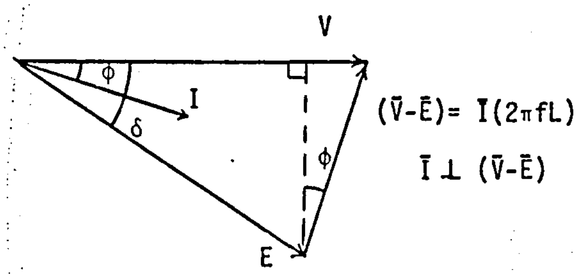

Figure 2 : Phasor Diagram

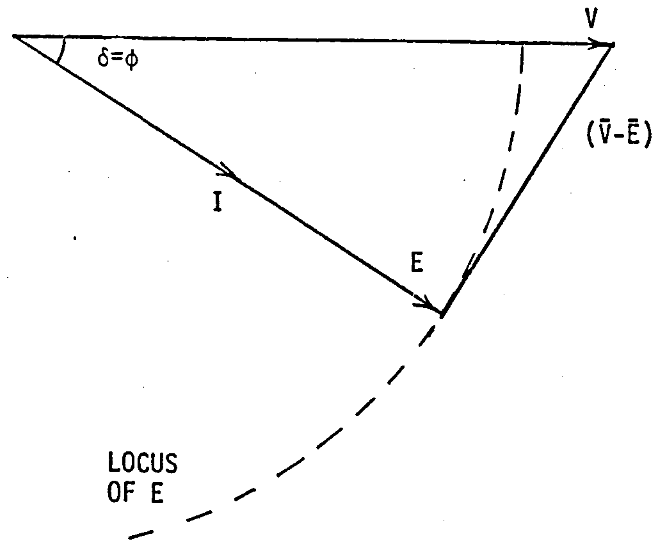

Figure 4 : Optimum Power Factor for E <V

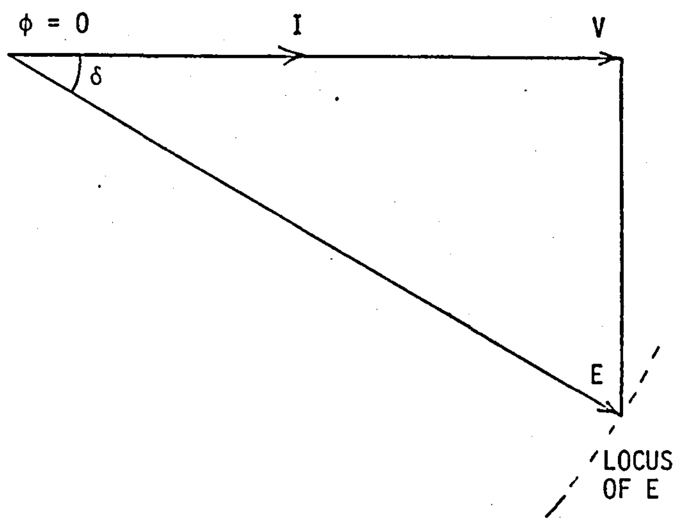

Figure 5 : Optimum Power Factor for E >V

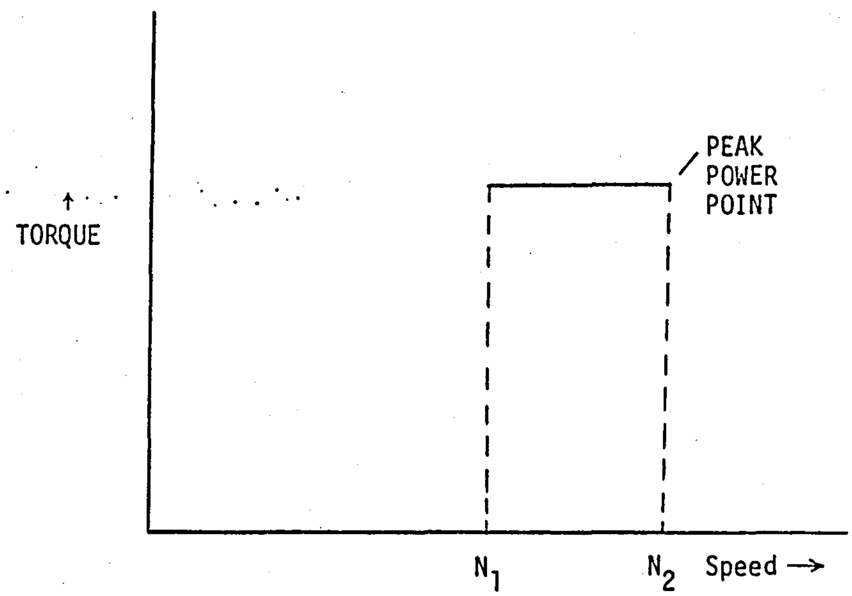

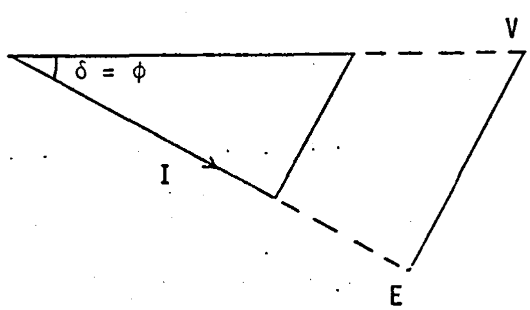

Figure 7 : Constant Torque Operation, E <V

Figure 8 :
Constant Torque Operation,E >V

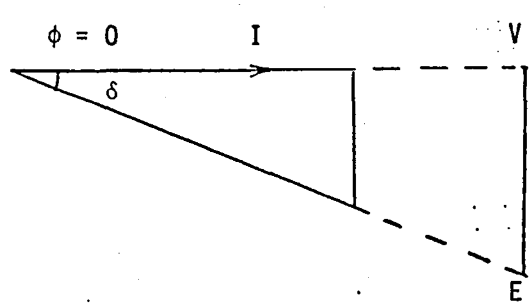

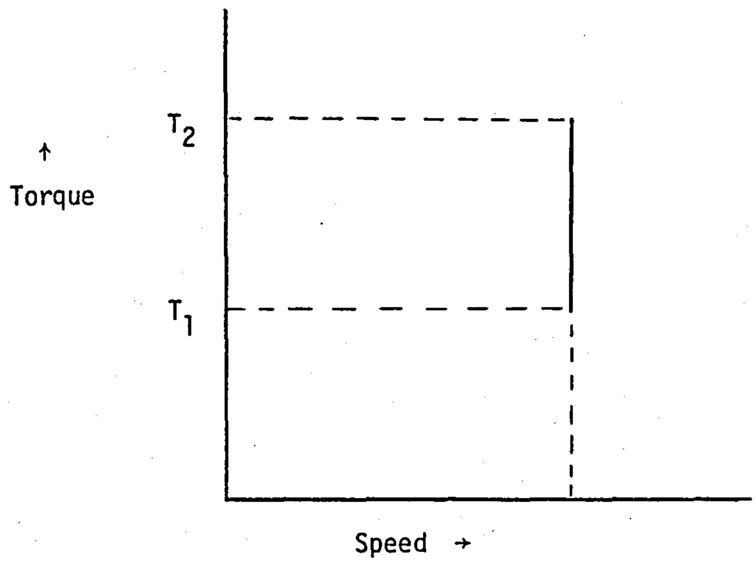

Figure 9 : Constant Speed Operation

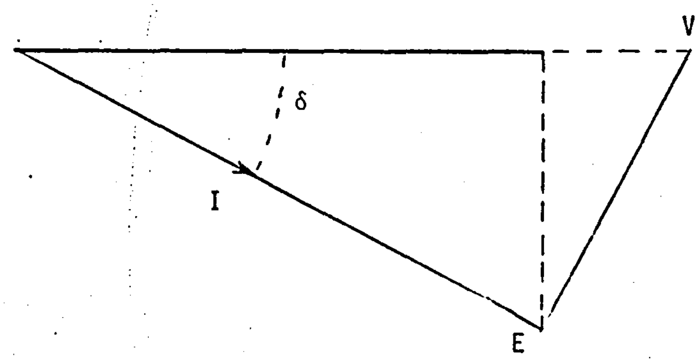

Figure 10 : Constant Speed Operation:Phasor Diagram

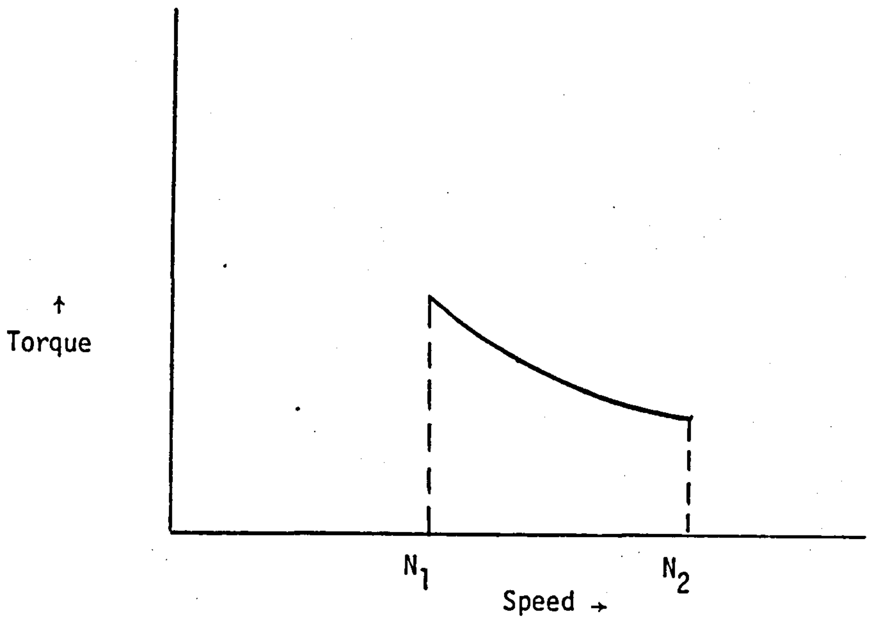

Figure 11 : Constant Power Operation

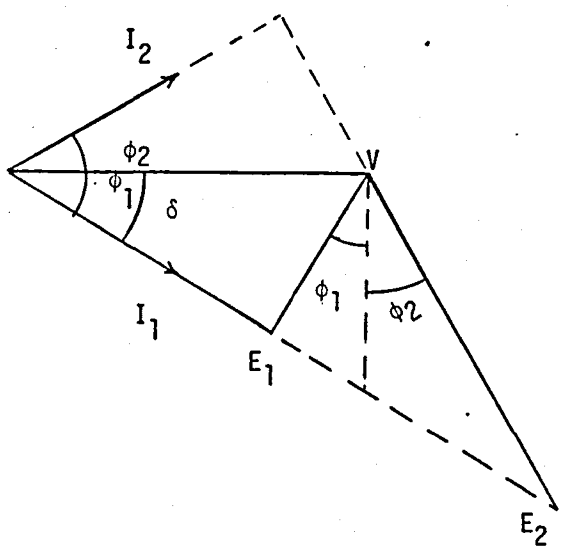

Figure 12 : Constant Power Operation : Phasor Diagram

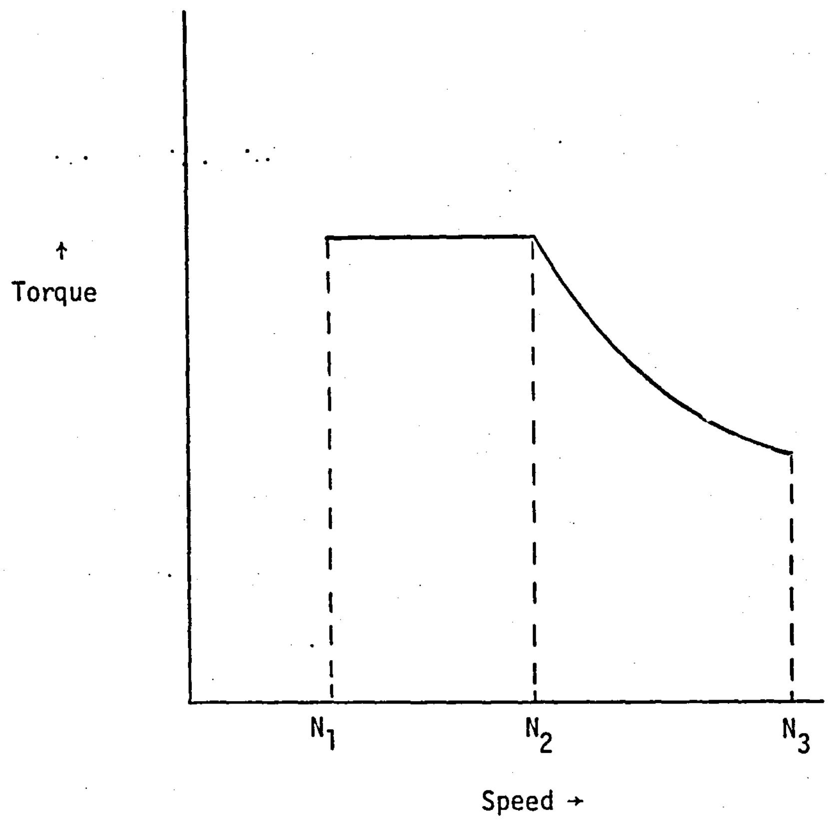

Figure 13 : Combination of Two Speed Torque Characteristics

End of Document